V. M. Sineglazov,
A. A. Zelenkov,
Sh. I. Askerov

MEMRISTORS AND NONVOLATILE RANDOM ACCESS MEMORY (NVRAM) IN NANOELECTRONICS

Training book

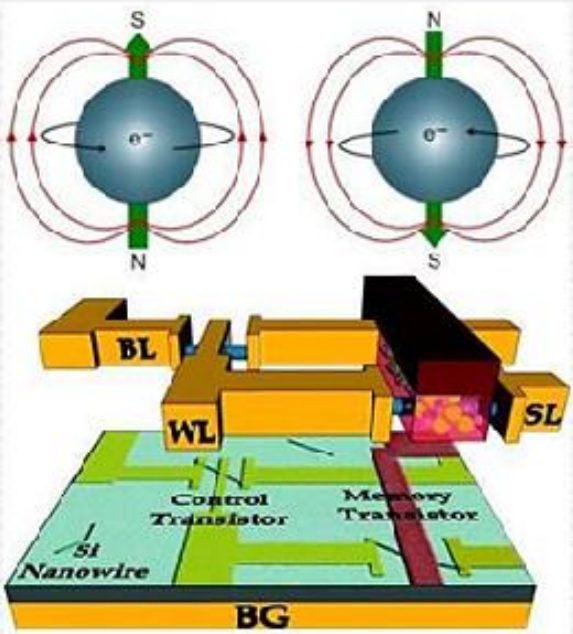

Osvita Ukraiyny

MINISTRY OF EDUCATION AND SCIENCE OF UKRAINE

National Aviation University

V. M. SINEGLAZOV, A. A. ZELENKOV,
Sh. I. ASKEROV

MEMRISTORS AND NONVOLATILE RANDOM ACCESS MEMORY (NVRAM) IN NANOELECTRONICS

Training book

Kyiv 2017
Osvita Ukraiyny

UDC 621.373.8(075.8)
BBC з86 я7
C 382

Reviewers:

V. I. Skurihin – Doctor of Engineering Science. Professor. Member of Academy of sciences of Ukraine
V. V. Vasiliev – Doctor of Engineering Science. Professor. Corresponding member of Academy of sciences of Ukraine

Approved by the Academic council of the National Aviation University, 17.03.2016

Sineglazov V.M., Zelenkov A.A., Askerov Sh.I.
C382 Memristors and nonvolatile random access memory (NVRAM) in nanoelectronics: training book / V. M. Sineglazov, A. A. Zelenkov, Sh. I. Askerov – K.: Osvita Ukraiyny, 2017. – 324 p.

ISBN

The manual is devoted to the physical principles of the memristor as a fourth fundamental element, whose existence was predicted theoretically in 1971, and in 2008 alone the memristor was realized physically.

The basic characteristics and models of the memristor as the basic element of the electrical circuits, along with the resistor, inductor and capacitor are considered. The basic note is shared to the effect of the resistive switching of the memristor, its physical realization, as well as building on its base of some types of nonvolatile random access memory (NVRAM), elements of which are dimensions of the order of several nanometers, and therefore their physical realization is in the field of nanotechnology. The properties of materials to realize new approaches to the development of computers and their basic elements are just manifested in the nanoscale.

UDC 621.373.8(075.8)
BBC з86 я7

ISBN

In the past few years in the periodical scientific literature there are a large number of publications related to the emergence of a new fourth fundamental element, called ***memristor***, as well as its possible physical realization and application in electronics.

The discovery of this element was held at the "pen tip" a professor of electrical engineering and computing system Department of the University of California at Berkeley Leon Chua in 1971.

Let's consider a historical background.

The concept of a resistor with memory existed even before Leon Chua's publication o the memristor. In 1960, professor Bernard Widrow of Stanford University developed a new circuit element named the "memistor". The memistor was a three-terminal device for which the conductance between two of the terminals was controlled by the time-integral of the current into the third terminal. Thus, the resistance of the memistor was controlled by charge. Memistors formed the basic components of the neural-network architecture called ADALINE (ADAptive Linear Neuron).

In 1968, F. Argall published a paper, "Switching phenomena in titanium oxide thin films", which shows results similar to that of the memristor model proposed by Stanley Williams and his team.

In 1971, Leon Chua mathematically predicted that there is a fourth fundamental circuit element characterized by a relationship between charge and flux linkage.

In 1976, Leon Chua and Sung Mo Kang published a paper entitled "Memtristive devices and systems", generalizing the theory of memristors and memristive systems.

In 1990, S. Thakoor, et al., demonstrated a tungsten-oxide variable-resistance device that is electrically reprogrammable. It is not clear whether the memistor device described has any relation with Chua's memristor.

In 1994, Buot and Rajgopal published an article entitled "Binary information storage at zero bias in quantum-well diodes". The article described current-voltage characteristics similar to that of the memristor in AlAs/GaAS/AlAs quantum-well diodes. The analysis showed no direct connection to Chua's memristor.

In 2000, Beck, et al., of IBM's Zurich Research Laboratory, described reproducible resistance switching effects in thin oxide films. The hysteretic features of these switches are similar to those of the memristor.

In 2001, Liu, et al., researches in the Space Vacuum Epitaxy Center of the University of Houston, presented results during a non-volatile memory conference held in San Diego, California, showing the importance of oxide bilayers to achieve high-to-low resistance ratio.

Apart from the devices mentioned above, it is interesting to note that between 1994 and 2008 there were many other devices developed with behavior similar to that of the memristor, but only the HP scientists were successful in finding a link between their work and the memristor postulated by Chua.

In 2008, thirty-seven years after Leon Chua's proposal, the memristor in device form was developed by Stanley Williams and his group in the Information and Quantum Systems (IQS) Lab at HP. Dmitry Strukov, Gregory Snider, Duncan Stewart, and Stanley Williams, of HP Labs, published an article identifying a link between the two-terminal resistance switching behavior found in nanoscale systems and Leon Chua's memristor.

Later in 2008, J. Joshua Yang, Matthew D. Pickett, Xuema Li, Douglas a. A. Ohlberg, Duncan r. Stewart and R. Stanley Williams published an article demonstrating the memristive switching behavior and mechanism in nanodevices.

Nanoelectronics is a relatively young field of physics and electronics, and the range of its researches and applications very quickly expends and deepens.

Achievements of nanoelectronics and nanotechnology have gained immense popularity. Extensive foreign and domestic publications as special research papers and reviews, and popular magazine essays are denoted nanoelectronics.

Nanoelectronics is the leading direction of nanotechnology development. Advances in microelectronics and expansion of technologies used in it are the basis for the creation of modern nanotechnology. Information technology and nanoelectronic systems continue to develop communication, processing and storage systems, industrial process control, digital information systems.

In history there are cases of the practical realization delay of discoveries after their theoretical studies.

The case of field-effect transistor is the most famous. The concept of field effect was known as early as 1930 before the invention of the bipolar transistor. However, the field effect transistor has get practical realization only in the 60th of the last century and has become a necessary part of CMOS (complementary metal-oxide semiconductor) technology. In those years it was impossible to carry out the realization of the FET due to the imperfection of the respective technologies.

Similar case has occurred with the discovery of the memristor. We now know that in order to realize the memristor, it is necessary to have a special nanotechnology, since the effect of the so-called memristance become "visible" only at nanoscale.

This manual is intended for students who do not have special training in order to understand the functioning principles of different memristor-based devices, as well as the prospects of their application.

Today the fundamental courses of electrical engineering and electronics are considering questions related to basic physical laws of electromagnetism and quantum physics.

In the study of passive elements such as resistor, capacitor and inductor, as a rule, we consider simple examples, which do not require at the early stages of learning the complex calculation methods. In this case, the resistance of the resistor is considered as a measure to counteract the passage of electrons through the atomic structure of the material. The capacitance is represented as the amount of charge that is retained in a closed volume.

One of the representations of the memristor is an expression $u(t) = M[q(t)]i(t)$, reminiscent of Ohm's law, studied in the school curriculum of physics. If the M is a constant, independent of the charge q, this expression is a simple Ohm's law and a memristor is represented as a linear resistor with some resistance R. If the parameter M has a nonlinear dependence on the charge passing through the element, the memristor becomes a nonlinear element with properties that are great interest in electronics.

It is necessary to note that skeptics argue that the memristor is not a fourth fundamental circuit element but an example of bad science. The crux of their argument rests on two fundamental misunderstandings:

first, skeptics overlook the expanded design space that arises from working with nonlinear circuit elements. The second and more profound misunderstanding concerns Leon Chua's mathematical definition of a memristor.

Thus, here is what we need to remember: one, a magnetic interaction is not necessary for memristance. Two, in nonlinear circuit elements, memristance is not the same thing as nonlinear resistance. Three, because no combination of passive devices can reproduce the properties of a memristor, memristance is a fundamental circuit quantity.

Since the memristor is a nonlinear element, therefore it is described by nonlinear differential equations, which are made using Kirchhoff's laws. The basic concepts of the analysis of nonlinear electric circuits, numerical methods for solving systems of nonlinear differential equations are included in the work programs of respective disciplines, enabling students to master the proposed material.

The development of high technologies in such branches of industries as microelectronics and the communication facilities under the general name "Information Technologies (IT)" determined growth of the economic of the developed countries over the last 40 years. Thus, consistent improvement of the characteristics and decreasing of the cost of the mikronanoelektroniks devices achieved first of all by reducing the linear dimensions (scaling) of the elements of logic and memory chips in accordance with the so-called Moore's law, that is every 18 months the productivity of computers without the need for radical innovations is doubled.

In 1975, Gordon Moore formulated his famous assumption, that the complexity of the chips will be doubled every two years. Technological progress allows to continuously reduce the sizes of transistors on a chip, so that the electrical signals will be pass through all the smaller distances to carry out the information processing. This means that the computerized devices will steadily become smaller, faster and cheaper. Thanks to constant application of innovations in design and technology of the semiconductor devices the chips almost exactly followed the forecast of Moore for almost 40 years.

However, the engineers knew that sooner or later this trend will stop. The thickness of the transistors is reduced to a value of tens atoms, and then the fundamental laws of physics will put a limit to the process. But, apparently, two basic practical problems occur:

• ensuring a high percentage of the useful chips with transistors which are placed close together and have such dimensions will be unacceptably expensive;

• intensity of the heat generated by an area with a high density of transistors location, can reach such a level that the elements are "melted."

Now these problems are solved by the use of two or more core processors. These processors have smaller dimensions and programmed for parallel processing of information.

Each core functions no faster than other processors, but as two (or more) core function in parallel, they can process more data in the same time while consuming less energy and releasing less heat.

Today, the smallest transistors have a width of 32 nm (32 nm technology). It is about 96 silicon atoms. Production of the elements with dimensions which are less than 22 nm (22 nm technology already exists, Table 1) with using a lithographic technique will be extremely difficult.

TABLE 1 **HISTORY OF PROCESSORS**

Type of a processor	Year of manufacture	Technology, nm
Intel 8086	1978	3000
Intel 80286	1982	1500
Intel 80386DX	1985	1000
Intel 80386SX	1988	1000
Intel 486DX	1989	800
Intel 386SL	1990	1000
Intel 486SX	1991	800
Intel 486SL	1992	800
Pentium	1993	350
Pentium II	1997	250
Pentium III	1999	180
Celeron M	2003	130
Core	2006	65
Core 2Duo	2008	45
Core i3	2009	32
Core i7	2010	30
Core i7-4960X	2014	22

However, it is well known that if the pace of development of CMOS – technology based on the silicon (CMOS is Complementary Metal-Oxide-Semiconductor), then due to the different fundamental physical limitations principles underlying the action of the logic and memory devices do not work. According to the perspective forecasts (if the rates of the technological and economic development will be kept) in the next decade a new scientific-technical and technological revolution may occur. Its foundation is the development, providing high data capacity (up to the several of atoms per bit) and a sharp decrease in the device power consumption for processing and storage of the information.

To change the paradigm of the development of the information technology instrumental base is necessary to search and study the fundamentally new effects in the materials based on new nanoscale structures. It is necessary to develop the alternative approaches to the creation of the analog or hybrid computing systems and information technology of the fundamentally different type, [13], [44], [45], and [48].

As a result of this it is necessary to note the achievements in the new field of science called spintronics (magnetoelectronics). The successes achieved in the technology of the manufacturing of nanosized structures, allowed to obtain the magnetic nanoheterostructures with unique quantum sized effects.

The possibility to combine the magnetic, semiconducting and dielectric materials holds the great perspectives in the control their magnetic and electrical properties. This, in turn, will allow to obtain the new nanostructures that may find practical application. With the development of a new class of materials called the magnetic semiconductors the integration of the magnetic structures in the semiconductor electronics is already existed.

To date, all the achievements of nanotechnology and nanoelectronics are aimed at a substantial increase of the computer productivity.

As is known, there is no computer productivity in the world, which would not have found its "brake" problem. It is an axiom.

Is there any reasonable limit of the computer productivity, that one would congratulate Humanity with a deserved victory? To answer this question it is necessary to come to the mirror and admire on the wonderful high productivity computer on own shoulders. Look closely at this thoughtful by Nature the frame with two ears, eyes, and other in-out interfaces: the system of the highest productivity is placed within, containing about10^{10} neurons in each cubic centimeter of the volume and decisive mind-blowing tasks in the real time without kilowatt power supply (only three meals a day are sufficiently) without any additional cooling by water or nitrogen (36.6 Celsius is quite enough).

There is one circumstance which strongly negates any attempts to compare the modern computer systems (even high productivity server clusters) with the human brain: the current computer architecture is not very suitable to emulate the brain. More precisely, it is quite not suitable. This is due to the fact that the brain is organized fundamentally dif-

ferently in comparison with the digital architecture of von Neumann computing.

One of the shortcomings of the von Neumann architecture (this is all computing equipment with which we deal, solving the problem) is the fact that the processing and storage of data is physically separated. It means that the information is stored in the memory, and processing is carried out in the processor. In the process of computer functioning it is necessary to move great amounts of data between the processor and memory.

The long-standing goal of all scientists and engineers is the creation of such device in which the calculations are made in a parallel manner as a result of combining processing and storage of the information in one place, to avoid unnecessary data transfer. In this case such architecture can significantly increase the efficiency of the computer systems approaching to creating artificial neural networks based on the new hardware base simulating activity of the biological neural networks (nerve cells of the living organism), [62], [35], and [80].

The modern science represents the principle of the brain functioning by the following way. According to modern concepts, the synapse is the "signal line" between neural cells. Its electrical properties directly depend on the conditions of its activity. That is, the smaller the time interval of the last communication between two neurons, the easier the synapse will react to the following "message", Fig. 1. We have almost complete analogy with the memristor resistance of which keeps the "news" about the last effect applied to it.

From this viewpoint, the investigation of the effects in nanostructures represents the exceptional interest since they functionally reproduce actions of the synapses of the biological systems. In particular the memristor that as well as the synapse of the brain represents the bipolar devices. From the standpoint of the electrical functionality, it can be considered as very close analogue.

The properties of the memristors reproduce functionally the activities of the synapses in neurons of the biological neural network because the memristors can continuously and reversibly change own resistance.

It allows to hope that artificial neural networks with nanoscale electronic "synapses" can be constructed on the base of the memristors.

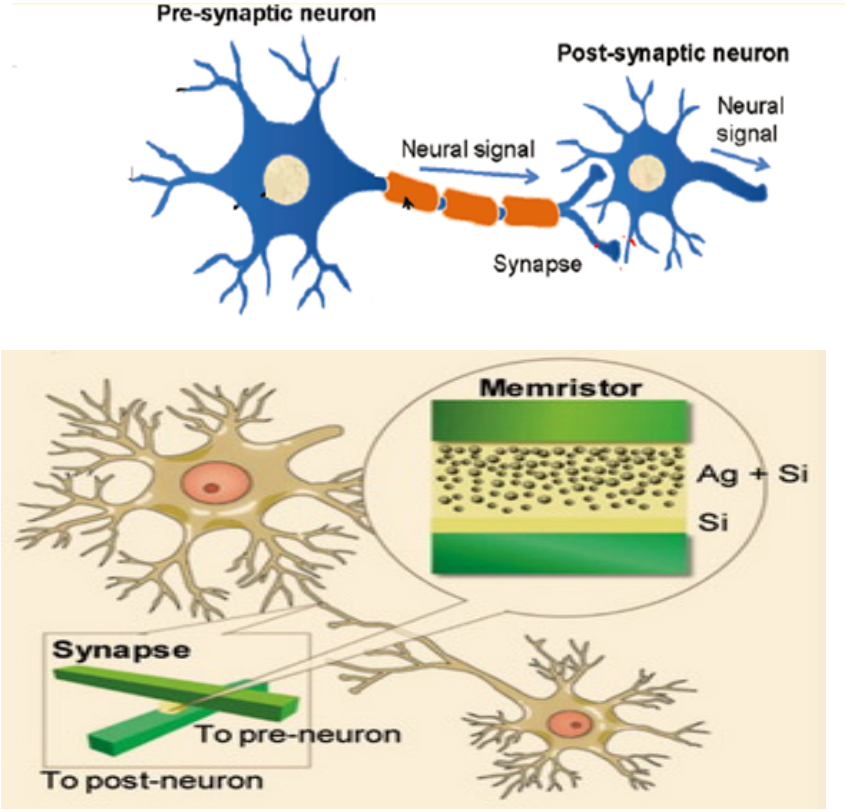

Fig. 1. Illustration of the electrical properties of the synapse

What's next? Is the development of the memristor-neural logic with new problems? ... To explore, innovate, work and analyze, explore again! As long last, the first 16-bit processor Intel86 is the forefather of the modern architecture x86. It had clock rate only 5 MHz, and was manufactured on the base of only 29 thousands of transistors. However, what was then?

It is important to note the following. For the development of the economic power of the country the substantial resources for the development of nanotechnology and nanoelectronics will be required, Fig. 2. However, we must not forget about well thought-out organization of personnel training, the organization of scientific research and implementation of results in manufacturing.

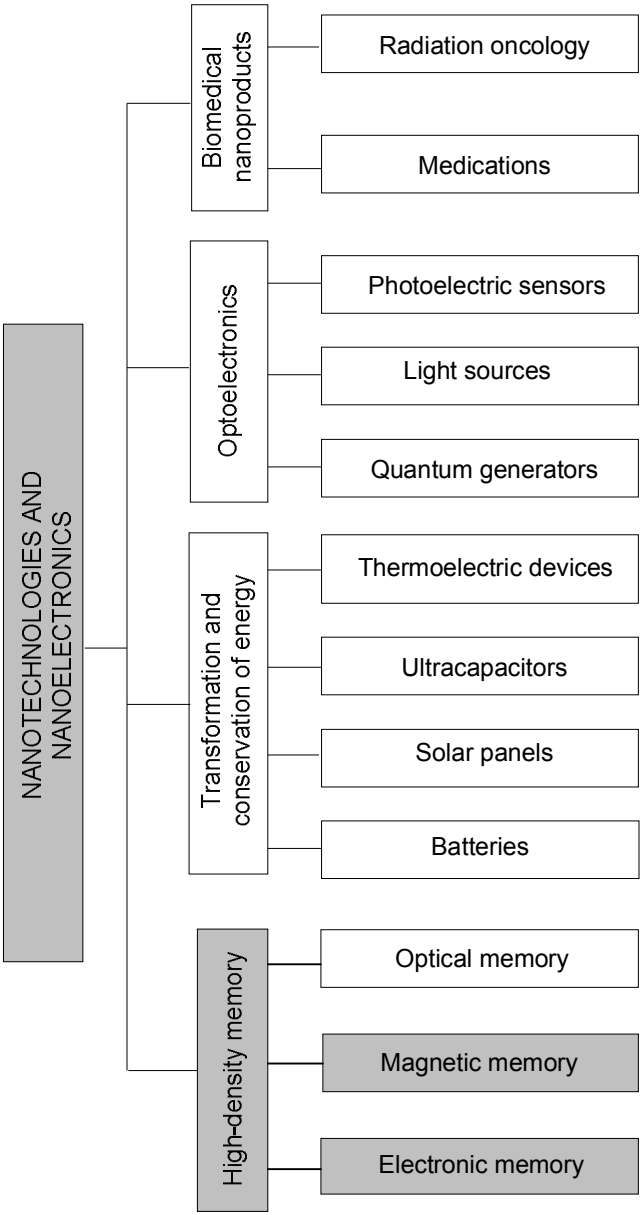

Fig. 2. Main of the nanotechnology application

PRINCIPLES AND METHODS OF PHYSICAL REALIZATION OF THE MEMRISTOR

- Basic characteristics of the fundamental elements
- Characteristics of memristor
- Principle of operation of the memristor
- General characteristic of the memristors

1.1 Basic characteristics of the fundamental elements

In 1971, American scientist L. Chua predicted the existence of a fourth fundamental element, taking into account the symmetry of the links between the well-known elements such as a resistor, capacitor and inductor. Obviously, there are six different mathematical relationships linking the pair of the four fundamental variables of electric circuits, namely the two local current i and charge q, as well as two differential: variables: the voltage u (or potential difference) and the magnetic flux Φ.

Of the possible $4^2 = 16$ combinations we must discard four trivial combinations $\left(\frac{di}{di}, \frac{du}{du} \ldots \right)$. The remaining 12 combinations need to be reduced by half, because they describe the same phenomenon $\left(\frac{du}{di} = R, \quad \frac{di}{du} = \frac{1}{R} \ldots \right)$. That leaves six combinations.

Any electrical circuit can be described by four physical quantities:

• the current strength i and the charge q at each point (node or section);

• the voltage u and magnetic flux Φ between two points (nodes or surfaces).

All these values are mutually related to each other, and these ratios are presented in the physical elements of any electrical or electronic circuit.

One of these relations determines the charge as the integral of the current:

$$q(t) = \int i(t)dt \quad \Rightarrow \quad dq = idt\,.$$

It shows the connection between two variables ($q \sim i$) above.

Another ratio determines the magnetic flux as the time integral of the electromotive force or the voltage. It follows from Faraday's law of induction:

$$\Phi(t) = \int u(t)dt \quad \Rightarrow \quad d\Phi = udt\,,$$

showing the relationship between the remaining two variables ($\Phi \sim u$).

Thus, there should be four fundamental elements of electrical circuits, which are described by the remaining four relationships between variables. Three ratios are known for a long time, namely:

• **resistor** (1827, Georg Ohm realizes the relationship of current i and voltage u in the form of $du = Rdi$ (R *is* resistance, measured in ohms):

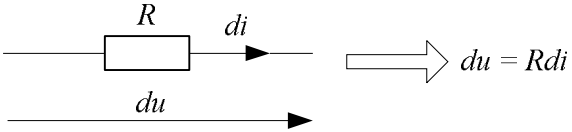

• **capacitor** (1745, Volta realizes the relationship between the voltage u and the charge q (C is capacitance, measured in farads):

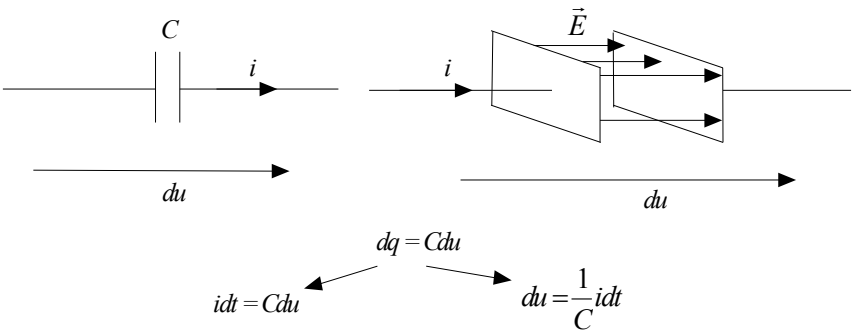

• **inductive coil** (1831, Faraday & Henry realize the relationship between the magnetic flux Φ and current strength i (L is coil inductance measured in henry):

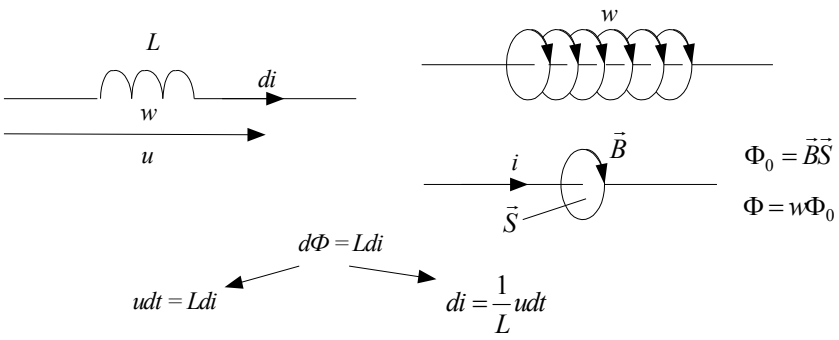

These three well-known passive elements are the basic (fundamental), as electrical circuit of any complexity can be reduced (in theory) to the equivalent circuit, built entirely of resistors, capacitors and inductors.

Three fundamental elements can be easily and reliably realized physically. The capacitor may be constructed from two parallel conducting plates. The inductance may be provided by a coil with a conductor wound on it, and the resistor may be formed of a material having a high resistivity (tungsten, constantan etc).

At the same time no one saw any of the material or a physical structure that would show the characteristics of the predicted element.

• **"missing" element** provides the rest of the functional relationship between charge q and magnetic flux Φ. This element was named the **memristor**, and today it is represented by passive element of the circuit, the resistance of which in some way dependent on the charge passing through it. If a memristor is disconnected from then its state does not change, that is a memristor "remembers" the last resistance value (memory resistor) with the respective symbol (parameter M is memristance, which is measured in Ω):

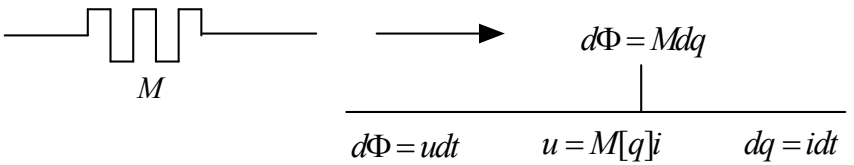

Generally memristance M should depend on the charge q. If a magnetic flux is represented by the time integral of the voltage then using the relations $d\Phi = udt$ and $dq = idt$ it is possible to write the relationship between current and voltage in the form:

$$udt = M(q)idt .$$

In the case $M = \text{const}$, that is a memristor is a linear element, the memristance M is identical to the resistance R and the ratio $udt = Midt$ is transformed into a well-known Ohm's law. If the parameter M is the function of the charge that is $M = M(q)$ then a memristor is nonlinear element with much more interesting properties.

Since memristance M depends on the charge, the element keeps the memory of past processes of the input current action. In fact, the definition of the memristor $M = \dfrac{d\Phi}{dq}$ is not common because the memristor can be defined as an element in which there is a nonlinear relationship between the integrals of current and voltage, as is pointed out in [72]. The last definition has the advantage that it does not introduce the concept of a magnetic flux, that is it does not require magnetism effects that essentially no role in the physical principles of operation memristor.

As it was nobed in [20] all devices, which are characterized by the presence of a double hysteresis loop (twisted loop) in the current-voltage characteristic passing through the origin, are the memristors, Fig. 1.1.

The current-voltage characteristic of such a non-linear element between charge q and magnetic flux Φ with applied sinusoidal voltage is frequency-dependent Lissajous figure (to be discussed below).

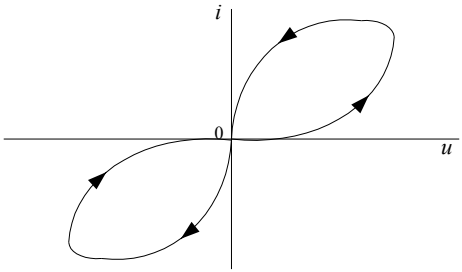

Fig.1.1. Current-voltage characteristic of a memristor

Any combinations of non-linear passive resistors, capacitors and inductors can not reproduce the electrical properties of a nonlinear memristor.

As we know, most useful functions of electrical circuits due to the nonlinear effects and respective devices. As will be shown, memristors compatible with integrated circuits can provide new functions, such as electronic switching of the resistance value (resistive switching).

As already noted, the current-voltage characteristic (CVC) of the memristor is a twisted hysteresis loop (pinched hysteresis loop), which means that the properties of the element depends on the applied effects. In this case, the resistance memristor (memristance M value) depends on the amount of charge that has passed through the element that is how long it flowed through the electric current.

Today, the definition of the memristor as a fundamental element of the following:

> **Memristor** is a passive element of nanoelectronics which can change its resistance depending on the charge flowing through it (the integral of current), described as a two-terminal network with nonlinear current-voltage characteristic having hysteresis.

It should be noted another definition, which appears in scientific papers:

> **Memristor** is passive element with two terminals, which behaves like a resistor if a small voltage is applied and a small current flows, and if a large voltage is applied so that relatively large current flows it reproducibly and reversibly switched to states with different electrical resistance, and stores any state sufficiently long period of time when the power source is disconnected.

Finally we may note that the following symmetrical relationships between the current and the voltage are possible, Table 1.1.

As seen from the table, the integral can be used in four different ways to write the relation between current and voltage: the integral is used or not. Note that the equations for the resistance and memristance

are identical, except that in the last case the integral sign is used on both sides of the ratio. However, these integrals can not be reduced, as a constant of integration can not be zero, [19], [37]. This constant "forces" memristor "to remember" previous state.

Table 1.1

Symmetric relationships between current $i(t)$ and voltage $u(t)$

Name of element	Law	Constant value k	Name of constant
Resistor	$u(t) = ki(t)$	$k = R$	resistance
Capacitor	$\int i(t)dt = ku(t)$	$k = C$	capacity
Inductor	$\int u(t)dt = ki(t)$	$k = L$	inductance
Memristor	$\int u(t)dt = k\int i(t)dt$	$k = M$	memristance

Figure 1.2 shows a variant of the symmetry between the four physical quantities.

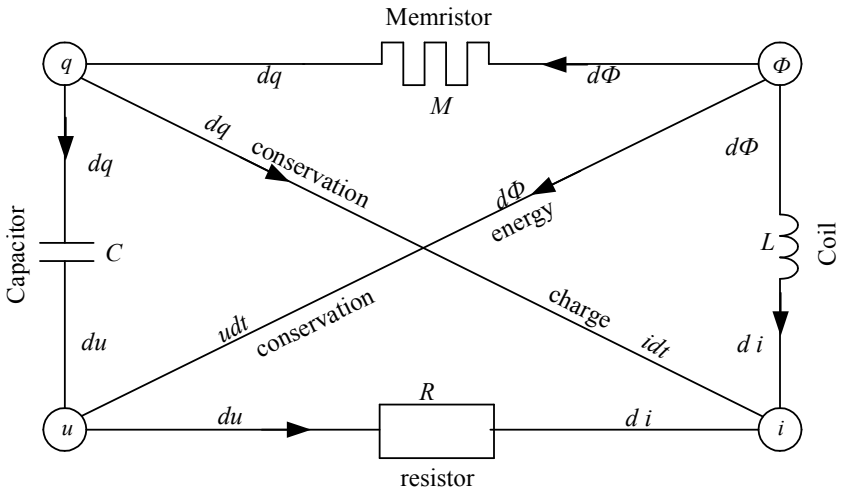

Fig. 1.2. Interconnection between the fundamental variables of electric circuits

Another variant of symmetry, published in some publications is shown in Fig. 1.3.

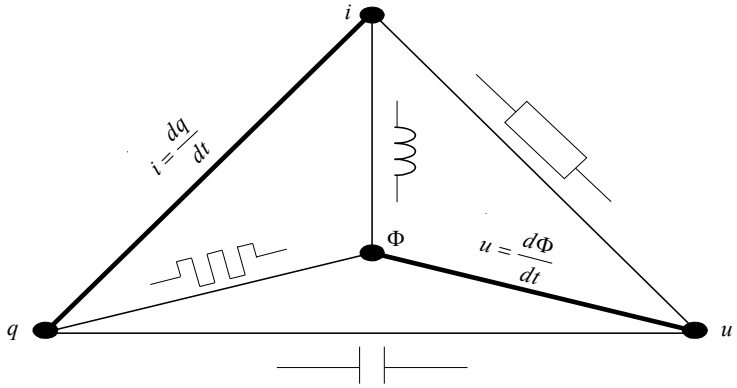

Fig. 1.3. Interconnection between the current, voltage, charge and magnetic flux

This symmetry associatively reminds theory of matter according to Aristotle: all matter is composed of the following four elements: earth, water, air and fire. Each of these elements is represented by two of the four properties: moisture, dryness, coldness and hotness, Fig. 1.4.

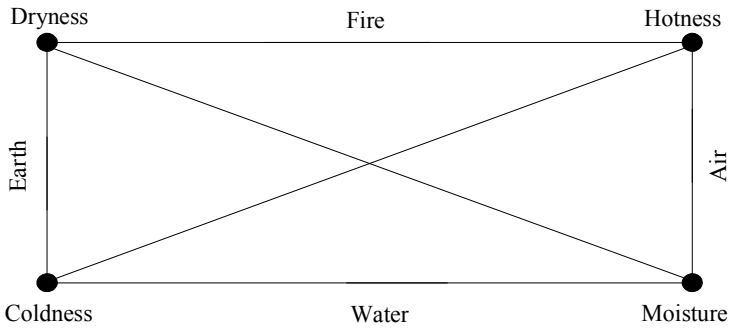

Fig. 1.4. Symmetrical conception of matter according to Aristotle

In conclusion, the development of new nanotechnologies has led to a wide practical application of memristors. Today, such researches are carried out throughout the world, including in Ukraine, and they are directed to creation of new elements of nonvolatile computer memory,

because the memristor demonstrates at least two significant differences from the traditional memory devices.

Firstly, a memristor is a two-terminal element, and therefore it may be easy integrated into the so-called multi-layer matrixes (Fig. 1.5) of mutually perpendicular metal conductors having nanosizes (crossbar).

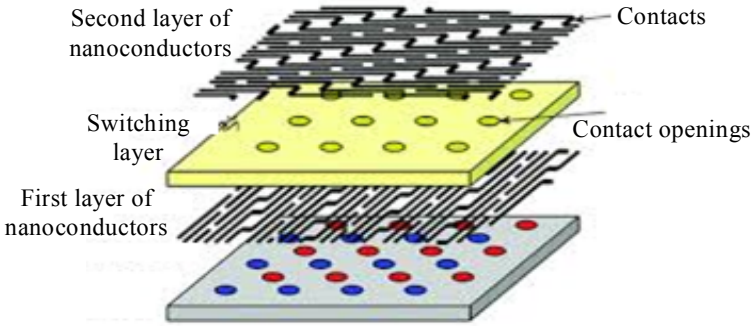

Fig. 1.5. Realization of multi-layer matrixes

Example implementation monolayer structure is shown in Fig. 1.6. This architecture is much more compact and does not require the transistors to access to memory cell that are used in modern architecture flash memory. Besides such logic of the control by the matrix is much simpler. It allows to significantly reduce the geometric dimensions of the respective devices, to increase the memory capacity and reduce expenses of energy. It can be expected that the memristor memory can be the only type of computer memory.

Secondly, the phenomenon of resistive switching (transition from a less to a greater conductive state memristor, the transition could not only be binary, but continuous) can be used to create devices, the architecture of which would be fundamentally different from the von Neumann architecture, at which all available electronics is built.

From the perspective of digital electronics can be said that memristor transitions from a state "0" to a state "1" and vice versa when the respective voltage polarity is applied and the memristor closes or opens the circuit passing through it.

Such state memristor "remembers" and can store long without limit, and it does not need a voltage source. Progress to date while switching memristor from one state to another is less than 1 μs. These properties

allow to apply memristor in several ways: the switch of the memory element and component of the logic element.

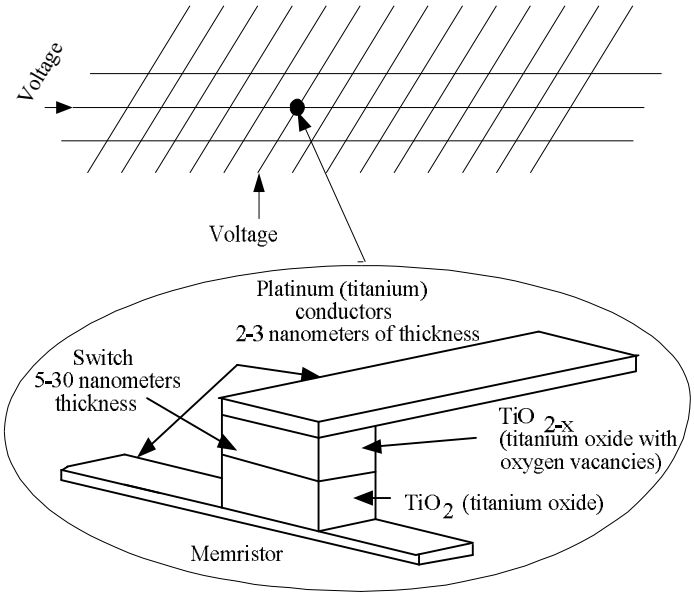

Fig. 1.6. Monolayer matrix of memristors

In particular, it has been demonstrated experimentally how to carry out the implication operation using two memristor and other logical operations [41] – [43]. Therefore, on the base of crossbars with memristors can construct a complete CPU. Each memristor can be used as an element of a logic gate, and a memory cell. Dynamic reconfiguration of memristors between memory and logic operations will allow to carry out calculations in the same chip, which stores the data. In this case the special processing unit may be excepted.

1.2 Characteristics of a memristor

Memristor is an element which is controlled by a charge if the relationship between the magnetic flux and the charge is expressed as a function of the electric charge $\Phi(q)$. Accordingly, the memristor is controlled by a magnetic flux, if the relationship is expressed as $q(\Phi)$.

It should be noted that the respective dependences are piecewise continuous differentiable functions.

Differentiating functional dependence $\Phi(q)$ on time gives the following relationship:

$$u(t) = \frac{d\Phi}{dt} = \frac{d\left[\Phi(q)\right]}{dq}\frac{dq}{dt} = M[q]i(t),$$

where

$$M[q] = \frac{d\Phi(q)}{dq}$$

is the memristance of the two-terminal network.

Similar arguments can be made for the relationship $q(\Phi)$:

$$i(t) = \frac{dq}{dt} = \frac{d\left[q(\Phi)\right]}{d\Phi}\frac{d\Phi}{dt} = W[\Phi]u(t),$$

where

$$W[\Phi] = \frac{dq(\Phi)}{d\Phi}$$

defines memconductance (memory conductance) of two-terminal network, which is measured in Simmons.

> Very often various publications (for example [22]) use the terms interchangeably, "memristance" $M(q)$ and the term "resistance" of the memristor $R(q)$ which has the same physical meaning. The same terminology applies for reverse dependencies "memconductance" $W(\Phi)$ and "conductance" of memristor $G(\Phi)$.

Values $M(q)$ and $W(\Phi)$ in any given time depend on the history of current flow through the element and the voltage across its terminals from moment $t = -\infty$ to moment $t = t_0$.

Obviously, the charge-controlled memristor is described by the functional dependency $u = M(q)i$, which is equivalent to Ohm's law, which depends on the amount of charge. The value $M(q)$ determines the slope

characteristic $\Phi(q)$ similar to the characteristics of other fundamental elements, Fig. 1.7.

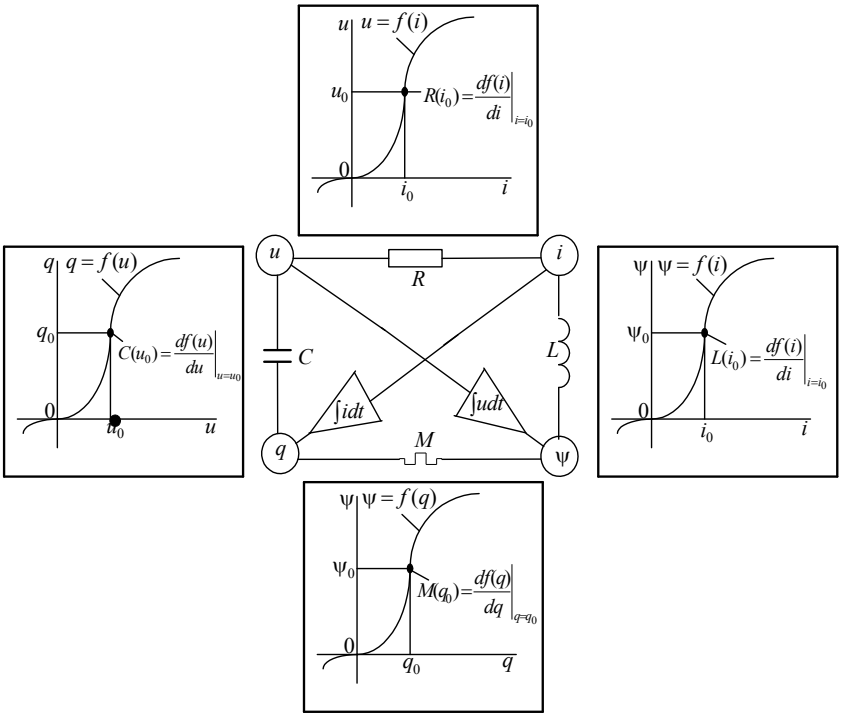

Fig. 1.7. Slope characteristics of fundamental elements

Dependencies $\Phi(q)$ and $u = M(q)i$ are equivalent, as is easily seen, if we integrate both sides of the expression $u = M(q)i$ with respect to time:

$$\int_{-\infty}^{t} u(\tau)d\tau = \int_{-\infty}^{t} M[q(\tau)]i(\tau)d\tau = \int_{-\infty}^{t} M[q(\tau)]\frac{dq(\tau)}{d\tau}d\tau$$

$$= \int_{q(-\infty)}^{q(t)} M[q(\tau)]dq(\tau) = \int_{q(-\infty)}^{q(t)} M(q)dq,$$

which implies that

$$\Phi(q) = \int_{q(-\infty)}^{q(t)} M(q)dq .$$

By analogy we may consider the dependency $i = W(\Phi)u$ where

$$q(\Phi) = \int_{\Phi(-\infty)}^{\Phi(t)} W(\Phi)d\Phi .$$

Example 1. Let's consider the memristor controlled by charge (Fig. 1.8, *a*), for which the relationship $\Phi(q)$ is defined analytically in the form of incomplete cubic polynomial, Fig. 1.8, *b*:

$$\Phi = a_1 q + a_3 q^3 = q + \frac{1}{3} q^3 .$$

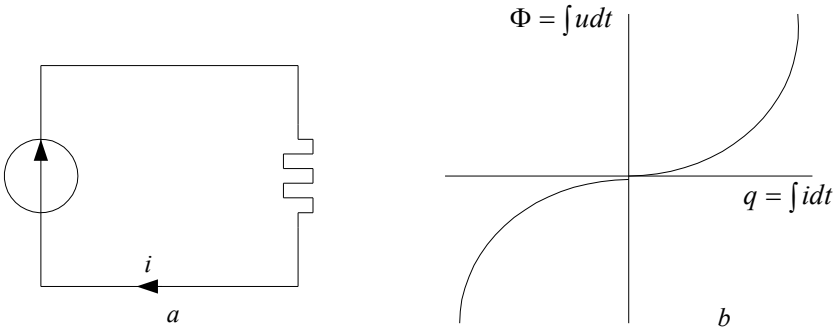

Fig. 1.8. Weber-Coulomb characteristic of the memristor

The source of current of the sinusoidal form is connected to the memristor so that the current in the circuit is given by expression:

$$i(t) = \begin{cases} I_m \sin \omega t, & t \geq 0 \\ 0, & t < 0. \end{cases}$$

The charge $q(t)$ is then determined in accordance with the general expression as an integral of current (assuming that the initial charge value $q_0 = q(0) = 0$):

$$q(t)=\int_0^t I_m \sin\omega\tau d\tau=-\frac{I_m}{\omega}\cos\omega\tau\Big|_0^t=\frac{I_m}{\omega}(1-\cos\omega t),\quad t\ge 0.$$

Substituting the expression for $q(t)$ into analytic expression that determines the flow, we get:

$$\Phi(t)=\frac{I_m}{\omega}(1-\cos\omega t)+\frac{1}{3}\frac{I_m^3}{\omega^3}(1-\cos\omega t)^3$$

$$=\frac{I_m}{\omega}(1-\cos\omega t)+\frac{1}{3}\frac{I_m^3}{\omega^3}(1-\cos\omega t)(1-\cos\omega t)^2$$

$$=\frac{I_m}{\omega}(1-\cos\omega t)\left[1+\frac{1}{3}\frac{I_m^2}{\omega^2}(1-\cos\omega t)^2\right].$$

Differentiating with respect to time this result, we obtain a general expression for the voltage across the memristor (Fig. 1.9):

$$u(t)=\frac{d\Phi(t)}{dt}=\left|(uv)'=u'v+v'u\right|=\frac{I_m}{\omega}\omega\sin\omega t\left[1+\frac{1}{3}\frac{I_m^2}{\omega^2}(1-\cos\omega t)^2\right]$$

$$+\frac{I_m}{\omega}(1-\cos\omega t)\frac{2}{3}\frac{I_m^2}{\omega^2}(1-\cos\omega t)\omega\sin\omega t$$

$$=I_m\left[1+\frac{I_m^2}{\omega^2}(1-\cos\omega t)^2\right]\sin\omega t.$$

$$\omega:=1\qquad I_m:=1\qquad t:=0,0.1,...,15$$

$$i(t):=I_m\sin(\omega t)\quad q(t):=\frac{I_m}{\omega}\left(1-\cos(\omega t)\right)\quad M(t):=1+\frac{I_m{}^2}{\omega^2}\left(1-\cos(\omega t)\right)^2$$

$$u(t):=\left[1+\frac{I_m{}^2}{\omega^2}\left(1-\cos(\omega t)\right)^2\right]\cdot I_m\sin(\omega t)$$

$$\Phi(t):=\frac{I_m}{\omega}\left(1-\cos(\omega t)\right)\cdot\left[1+\frac{1}{3}\frac{I_m{}^2}{\omega^2}\left(1-\cos(\omega t)\right)^2\right]$$

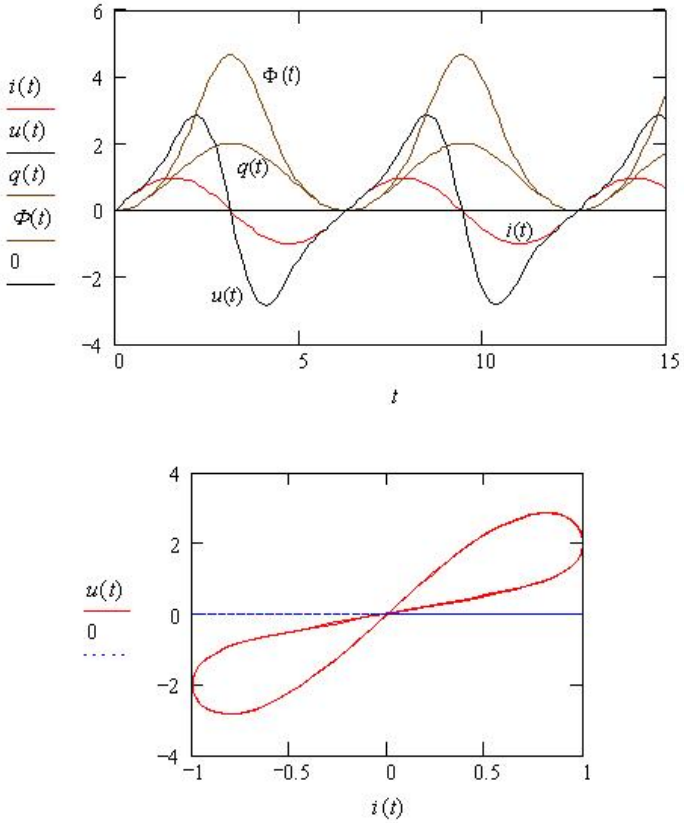

Fig. 1.9. Characteristics of the memristor controlled by charge

Graph of the dependency $\{i(t), u(t)\}$ (that is the volt-ampere characteristic of the memristor in accordance with a given expression for the current $i(t)$ and the voltage $u(t)$ obtained by the expression) is shown in Fig. 1.9 (for conditionally accepted values $I_m = 1,\ \omega = 1$).

The form of graphic, as noted above, is pinched at the origin of the hysteresis loop.

The hysteresis is explained by the fact that the maximum and minimum values of the input current and the voltage across the memristor achieved at different times, that is if $i(t_1) = i_{\max}$ then $u(t_1 + \neq u_{\max}$ and $u(t_2) = u_{\max}$ but then $t_2 \neq t_1$ as it is seen in Fig. 1.9.

Thus, the dependence $\{i(t),u(t)\}$ on the $i-u$ plane for any passive memristor with positive memristance

$$M(q)=\frac{d\Phi(q)}{dq}>0$$

always represents a hysteresis loop pinched in origin.

The area of this loop is narrowed if the frequency increases and approaches to the linear dependence with resistance $R=M(0)$ equaled to the value $\mathrm{tg}\alpha$, where $\alpha-$ the angle of inclination of the tangent to the curve $\Phi(q)$ at $q=0$.

In addition, the curve $\{i(t),u(t)\}$ can not cross the axis $i(t)$, as the memristor is a passive element, for which $M(q)>0$. This means that the hysteresis loop should be limited to the first and third quadrants.

Let's find the value of memristance $M(q)$ according to the definition:

$$M(q)=\frac{d\Phi(q)}{dq}=\left(q+\frac{1}{3}q^3\right)'=1+q^2.$$

Substitution of the obtained previously expression for $q(t)$ gives:

$$M[q(t)]=1+\left[\frac{I_m}{\omega}(1-\cos\omega t)\right]^2,\ t\geq 0$$

which implies that $M(q)>0$.

Substituting $M(q)$ and $i(t)$ in the general expression for the memristor, we determine the voltage across the memristor:

$$u(t)=M(q)i(t)=I_m\left[1+\frac{I_m^2}{\omega^2}(1-\cos\omega t)^2\right]\sin\omega t,$$

which coincides with the expression obtained previously.

Since $M(q)$ is a finite value for all finite values of charge q, then $u(t)=0$ if and only if $i(t)=0$ for any input action $i(t)$. Similarly, for all Φ-controlled memristor, for which memconductance is a finite quantity

for all finite values Φ, $i(t)=0$ if and only if $u(t)=0$ for any input action $u(t)$.

A graph of the dependency $\{M(t), i(t)\}$ is a hysteresis loop, but not pinched at the origin, since $M(t)>0$ for any instant of the time, Fig. 1.10.

$$\omega := 1 \qquad I_m := 1 \qquad t := 0, 0.1, ..., 15$$

$$i(t) := I_m \sin(\omega t) \quad q(t) := \frac{I_m}{\omega}\left(1-\cos(\omega t)\right) \quad M(t) := 1 + \frac{I_m^{\,2}}{\omega^2}\left(1-\cos(\omega t)\right)^2$$

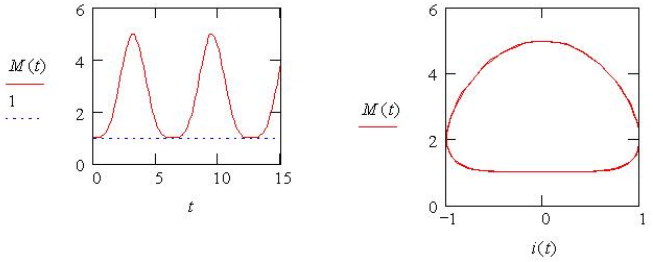

$$q(t) := -2, -1.9...2 \quad M(q) := 1 + q^2 \quad \Phi(q) := q\frac{1}{3} + q^3$$

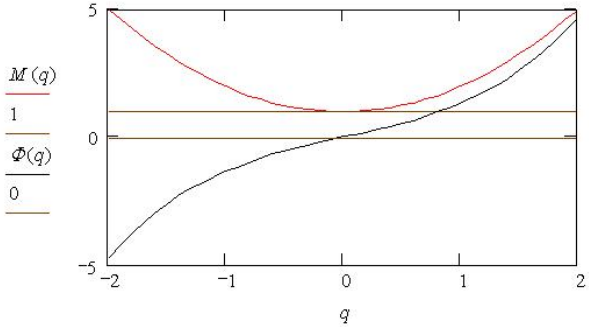

Fig. 1.10. Graphs of dependencies $M(t), M(q)$ and $\Phi(q)$

It should be noted that from the obtained graphs it follows that when $i(t)$ and $u(t)$ simultaneously take both positive and negative values, $\Phi(t)$ and $q(t)$ are nonnegative. We note also that the hysteresis loop $\{i(t), u(t)\}$ is odd with respect to the origin.

Also note that all the considered above forms of signals and the hysteresis loops are demonstrations of the memristor only and can not be used to predict its response $u(t)$ at any other form of input action, which is different from $i(t) = I_m \sin \omega t$ (or response $i(t)$ when the form of action is $u(t) = U_m \sin \omega t$).

This is easily seen that in the case if the amplitude I_m (or U_m), frequency ω or the shape of the action change then completely different responses are obtained.

For example, for the considered above example the results are shown in Fig. 1.11 for case when the amplitude of the current changes up to $I_m = 5$ A .

A simple comparison of the results in Figs 1.9 and 1.11 shows the correctness of these arguments (for comparison of graphs the scales for the current and the charge are changed).

From the equations obtained above:

$$q(t) = \frac{I_m}{\omega}(1 - \cos \omega t),$$

$$u(t) = I_m \left[1 + \frac{I_m^2}{\omega^2}(1 - \cos \omega t)^2 \right] \sin \omega t,$$

$$\Phi(t) = \frac{I_m}{\omega}(1 - \cos \omega t) \left[1 + \frac{1}{3} \frac{I_m^2}{\omega^2}(1 - \cos \omega t)^2 \right],$$

$$M(q) = 1 + \left[\frac{I_m}{\omega}(1 - \cos \omega t) \right]^2$$

it follows that, for example, at a constant amplitude I_m the value of charge $q(t) \to 0$, the voltage $u(t)$ tends to a sinusoidal form, and the value $M(q)$ tends to 1 ohm if the frequency ω increases (up to $\omega \to \infty$).

The hysteresis curve $\{i(t), u(t)\}$ narrows with increasing frequency, and is transformed into a straight line passing through the origin with some slope. Fig. 1.12 shows the change of the current-voltage characteristics of a memristor at change of frequency: $\omega =$ 0,5 Hz, 0,75 Hz and 5 Hz respectively.

$$\omega := 1 \qquad I_m := 5$$

$$t := 0, 0.1, ..., 15$$

$$i(t) := I_m \sin(\omega t)$$

$$q(t) := \frac{I_m}{\omega}\left(1 - \cos(\omega t)\right)$$

$$M(t) := 1 + \frac{I_m^{\,2}}{\omega^2}\left(1 - \cos(\omega t)\right)^2$$

$$u(t) := \left[1 + \frac{I_m^{\,2}}{\omega^2}\left(1 - \cos(\omega t)\right)^2\right] \cdot I_m \sin(\omega t)$$

$$\Phi(t) := \frac{I_m}{\omega}\left(1 - \cos(\omega t)\right) \cdot \left[1 + \frac{1}{3}\frac{I_m^{\,2}}{\omega^2}\left(1 - \cos(\omega t)\right)^2\right]$$

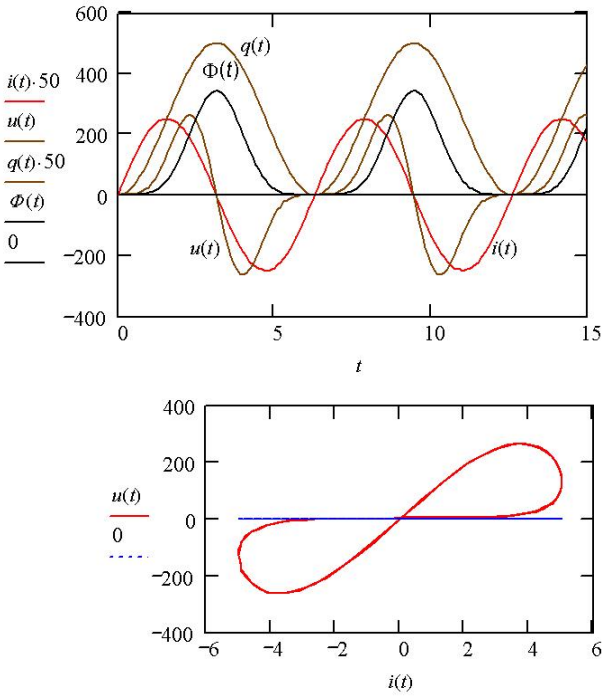

Fig. 1.11. The response of the memristor on the amplitude of action equaled $I_m = 5$ A

$$\omega := 0.5 \qquad I_m := 1 \qquad t := 0, 0.001, ..., 15$$

$$i(t) := I_m \sin(\omega t) \quad u(t) := \left[1 + \frac{I_m^{\,2}}{\omega^2}\left(1 - \cos(\omega t)\right)^2\right] \cdot I_m \sin(\omega t)$$

$$\omega_1 := 0.75 \;\; i_1(t) := I_m \sin(\omega_1 t) \;\; u_1(t) := \left[1 + \frac{I_m^{\,2}}{\omega_1^{\,2}}\left(1 - \cos(\omega_1 t)\right)^2\right] \cdot I_m \sin(\omega_1 t)$$

$$\omega_2 := 5 \;\; i_2(t) := I_m \sin(\omega_2 t) \;\; u_2(t) := \left[1 + \frac{I_m^{\,2}}{\omega_2^{\,2}}\left(1 - \cos(\omega_2 t)\right)^2\right] \cdot I_m \sin(\omega_2 t)$$

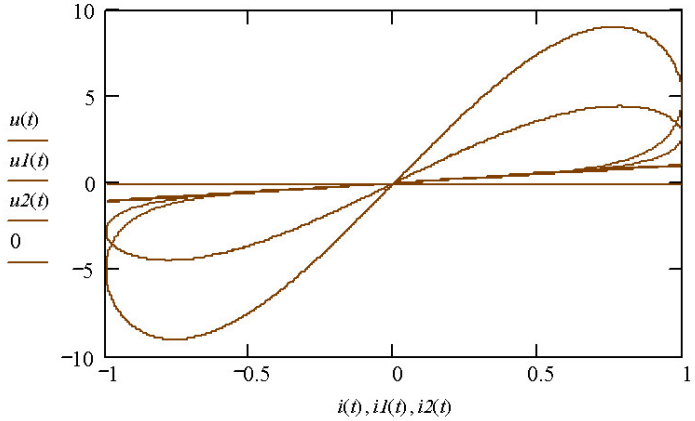

Fig. 1.12. Change CVC of the memristor with increasing frequency of the acting signal

The charge q and the flux Φ decreasing in value tend to the origin and remain at rest state. Under these limit conditions, the memristor is a linear resistor, its value is determined by the slope of the straight at the origin and in the given case is equal to 1 Ω.

There are a few special cases when the hysteresis loop $\{i(t), u(t)\}$ degenerates into a single-valued function. Consider a few examples.

Example 2. Suppose that the current $i(t) = \cos t \quad (t \geq 0)$ flows through the memristor. Then the charge $q(t)$ is determined by the expression $q(t) = \sin t$.

The dependence $\Phi(q)$ remains the same as in Example 1:

$$\Phi(q) = q + \frac{1}{3}q^3 = \sin t + \frac{1}{3}\sin^3 t\,.$$

Then the voltage across the memristor is:

$$u(t) = \frac{d\Phi}{dt} = \cos t + \sin^2 t \cos t = \cos t(1 + \sin^2 t).$$

In this case, the hysteresis loop represents a single-valued function, passing through zero, that is and in this case it is pinched at the origin. The corresponding dependences are shown in Fig. 1.13.

$$t := 0, 0.1, ..., 15 \quad i(t) := \cos(t) \quad q(t) := \sin(t) \quad M(t) := 1 + \left(1 - \cos(t)\right)^2$$

$$u(t) := \left[1 + \left(1 - \sin(t)\right)^2\right] \cdot \cos(t) \qquad \Phi(t) := \sin(t) + \frac{1}{3}\sin(t)^3.$$

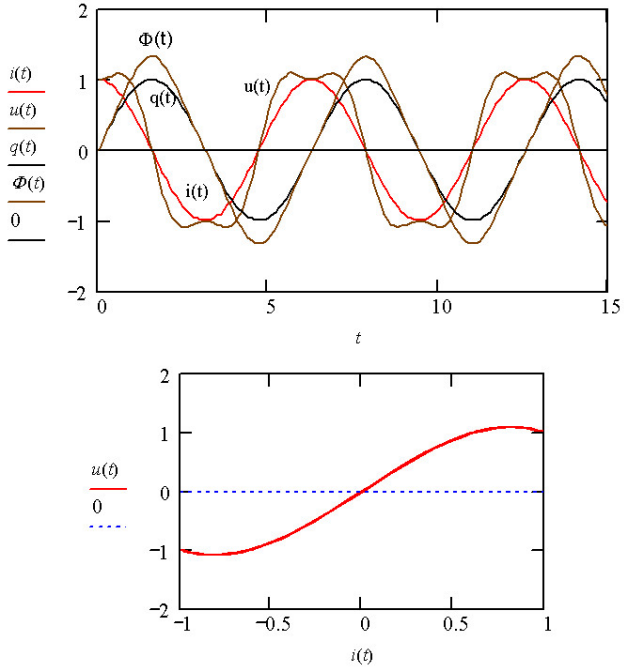

Fig. 1.13. Hysteresis loop degenerates into single-valued function

$$\text{for } \Phi(q) = q + \frac{1}{3}q^3$$

Example 3. Another case can occur when

$$M(q^*) = \left.\frac{d\Phi(q)}{dq}\right|_{q=q^*} = 0$$

at a certain point of the curve $\Phi(q)$. For example, for $\Phi(q) = \frac{1}{3}q^3$.

Then it is obvious that $M(q^*) = 0$ at $q^* = 0$, Fig. 1.14.

$$i(t) := \cos(t) \quad q(t) := \sin(t) \quad M(q) := q^2 \quad t := 0, 0.1, ..., 15$$

$$u(t) := (\sin(t))^2 \cdot \cos(t) \quad \Phi(t) := \frac{1}{3}\sin(t)^3$$

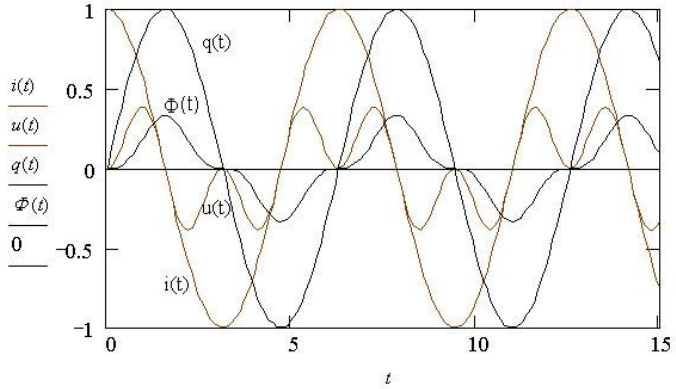

$$q(t) := 2, -1.9, ..., 2 \qquad \Phi(q) := \frac{1}{3}q^3$$

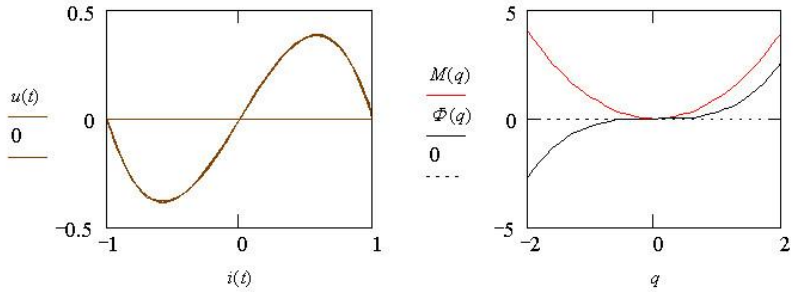

Fig. 1.14. Hysteresis loop degenerates into single-valued function

Assuming that the action is $i(t)=\cos t$, let's define $q(t), u(t)$ and $\Phi(t)$:

$$q(t)=\int i(t)dt=\sin t,$$

$$u(t)=\frac{d\Phi}{dt}=\left[\frac{1}{3}\sin^3 t\right]'=\sin^2 t\cos t,\quad \Phi(t)=\frac{1}{3}\sin^3 t.$$

Graphs of the corresponding dependences are shown in Fig. 1.14. As can be seen from the graph the dependence $\{i(t),u(t)\}$ includes the points of the axis $i(t)$. In this case the curve as before passes through the origin and is tangent to certain points of the axis $i(t)$.

In conclusion, we note the following. In general, the possible characteristics of the respective four fundamental elements may have the form shown in Fig. 1.15: current-voltage (*a*), Weber-voltage (*b*), coulomb-voltage (*c*) and coulomb-Weber (*d*) characteristics.

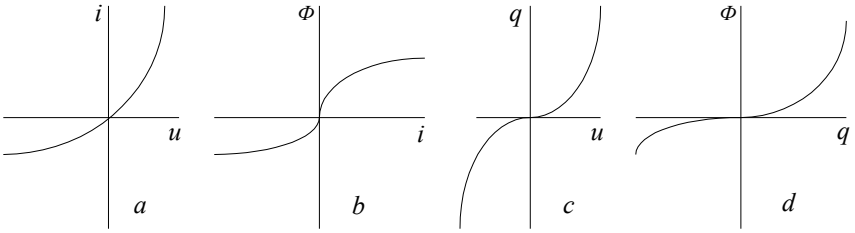

Fig. 1.15. Characteristics of the four fundamental elements

As for the dependency $\Phi(q)$, describing the behavior of the memristor, it is monotonically increasing. Memristance is determined by the slope ratio of the curve at any point (see Fig. 1.6), like the dynamic resistance of the nonlinear resistor.

Obviously, memristor is a passive element, if and only if a memristance $M(q)$ is nonnegative [19]. If $M(q)\geq 0$ then the instantaneous power dissipated by the memristor is defined as

$$p(t)=M(q)[i(t)]^2$$

and is always positive, that is a memristor is really a passive element like a resistor. This means that the curve $\Phi(q)$ is a monotonically increasing function.

An important feature of the memristor is the existence of the pinched hysteresis loop representing its current-voltage characteristic. For comparison, the current-voltage characteristics for the instantaneous values of the fundamental elements are shown in Fig. 1.16.

If any device has a hysteresis VAC, then such device is either memristor or memristor system [20], [22].

$$\omega := 1 \quad iR(t) := 1 \cdot \sin(\omega \cdot t) \quad t := 0, 0.01, ..., 10 \quad iL(t) := 1 \cdot \sin\left(\omega \cdot t - \frac{\pi}{2}\right)$$

$$uR(t) := 1 \cdot \sin(\omega \cdot t) \qquad uL(t) := 1 \cdot \sin(\omega \cdot t)$$

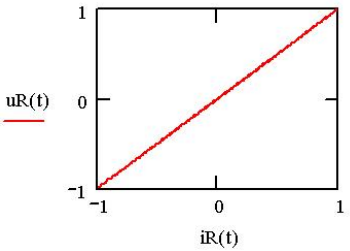

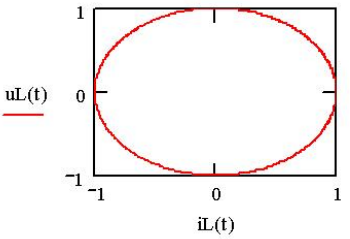

$$t := 0, 0.01, ..., 15 \qquad iC(t) := 1 \cdot \sin\left(\omega \cdot t + \frac{\pi}{2}\right) \qquad iM(t) := 1 \cdot \sin(\omega \cdot t)$$

$$uC(t) := 1 \cdot \sin(\omega \cdot t) \quad uM(t) := \left[1 + \frac{1}{\omega^2} \cdot (1 - \cos(\omega \cdot t))^2\right] \cdot \sin(\omega \cdot t)$$

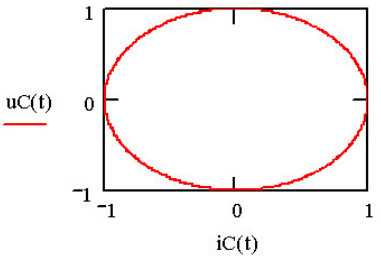

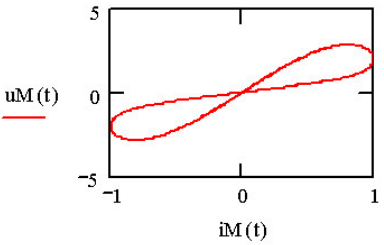

Fig. 1.16. Current-voltage characteristics of the fundamental elements

Another important feature memristor, as already was noted, is that the hysteresis curve is narrowed with increasing the frequency of the applied action (see Fig. 1.12).

Note also that to understand the properties of the memristor there are several physical analogies. One of them is given in [35], [2]. Memristor is represented as a pipe through which water flows. The pressure at the its input is similar to the voltage applied to the memristor, and the water is an analogue of an electrical charge. The rate of water flow through the pipe is an analog of the electric current.

If the pipe diameter increases, the flow of water through it accelerates similar increase of the current through the resistor with a small resistance value. Thus, the analogue of the memristor is a pipe whose diameter is increased or decreased depending on the water flow direction. Pipe diameter increases when the water flows in one direction, whereby the flow rate increases, and, accordingly, the pipe diameter decreases, when the water flows in the opposite direction, whereby its flow rate decreases, Fig. 1.17.

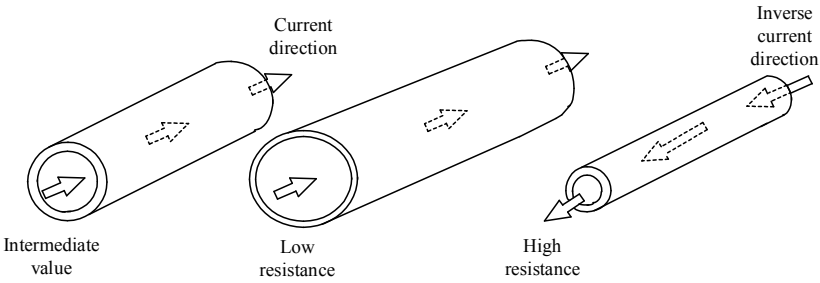

Fig. 1.17. Physical analogy of the memristor

If the water is not flowing, the pipe diameter retains the last value and will store as long as the water flow again resumes. Thus, the pipe "remembers" the amount of water that flowed through it before disconnecting.

1.3 The operating principle of the memristor

The first examples of a memristors was obtained in 2008 by HP's laboratory (Hewlett Packard), whose photograph obtained by using an atomic force microscope, was published in many scientific periodical journals, Fig. 1.18.

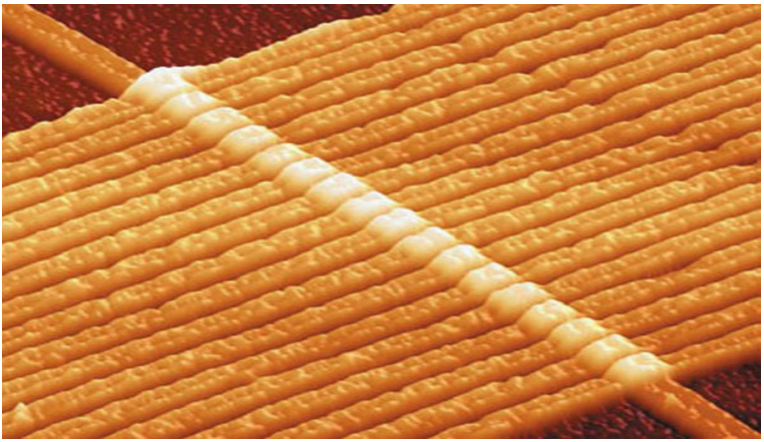

Fig. 1.18. Crossbar including 17 memristors

The memristors were distributed between the lower and upper conductors of the so-called crossbar which consists of one common platinum nanowire of 50 nm wide and superimposed perpendicular to it 17 other such nanowires.

The photomicrograph shows 17 memristors.

A simple physical model of the memristor is shown in Fig. 1.19. It contains a double layer of a thin titanium dioxide (TiO_2) of 5–20 nm thick film and thin film of oxygen-depleted titanium oxide (TiO_{2-x}), which form the so-called memristor active region [56], [57].

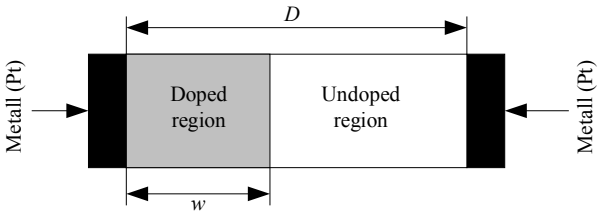

Fig. 1.19. A simple physical model of the memristor

Thus, the active region contains a material TiO_2 which is a semiconductor of high specific resistance (essentially it is an insulator), and

the doped material TiO_{2-x}, in which the ratio between the atoms of titanium and oxygen such that there oxygen atoms are less, so that the two layers have different specific conductivity.

Semiconductors are known are doped (impurity is introduced) to make them either *p*-type or *n*-type. For example, if the silicon is doped by impurity of the arsenide, it becomes the *n*-type semiconductor. Pure titanium dioxide TiO_2, which also is a semiconductor, has a high resistance (as in the case of the silicon), and may be doped to make it conductive.

If the oxygen atom which is negatively charged is moved from its place in TiO_2, it creates positively charged oxygen vacancy (hole). These oxygen vacancies can be moved to the current direction by the applied electric field. The idea of such movement allows to create the memristor as a two-layer structure consisting of two thin conductive and non-conductive layers of 5–20 nm thick. This active region is sandwiched between two metal electrodes (see Fig. 1.19).

Let's designate the thickness of the doped region through *w*, the thickness of entire active region as D, so that the thickness of the undoped region is $D - w$.

The functioning of the memristor is based on the difference of the conductivities of these very similar materials. Material TiO_2 of the stoichiometric composition is known as the "rutile" which is represented by the tetragonal crystal structure and is an insulator.

The **stoichiometry** is a system of laws, rules and terms, justifying the calculations of the composition of substances and the quantitative relationships between the masses of substances in chemical reactions. In stoichiometric compounds chemical elements present in well-defined ratios (composition of the constant stoichiometric compound). Examples of stoichiometric co mpositions may be water H_20, titanium dioxide TiO_2(titanium (IV)), as well as many inorganic compositions.

Substances for which there are deviations from the law of the stoichiometry is called non-stoichiometric. Generally, titanium

dioxide is an insulator. However, its electrical properties can be controlled by means of so-called oxygen vacancies. To increase the electrical conductivity, it is necessary to increase the number of oxygen vacancies and to obtain a non-stoichiometric titanium dioxide TiO_{2-x}, for which there are various ways. The obtained titanium dioxide has an alternating structure in which one titanium atom may contain from 0.65 to 1.25 oxygen atoms.

If the initial materials come into chemical reaction in strictly defined proportions, and a result of the reaction are products, the number of which may be exactly calculated, such reactions are called stoichiometric, and describing their equations are stoichiometric equations.

Thus, the material TiO_{2-x} is TiO_2, in which from the crystal oxygen is partly removed, so that it has a slightly lower concentration of oxygen atoms (less than two oxygen atoms per one titanium atom). Very often, it takes $x = 1.3$.

The process of obtaining the material TiO_{2-x} is heating to very high temperatures (from 600 K to 900 K) with following cooling. The resistance of the obtained material decreases as a result of removal of the oxygen atoms.

Let's conditionally assume that the memristor has the cubic structure, Fig. 1.20, *a*.

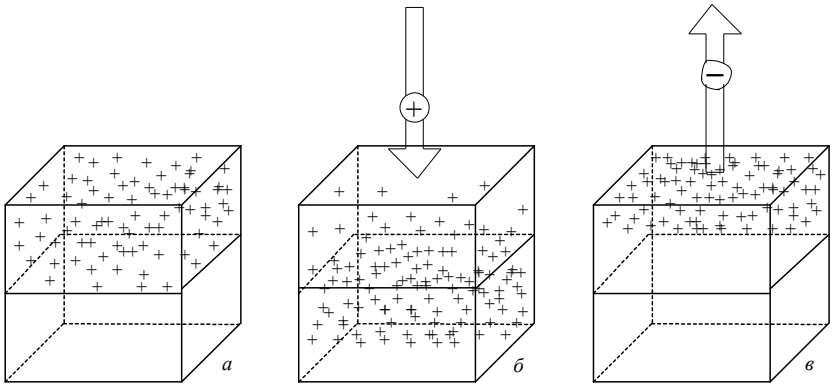

Fig. 1.20. The distribution of oxygen vacancies, depending the polarity of the applied voltage

The lower layer is a high-purity titanium dioxide having the high resistance value, the upper layer is a depleted by oxygen titanium dioxide TiO_{2-x} in which there are positive oxygen vacancies ("holes" which are formed after the removal of oxygen atoms).

The application of positive potential to the upper platinum electrode (Fig. 1.20, *b*) leads to the fact that the positively charged "holes" are repelled and migrate to the lower layer in the direction of undoped region TiO_2. Such a change of the internal structure of the film corresponds to the flow of current through the semiconductor. As a result a virtual boundary between the regions (see Fig. 1.19) is also shifted down and increases the thickness of the layer TiO_{2-x}, which in turn increases the conductivity of all memristor as a whole.

If the polarity of the applied voltage is changed (Fig. 1.20, *c*), the oxygen vacancies are attracted, so that some of them leave from the layer TiO_2. As a result a virtual boundary between the layers moves up and its thickness increasing. It means that the resistivity of the memristor increases as a whole.

Experiments show that if the virtual boundary change only on 0.3 nm then the resistance value change in 1000 times.

It should be noted that when a negative polarity of the voltage is applied to the memristor (the "holes" are shifted back to the upper layer), the “holes” are not repeated with precision the path through which current is passed through memristor. Thus, the value of the current flowing through the memristor depends on the voltage applied to it in the past.

So the virtual boundary between doped and undoped regions drifts in the respective direction depending on the polarity of the applied voltage. It means that the doped region thickness varies.

In the extreme positions of the boundary electrical resistance of the active region will either be high (case $w = 0$ with the designation of this state as R_{off}) or low (the case $w = D$ with the designation of this state as R_{on}). This generalization is shown in Fig. 1.21.

It is obvious that the impedance of the memristor structure can be represented as a series combination of two resistors, whose values depend on the position of the virtual boundary (the value w, Fig. 1.21). In this case, the general expression for memristance $M(q)$ can be written as:

$$M(q) = R_{\text{on}} \frac{w}{D} + R_{\text{off}} \left(1 - \frac{w}{D}\right).$$

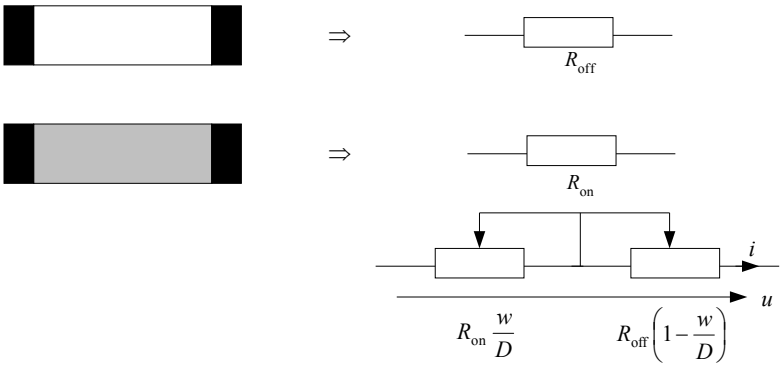

Fig. 1.21. The change of the memristor resistance according to its state

If the applied voltage is switched off, the oxygen ions do not move, and the boundary between the two regions "freezes". The state of the memristor at this time is defined by its resistance which is proportional to the charge which has passed through the memristor to this instant of time. The effect of "resistance memory" increases by nanoscale memristor due to the fact that the "holes" do not need to pass long distances.

Thus the memristor does not accumulate the charge like a capacitor and does not maintain the magnetic flux as the inductor. His functioning (change of its properties) is provided by chemical reactions in a thin (from 3 to 20 nm) two-layer film of titanium dioxide. One of the layers of the film, as was noted above, is slightly depleted by oxygen and oxygen vacancies migrate between the layers in one direction and then in inverse direction under the influence of an applied voltage.

In other words, due to the diffusion of oxygen ions under the influence of an applied electric field the thickness of these layers vary: the thickness of one of them increases and the thickness of the second layer decreases respectively due to the polarity of the voltage source.

1.4 General characteristic of the memristors

To sum up the memristor, the properties discussed above, we note the following.

• The fact that memristors were "hidden" in Maxwell's equations for more than 100 years, apparently, was due to the fact that the equations

were not formulated at that time in a form, which is used today. In addition, these devices are very small in size and, therefore, could not be detected until nanoelectronics with the respective nanotechnologies is appeared which study transfer of charges in solid-state semiconductors.

• The researchers of HP–laboratory used the fact of nonlinearity to obtain the memristor. They began to study the small electrical devices with sizes D of a few tens of nanometers (instead of searching among magnetic systems), for which a nonlinear relationship between the integrals of the current and the voltage is satisfied, so that the value M became a nonlinear function of the charge.

• Most memristors realized in practice are based on titanium dioxide TiO_2 in pure state having a large resistance. However, when TiO_2 is doped with other elements, these dopants (that is oxygen ions) in an electric field of high intensity can drift in the direction of the electric current. If the voltage is applied to the two-layer film then impurities begin to spread in volume TiO_2 and thus change the resistance of the active layer.

• The electric field at the same time reaches enormous values. In particular, if the voltage of 1 volt is applied to the section of 20 nm then electric field intensity is equal to:

$$E = \frac{U}{l} = \frac{1}{20 \cdot 10^{-9}} = 5 \cdot 10^{7} \frac{\text{V}}{\text{m}}.$$

• The memristance of the memristor changes over time only when an alternating current flows through it. It means that the memristor is a AC unit.

• The device functions as a memristor, not a resistor, due to the presence of the dynamic state variable w that defines the boundary between two layers of high and low conductivity. State variable describes how memristance changes over time. The state variable is proportional to the charge q.

• Influence of memristance on the electrical behavior of the device affects only when the device itself becomes very small (at the nanoscale).

• Expression for memristance M is not explicitly connected with the magnetic flux, although its value is defined as the ratio between the flux and the electric charge. The absence of magnetic flux in an explicit form can be explained by the use of the law of electromagnetic induction, if we rewrite the definition of memristance as

$$M(q) = \frac{d\Phi}{dq} = \frac{udt}{idt} = \frac{u}{i}.$$

The expression looks like a usual resistance, but the dependence of the memristance from a charge shows that it is not.

• Absence of the magnetic flux in an explicit form is the subject of scientific and nonscientific dispute about the fact of discovery of the memristor. The polemics about it is considering so far [52], [84].

• If the voltage applied to the memristor switch off, the dynamic movement of a virtual boundary between the two layers of the active region is stopped and the value of memristor resistance is retained, that is remembered. This stored state of the device is held up until another voltage will be applied to the memristor, which will cause the transfer of the charges. When the voltage switched off the previous state is retained arbitrarily long.

• Memristor does not keep its own properties in the form of a charge, and it was not afraid of the charge leakage in the chip nanometer scale (nanocircuits), and it is completely nonvolatile, and the data can be stored in the memristor as long as there are the materials from which it is made. However, the memristor is not stored either electric or magnetic energy.

• Current-voltage characteristic of a memristor has the form of the hysteresis loop when AC voltage is applied. In this case the loop is pinched (twisted) at the coordinate plane $i(u)$, Fig. 1.1. It follows from the relationship:

$$u(t) = M(x,t)i(t).$$

When $u = 0$, then $i = 0$ and vice versa. This fact also shows that the memristor is not a device that stores energy.

The current-voltage characteristic is ambiguous like Lissajous figures that arise while moving a point in two perpendicular directions with different frequencies.

• Hysteresis loop is formed because the current passing through memristor does not change linearly with the applied voltage, unlike the resistor which follows Ohm's law.

Indeed, the virtual boundary w between the respective layers shifts by the charge carriers when a current passes through the memristor, Fig. 1.22.

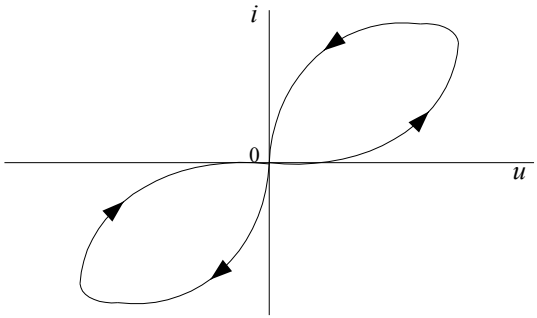

Fig. 1.22. The dependency $i(u)$ of the memristor

If the charge carriers are pushing the boundary in the side, in which the instant resistance of the two-component memristor decreases over time, this means that the current increases with the increase of the applied voltage according to the nonlinear low (see on the curve $i(u)$ in the upper right corner, Fig. 1.22).

• A memristor is a frequency dependent element that is the memristance value M depends on the frequency of the applied signal. In this case, if the frequency increases, there is less time for the boundary to change its direction of movement to the right or left, because the flow of charge carriers changes direction faster and faster, so that the current-voltage characteristic is narrowed, Fig. 1.23.

With a relatively high frequency hysteresis loop is transformed into a straight line (see Fig. 1.12).

• Memristors can be created on the base of the multi-layer materials to get a wide range and high rate of resistance switching upon application of the respective signal. There are already examples of cells with a side of 3 nm and a switching speed of about one nanosecond.

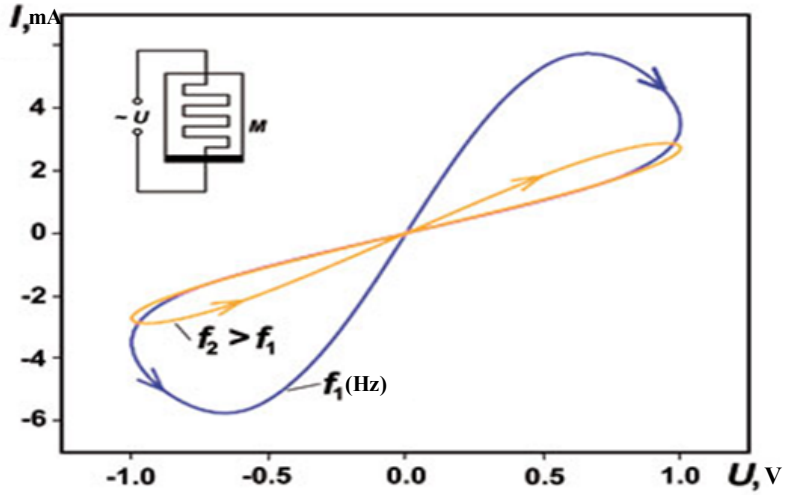

Fig. 1.23. The dependence of the current-voltage characteristics of a memristor from frequency

• Memristors today are the only inorganic material, approaching in their functions to the synapses of the brain (the synapse is the connection between nerve cells in the brain (neurons)). The rate of the signal transfer by synapse depends on the neuron activation time: the smaller the time interval between the activation, the faster the signal is transmitted at the synapse. Similarly memristor functions: if the current is applied to the memristor with intervals, for example, 20 ms then the resistance of the memristor is two times less than at intervals of 40 ms.

MATHEMATICAL MODELS OF MEMRISTOR

- Linear mathematical model of the memristor
- Nonlinear mathematical model of the memristor

2.1 Linear mathematical model of the memristor

The definition of a broad class of systems called memristive systems was given in [20]. These systems are described by the equations:

$$u(t) = M(w, i)i(t), \qquad \frac{dw}{dt} = f(w, i),$$

where w defines the state variable, M and f may be time functions, u and i are the voltage and current respectively.

The first equation $u(t) = M(w, i)i(t)$ looks, as already mentioned, like the nonlinear version of Ohm's law and determine how the voltage across the memristor depends on the current passing through it, and on some state variable. However, the difference lies in the fact that this expression depends on the state variable w. This variable describes the system inside. This time dependence of a state variable provides the storage of the system. The thickness of the titanium dioxide film TiO_2 plays the role of a state variable of the memristor. Increase or decrease in this thickness causes increase and decrease the resistance of the entire structure. This means that the resistance of the structure will vary depending on what amount of charge passed through the element and generally this resistance can not be constant.

The second equation expresses that fact in what way change of the state variable depends on the amount of charge flowing through the memristor. Thickness of the film of the memristor depends on the distribution of oxygen vacancies through the material.

Consider the simple linear mathematical model of the memristor, proposed in [10], [34], and [70]. The linear model of a virtual boundary movement suggests that oxygen vacancies are free in crossing the entire thickness of the structure without taking into account boundary condi-

tions. The usefulness of this model is defined by the ease of use and finished form solution.

Let voltage applied to the memristor creates a uniform electric field. Velocity of carriers drift is defined as

$$v = \frac{dw(t)}{dt}.$$

Obviously, the speed v is directly proportional to the electric field intensity $E = \frac{u}{D}$ and the charge carrier mobility μ_D in the diffusion process that is we may write that

$$v = \mu_D E,$$

where the value μ_D has the dimension equaled $\left[\frac{\text{m}^2}{\text{s} \cdot \text{V}}\right]$.

Then for a linear relationship between the rate of diffusion and electric field intensity the speed of movement of virtual boundary w separating the doped and undoped regions is defined as follows:

$$v = \frac{dw(t)}{dt} = \frac{\mu_D u(t)}{D} = \frac{\mu_D R_{\text{on}}}{D} i(t),$$

where the value R_{on} is the resistance of the completely doped active region of the memristor.

Introducing this expression in the form

$$dw = \frac{\mu_D R_{\text{on}}}{D} i(t) dt,$$

and integrating both sides with respect to time: we get

$$\int_0^t dw(t) = \frac{\mu_D R_{on}}{D} \int_0^t i(\tau) d\tau,$$

from which we obtain

$$w(t) = \frac{\mu_D R_{\text{on}}}{D} [q(t) - q(0)] + w(0).$$

Assuming $q(0) = 0$ we get:

$$w(t) = w_0 + \frac{\mu_D R_{\text{on}}}{D} q(t),$$

where the value $w(0) = w_0$ determines the initial value of the position of the virtual boundary.

Memristance of the structure corresponding to this position of the boundary w with respect to the entire thickness of the structure is given by:

$$M = R_{\text{on}} \frac{w}{D} + R_{\text{off}} \left(1 - \frac{w}{D}\right),$$

where the value R_{off} is the resistance of the undoped region.

Substituting the expression $w(t)$, we get:

$$\begin{aligned} M(q) &= R_{\text{on}} \frac{w_0}{D} + \frac{\mu_D R_{\text{on}}^2}{D^2} q(t) + R_{\text{off}} \left[1 - \frac{w_0}{D} - \frac{\mu_D R_{\text{on}}}{D^2} q(t)\right] \\ &= R_{\text{on}} \frac{w_0}{D} + R_{\text{off}} \left[1 - \frac{w_0}{D}\right] - \frac{\mu_D R_{\text{on}}}{D^2} \left[R_{\text{off}} - R_{\text{on}}\right] q(t) \\ &= \left|R_{\text{off}} - R_{\text{on}} = \Delta R\right| = R_0 - \frac{\mu_D R_{\text{on}} \Delta R}{D^2} q(t) = R_0 - \frac{\Delta R}{Q_0} q(t), \end{aligned}$$

where

$$R_0 = R_{\text{on}} \frac{w_0}{D} + R_{\text{off}} \left(1 - \frac{w_0}{D}\right),$$

is the initial resistance of the memristor, and the value

$$Q_0 = \frac{D^2}{\mu_D R_{\text{on}}}$$

determines the amount of charge that is required to change the state of the structure, from w_0.

It is obvious that the second term in the expression for memristance

$$M[q] = R_0 - \frac{\mu_D R_{\text{on}} \Delta R}{D^2} q(t),$$

depending on the charge $q(t)$ carries in a substantial contribution into the memristance value. This term increases in magnitude with increasing mobility of impurities and reduction of the entire active area of the film thickness *D*. For any material this term is 10^6 greater in absolute value for the case of nanoscale (10^{-9}), compared with microscale (10^{-6}) due to the presence of the factor $\frac{1}{D^2}$.

It is therefore memristance *M* is much more important parameter for understanding the processes in the electronic devices when their dimensions are reduced to the nanoscale.

We also note that the expression for memristance was written in the form that takes into account the material properties and geometrical dimensions of the device itself. Similarly, it has been done for a capacitor, whose capacitance is expressed as:

$$C = \frac{\varepsilon_a S}{d},$$

where ε_a, S and *d* are the dielectric constant, the area of the plates and the distance between the plates, respectively. By analogy the value of the resistor and the inductance of the coil are also defined in terms of the properties of materials and geometry dimensions:

$$R = \rho \frac{l}{S}, \quad L = w^2 \frac{\mu S}{l}.$$

According to the definition of the memristance we obtain:

$$M[q(t)] = \frac{d\Phi}{dq} = \frac{udt}{idt} = \frac{u(t)}{i(t)}.$$

Then, the voltage $u(t)$ can be determined as follows:

$$u(t) = M[q(t)]i(t) = \left[R_0 - \frac{\Delta R}{Q_0} q(t) \right] i(t) = \left[R_0 - \frac{\Delta R}{Q_0} q(t) \right] \frac{dq}{dt},$$

and integrating both sides of this expression with respect to time, we obtain the dependence of the magnetic flux over time (assuming $q(0) = 0$):

$$\Phi(t)=\int_0^t u(t)dt=R_0\int_0^t dq(\tau)-\frac{\Delta R}{Q_0}\int_0^t q(\tau)d\tau=R_0\,q(t)-\frac{\Delta R}{Q_0}\frac{q^2(t)}{2}.$$

We solve the resulting equation for the charge $q(t)$, which (it is clear from the expression) is bound up with the magnetic flux by the quadratic dependence:

$$\frac{\Delta R}{2Q_0}q^2-R_0q+\Phi=0,$$

$$q(t)=\frac{\left[R_0-\sqrt{R_0^2-\dfrac{2\Delta R}{Q_0}\Phi}\right]Q_0}{\Delta R}=\frac{Q_0R_0}{\Delta R}-\frac{Q_0R_0}{\Delta R}\sqrt{1-\frac{2\Phi\Delta R}{Q_0R_0^2}}$$

$$=\frac{Q_0R_0}{\Delta R}\left[1-\sqrt{1-\frac{2\Delta R\Phi(t)}{Q_0R_0^2}}\right].$$

Thus, the time dependence of the charge is given by the expression:

$$q(t)=\frac{Q_0R_0}{\Delta R}\left[1-\sqrt{1-\frac{2\Delta R\Phi(t)}{Q_0R_0^2}}\right].$$

Substituting the obtained expression for $q(t)$ into relation of memristance, we get:

$$M[q(t)]=R_0-\frac{\Delta R}{Q_0}q(t)=R_0\sqrt{1-\frac{2\Delta R}{Q_0R_0^2}\Phi(t)}.$$

The current flowing through the memristor is given by the relationship:

$$i(t)=\frac{u(t)}{M[q(t)]}=\frac{u(t)}{R_0\sqrt{1-\dfrac{2\Delta R}{Q_0R_0^2}\Phi(t)}}.$$

The graphs of the respective dependencies $u(t)$, $i(t)$, $q(t)$, $\Phi(t)$ and the graph of the current-voltage characteristic $i=f(u)$ for the linear model of the memristor are shown in Fig. 2.1. It should be noted that the

charge q is an unambiguous function of the magnetic flux, as it should be in the memristor.

$$U_m := 1 \quad \omega := 1 \quad R_{\text{off}} := 16 \cdot 10^3 \quad R_{\text{on}} := 100 \quad \mu_D := 10^{-14}$$

$$D := 35 \cdot 10^{-9} \quad w_0 := 0.5D$$

$$Q_0 := \frac{D^2}{\mu_D \cdot R_{\text{on}}} \quad R_0 := R_{\text{on}} \frac{w_0}{D} + R_{\text{off}} \left(1 - \frac{w_0}{D}\right) \quad \Delta R := R_{\text{off}} - R_{\text{on}}$$

$$t := 0, 0.0005 \ldots 20 \quad u(t) := U_m \sin(\omega \cdot t) \qquad \Phi(t) := \frac{U_m}{\omega} \cdot (1 - \cos(\omega \cdot t))$$

$$i(t) := \frac{u(t)}{R_0 \sqrt{1 - \frac{2\Delta R}{Q_0 (R_0)^2} \cdot \Phi(t)}} \qquad q(t) := \frac{Q_0 R_0}{\Delta R} \left[1 - \sqrt{1 - \frac{2\Delta R}{Q_0 (R_0)^2} \cdot \Phi(t)}\right]$$

$$w(t) := w_0 + \frac{\mu_D R_{\text{on}}}{D} q(t) \qquad x(t) := \frac{w(t)}{D}$$

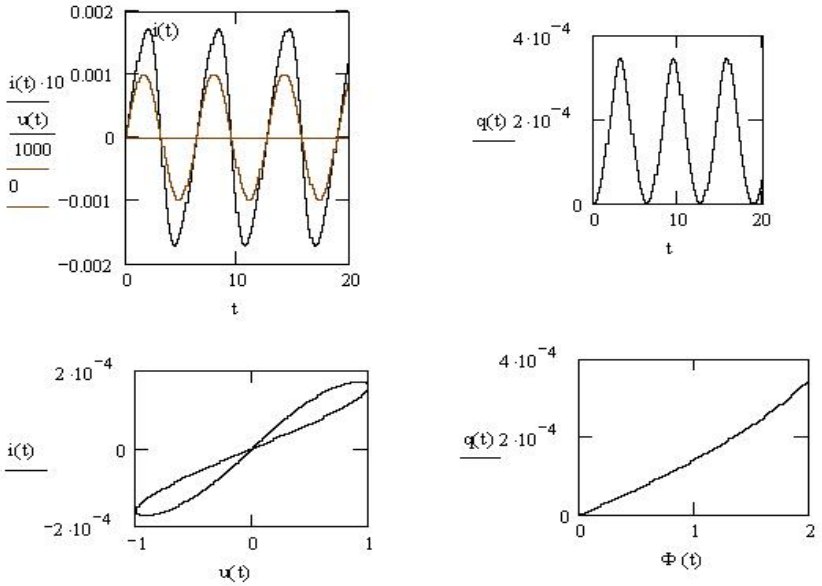

Fig. 2.1. Graphs of dependencies $u(t)$, $i(t)$, $q(t)$, $\Phi(t)$, $i = f(u)$ for the linear model of the memristor

The analysis and the modeling of memristive circuits can use the normalized value of the state variable which is given by the expression:

$$x(t) = \frac{w(t)}{D}.$$

Besides the coefficient r is used which is defined by the ratio of the resistances in extreme conditions (for $w = D$ and $w = 0$ we have the resistances R_{on} and R_{off} respectively):

$$r = \frac{R_{\text{off}}}{R_{\text{on}}}.$$

In this case, easy to obtain the following expressions:

$$M[q] = R_{\text{on}} \frac{w}{D} + R_{\text{off}} \left(1 - \frac{w}{D}\right) = R_{\text{on}} \left[x + r(1-x)\right],$$

$$x(t) = x_0 + \frac{q(t)}{Q_0}.$$

It is also obvious that the equation

$$w(t) = w_0 + \mu_D \frac{R_{\text{on}}}{\text{D}} q(t),$$

defining the state variable $w(t)$ is valid only when the values w are in the range $[0, D]$ or the values of the normalized state variable x are in the range $[0, 1]$.

Figure 2.2 shows the graphs of change in time $M(t)$ and $x(t)$.

$$U_m := 1 \quad \omega := 1 \quad R_{\text{off}} := 16 \cdot 10^3 \quad R_{\text{on}} := 100 \quad \mu_D := 10^{-14}$$

$$D := 35 \cdot 10^{-9} \quad w_0 := 0.5D$$

$$Q_0 := \frac{D^2}{\mu_D \cdot R_{\text{on}}} \quad R_0 := R_{\text{on}} \frac{w_0}{D} + R_{\text{off}} \left(1 - \frac{w_0}{D}\right) \quad \Delta R := R_{\text{off}} - R_{\text{on}}$$

$$t := 0, 0.00095 \ldots 20 \quad u(t) := U_m \sin(\omega \cdot t) \qquad \Phi(t) := \frac{U_m}{\omega} \cdot \left(1 - \cos(\omega \cdot t)\right)$$

$$q(t) := \frac{Q_0 R_0}{\Delta R}\left[1 - \sqrt{1 - \frac{2\Delta R}{Q_0 (R_0)^2} \cdot \Phi(t)}\right] \qquad M(t) := R_0 \sqrt{1 - \frac{2\Delta R}{Q_0 (R_0)^2} \cdot \Phi(t)}$$

$$w(t) := w_0 + \frac{\mu_D R_{on}}{D} q(t) \qquad x(t) := \frac{w(t)}{D}$$

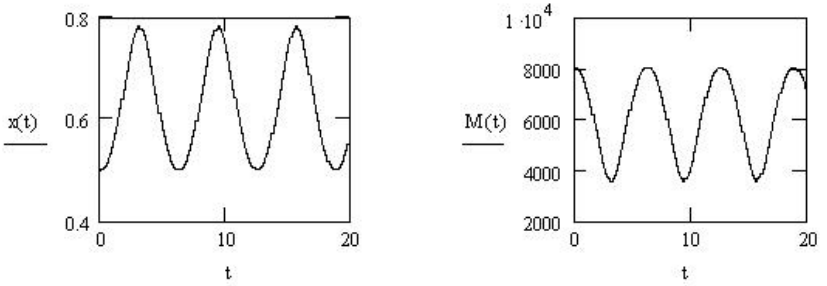

Fig. 2.2. Graphs of dependencies $M(t)$ and normalized state variable $x(t)$

As noted above, the value w is proportional to the charge $q(t)$ that passes through memristor, as long as its value is closer to the value D (or 0).

Also note the following important fact.

If we transform the equation

$$u(t) = M[w(t),\ i(t)]\, i(t)$$

in the form

$$u(t) = R_{on}\left[x(t) + r(1 - x(t))\right] i(t),$$

taking into account the fact that

$$\frac{dw(t)}{dt} = \frac{\mu_D u(t)}{D} = \frac{\mu_d R_{on}}{D} i(t)$$

or by introducing a normalized variable $x = \frac{w}{D}$,

$$\frac{dx(t)}{dt} = \frac{\mu_d R_{on}}{D^2} i(t) = \frac{R_{on}}{\beta} i(t),$$

the initial expression for $u(t)$ can be obtained in the form of:

$$u(t) = \beta\left[x(t) + r(1 - x(t))\right]\frac{dx(t)}{dt}.$$

Integrating the voltage over time we may determine the magnetic flux:

$$\Phi(t) = \int u(t)dt = \beta\int xdx + \beta r\int dx - \beta r\int xdx$$

$$= \beta\frac{x^2}{2} + \beta rx - \beta r\frac{x^2}{2} + \beta C = \beta\left[-\frac{r-1}{2}x^2 + rx + C\right],$$

where the constant C is the constant of integration, which is determined by the initial values of the state variable.

The constant of integration C contains "past events" created by the input current, and plays an important role in the nonlinear structure. Memristor memory effect refers to the constant C. This constant can not be eliminated by subtracting from $x(t)$, it is saved and after a time differentiation of $x(t)$. That is why the memristor reaction depends on the prior history.

In conclusion we note that in real systems with nanoscale significant nonlinear effects in the drift of oxygen vacancies within the active region appear in achieving boundaries due to strong electric fields. In this case the form of voltage-current characteristic varies considerably, as will be discussed below.

2.2 Nonlinear mathematical model of the memristor

The need to get the reliable models, which take into account the nonlinear dynamics of the movement of impurities, is an important task in the study of memristor systems, especially in cases where their physical dimensions are in the nanometer range.

Dynamic processes in the memristor are described by the examples of many analytical models that approximate the kinematics of the inner impurities.

Although the linear model reproduces the hysteresis loop $i-u$ of the volt-ampere characteristic, however, a serious shortcoming is the

simplification of the foundations of electrodynamics. First of all, a small value of the voltage applied to the region having nanosizes causes a very large electric field, which undoubtedly leads to nonlinear movement of the virtual boundary. The value w never reaches 0, as this would mean that physically memristor has no oxygen vacancies. In another simple case ($w = D$) the entire area of the two-layer structure should be a fully doped by the oxygen vacancies.

Obviously, to simulate the process of state change it is required that the rate of change of this state $\frac{dw}{dt}$ was greatest in the center of the structure $\left(w = \frac{D}{2} \right)$ and would be reduced to zero, when the value w was close to the boundaries ($w = 0,\ w = D$). These restrictions can be carried out by multiplication by a so-called window function $f(x)$, where x is as above, normalized state variable equaled $\frac{w}{D}$.

As is known, the thickness of the doped region at some time t depends on the number of charges that have passed through the structure and, therefore, the time derivative of the function $w(t)$ is a function of the current:

$$\frac{dw}{dt} = v_D = \mu_D E = \mu_d \frac{u}{D} = \mu_D \frac{R_{\text{on}}}{D} i(t),$$

where v_D is the sped at which a virtual boundary moves between doped and undoped regions, μ_D is the average mobility of the impurities, E is the electric field intensity applied to the doped region with the passage of current $i(t)$, R_{on} is the total resistance of the structure, where the active region is doped completely.

If we assume that the electric field is small enough, then the linear model of impurity drift can sufficiently precisely approximate the dynamics of the operation of the memristor. However, this model is not suitable when the process is considered on the boundaries. This is due to the influence of an inhomogeneous electric field which restrains drift of impurities.

Restrictions of the linear model appear in its extreme states, that is when the state is saturated ($w \to D$) and in the initial state ($w \to 0$). These two extreme cases are achieved when the voltage applied to memristor has the sinusoidal form.

To take into account the nonlinearity we introduce a window function $f(w)$:

$$\frac{dw}{dt} = \mu_D \frac{R_{\text{on}}}{D} i(t) f(w),$$

or introducing a normalized variable $x = \frac{w}{D}$,

$$\frac{dx}{dt} = \mu_D \frac{R_{\text{on}}}{D^2} i(t) f(x).$$

Window function simulates the nonlinear dynamics of impurities in the active two-layer structure. The following conditions must be carried out:

• to take into account the boundary conditions at both electrodes of the memristor structure;

• to take into account the nonlinearity of impurities drift across the active area of the device;

• to provide the connection between linear and nonlinear models of the drift of impurities;

• to provide scalability, that is the range $f(x)$ should be such as to satisfy the condition $0 \le f(x) \le 1$;

• to use the built-in parametric control to adjust the model.

Consider a few models.

It was proposed in [34] to use a function $f(x)$ in the form:

$$f_p(x) = 1 - [2x - 1]^{2p},$$

where p is a positive integer, called the parameter of the model. This window function ensures a zero drift at the boundaries ($f(0) = f(1) = 0$), as seen from the relation.

For the value $p = 1$ the nonlinear drift is taken into account throughout the active region of thickness D, and for $p \to \infty$ the model be-

comes the linear one (the value $2x-1<1$) for the model, that is $f_p(x)\to 1$.

Thus, we may control by the rate of change function by means of the change of the parameter *p*. Low values of the parameter *p* correspond to lower rate of change *w* and vice versa. Figure 2.3 shows a window function graphs for different values of the parameter *p*.

$$x := 0, 0.01 \ldots 1 \qquad p := 1 \qquad f_1(x) := 1-(2x-1)^{2p}$$
$$p := 5 \qquad f_2(x) := 1-(2x-1)^{2p}$$
$$p := 10 \qquad f_3(x) := 1-(2x-1)^{2p}$$

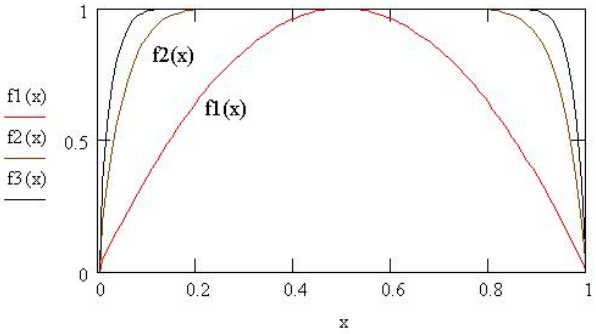

Fig. 2.3. Graphs of window function for different values of parameter *p*

The modified equation of change of the rate $\frac{dx}{dt}$ is as follows:

$$\frac{dx}{dt} = \frac{\mu_D R_{\text{on}}}{D^2} i(t) f_p(x) = ki(t)[1-(2x-1)^{2p}].$$

The considered a nonlinear model is more precise than linear one. The decision of the model can be carried out as for the time function for arbitrary values of *p*. We may use numerical methods of solving in the modeling process based on previously obtained relations.

The following is an algorithm for calculating the corresponding functions:

$$M[w(t_i)] = R_{\text{on}}\left[\frac{w(t_i)}{D}\right] + R_{\text{off}}\left[1-\frac{w(t_i)}{D}\right],$$

$$i(t_{i+1}) = \frac{u(t_{i+1})}{M[w(t_i)]},$$

$$v_D(t_{i+1}) = \frac{\mu_D R_{on}}{D} i(t_{i+1}) f_p\left[\frac{w(t_i)}{D}\right],$$

$$w(t_{i+1}) = v_D(t_{i+1})[t_{i+1} - t_i] + w(t_i),$$

$$q(t_{i+1}) = \frac{\Phi(t_{i+1})}{M[w(t_i)]},$$

where the magnetic flux $\Phi(t)$ is defined from the expression:

$$\Phi(t) = \int_0^t u(\tau) d\tau.$$

It should be noted peculiarities of the function $f_p(x)$ when the doped region covers the entire thickness of the structure (x = 1). In this case the function $f_p(x=1) = 0$ for all values p. Then the value $v_D(t_{i+1}) \equiv 0$ and the value $w(t_{i+1}) = w(t_i)$, that is it does not change in the next steps of the simulation. This "loop" continues until the end of the simulation regardless of the change of current direction. It leads to incorrect results.

Thus, for the considered model all conditions are carried out except scalability condition $0 \le f(x) \le 1$, namely, if the function $f_p(x)$ reaches such boundary value (x = 0 or x = 1), then the state of the device can not be further adjusted. This case is called the terminal state problem, [34].

Consider the particular case of the model, when p = 1, that is the window function takes the form:

$$f_1(x) = 1 - [2x - 1]^2,$$

and the ratio for the rate of change of the state variable is written as

$$\frac{dx}{dt} = ki(t)[1 - (2x - 1)^2].$$

Let us solve the equation for state variable $x(t)$, taking into account that $idt = dq$:

$$dx = k\left[1-(2x-1)^2\right]idt = k\left[1-(2x-1)^2\right]dq = 4x(1-x)kdq,$$

from which it follows:

$$\frac{dx}{4x(1-x)} = kdq$$

or

$$\frac{1}{4}\int\frac{dx}{x(1-x)} = k\int dq.$$

We represent the integrand on the left, as follows:

$$\frac{1}{x(1-x)} = \frac{1}{x} + \frac{1}{1-x} = \frac{1}{x} - \frac{1}{x-1}.$$

Then we get:

$$\frac{1}{4}\ln x - \frac{1}{4}\ln(x-1) = k[q(t)-q(0)] = k[q(t)-q_0]$$

or

$$\ln\frac{x}{x-1} = 4k[q(t)-q_0],$$

where q_0 is the initial value of the charge at the time $t=0$.

It's obvious that

$$\frac{x-1}{x} = \exp\{-4k[q(t)-q_0]\}.$$

Let's define the memristance of the structure in accordance with the obtained result:

$$M(x) = xR_{\text{on}} + R_{\text{off}}(1-x) = x\left[R_{on} + R_{\text{off}}\frac{1-x}{x}\right]$$
$$= x\left[R_{\text{on}} + R_{off}\exp\{-4k[q(t)-q_0]\}\right],$$

then

$$\frac{M(x)}{x} = R_{\text{on}} + R_{\text{off}} \exp\{-4k[q(t) + q_0]\}.$$

Represent the value $\frac{1}{x}$ in the form:

$$\frac{1}{x} = \frac{1-x}{x} + 1 = \exp\{-4k[q(t) + q_0]\} + 1.$$

Substituting this value in the expression for memristance, we get:

$$M(x) = M[q(t)] = \frac{R_{\text{on}} + R_{\text{off}} \exp\{-4k[q(t) + q_0]\}}{\exp\{-4k[q(t) + q_0]\} + 1}$$
$$= R_{\text{off}} + \frac{R_{\text{on}} - R_{\text{off}}}{\exp\{-4k[q(t) + q_0]\} + 1}.$$

Thus, the final expression for memristance is:

$$M[q(t)] = R_{\text{off}} - \frac{R_{\text{off}} - R_{\text{on}}}{\exp\{-4k[q(t) + q_0]\} + 1}.$$

Changing the normalized state variable $x(t)$ in time, as it follows from the above arguments, is determined from the relationship:

$$x(t) = \frac{1}{\exp\{-4k[q(t) + q_0]\} + 1}.$$

The results of simulation of the nonlinear model of the memristor are shown in Fig. 2.4 at the value of the parameter $p = 1$ and input signal $i(t) = I_m \sin \omega t$.

$$t := 0, 0.001...15 \quad \omega := 1 \quad I_m := 1 \quad \mu_D := 10^{-18}$$
$$D := 5 \cdot 10^{-9} \quad R_{\text{off}} := 1600 \quad R_{\text{on}} := 100$$
$$k := \frac{\mu_D \cdot R_{\text{on}}}{D^2} \quad i(t) := I_m \sin(\omega \cdot t) \quad q(t) := \frac{I_m}{\omega}\left(1 - \cos(\omega \cdot t)\right)$$
$$M(t) := R_{\text{off}} - \frac{R_{\text{off}} - R_{\text{on}}}{\exp\left(-4kq(t)\right) + 1} \quad x(t) := \frac{1}{\exp\left(-4kq(t)\right) + 1} \quad u(t) := M(t) \cdot i(t)$$

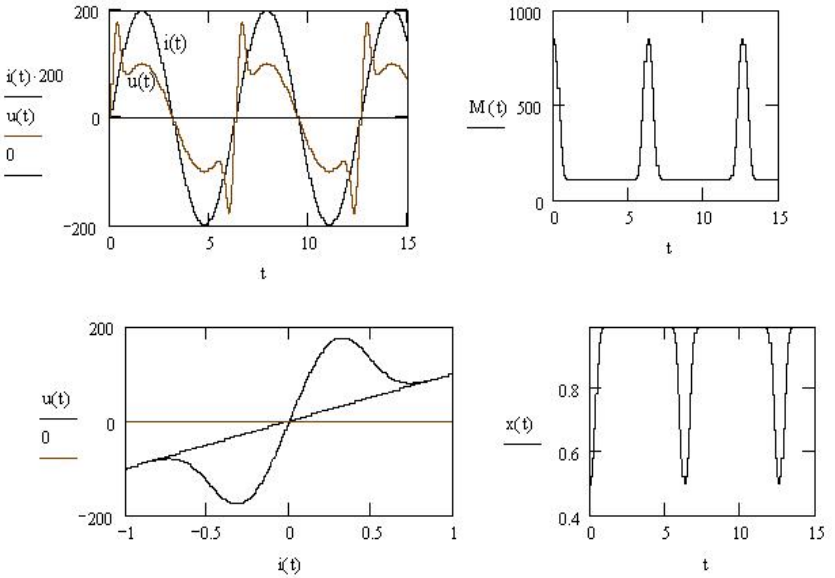

Fig. 2.4. Simulation results of the memristor described by the Nonlinear model

Let's find the charge $q(t)$ from the ratio

$$q(t) = \int_0^t i(\tau)d\tau = \frac{I_m}{\omega}\left(1 - \cos(\omega t)\right)$$

and the voltage $u(t)$ across the memristor from the relation

$$u(t) = M[q(t)]i(t).$$

Next we can build a current-voltage characteristic of the memristor $\{i(t), u(t)\}$, Fig. 2.4.

Comparing the current-voltage characteristics of the linear (see Fig. 2.1) and nonlinear (Fig. 2.4) models, it is necessary to note that the window function increases the effect of the nonlinearity of the ion drift when the value w is sufficiently close to zero or D. Current-voltage characteristics differ significantly by more abrupt transitions from state R_{off} to state R_{on}, and vice versa (so-called effect of the resistive switching). These effects will be considered in more detail in chapter 5.

The window function was proposed in [77], [78] in the form:

$$f(w) = \frac{w(D-w)}{D^2},$$

which may be rewritten in terms of the normalized state variable $x(t)$ as the following:

$$f(x) = x - x^2.$$

The boundary condition in the state "off" ($x = 0$) is satisfied because $f(x) \equiv 0$. However, this function has not enough flexibility and the problem of final state remains.

It may be noted that the proposed function is essentially a scaled function considered above. Indeed, for $p = 1$, we have:

$$f_1(x) = 1 - (2x-1)^2 = 4(x - x^2),$$

that is the factor 4 is added.

Another window function is proposed in [11]:

$$f_p(x) = 1 - [x - \text{sgn}(-i)]^p,$$

$$\text{sgn}(i) = \begin{cases} 1, & i \geq 0, \\ 0, & i < 0. \end{cases}$$

A positive (negative) value of the current is associated with the increase (decrease) of the doped region width Graphs $f_p(x)$ for different values of p are shown in Fig. 2.5. The results of simulation of the memristor with the given window function are shown in Fig. 2.6.

In this case, if the process begins with $x = 0$ then $f_p(0) = 1$. With the increase in x so that $x \to 1$ $(w \to D)$ the function $f_p(1) = 0$. When the current changes the direction, the function $f_p(x)$ immediately "switches" to 1. As x decreases, so that $x \to 0$ the function $f_p(x)$ is also decreases to zero. When the current changes its direction again, the cycle repeats.

Nonlinearity of impurities movement, as already noted, appears in two extreme values $x \to 0$ and $x \to D$.

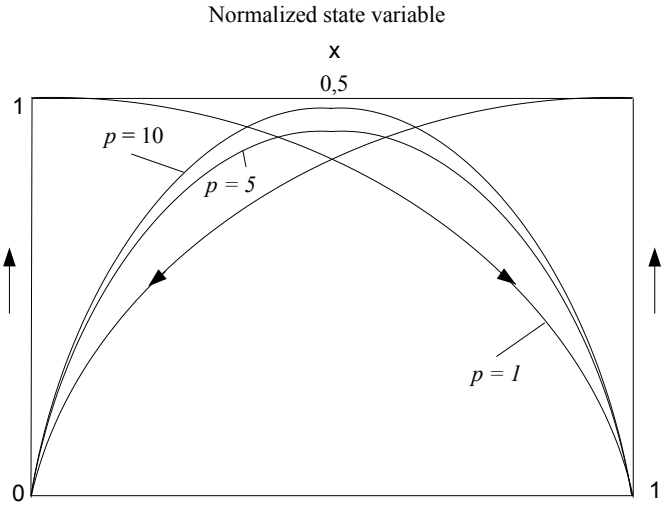

Fig. 2.5. Graphs of the window function for the different values p

The parabola curve was proposed in [71], which is symmetrical at $x = 0.5$. We may write the expression for the window function in the form:

$$f(x) = -Ax^2 + Bx + C,$$

where the coefficients A, B and C are determined by the following conditions:

$$\left.\frac{df}{dx}\right|_{x=0,5} = 0, \qquad f(x)\big|_{x=0,5} = 1, \qquad f(0) = f(1) = 0.$$

A simple calculation of the coefficients ($A = B = 4$, $C = 0$) results to a relation considered above, that is

$$f(x) = -4x^2 + 4x$$

for the case of $p = 1$. In order to attain both flexibility and scalability of model it is proposed modification of the window function based on the smooth parabolic function:

$$f(x) = x - x^2 = -\left[(x-0,5)^2 - 0,25\right] = 1 - \left[(x-0,5)^2 + 0,75\right].$$

formula1_all:=

$\delta \leftarrow 4 \cdot 10^{-5}$

$p \leftarrow 1$

$D \leftarrow 30 \cdot 10^{-9}$

$Q_0 \leftarrow 6 \cdot 10^{-5}$

$\mu_D \leftarrow 6 \cdot 10^{-14}$

$w_0 \leftarrow 0.2 \cdot D$

$i_0 \leftarrow 0$

$Ron \leftarrow 100$

$Roff \leftarrow 10000$

$\omega \leftarrow 10$

$t_0 \leftarrow 0$

for $j \in 0 .. 35998$

$t_{j+1} \leftarrow (j + 1) \cdot \delta$

$M_j \leftarrow Ron \cdot \left(\frac{w_j}{D}\right) + Roff \cdot \left(1 - \frac{w_j}{D}\right)$

$u_{j+1} \leftarrow 1 \cdot \sin\left(\omega \cdot t_{j+1}\right)$

$i_{j+1} \leftarrow \frac{u_{j+1}}{M_j}$

$v_{j+1} \leftarrow \frac{D}{Q_0} \cdot i_{j+1} \left[1 - \left[\frac{w_j}{D} - \frac{1}{1 + \exp\left[-100 \left[(-i)_{j+1}\right]\right]} \right] \right]^{2 \cdot p}$

$w_{j+1} \leftarrow v_{j+1} \left(t_{j+1} - t_j\right) + w_j$

$x_{j+1} \leftarrow \frac{w_{j+1}}{D}$

t

w

u

x

i

$s \leftarrow augment(t, i, x, v, u)$

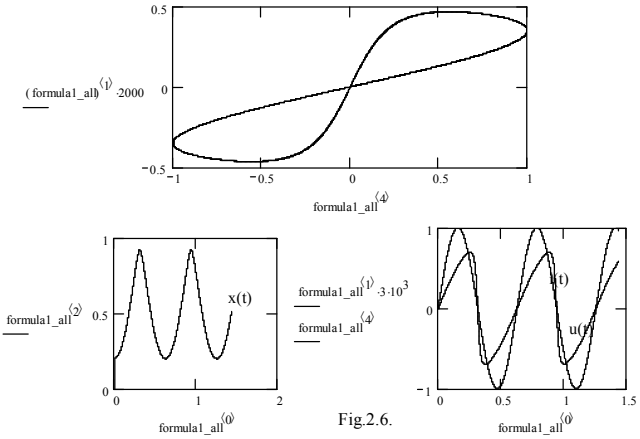

Fig.2.6.

Fig. 2.6. The results of a memristor simulation

Finally, the introduction of the control parameter p gives:

$$f(x) = 1 - \left[(x - 0{,}5)^2 + 0{,}75 \right]^p .$$

Note that for p = 1, this model is identical to the model described above. Figure 2.7 shows the graphs of the window functions for different values of the parameter p.

$$x := 0, 0.01 ... 1 \quad p_1 := 1 \quad p_2 := 5 \quad p_3 := 10 \quad p_4 := 40$$

$$f_1(x) := 1 - \left[(x - 0.5)^2 + 0.75 \right]^{p_1} \quad f_2(x) := 1 - \left[(x - 0.5)^2 + 0.75 \right]^{p_2}$$

$$f_3(x) := 1 - \left[(x - 0.5)^2 + 0.75 \right]^{p_3} \quad f_4(x) := 1 - \left[(x - 0.5)^2 + 0.75 \right]^{p_4}$$

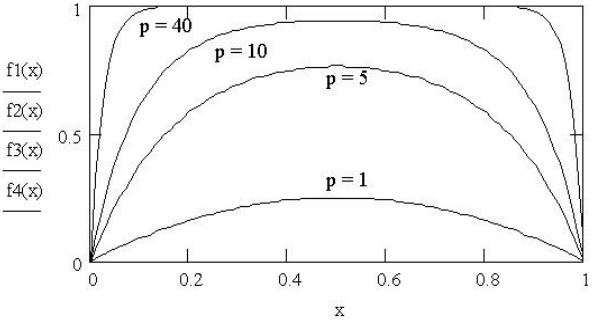

Fig. 2.7. Graphs of the window function $f(x) = 1 - \left[(x - 0{,}5)^2 + 0{,}75 \right]^p$

In this case the window function satisfies all conditions and improves shortcomings of the models considered above.

Introduced parameter p performs the following functions:

• parameter p allows to scale the window function from the top that is the maximum value of the function $f_{\max}(x)$ can take any value in the interval $0 \le f_{\max}(x) \le 1$;

• parameter p can take any real number unlike the models proposed in [34] and [35]; it allows to increase its flexibility. The values of p = 1, 2, 4, 8 and 10 may be selected to show the individual drift across the nonlinear two-layer structure, while a very large value of p can provide the bond withe the linear drift model (p = 60, 80);

• the limit values are determined by the window function as zero values at the edges of the two-layer structure, while the impurities drift is

strongly suppressed near metal contacts of the structure. On the other hand the problem of the final state is solved fundamentally in this case.

In special cases, when the drift of impurities such that $f_{\max}(x) \geq 1$ or $f_{\max}(x) < 0$ the function of the window may be adjusted be the introduction of another scalar parameter *c*. For any particular values of *p* the value $f_{\max}(x)$ can be scaled, and from the top and from the below with the respective value *c*:

$$f(x) = c\left[1 - \left[(x-0,5)^2 + 0,75\right]^p\right].$$

The graphs of the window function are shown in Fig. 2.8 for various values of the parameter *c* with a fixed value of *p* = 10.

$x := 0, 0.01 ... 1 \quad p := 10 \quad c_1 := 0.2 \quad c_2 := 0.4 \quad c_3 := 0.8 \quad c_4 := 1.6$

$f_1(x) := c_1\left[\left[1-(x-0.5)^2+0.75\right]^p\right] \quad f_2(x) := c_2\left[\left[1-(x-0.5)^2+0.75\right]^p\right]$

$f_3(x) := c_3\left[\left[1-(x-0.5)^2+0.75\right]^p\right] \quad f_4(x) := c_4\left[\left[1-(x-0.5)^2+0.75\right]^p\right]$

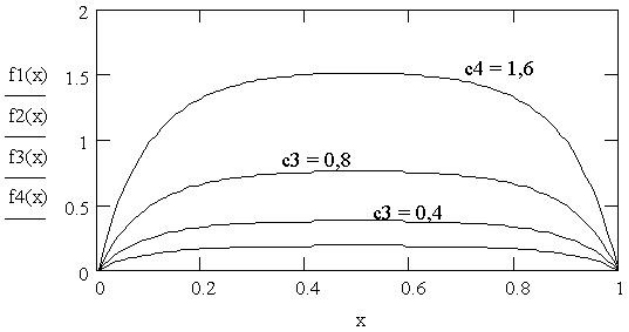

Fig. 2.8. Graphs of the window function $f(x) = c\left[1 - \left[(x-0,5)^2 + 0,75\right]^p\right]$

In general, the memristor as the device is characterized by the parameters μ_D, w_0, D, R_{on} and R_{off}. The higher the value w_0, the wider the loop in the $i-u$ graph. However, no values μ_D or values w_0 may be set arbitrarily, because the imaginary numbers may appear in equations. Furthermore, the model operates with a wider range of parameter val-

ues, if the size of the initial-doped region is less than half the total thickness D of the structure.

As already noted, the "long" structures with high values D indicate smaller memristive effect than the "short" structures, as

$$M(q) = R_0 - \frac{\mu_D R_{\text{on}} \Delta R}{D^2} q(t),$$

because the values $M(q)$ are inversely proportional to D^2.

The values R_{on} and R_{off} may be arbitrarily selected in accordance with their definitions. The ratio $r = \frac{R_{\text{off}}}{R_{\text{on}}}$ must be greater than 10, although the values $r = 100 - 2000$ are used more frequently in the simulation. It should be noted that an increase of the value r narrows the hysteresis loop to a straight line. For any given value D the hysteresis effect is greater if $\Delta R >> R_0$ [34].

The results of simulation of the nonlinear model of the memristor with parameters:

$$\mu_D = 10^{-14} \frac{\text{m}^2}{\text{V} \cdot \text{s}};\ D = 40 \text{ nm};\ x_0 = 0,4;\ R_{\text{on}} = 100\ \Omega;\ R_{\text{off}} = 10000\ \Omega;$$

$$u(t) = 1 \cdot \sin \omega t \text{ V};\ \omega = 8\pi \frac{\text{rad}}{\text{s}}.$$

are shown in Fig. 2.9.

Step simulation was selected as $\delta = 2 \cdot 10^{-6}$ s. The used window function has the form:

$$f(x) = \frac{w(D-w)}{D^2} = x - x^2.$$

It should be noted that in the case of the nonlinear model the periods of the current and the input voltage coincide and the phase shift between them is equal to zero, but the current curve and the hysteresis curve are sharper because the respective window function is used in comparison with the linear model, (look of Fig. 2.1).

formula1_all :=

$P \leftarrow 7$

$\delta \leftarrow 2 \cdot 10^{-6}$

$D \leftarrow 40 \cdot 10^{-9}$

$Q_0 \leftarrow 6 \cdot 10^{-6}$

$\mu_D \leftarrow 6.4 \cdot 10^{-14}$

$w_0 \leftarrow 0.3 \cdot D$

$i_0 \leftarrow 0$

$Ron \leftarrow 100$

$Roff \leftarrow 10000$

$\omega \leftarrow 8 \cdot \pi$

$t_0 \leftarrow 0$

for $j \in 0 .. 199998$

$t_{j+1} \leftarrow (j + 1) \cdot \delta$

$M_j \leftarrow Ron \cdot \left(\frac{w_j}{D} \right) + Roff \cdot \left(1 - \frac{w_j}{D} \right)$

$u_{j+1} \leftarrow 1 \cdot \sin\left(\omega \cdot t_{j+1}\right)$

$i_{j+1} \leftarrow \frac{u_{j+1}}{M_j}$

$v_{j+1} \leftarrow \frac{D}{Q_0} \cdot i_{j+1} \cdot \frac{w_j \cdot \left(D - w_j\right)}{D^2}$

$w_{j+1} \leftarrow v_{j+1} \cdot \left(t_{j+1} - t_j\right) + w_j$

$x_{j+1} \leftarrow \frac{w_{j+1}}{D}$

$q_{j+1} \leftarrow \frac{\frac{1}{\omega} \cdot \left(1 - \cos\left(\omega \cdot t_{j+1}\right)\right)}{M_j}$

t

w

u

i

q

$s \leftarrow augment(t, i, q, x, u)$

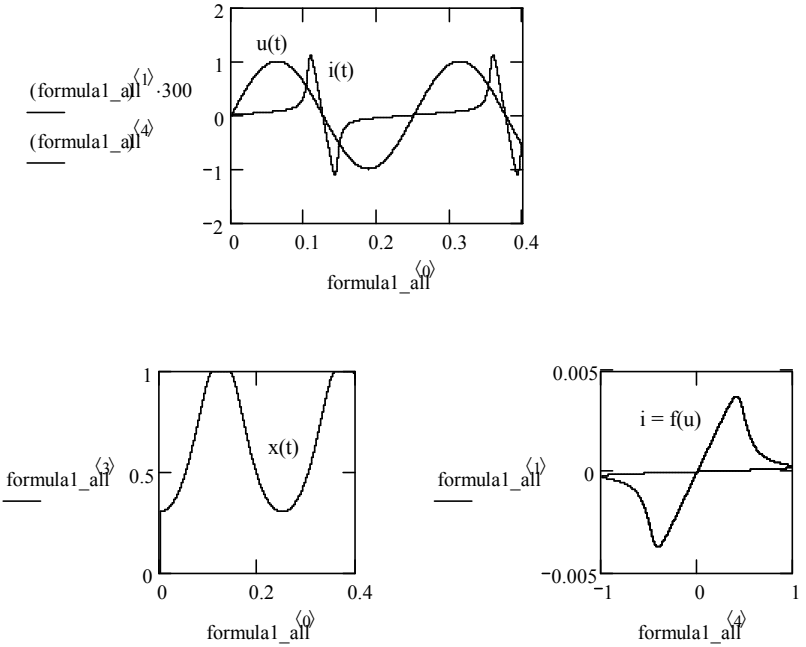

Fig. 2.9. Characteristics of the nonlinear model of the memristor with the window function $f(x) = x - x^2$

The results of simulation of nonlinear model with the same parameters, but with window function a different $f(x) = 1 - (2x-1)^{2p}$ are shown in Fig. 2.10.

Comparing the graphs in Fig. 2.9 (p = 1) and Fig. 2.10 (p = 9), we note a significant influence of the parameter p on the current-voltage characteristic of the memristor.

The dynamic models of the linear and the nonlinear memristors are considered. The following conclusions can be obtained from these results.

Nonlinear models give results closer to the experimental data obtained in the research of real physical samples in comparison with the linear models. Nonlinear models with the respective window functions provide a more complete understanding of the dynamics of the processes.

formula1_all :=

$\delta \leftarrow 2 \cdot 10^{-6}$

$p \leftarrow 9$

$D \leftarrow 40 \cdot 10^{-9}$

$Q_0 \leftarrow 6 \cdot 10^{-6}$

$\mu_D \leftarrow 6.4 \cdot 10^{-14}$

$w_0 \leftarrow 0.3 \cdot D$

$i_0 \leftarrow 0$

$Ron \leftarrow 100$

$Roff \leftarrow 10000$

$\omega \leftarrow 8 \cdot \pi$

$t_0 \leftarrow 0$

for $j \in 0 .. 199998$

$t_{j+1} \leftarrow (j + 1) \cdot \delta$

$M_j \leftarrow Ron \cdot \left(\frac{w_j}{D} \right) + Roff \cdot \left(1 - \frac{w_j}{D} \right)$

$u_{j+1} \leftarrow 1 \cdot \sin\left(\omega \cdot t_{j+1} \right)$

$i_{j+1} \leftarrow \frac{u_{j+1}}{M_j}$

$v_{j+1} \leftarrow \frac{D}{Q_0} \cdot i_{j+1} \cdot \left[1 - \left(\frac{2 \cdot w_j}{D} - 1 \right)^{2 \cdot p} \right] \cdot \frac{1}{4}$

$w_{j+1} \leftarrow v_{j+1} \cdot \left(t_{j+1} - t_j \right) + w_j$

$x_{j+1} \leftarrow \frac{w_{j+1}}{D}$

$q_{j+1} \leftarrow \frac{\frac{1}{\omega} \cdot \left(1 - \cos\left(\omega \cdot t_{j+1} \right) \right)}{M_j}$

t

w

u

i

q

$s \leftarrow augment\ (t, i, q, x, u)$

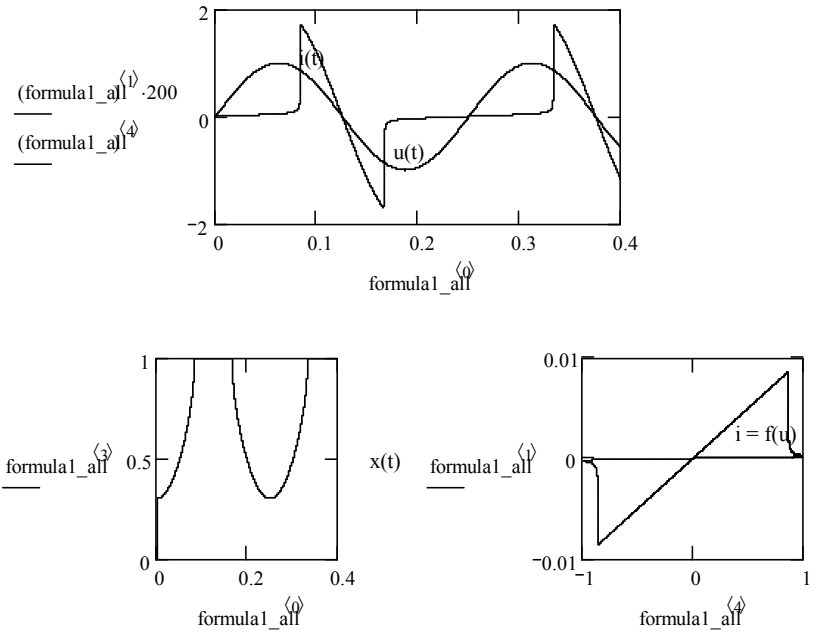

Fig. 2.10. Characteristics of the nonlinear model of the memristor with the window function $f(x) = 1 - (2x-1)^{2p}$ with the parameter $p = 9$

INTERPRETATION OF THE MEMRISTOR IN THE THEORY OF ELECTROMAGNETISM

- Electromagnetic properties of the medium
- Memristance and the memristive medium

3.1 Electromagnetic properties of the medium

When the separate concepts of the circuit theory are not applicable, the only possible methods of the research are methods of the electromagnetic field theory. The electromagnetic processes are characterized by the point values namely electric and magnetic fields, intensity, current densities and others.

In the study of electromagnetic fields it is necessary to consider the characteristics of the medium in each point namely the specific electric conductivity, permittivity and absolute magnetic permeability.

To characterize the properties of electric and magnetic circuits some constants called parameters of the circuit are used: the resistance, the inductance and the capacitance, which characterize any separate sections of the circuits (circuits with the lumped parameters), or their unit length (circuits with the distributed parameters), [103].

It is known that if a voltage is applied to the capacitor plates, the electric charges will accumulate on them. Similarly, the current flow through the coil causes the storage of the magnetic energy on this element. If the current flows through the resistor then at its terminals the potential difference occurs (the voltage). The inductance and the capacitance store the energy, while the resistor converts the electrical energy into heat. These well-known conclusions are in full accordance with Maxwell's electromagnetic theory. The fundamental relations which connect the electric current, density of the electric and magnetic fluxes with the electric and magnetic field intensity, have one correspondence with the equations of the electric circuit elements.

The study of the memristors is usually focused on the examination of the behavior of the current-voltage characteristics, but the relationships between the magnetic flux and charges are not fully taken into account.

First of all, let's consider the correspondence between the circuit theory and the electromagnetism.

Well-known elements of the electrical circuits R, L and C are given by the respective ratios:

$$v = iR, \quad q = Cv, \quad \Phi = Li,$$

that connect the electric and the magnetic quantities with each other.

The fundamental equations of electromagnetism can be written as:

$$\vec{\delta} = \gamma \vec{E}, \qquad \vec{D} = \varepsilon_a \vec{E}, \qquad \vec{B} = \mu_a \vec{H},$$

where $\vec{\delta}$ is the density of the conduction current, $\vec{D}$ is the vector of the electric induction (electric displacement), $\vec{B}$ is the vector of the magnetic induction, $\vec{E}, \vec{H}$ are the vectors of the electric and magnetic field intensity respectively. The medium is characterized conductivity γ, and the absolute values of the electric and magnetic permeability ($\varepsilon_0 = \frac{1}{36\pi} 10^{-9} \frac{\text{F}}{\text{m}}, \mu_0 = 4\pi \cdot 10^{-7} \frac{\text{H}}{\text{m}}, \varepsilon_a = \varepsilon_0 \varepsilon$, $\mu_a = \mu_0 \mu$). These values are used in electromagnetism are equivalent to the resistance, the inductance and the capacitance in the circuit theory. For example, the permittivity is connected with the capacitance and its unit is $\left[\frac{\text{F}}{\text{m}}\right]$. It is important to note that the values γ, ε, μ that correspond to the electrical circuit elements R, L, C represent the electromagnetic properties of the medium.

3.2 Memristance and the memristive medium

As is known, the memristor relates the magnetic flux Φ with the electric charge q by the ratio:

$$\Phi = M(q)q,$$

where M is the memristance of the element.

We introduce the following relation [23], [82]:

$$\vec{\mathbf{B}} = \chi \vec{\mathbf{D}}.$$

which is the electromagnetic equivalent of the equation $\Phi = M(q)q$, where the value χ is specific memristance of the medium. This equation states that the density of the electrical flux $\left[\frac{\mathrm{V}}{\mathrm{m}^2}\right]$ leads to creation of the magnetic flux density in the memristive medium.

Let's apply the divergence operation to both sides of the equation:

$$\mathrm{div}\vec{\mathbf{B}} = \chi \mathrm{div}\vec{\mathbf{D}},$$

which is true for a homogeneous and isotropic memristive medium.

As is known, the divergence of the electric flux density is equal to the volume density of the charge ρ in a certain volume V, that is $\mathrm{div}\vec{\mathbf{D}} = \rho_v$ and hence we have

$$\mathrm{div}\vec{\mathbf{B}} = \chi\rho_v.$$

This equation represents the effect of the memristance of the medium in terms of Maxwell's equations. In fact, the divergence of the magnetic induction is zero, since there is naturally no magnetic charge density. However, in the field theory (in particular, when we consider the propagation of electromagnetic waves and antennae theory) the concept of fictitious magnetic charges in the right part of the Maxwell equations is introduced. This technique is used in the simulation of electromagnetic processes in certain types of antennas.

For example, the loop antenna can be represented by an equivalent symmetric dipole antenna, on which a so-called magnetic current flows. This configuration produces the same electromagnetic field at a point of observation, like a loop antenna. But such mathematical models do not give any physical understanding about the existence of magnetic monopoles.

The equation $\mathrm{div}\vec{\mathbf{B}} = \chi\rho_v$ can be transformed in accordance with the theorem of Gauss.

As is known, the flux of the vector $\vec{\mathbf{A}}$ through a closed surface S is equal to the integral of $\mathrm{div}\vec{\mathbf{A}}$. The integral is taken over the volume bounded by this surface:

$$\oint_S \vec{\mathbf{A}}\mathbf{d}\vec{\mathbf{S}} = \int_V \mathrm{div}\vec{\mathbf{A}}dV..$$

Then we can write:

$$\oint_S \vec{\mathbf{B}}d\vec{\mathbf{S}} = \left| \oint_S \vec{\mathbf{A}}d\vec{\mathbf{S}} = \int_V \mathrm{div}\vec{\mathbf{A}}dV \right| = \int_V \mathrm{div}\vec{\mathbf{B}}dV = \left| \mathrm{div}\vec{\mathbf{B}} = \chi\rho_v \right| = \chi\int_V \rho_v dV,$$

where V is the volume surrounding the charges; S is a closed surface bounded by volume V; $\mathbf{d}\vec{\mathbf{S}} = \vec{\mathbf{n}}dS$, $\vec{\mathbf{n}}$ is the unit vector which is normal to the surface dS.

The electromagnetic properties of the medium within the volume may be modeled by the value χ. The obtained equation says that electric charges accumulated in memristive medium, create a magnetic flux density which permeates the closed surface bounded by the volume. Note that the equation $\mathrm{div}\vec{\mathbf{B}} = \chi\rho_v$ is true as well for the static case, when the charges and the field does not change over time.

Let's assume the existence of a certain density of the external current $\vec{\boldsymbol{\delta}}_{\text{ext}}$ in the memristive medium. First of all, we introduce the continuity equation of the form:

$$\mathrm{div}\vec{\boldsymbol{\delta}}_{\text{ext}} + \frac{\partial\rho_v}{\partial t} = 0,$$

where $\vec{\boldsymbol{\delta}}_{\text{ext}}$ is the external conduction current density produced by external energy sources, [103].

In accordance with the first Maxwell's equation:

$$\mathrm{rot}\vec{\mathbf{H}} = \frac{\partial\vec{\mathbf{D}}}{\partial t} + \vec{\boldsymbol{\delta}}_{\text{ext}} + \gamma\vec{\mathbf{E}},$$

where γ is the electrical conductivity of the medium $\left[\frac{1}{\Omega\cdot\mathrm{m}}\right]$, and $\gamma\vec{\mathbf{E}} = \vec{\boldsymbol{\delta}}$ is the conduction current density produced by the motion of charges in the presence of the field $\vec{\mathbf{E}}$.

The second Maxwell's equation can be written as

$$\mathrm{rot}\,\vec{\mathbf{E}} = -\frac{\partial\vec{\mathbf{B}}}{\partial t} + \vec{\mathbf{M}},$$

where $\vec{\mathbf{M}}$ is some unknown vector.

Let's carry out the operation of divergence on the left and right hand sides of the equation:

$$\text{divrot}\vec{\mathbf{E}} = \text{div}\vec{\mathbf{M}} - \text{div}\left[\frac{\partial \vec{\mathbf{B}}}{\partial t}\right].$$

From vector analysis it is known that $\text{divrot}\vec{\mathbf{A}} = 0,$ then we get

$$\text{div}\vec{\mathbf{M}} - \frac{\partial}{\partial t}\text{div}\vec{\mathbf{B}} = 0.$$

Taking into account that $\text{div}\vec{\mathbf{B}} = \chi \text{div}\vec{\mathbf{D}}$, $\text{div}\vec{\mathbf{D}} = \rho_V$, we can write:

$$\text{div}\vec{\mathbf{M}} - \chi\frac{\partial \rho_V}{\partial t} = 0,$$

from which we obtain:

$$\text{div}\vec{\mathbf{M}} + \chi \text{div}\vec{\boldsymbol{\delta}}_{\text{ext}} = 0,$$

and hence

$$\vec{\mathbf{M}} = -\chi\vec{\boldsymbol{\delta}}_{\text{ext}}.$$

Let's write the second Maxwell's equation in the form:

$$\text{rot}\vec{\mathbf{E}} = -\frac{\partial \vec{\mathbf{B}}}{\partial t} - \chi\vec{\boldsymbol{\delta}}_{\text{ext}} - \vec{\boldsymbol{\delta}}_{\text{ext m}} = -\frac{\partial \vec{\mathbf{B}}}{\partial t} - \chi\vec{\boldsymbol{\delta}}_{\text{ext}} - \gamma_{\text{m}}\vec{\mathbf{H}},$$

where γ_{m} is the specific magnetic conductivity $\left[\frac{\Omega}{\text{m}}\right]$.

The equation

$$\text{rot}\vec{\mathbf{E}} = -\frac{\partial \vec{\mathbf{B}}}{\partial t} - \chi\vec{\boldsymbol{\delta}}_{\text{ext}} - \gamma_{\text{m}}\vec{\mathbf{H}},$$

represents an enhanced version of the second Maxwell's equations in the memristive medium.

Let's apply the operation of divergence for the second Maxwell's equation:

$$\operatorname{divrot}\vec{\mathbf{E}} = -\frac{\partial}{\partial t}\operatorname{div}\vec{\mathbf{B}} - \chi\operatorname{div}\vec{\boldsymbol{\delta}}_{\text{ext}} - \gamma_{\text{m}}\operatorname{div}\vec{\mathbf{H}}$$

$$= \left| \operatorname{div}\vec{\mathbf{H}} = \frac{1}{\mu_a}\operatorname{div}\vec{\mathbf{B}},\ \ \operatorname{div}\vec{\mathbf{B}} = \chi\rho_V \right|$$

$$= \chi\left[\frac{\partial\rho_V}{\partial t} + \operatorname{div}\vec{\boldsymbol{\delta}}_{\text{ext}} + \frac{\gamma_{\text{m}}}{\mu_a}\rho_V \right] = 0.$$

According to Stokes' theorem

$$\oint_L \vec{\mathbf{A}}\mathbf{d}\vec{\mathbf{l}} = \int_S \operatorname{rot}\vec{\mathbf{A}}dS$$

we can write:

$$\oint_L \vec{\mathbf{E}}\mathbf{d}\vec{\mathbf{l}} = \int_S \left[\frac{\partial\vec{\mathbf{B}}}{\partial t} + \chi\vec{\boldsymbol{\delta}}_{\text{ext}} + \gamma_{\text{m}}\vec{\mathbf{H}} \right]\mathbf{d}\vec{\mathbf{S}}.$$

This equation means that the time variation of the magnetic induction, the density of the conduction currents through the surface S of the memristive medium creates the electric field along a loop L that surrounds this surface.

On the other hand, as was already noted, the memristive system has a memory property. The memristor satisfies to the expression

$$\Phi = Mq \Rightarrow \left| \begin{matrix} \Phi = \int v(t)dt \\ q = \int i(t)dt \end{matrix} \right| \Rightarrow \int v(t)dt = M\int i(t)dt,$$

which may be transformed as following:

$$\int (v - Mi)dt = 0.$$

The respective expression that satisfies this equation is written in the form:

$$v(t) = Mi(t) + C,$$

where the constant C is the integration constant. The memristor remembers (mathematically) its previous state because of this constant

[82], [37]. Taking into account the equation $\vec{\mathbf{B}} = \chi\vec{\mathbf{D}}$ which defines the memristive medium we may write that

$$\frac{\partial\vec{\mathbf{B}}}{\partial t} = \chi\frac{\partial\vec{\mathbf{D}}}{\partial t},$$

if we differentiate over time both sides of the equation. From Maxwell's equations it follows (under the condition that $\gamma = 0$) that

$$\mathrm{rot}\vec{\mathbf{H}} = \frac{\partial\vec{\mathbf{D}}}{\partial t}, \qquad \mathrm{rot}\vec{\mathbf{E}} = -\frac{\partial\vec{\mathbf{B}}}{\partial t}.$$

Then we obtain the equation

$$\mathrm{rot}\vec{\mathbf{E}} = -\chi\mathrm{rot}\vec{\mathbf{H}},$$

which can be transformed as

$$\mathrm{rot}\left\{\vec{\mathbf{E}} + \chi\vec{\mathbf{H}}\right\} = 0.$$

From vector analysis it follows that

$$\mathrm{rotgrad}w = 0,$$

where w is the scalar function.

Then it is obvious that the equation

$$\vec{\mathbf{E}} + \chi\vec{\mathbf{H}} = \mathrm{grad}\, w = \nabla w$$

satisfies to the equation obtained above.

Thus, the equation

$$\vec{\mathbf{E}} = -\chi\vec{\mathbf{H}} + \nabla w$$

is an analogue of the equation $v = Mi + C$. The memristive medium remembers its last state according to the presence of the term ∇w as in the memristor.

Thus, if in accordance with the definition the memristor set the ratio between the magnetic flux and electric charge, then from the standpoint of electromagnetic theory, this expression can be written as the ratio

between the electric $\vec{\mathbf{D}}$ and magnetic $\vec{\mathbf{B}}$ induction. This approach leads to two equations:

$$\operatorname{div}\vec{\mathbf{B}} = \chi\rho_V,$$

$$\operatorname{rot}\vec{\mathbf{E}} = -\frac{\partial\vec{\mathbf{B}}}{\partial t} - \chi\vec{\boldsymbol{\delta}}_{\text{ext}} - \gamma_{\text{m}}\vec{\mathbf{H}},$$

which are an extension of Maxwell's equations (the so-called Maxwell-Gauss and the Faraday-Maxwell) in the memristive medium. The equation $\operatorname{div}\vec{\mathbf{B}} = \chi\rho_V$ says that the density of the electrical charge creates a magnetic induction $\vec{\mathbf{B}}$ instead of electrical induction in the memristive medium. The second equation indicates that the electric current density will induce the electric field $\vec{\mathbf{E}}$ in the memristive medium.

Let's consider the interpretation of the memristor from the position of the electromagnetic field, given in [23], in which the concept of the so-called quasi-static expansion of Maxwell's equations was used. This representation is usually used when we need to give an explanation of the fundamental elements of the electrical circuits within the electromagnetic field theory.

Let's write the system of Maxwell's equations in differential form, [103]:

$$\operatorname{rot}\vec{\mathbf{H}} = \frac{\partial\vec{\mathbf{D}}}{\partial t} + \vec{\boldsymbol{\delta}}, \qquad \operatorname{rot}\vec{\mathbf{E}} = -\frac{\partial\vec{\mathbf{B}}}{\partial t},$$

$$\operatorname{div}\vec{\mathbf{D}} = \rho, \qquad \operatorname{div}\vec{\mathbf{B}} = 0,$$

where, as before, $\vec{\mathbf{E}}$ is the electric field intensity, $\vec{\mathbf{D}}$ is the electric induction, $\vec{\mathbf{B}}$ is the magnetic induction, $\vec{\mathbf{H}}$ is the magnetic field intensity, $\vec{\delta}$ is the density of the electrical conduction current, ρ is the volume density of the electric charge.

The idea of a quasi-static expansion includes a process of successive approximations for **the electromagnetic fields, which change over time**. This approach allows to study the electrical circuits in which temporal changes of the electromagnetic fields are quite slow. It is typical for the particular case of the electric circuits.

Let's consider a complete family of electromagnetic fields, for which their rate of change over time is variable. The family of these fields can be described by a parameter α, which is the rate of change of the charge density ρ over time.

Introducing the variable $\tau = \alpha t$, we can write the respective derivatives of the fields with respect to time as follows:

$$\frac{\partial \vec{\mathbf{B}}}{\partial t} = \frac{\partial \vec{\mathbf{B}}}{\partial \tau}\frac{\partial \tau}{\partial t} = \alpha \frac{\partial \vec{\mathbf{B}}}{\partial \tau}, \qquad \frac{\partial \vec{\mathbf{D}}}{\partial t} = \alpha \frac{\partial \vec{\mathbf{D}}}{\partial \tau}.$$

Maxwell's equations in this case take the form of:

$$\operatorname{rot} \vec{\mathbf{H}} = \vec{\boldsymbol{\delta}} + \alpha \frac{\partial \vec{\mathbf{D}}}{\partial \tau}, \qquad \operatorname{rot} \vec{\mathbf{E}} = -\alpha \frac{\partial \vec{\mathbf{B}}}{\partial \tau},$$

which allow to consider the different values of the variable τ corresponding to different time scales of the excitations. In these equations the vectors $\vec{\mathbf{E}}$, $\vec{\mathbf{D}}$, $\vec{\mathbf{B}}$, $\vec{\mathbf{H}}$ and the vector $\vec{\delta}$ are also functions α and τ together with the space coordinates x, y, z.

Let's expand, for example, the vector $\vec{\mathbf{E}}$ by the extent α:

$$\vec{\mathbf{E}}(x, y, z, \alpha, \tau) = \vec{\mathbf{E}}_0(x, y, z, \tau) + \alpha \vec{\mathbf{E}}_1(x, y, z, \tau) + \alpha^2 \vec{\mathbf{E}}_2(x, y, z, \tau) + \ldots,$$

where the terms of the first and the second order are:

$$\vec{\mathbf{E}}_0(x, y, z, \tau) = \left[\vec{\mathbf{E}}(x, y, z, \alpha, \tau) \right]_{\alpha=0}, \quad \vec{\mathbf{E}}_1(x, y, z, \tau) = \left[\frac{\partial \vec{\mathbf{E}}(x, y, z, \alpha, \tau)}{\partial \alpha} \right]_{\alpha=0}.$$

The similar expansions we may write for other vectors of the electromagnetic field and substitute into the Maxwell's equations. Then we have, for example, the expression for $\operatorname{rot} \vec{\mathbf{E}}$ as following:

$$\operatorname{rot} \vec{\mathbf{E}} = \operatorname{rot} \vec{\mathbf{E}}_0 + \alpha \operatorname{rot} \vec{\mathbf{E}}_1 + \alpha^2 \operatorname{rot} \vec{\mathbf{E}}_2 + \ldots$$

It is evident that the second equation of the system may be written in the form:

$$\operatorname{rot} \vec{\mathbf{E}}_0 + \alpha \left[\operatorname{rot} \vec{\mathbf{E}}_1 + \frac{\partial \vec{\mathbf{B}}_0}{\partial \tau} \right] + \alpha^2 \left[\operatorname{rot} \vec{\mathbf{E}}_2 + \frac{\partial \vec{\mathbf{B}}_1}{\partial \tau} \right] + \ldots = 0,$$

which must be satisfied for all values α. It is truth if the coefficients α of all degrees are separately equaled zero. By analogy we may write the first equation of the system. In general, we obtain the so-called Maxwell's equations of the *n*-th order, *n* = 0, 1, 2… For example Maxwell's equations of the zero order are written in the form:

$$\operatorname{rot}\vec{\mathbf{H}}_0 = \vec{\boldsymbol{\delta}}_0, \qquad \operatorname{rot}\vec{\mathbf{E}}_0 = 0,$$

the equations of the second order are written as follows:

$$\operatorname{rot}\vec{\mathbf{H}}_1 = \vec{\boldsymbol{\delta}}_1 + \frac{\partial\vec{\mathbf{D}}_0}{\partial\tau}, \qquad \operatorname{rot}\vec{\mathbf{E}}_1 = -\frac{\partial\vec{\mathbf{B}}_0}{\partial\tau}.$$

To obtain the expressions describing the quasi-static electromagnetic field we have to take into account only the first two terms of expansion neglecting by the rest terms and assuming that $\alpha = 1$. Then the approximation of the vectors of the electromagnetic field is written in the form:

$$\vec{\mathbf{E}} \approx \vec{\mathbf{E}}_0 + \vec{\mathbf{E}}_1, \qquad \vec{\boldsymbol{\delta}} \approx \vec{\boldsymbol{\delta}}_0 + \vec{\boldsymbol{\delta}}_1$$

$$\vec{\mathbf{D}} \approx \vec{\mathbf{D}}_0 + \vec{\mathbf{D}}_1, \qquad \vec{\mathbf{H}} \approx \vec{\mathbf{H}}_0 + \vec{\mathbf{H}}_1, \qquad \vec{\mathbf{B}} \approx \vec{\mathbf{B}}_0 + \vec{\mathbf{B}}_1.$$

Three fundamental elements, namely, the resistor, the inductor and the capacitor, may be analyzed as the electromagnetic systems, whose quasi-static solutions corresponds to some combinations of solutions of the first and second order equations.

However, in such explanation the following connection was not considered. It is case when the electromagnetic fields of the first order are connected between each other. But the electromagnetic fields of the zero order in comparison with the fields of the first order are epsilon squared and may be ignored.

It was assumed [23] that the two terminals device exists in which the vectors $\vec{\mathbf{B}}_1$ and $\vec{\mathbf{D}}_1$ are connected some equation in which these values are considered simultaneously. At the same time the device is made from the nonlinear material for which the fields of the first order are connected.

Let's assume that relationships between the fields of the first order are written in the form:

$$\vec{\mathbf{B}}_1 = \mathcal{B}(\vec{\mathbf{H}}_1), \qquad \vec{\mathbf{D}}_1 = \mathfrak{D}(\vec{\mathbf{E}}_1), \qquad \vec{\boldsymbol{\delta}}_1 = \mathcal{A}(\vec{\mathbf{E}}_1),$$

where the functions $\mathcal{B}$, $\mathfrak{D}$ and $\mathcal{A}$ are the continuous functions defined only in the space with the coordinates x, y, z.

Neglecting by the vector $\vec{\mathbf{D}}_0$ in the equation

$$\operatorname{rot}\vec{\mathbf{H}}_1 = \vec{\boldsymbol{\delta}}_1 + \frac{\partial\vec{\mathbf{D}}_0}{\partial\tau},$$

we may write

$$\operatorname{rot}\vec{\mathbf{H}}_1 = \vec{\boldsymbol{\delta}}_1 = \mathrm{A}\left(\vec{\mathbf{E}}_1\right).$$

Since the spatial operator of the differentiation do not contain of the time derivatives, then this relationship shows that the fields of the first order $\vec{\mathbf{H}}_1$ and $\vec{\mathbf{E}}_1$ are connected between each other:

$$\vec{\mathbf{E}}_1 = F(\vec{\mathbf{H}}_1)$$

Then the equation for $\vec{\mathbf{D}}_1$ may be written as:

$$\vec{\mathbf{D}}_1 = \mathfrak{D} \otimes F(\vec{\mathbf{H}}_1),$$

where the operator $\otimes$ is the composition of the two functions. The dependency between $\vec{\mathbf{B}}_1$ and $\vec{\mathbf{H}}_1$ may be rewritten as the inverse dependency:

$$\vec{\mathbf{H}}_1 = \mathcal{B}^{-1}(\vec{\mathbf{B}}_1).$$

The substitution of this expression gives the dependency between the vectors $\vec{\mathbf{D}}_1$ and $\vec{\mathbf{B}}_1$:

$$\vec{\mathbf{D}}_1 = \mathfrak{D} \otimes F \otimes \left[\mathcal{B}^{-1}(\vec{\mathbf{B}}_1)\right] \equiv M(\vec{\mathbf{B}}_1).$$

This equation predicts that the instantaneous relationships may be set between the vectors $\vec{\mathbf{D}}_1$ and $\vec{\mathbf{B}}_1$ that it is realized in the memristor.

Thus the Maxwell's equations may be used for the quasi-static representation of the electromagnetic values in the memristor.

RESEARCHING OF THE ELECTRIC CIRCUITS WITH MEMRISTORS

- Statement of the problem
- Researching of the circuit with the memristor
- Ideal *MC* -circuit with the linear model of the memristor
- Ideal *ML* -circuit with the linear model of the memristor
- *MLC* -circuits with the nonlinear model of the memristor

4.1 Statement of the problem

Let's consider the properties of the ideal memristor. According to the definition the memristor *M* connects the charge q and the magnetic flux Φ in the circuit and supplements such elements as the resistor *R*. the capacitor *C* and the inductor *L* as ingredient of the ideal electric circuits. The properties of elements *R*, *L* and *C* are considered in any standard course of electrical engineering and electronics. Next we will consider the properties of ideal *MC*, *ML* and *MLC* circuits to complete the program of the course.

The properties of the electric circuits including three ideal elements *R*, *L* and *C* are the subject of study of the respective sections of the physic and technical disciplines. These circuits show the wide variety of the processes which occur in them. There are the exponential charge and discharge in the *RC*-circuit with the time constant $\tau_{RC} = RC$, the exponential increase and decrease of the current in the *RL*-circuit with the time constant $\tau_{LR} = \frac{L}{R}$, the undamped oscillations in the ideal LC-circuit with the frequency $\omega_0 = \frac{1}{\sqrt{LC}}$, resonant oscillations in the *RCL*-circuit which are induced by the alternating voltage source with the frequency $\omega \sim \omega_0$.

These ideal circuits are described by the Kirchhoff's laws. The Kirchhoffs Current Law (KCL) follows from the continuity equation, the

Kirchhoffs Voltage Law (KVL) follows from the second Maxwell's equation if the time dependency of the magnetic field created by the current does not take into account. It means that $\oint \vec{\mathbf{E}} d\vec{\mathbf{l}} = 0$, where the line integral of the electric field E is taken along any closed loop in the circuit.

Study of the elementary circuits with the ideal elements provides the using of visual methods and understanding of the real circuits in which each capacitor has final resistance, each energy source has the internal resistance, and each resistor has the inductive component at ultrahigh frequency. It is evident that real electric circuits may be modeled with using considered above three fundamental elements and the ideal voltage source.

As was noted the physic model of the memristor is represented by the resistor whose value is proportional to the charge q which passed through it to some time moment t. It follows from the definition of the memristor and the electromagnetic induction law:

$$d\Phi = Mdq \quad \Rightarrow vdt = M(q)idt \quad \Rightarrow v = M(q)i.$$

To research the characteristics of the electric circuits with the memristors at first we will consider the linear model of the carriers drift to describe the dependency of the effective resistance of the memristor (that is the memristance) from the charge q, which passed through it.

Such simplification allows to obtain the analytical complete results. Next we will show that the time constant of the damped charge (damped current) in the ideal $MC(ML)$ circuit depends on the polarity of the memristor.

4.2 Researching of the circuit with the memristor

The scheme of the electric circuit with the memristor is shown in Fig. 4.1.

The value of the effective resistance of the memristor is defined according to the general expression:

$$M(q) = \frac{w}{D} R_{\text{on}} + \left(1 - \frac{w}{D}\right) R_{\text{off}}.$$

The value of the effective resistance of the memristor is defined according to the general expression:

$$M(q) = \frac{w}{D} R_{\text{on}} + \left(1 - \frac{w}{D}\right) R_{\text{off}}.$$

As before, the value w represents the virtual boundary between the doped and undoped regions, the position of which depends on the mobility of the ions (oxygen vacancies) and the value of the applied electric field (voltage), Fig. 4.2.

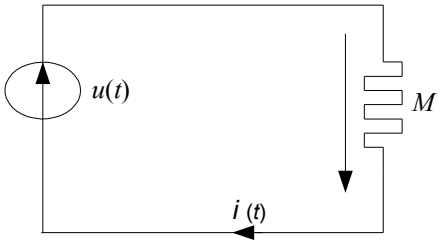

Fig. 4.1. Electrical circuit with the memristor

The current flowing in the memristor is defined by the uniform electric field applied to the memristor:

$$E = \frac{R_{\text{on}}}{D} i(t)$$

The resistance R_{off} is much greater than the resistance R_{on} so that the ratio is $\frac{R_{\text{off}}}{R_{\text{on}}} \sim 10^2 >> 1$ and $\Delta R = R_{\text{off}} - R_{\text{on}} \approx R_{\text{off}}$.

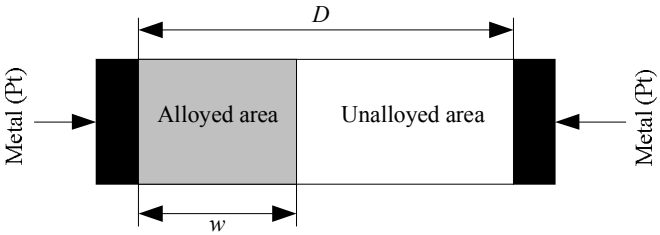

Fig. 4.2. The position of the virtual boundary w

If the alternating voltage $u(t)$ is applied to the terminals of the memristor then the current may be defined from the expression given by KVL:

$$u(t) = M(q)i(t).$$

The properties of the memristor depend on the time dependency of the size of the doped region $w(t)$. For the simplest linear model the virtual boundary between the regions drifts with the constant speed, given by the ratio:

$$v_D = \frac{dw}{dt} = \eta \frac{\mu_D R_{\text{on}}}{D} i(t).$$

Since the drift of the oxygen vacancies may be either expand or constrict the doped region then the polarity of the memristor may be characterized by the coefficient $\eta = \pm 1$, where $\eta = 1$ corresponds to the expansion of the doped region, [34].

It is necessary to note that the switching of the memristor polarity mean change of the voltage source polarity or change of the capacitor plates (in *MC*-circuit), or change of the initial current direction (in *ML*-circuit).

Let's write the expression for the memristance $M(q)$ in the following form (see the section 2.1):

$$M(q) = R_0 - \eta \frac{\Delta R}{Q_0} q(t),$$

where R_0 as before represents the initial value of the memristor resistance (initial memristance):

$$R_0 = R_{\text{on}} \frac{w_0}{D} + R_{\text{off}} \left(1 - \frac{w_0}{D}\right),$$

The obtained expression shows that the memristance $M(q)$ depends on only the charge $q(t)$ which passed through the memristor. Note that for the given value D the memristive effect becomes essential if $\Delta R >> R_0$.

According to the results obtained in the section 2.1 the expressions for the charge $q(t)$ and the current $i(t)$ may be written in the form:

$$q(t) = \frac{Q_0 R_0}{\Delta R}\left[1 - \sqrt{1 - \eta \frac{2\Delta R}{Q_0 R_0^2}\Phi(t)}\right],$$

$$i(t) = \frac{u(t)}{R_0}\frac{1}{\sqrt{1 - \eta \frac{2\Delta R}{Q_0 R_0^2}\Phi(t)}} = \frac{u(t)}{M[q(t)]}.$$

For the linear model of the ideal memristor these equations represent the analytical results which allow to construct the volt-ampere characteristic of the memristor. The equation for $q(t)$ shows that the charge is the function of the magnetic flux according to the general expression $d\Phi = M(q)dq,$ and the equation for $i(t)$ shows that the phase shift between the voltage and the current equals zero in the memristor. It means that the memristor absorbs the energy.

If the alternating voltage $u(t) = U_m \sin \omega t$ is applied to the memristor then the magnetic flux is defined by the ratio:

$$\Phi(t) = \int_0^t u(\tau)d\tau = \frac{U_m}{\omega}(1 - \cos \omega t).$$

It is necessary to note the following

$$U_m \sin(\pi - \omega t) = U_m(\sin \pi \cos \omega t - \cos \pi \sin \omega t) = U_m \sin \omega t,$$

however

$$\Phi(t) = \frac{U_m}{\omega}[1 - \cos(\pi - \omega t)] = \frac{U_m}{\omega}[1 - (\cos \pi \cos \omega t + \sin \pi \sin \omega t)]$$

$$= \frac{U_m}{\omega}[1 + \cos \omega t] \neq \frac{U_m}{\omega}[1 - \cos \omega t].$$

It is evident that the current $i(t)$ will be multi-valued function of the voltage $u(t)$. It follows from the expression for $i(t)$. That's why we

obtain the pinched hysteresis in the volt-ampere characteristic of the memristor, Fig. 4.3.

$$Um := 1 \quad \mu d := 1.1 \cdot 10^{-14} \quad Rof := 1600 \quad Ron := 100$$

$$t := 0, 0.001 .. 6 \quad r := \frac{Rof}{Ron} \quad D := 25 \cdot 10^{-9} \quad Qd := \frac{D^2}{\mu d \cdot Ron}$$

$$w1 := 5 \quad w2 := 6 \quad w3 := 11$$

$$u1(t) := Um \sin(w1 \cdot t) \quad u2(t) := Um \sin(w2 \cdot t) \quad u3(t) := Um \sin(w3 \cdot t)$$

$$\Phi 1(t) := \frac{Um}{w1} \cdot (1 - \cos(w1 \cdot t)) \quad \Phi 2(t) := \frac{Um}{w2} \cdot (1 - \cos(w2 \cdot t)) \quad \Phi 3(t) := \frac{Um}{w3} \cdot (1 - \cos(w3 \cdot t))$$

$$i1(t) := \frac{u1(t)}{Rof \cdot \sqrt{1 - \frac{2 \cdot \mu d \cdot \Phi 1(t)}{r \cdot D^2}}} \quad i2(t) := \frac{u2(t)}{Rof \cdot \sqrt{1 - \frac{2 \cdot \mu d \cdot \Phi 2(t)}{r \cdot D^2}}} \quad i3(t) := \frac{u3(t)}{Rof \cdot \sqrt{1 - \frac{2 \cdot \mu d \cdot \Phi 3(t)}{r \cdot D^2}}}$$

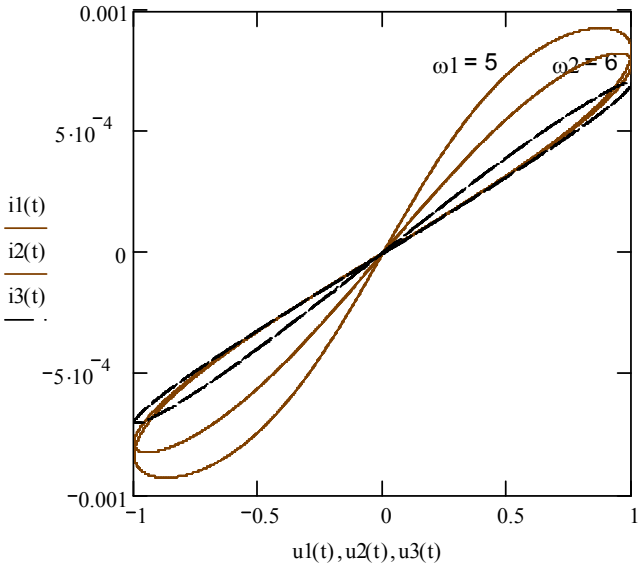

Fig. 4.3. Volt-ampere characteristics of the memristor

Since the value of the magnetic flux is inversely proportional to the frequency ω then the memristive effect dominates only at low frequencies. In this case the following inequality is carried out:

$$\omega < \omega_0 = \frac{2\pi}{t_0},$$

where t_0 is the time interval needed charge carriers to pass the distance D under the applied constant voltage of the value $U_{\max}$. The value t_0 is defined from the expression:

$$t_0 = \frac{D^2}{\mu_D U_{\max}}.$$

The values t_0 and ω_0 provide the respective time scale for the memristive circuit.

The obtained results are correct for the linear model of transfer of the charge carriers. At the same time the model is correct when the charge passing through the memristor is less than $q_{\max}(t) = Q_0\left(1 - \frac{w_0}{D}\right)$ for the case $\eta = 1$ or $q_{\max}(t) = Q_0 \frac{w_0}{D}$ for the case $\eta = -1$.

It is easy to obtain the variety of the characteristics $\{i(t), u(t)\}$ for the different values of the frequency ω using written above the equations for $i(t)$ and $u(t)$. The respective theoretical curves of the volt-ampere characteristics of the memristor are shown in Fig. 4.3.

If the frequency decreases then the size of the doped region increases and the value of the memristance decreases. Thus the "size" of the hysteresis loop is inversely proportional to the frequency ω.

At high frequencies the size of the doped region practically does not change.

Thus the effect of memristance occurs when the size of the active region of the memristor is within nanoscale. It is explained by the fact that mobility of carriers is respectively low.

Let's consider the ideal electric circuit with two series connected memristors. It follows from KVL if two memristors have the same polarity ($\eta_1 = \eta_2$) then the values of memristances are added like the resistances of two resistors in series (Fig. 4.4, *a*):

$$M_{\Sigma}\ (\mathrm{q}) = (R_{01} + R_{02}) - \eta \frac{(\Delta R_1 + \Delta R_2) q(t)}{Q_0}.$$

The memristive effect is retained because the doped regions in both memristors are expanded or constricted simultaneously.

In the case of the opposite polarities (Fig. 4.4, *b*) we have $\eta_1 \eta_2 = -1$ and the terms depending on the charge $q(t)$ are abstracted (suppressed). Then the equivalent memristance is

$$M_{\Sigma}\ (q) = (R_{01} + R_{02}) - \eta \frac{(\Delta R_1 - \Delta R_2) q(t)}{Q_0}.$$

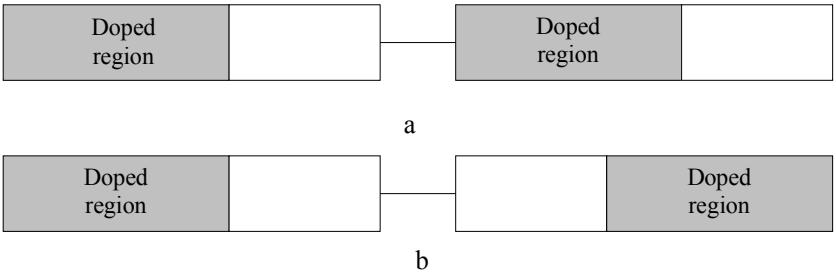

Fig. 4.4. Series connected memristors

4.3 Ideal *MC*-circuit with the linear model of the memristor

Let's consider the electric circuit with the series connected the ideal memristor and the capacitor without the voltage source. We assume that the capacitor has the initial charge q_0, Fig. 4.5.

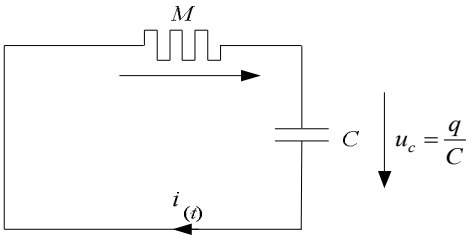

Fig. 4.5. The circuit of discharge of the capacitor

The effective resistance of the memristor is defined its polarity (that is the doped region either increases or decreases).

The decat time constant of *MC*-circuit depends on the resistance of the memristor and therefore discharge of the capacitor will depend on the polarity of the memristor. According to the KVL we may write:

$$M_C[q(t)]\frac{dq}{dt}+\frac{q}{C}=0,$$

where $q(t)$ is the charge on the capacitor, $\frac{dq}{dt}$ is the current in the circuit.

The value of the memristance as was shown above is defined by the relationship:

$$M[q(t)]=R_0-\eta\frac{\Delta R}{Q_0}q(t).$$

Taking into account that the initial charge on the capacitor equals q_0 and $q(t)$ is the charge remaining at the moment *t* then it is evident that the value of the charge which passed through the memristor is defined as:

$$M_C[q(t)]=R_0-\eta\Delta R\frac{q_0-q(t)}{Q_0}.$$

Substituting the value M_C into the KVL equation we obtain the nonlinear differential equation:

$$\frac{dq}{dt}=-\frac{q}{CM_C[q(t)]}=\frac{q}{CR_0-C\eta\Delta R\frac{q_0}{Q_0}+C\eta\Delta R\frac{q}{Q_0}}=-\frac{q}{a+bq},$$

where

$$a=C\left[R_0-\eta\frac{\Delta Rq_0}{Q_0}\right],\quad b=\frac{\eta\Delta RC}{Q_0}.$$

The analytical solution of the differential equation leads to the implicit equation:

$$q(t) = \frac{q_0 \exp\left[-\frac{t}{M_0 C}\right] \exp\left[\frac{\eta \Delta R}{M_0 Q_q} q_0\right]}{\exp\left[\frac{\eta \Delta R}{M_0 Q_q} q(t)\right]}$$

$$= q_0 \exp\left[-\frac{t}{M_0 C}\right] \exp\left[\frac{\eta \Delta R}{M_0 Q_q}[q_0 - q(t)]\right],$$

where the value

$$M_0 = R_0 - \eta \frac{\Delta R q_0}{Q_0}$$

represents the value of the memristance when the total charge q_0 passed through the memristor. If we substitute the time moment $t = 0$ then we obtain

$$q(t)\big|_{t=0} = q_0 .$$

The initial value of the discharge current $i(0)$ we may calculate from the initial equation:

$$M_C(q) \frac{dq}{dt}\Big|_{t=0} + \frac{q_0}{C} = 0.$$

Since

$$M_C[q(0)] = M_C[q_0] = R_0 - \eta \Delta R \frac{q_0 - q_0}{Q_0} = R_0,$$

then the initial value of the current is:

$$i(0) = \frac{dq}{dt}\Big|_{t=0} = -\frac{q_0}{M_C(q_0) C} = -\frac{q_0}{R_0 C}.$$

The numerical integration of the nonlinear differential equation gives $q - t$ graphs shown in Fig. 4.6.

formula1_all :=

$\delta \leftarrow 10^{-4}$

$D \leftarrow 5 \cdot 10^{-8}$

$q_0 \leftarrow 2 \cdot 10^{-4}$

$Q_0 \leftarrow 10^{-3}$

$c \leftarrow 1 \cdot 10^{-6}$

$w_0 \leftarrow 0.5 \cdot D$

$i_0 \leftarrow 0$

$R_{on} \leftarrow 100$

$R_{off} \leftarrow 2000$

$n \leftarrow 1$

$t_0 \leftarrow 0$

for $j \in 0..30$

$t_{j+1} \leftarrow j \cdot \delta$

$w_{j+1} \leftarrow w_j - n \cdot \frac{D}{Q_0} \cdot i_j \cdot \delta$

$i_{j+1} \leftarrow \frac{-q_j}{c \cdot \left[\frac{w_{j+1}}{D} \cdot R_{on} + \left(1 - \frac{w_{j+1}}{D} \right) \cdot R_{off} \right]}$

$q_{j+1} \leftarrow q_j + i_{j+1} \cdot \delta$

t

i

q

$s \leftarrow \text{augment}(t, i, q, w)$

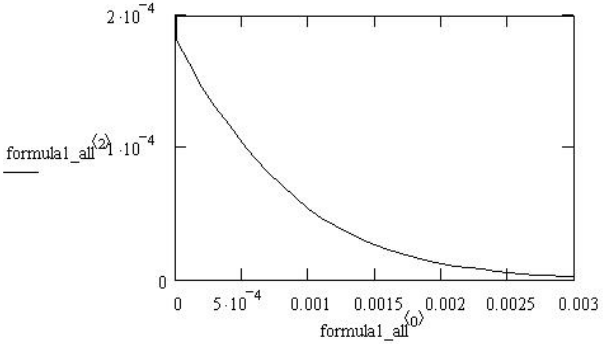

Fig. 4.6. The numerical integration of the nonlinear differential equation gives $q-t$ graph

It is evident that the initial value of the current in the considered circuit does depend on the polarity of the memristor η. For great values of the argument t the charge of the capacitor $q(t)$ decreases according to the exponential law.

Since the decreasing or increasing of the memristance depends on the polarity of the memristor then *MC*-circuit will discharge faster for $\eta = 1$ than *RC*-circuit with the same resistance R_0. The *RC*-circuit will discharge faster than the *MC*-circuit with $\eta = -1$, Fig. 4.7.

The solution $q(t)$ obtained for the linear model of drift of the charge carriers is correct for the charge

$$q_0 \le Q_0\left(1 - \frac{w_0}{D}\right), \quad \eta = 1.$$

In this case the memristance $M_0 \ge R_{\text{on}}$ and is the positive value.

By analogy we may consider the ideal *MC*-circuit containing the direct voltage source V_0 and the discharged capacitor ($q_0 = 0$). This problem is solved as the inverse task for the considered above *MC*-circuit with the capacitor charged to the value $q_0 = V_0 C$ without the voltage source.

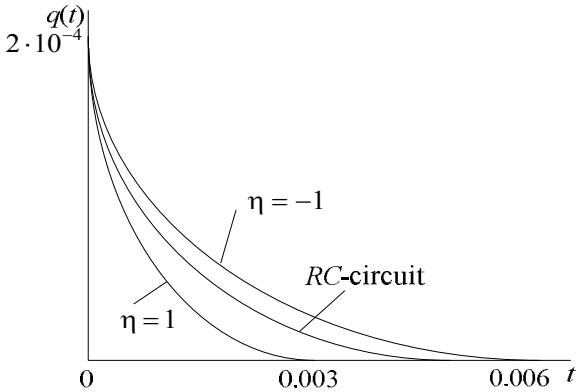

Fig. 4.7. Graphs $q(t)$ for different values of η

4.4 Ideal *ML*-circuit with the linear model of the memristor

Ass known the ideal *RC*- and *RL*-circuits are described by the same (on structure) differential equations:

$$RC \quad \Rightarrow \quad R\frac{dq}{dt}+\frac{q}{C}=0, \qquad RL \quad \Rightarrow \quad L\frac{di}{dt}+iR=0$$

.

Taking into account that the time constants are equal to

$$\tau_{RC}=RC, \quad \tau_{RL}=\frac{L}{R},$$

we may write

$$RC \quad \Rightarrow \quad \frac{dq}{dt}+\frac{q}{\tau_{RC}}=0, \qquad RL \quad \Rightarrow \quad \frac{di}{dt}+\frac{i}{\tau_{RL}}=0$$

with the initial conditions q_0 and i_0.

That's why the transients in such circuits have the identical solutions:

$$q(t)=q_0\exp\left[-\frac{t}{\tau_{RC}}\right], \qquad i(t)=i_0\exp\left[-\frac{t}{\tau_{RL}}\right].$$

However for the *MC*- and *ML*-circuits such equivalence is not correct.

Let's consider the ideal *ML*-circuit with the initial current i_0, Fig. 4.8.

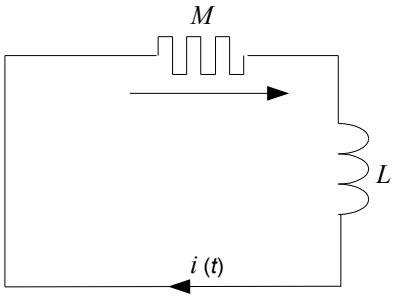

Fig.4.8. Electric $ML-$ circuit with the initial current

According to the KVL we may write:

$$L\frac{di}{dt} + M[q(t)]i(t) = 0,$$

or taking into account that $idt = dq$, and $dt = \frac{dq}{i}$ we get:

$$Li\frac{di}{dq} + \left(R_0 - \eta\frac{\Delta Rq(t)}{Q_0}\right)i(t) = 0.$$

If we cancel both part of the equation by $i(t)$ then we may write the following expression:

$$\frac{di}{dq} + \frac{R_0}{L} - \eta\frac{\Delta Rq(t)}{LQ_0} = 0.$$

The integration of the obtained equation gives:

$$di = \eta\frac{\Delta Rq(t)}{LQ_0}dq - \frac{R_0}{L}dq,$$

$$\int di = \eta\frac{\Delta R}{LQ_0}\int qdq - \frac{R_0}{L}\int dq,$$

$$i(q) = \eta\frac{\Delta R}{2LQ_0}q^2 - \frac{R_0}{L}q + C.$$

Here the value C is some constant.

For $q = 0$ the initial value of the current equals $i(0) = i_0 = C$.

Thus the solution of the obtained equation may be written in the form:

$$i(q) = Aq^2 - Bq + i_0,$$

where the coefficients are:

$$A = \eta\frac{\Delta R}{2LQ_0}, \quad B = \frac{R_0}{L}.$$

The solution of the squared equation gives the values of the roots:

$$q_{1,2} = \frac{B \pm \sqrt{B^2 - 4Ai_0}}{2A} = \frac{\dfrac{R_0}{L} \pm \sqrt{\dfrac{R_0^2}{L^2} - 2\eta \dfrac{\Delta R}{LQ_0} i_0}}{\eta \dfrac{\Delta R}{LQ_0}}$$

$$= \frac{R_0 Q_0 \pm \sqrt{R_0^2 Q_0^2 - 2\eta \Delta R Q_0 L i_0}}{\eta \Delta R}.$$

Thus we have the values of two roots for $\eta = 1$:

$$q_1 = \frac{R_0 Q_0}{\Delta R} + \sqrt{\left[\frac{R_0 Q_0}{\Delta R}\right]^2 - \frac{2Q_0 L}{\Delta R} i_0} = \frac{R_0 Q_0}{\Delta R}\left[1 + \sqrt{1 - \frac{2\Delta R L}{Q_0 R_0^2} i_0}\right],$$

$$q_2 = \frac{R_0 Q_0}{\Delta R}\left[1 - \sqrt{1 - \frac{2\Delta R L}{Q_0 R_0^2} i_0}\right].$$

Then the equation for $i(q)$ may be represented in the following form:

$$i(q) = (q - q_1)(q - q_2).$$

Using the method of expansion we may represent the expression for the charge $q(t)$ as the sum of the rational fractions:

$$q(t) = i_0 \frac{2Q_0 L}{\Delta R} \frac{\exp\left[\dfrac{t}{\tau_{ML}}\right] - 1}{q_1 \exp\left[\dfrac{t}{\tau_{ML}}\right] - q_2},$$

where the value τ_{ML} is the time constant of the *ML*-circuit defined by means of the expression:

$$\tau_{ML} = \frac{L}{R_0 \sqrt{1 - 2\eta \dfrac{\Delta R L i_0}{Q_0 R_0^2}}}.$$

Let's find the current flowing in the circuit according to the general expression:

$$i(t)=\frac{dq}{dt}=i_0\frac{2Q_0L}{\Delta R}\frac{d}{dt}\left[\frac{\exp\left[\frac{t}{\tau_{ML}}\right]-1}{q_1\exp\left[\frac{t}{\tau_{ML}}\right]-q_2}\right],$$

$$\frac{d}{dt}\left[\frac{\exp\left[\frac{t}{\tau_{ML}}\right]-1}{q_1\exp\left[\frac{t}{\tau_{ML}}\right]-q_2}\right]$$

$$=\frac{\frac{1}{\tau_{ML}}\exp\left[\frac{t}{\tau_{ML}}\right]\left[q_1\exp\left[\frac{t}{\tau_{ML}}\right]-q_2\right]-\frac{1}{\tau_{ML}}q_1\exp\left[\frac{t}{\tau_{ML}}\right]\left[\exp\left[\frac{t}{\tau_{ML}}\right]-1\right]}{\left[q_1\exp\left[\frac{t}{\tau_{ML}}\right]-q_2\right]^2}$$

$$=\frac{\frac{1}{\tau_{ML}}\exp\left[\frac{t}{\tau_{ML}}\right]\left[q_1\exp\left[\frac{t}{\tau_{ML}}\right]-q_2-q_1\exp\left[\frac{t}{\tau_{ML}}\right]+q_1\right]}{\left[q_1\exp\left[\frac{t}{\tau_{ML}}\right]-q_2\right]^2}$$

$$=\frac{\exp\left[\frac{t}{\tau_{ML}}\right]\left[q_1-q_2\right]}{\tau_{ML}\left[q_1\exp\left[\frac{t}{\tau_{ML}}\right]-q_2\right]^2}=\frac{\exp\left[\frac{t}{\tau_{ML}}\right]\frac{2Q_0R_0}{\Delta R}\sqrt{1-2\eta\frac{\Delta RLi_0}{Q_0R_0}}}{\tau_{ML}^2\left[q_1\exp\left[\frac{t}{\tau_{ML}}\right]-q_2\right]^2}$$

$$=\frac{\exp\left[\frac{t}{\tau_{ML}}\right]\frac{2Q_0R_0}{\Delta R}\frac{L}{R_0}\frac{1}{\tau_{ML}}}{\tau_{ML}\left[q_1\exp\left[\frac{t}{\tau_{ML}}\right]-q_2\right]^2}=\frac{\exp\left[\frac{t}{\tau_{ML}}\right]\frac{2Q_0L}{\Delta R}}{\tau_{ML}^2\left[q_1\exp\left[\frac{t}{\tau_{ML}}\right]-q_2\right]^2}.$$

Thus the current in the *ML*-circuit is given by the expression:

$$i(t) = i_0 \frac{2Q_0 L}{\Delta R} \frac{2Q_0 L}{\Delta R} \frac{\exp\left[\dfrac{t}{\tau_{ML}}\right]}{\tau_{ML}^2 \left[q_1 \exp\left[\dfrac{t}{\tau_{ML}}\right] - q_2\right]^2}$$

$$= i_0 \left[\frac{2Q_0 L}{\Delta R \tau_{ML}}\right]^2 \frac{\exp\left[\dfrac{t}{\tau_{ML}}\right]}{\left[q_1 \exp\left[\dfrac{t}{\tau_{ML}}\right] - q_2\right]^2}.$$

The obtained expressions for $q(t)$ and $i(t)$ are the analytical results for the ideal *ML*-circuit describing by the linear model of drift of carriers in the memristor.

For small values of *t* we obtain the following approximation:

$$\sqrt{1 - 2\eta \frac{\Delta R L}{Q_0 R_0^2} i_0} \to 1, \quad q_2 = \frac{R_0 Q_0}{\Delta R}\left[1 - \sqrt{1 - 2\eta \frac{\Delta R L}{Q_0 R_0^2} i_0}\right] \to 0,$$

$$q_1 = \frac{R_0 Q_0}{\Delta R}\left[1 + \sqrt{1 - 2\eta \frac{\Delta R L}{Q_0 R_0^2} i_0}\right] \to 2\frac{R_0 Q_0}{\Delta R}.$$

In this case the value of the current is defined by the following law:

$$i(t) = i_0 \left[\frac{2Q_0 L}{\Delta R \tau_{ML}}\right]^2 \frac{\exp\left[\dfrac{t}{\tau_{ML}}\right]}{q_1^2 \exp\left[\dfrac{2t}{\tau_{ML}}\right]} = i_0 \left[\frac{2Q_0 L}{\Delta R \tau_{ML}}\right]^2 \frac{1}{q_1^2} \exp\left[\frac{-t}{\tau_{ML}}\right]$$

$$= i_0 \left[\frac{2Q_0 L}{\Delta R \tau_{ML}}\right]^2 \left[\frac{\Delta R \tau_{ML}}{2Q_0 L}\right]^2 \frac{L^2}{R_0^2 \tau_{ML}^2} \exp\left[\frac{-t}{\tau_{ML}}\right] = i_0 \frac{L^2}{R_0^2 \tau_{ML}^2} \exp\left[\frac{-t}{\tau_{ML}}\right].$$

It is evident that the value τ_{ML} defined by the expression

$$\tau_{ML} = \frac{L}{R_0\sqrt{1-2\eta\dfrac{\Delta R L i_0}{Q_0 R_0^2}}}$$

tends to the value $\dfrac{L}{R_0}$ for small values t. Let's expand the function $\exp\left[-\dfrac{t}{\tau_{ML}}\right]$ into the series and neglect by terms containing t^2. Then we get the final expression for the current at small values t:

$$i(t) = i_0 \exp\left[\frac{-t}{\tau_{ML}}\right] = i_0\left[1-\frac{t}{\tau_{Ml}}\right] = i_0\left[1-\frac{R_0}{L}t\right].$$

For the great values of t the current damps according to the exponential law:

$$i(t) = i_0\left[\frac{2Q_0L}{\Delta R\tau_{ML}}\right]^2 \frac{1}{\exp\left[\dfrac{t}{\tau_{ML}}\right]\left[q_1-\dfrac{q_2}{\exp\left[\dfrac{t}{\tau_{ML}}\right]}\right]^2} = i_0\left[\frac{2Q_0L}{q_1\Delta R\tau_{ML}}\right]^2 \exp\left[-\frac{t}{\tau_{ML}}\right].$$

Since the time constant τ_{ML} depends on the polarity of the memristor $\left(\tau_{ML}(\eta=1) > \tau_{ML}(\eta=-1)\right)$ then the *ML*-circuit for $\eta=1$ discharges more slowly than its *RL*-copy. For value $\eta=-1$. *ML*-circuit discharges faster than *RL*-circuit, Fig. 4.9.

The solution of the equation for the current in the *ML*-circuit under the action of the direct voltage U_0 is not simple.

It is necessary to recall that in *RL*-circuit the current approaches asymptotically to the maximum value $\dfrac{U_0}{R}$ for $t >> \tau_{RL} = \dfrac{L}{R}$. The differential equation

$$L\frac{di}{dt} + \left[R_0 - \eta\frac{\Delta R q(t)}{Q_0}\right] i(t) = u(t),$$

written according to the KVL shows that this problem is sufficiently complex one.

$$q0 := 0.45\cdot 10^{-4} \qquad t0 := 10^{-4} \qquad Ron := 100 \qquad Q0 := 10^{-4} \qquad D := 10\cdot 10^{-9}$$

$$R0 := 15.5\cdot Ron \qquad n := 1 \qquad L0 := t0\cdot Ron \qquad L := L0\cdot 30 \qquad dR := 29\cdot Ron \qquad i0 := 0.135$$

$$t := 0, 0.00001 .. 0.001 \qquad Tm := \frac{L}{R0\cdot\sqrt{1-\frac{2\cdot n\cdot dR\cdot L\cdot i0}{Q0\cdot R0^2}}}$$

$$q1 := \frac{Q0\cdot R0}{dR}\cdot\left(1+\sqrt{1-\frac{2\cdot n\cdot dR\cdot L\cdot i0}{Q0\cdot R0^2}}\right) \qquad q2 := \frac{Q0\cdot R0}{dR}\cdot\left(1-\sqrt{1-\frac{2\cdot n\cdot dR\cdot L\cdot i0}{Q0\cdot R0^2}}\right)$$

$$i(t) := i0\cdot\left(\frac{2\cdot Q0\cdot L}{dR\cdot Tm}\right)^2\cdot\frac{\exp\left(t\cdot\frac{1}{Tm}\right)}{\left(q1\cdot\exp\left(t\cdot\frac{1}{Tm}\right)-q2\right)^2} \qquad q(t) := \left(\frac{2\cdot Q0\cdot L\cdot i0}{dR}\right)\cdot\left[\frac{\exp\left(t\cdot\frac{1}{Tm}\right)-1}{\left(q1\cdot\exp\left(t\cdot\frac{1}{Tm}\right)-q2\right)}\right]$$

$$n1 := -1 \qquad Tm1 := \frac{L}{R0\cdot\sqrt{1-\frac{2\cdot n1\cdot dR\cdot L\cdot i0}{Q0\cdot R0^2}}} \qquad t := 0, 0.00001 .. 0.001$$

$$q11 := \frac{Q0\cdot R0}{dR}\cdot\left(1+\sqrt{1-\frac{2\cdot n1\cdot dR\cdot L\cdot i0}{Q0\cdot R0^2}}\right) \qquad q21 := \frac{Q0\cdot R0}{dR}\cdot\left(1-\sqrt{1-\frac{2\cdot n1\cdot dR\cdot L\cdot i0}{Q0\cdot R0^2}}\right)$$

$$i2(t) := i0\cdot\left(\frac{2\cdot Q0\cdot L}{dR\cdot Tm1}\right)^2\cdot\frac{\exp\left(t\cdot\frac{1}{Tm1}\right)}{\left(q11\cdot\exp\left(t\cdot\frac{1}{Tm1}\right)-q21\right)^2} \qquad i1(t) := i0\cdot\exp\left(\frac{-t\cdot R0}{L}\right) \qquad y(t) := 0.5 + n\cdot\frac{q(t)}{Q0}$$

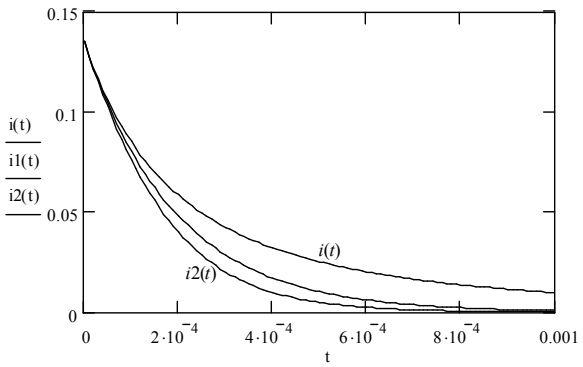

Fig. 4.9. The graphs of the transients in the *ML*-circuit

It is explained by the fact that the current $i(t)$ approaches asymptotically to the maximum value and may accumulate the great charge according to the expression:

$$q(t) = \int_0^t i(\tau) d\tau,$$

which passes through the memristor. Hence for any nonzero value of the voltage the linear model of the memristor does not correspond to the real processes at the great time interval when the value $w(t)$ defined from the expression

$$w(t) = w_0 + \eta \frac{Dq(t)}{Q_0},$$

exceeds the value D (for $\eta = 1$) or has the negative value (for $\eta = -1$).

This shortcoming of the linear model shows that fact when the vacancies of the oxygen reach any from the two ends of the active region then their displacement is suppressed sufficiently strongly by the nonhomogeneous electric field.

Thus, unlike the ideal *RL*-circuit the steady-state component of the current in the ideal *ML*-circuit is defined by the resistance R_0 and the inductance L.

4.5 *MLC*-circuits with the nonlinear model of the memristor

The linear model of drift of the charge carriers in the memristor which was considered in the previous sections allows to obtain the convenient results in the analytical final form. It is easy to show that these results lead to the well-known expressions obtained for R, RC and RL circuits if we neglect by the memristive effect in the case when $\Delta R \to 0$.

We considered above that the basic shortcoming of the linear model is the fact that it does not take into account the boundary effects. The virtual boundary between the doped and undoped regions moves in the material of the memristor with the speed v_D. This speed is strongly suppressed at the ends where $w \approx 0$ and $w \approx D$. To eliminate this shortcoming it is necessary to introduce the window function $f(x)$ by the following way:

$$\frac{dw}{dt} = \eta \frac{\mu_D R_{\text{on}}}{D} f\left(\frac{w}{D}\right) i(t).$$

Let' assume that the window function is given by the expression:

$$f_p(x) = 1 - (2x-1)^{2p},$$

where the value x equals $\frac{w}{D} = x$ and the value p is the positive integer. Then the equation $f_p(x) = 0$ has the two real roots and $2(p-1)$ complex roots.

Let's consider the *MC*-circuit describing by the nonlinear model and assume that the capacitor is charged to initial value q_0. If the external voltage source is absent then the circuit equation according to the KVL may be written as:

$$M[q(t)]i(t) + \frac{q(t)}{C} = 0.$$

Then the current flowing in the circuit is defined by the expression:

$$i(t) = -\frac{q(t)}{C}\frac{1}{M[q(t)]} = -\frac{q(t)}{C}\frac{1}{\frac{w}{D}R_{\text{on}} + \left[1 - \frac{w}{D}\right]R_{\text{off}}}.$$

To solve the equation with the given window function we may use the following algorithm:

$$w_{j+1} + \eta \frac{D}{Q_0}\left(1 - \left(\frac{2w_j}{D} - 1\right)^{2p}\right) i_j \Delta t,$$

$$i_{j+1} = -\frac{q_j}{C}\frac{1}{\left[\frac{w_{j+1}}{D}R_{\text{on}} + \left[1 - \frac{w_{j+1}}{D}\right]R_{\text{off}}\right]},$$

$$q_{j+1} = q_j + i_j \Delta t,$$

where the value Δt is the discrete step at which we have the stable operation of the algorithm.

The graph of the dependency $q(t)$ obtained with the help of the window function is shown in Fig. 4.10. It is necessary to note that for the value of the parameter $p=1$ we have the model in which the nonlinear drift of carriers passes through total active region of the memristor. For the value $p=10$ we have the model in which drift of carriers is strongly suppressed only close to ends (boundaries).

formula1_all :=

$p \leftarrow 1$

$\delta \leftarrow 10^{-4}$

$D \leftarrow 5 \cdot 10^{-8}$

$q_0 \leftarrow 20 \cdot 10^{-4}$

$Q_0 \leftarrow 25 \cdot 10^{-4}$

$c \leftarrow 1 \cdot 10^{-6}$

$w_0 \leftarrow 0.5 \cdot D$

$i_0 \leftarrow 0$

$R_{on} \leftarrow 100$

$R_{off} \leftarrow 2000$

$n \leftarrow 1$

$t_0 \leftarrow 0$

for $j \in 0..60$

$t_{j+1} \leftarrow j \cdot \delta$

$w_{j+1} \leftarrow w_j + n \cdot \frac{D}{Q_0} \cdot i_j \cdot \delta \left[1 - \left(\frac{2 \cdot w_j}{D} - 1 \right)^{2 \cdot p} \right]$

$i_{j+1} \leftarrow \frac{-q_j}{c \cdot \left[\frac{w_{j+1}}{D} \cdot R_{on} + \left(1 - \frac{w_{j+1}}{D} \right) \cdot R_{off} \right]}$

$q_{j+1} \leftarrow q_j + i_{j+1} \cdot \delta$

t

i

q

$s \leftarrow \text{augment}(t, i, q, w)$

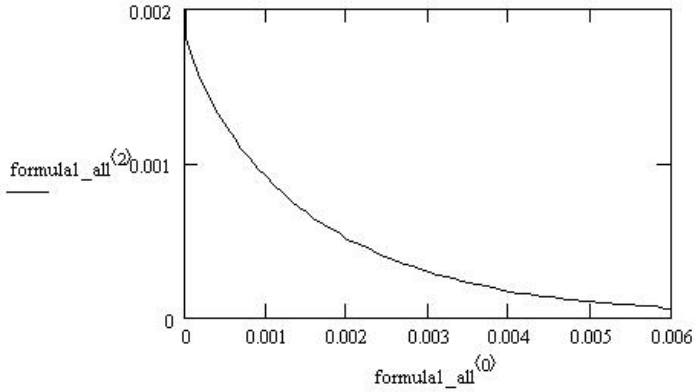

Fig. 4.10. The graph of $q(t)$ calculated with the use of the window function

It is evident that the select of the window function allows to get the results like the processes in the real samples.

Before the consideration of the processes in the *MLC*-circuits with the nonlinear drift of charge carriers it is necessary to recall the results of the analysis of the transients in the linear *RLC*-circuit which is described by the linear second order differential equation.

Let's assume that the initial charge on the capacitor equals q_0 and the voltage source is absent. In this case the differential equation describing the circuit is

$$iR + L\frac{di}{dt} + \frac{1}{C}\int i(t)dt = 0.$$

Taking into account that the current in the circuit is $i = \frac{dq}{dt}$ we may rewrite the equation in the following form:

$$iR + L\frac{di}{dt} + \frac{1}{C}\int i(t)dt = 0.$$

The characteristic equation is:

$$p^2 + \frac{R}{L}p + \frac{1}{LC} = 0.$$

Assuming that $\frac{R}{2L}=\delta,\quad \frac{1}{LC}=\omega_0^2$ we find the roots of the equation:

$$p_1=-\delta+\sqrt{\delta^2-\omega_0^2},\qquad p_2=-\delta-\sqrt{\delta^2-\omega_0^2},$$

so that the solution of the differential equation is written in the form:

$$q(t)=A_1\exp(p_1t)+A_2\exp(p_2t),$$

where the values A_1 and A_2 are the integration constants defined by the following way.

Since the initial value of the current at the time moment $t=0$ equals zero then $\frac{dq}{dt}\Big|_{t=0}=i(0)=0.$ Taking into account that $q(0)=q_0$ we may write the system of equations:

$$q(0)=A_1+A_2,$$

$$\frac{dq}{dt}\Big|_{t=0}=p_1A_1+p_2A_2,$$

from which it follows that

$$A_1=-q_0\frac{p_2}{p_1-p_2},\quad A_2=q_0\frac{p_1}{p_1-p_2}.$$

Thus the dependency $q(t)$ is described by the following expression:

$$q(t)=\frac{q_0}{p_1-p_2}\left[p_1e^{p_2t}-p_2e^{p_1t}\right]$$

$$=\frac{q_0}{2\sqrt{\delta^2-\omega_0^2}}\left[-\delta e^{p_2t}+\sqrt{\delta^2-\omega_0^2}e^{p_2t}+\delta e^{p_1t}+\sqrt{\delta^2-\omega_0^2}e^{p_1t}\right]$$

$$=\left|\delta^2-\omega_0^2=\underline{\omega}^2\right|=\frac{q_0}{2\sqrt{\delta^2-\omega_0^2}}e^{-\delta t}\left[2\sqrt{\delta^2-\omega_0^2}\left[\frac{e^{\underline{\omega}t}+e^{-\underline{\omega}t}}{2}\right]\right.$$

$$\left.+2\delta\left[\frac{e^{\underline{\omega}t}-e^{-\underline{\omega}t}}{2}\right]\right]=\frac{q_0}{\underline{\omega}}e^{-\delta t}[\underline{\omega}\mathrm{ch}\underline{\omega}t+\delta\mathrm{sh}\underline{\omega}t]$$

$$= \frac{q_0}{\underline{\omega}} e^{-\delta t} \sqrt{\underline{\omega}^2 + \delta^2} \operatorname{sh}(\underline{\omega} t + \varphi),$$

where $\operatorname{th}\varphi = \frac{\underline{\omega}}{\delta}$, $\operatorname{sh}\varphi = \frac{\underline{\omega}}{\omega_0}$ as it follows from the triangle, Fig. 4.11.

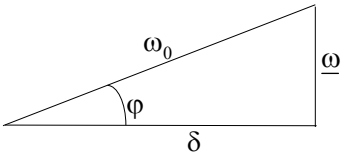

Fig. 4.11. The relationships between the frequencies in *RLC*-circuit

Finally we have:

$$q(t) = q_0 \frac{\omega_0}{\underline{\omega}} e^{-\delta t} \operatorname{sh}(\underline{\omega} t + \varphi).$$

Under the condition $\delta > \omega_0$ or $\frac{R}{2L} > \frac{1}{\sqrt{LC}}$ the discharge of the capacitor will be aperiodic. In this case the inequality $R > 2\sqrt{\frac{L}{C}} = 2\rho$ is satisfied.

The value ρ is the characteristic resistance of the circuit. Under the condition $\delta < \omega_0$ ($R < 2\rho$) the characteristic roots are the complex numbers. It means that the discharge of the capacitor will be oscillatory. In this case:

$$p_1 = -\delta + j\underline{\omega}, \quad p_2 = -\delta - j\underline{\omega}, \quad \underline{\omega} \to j\underline{\omega}, \quad \operatorname{sh}\underline{\omega} t \to j \sin \underline{\omega} t.$$

and the expression for $q(t)$ is:

$$q(t) = q_0 \frac{\omega_0}{\underline{\omega}} e^{-\delta t} \sin(\underline{\omega} t + \varphi).$$

Taking into account that $\tau_{RL} = \frac{L}{R}$, $\delta = \frac{R}{2L}$ or $\delta = \frac{1}{2\tau_{RL}}$ we may write the final solution:

$$q(t) = \begin{cases} q_0 \dfrac{\omega_0}{\underline{\omega}} \exp\left(-\dfrac{t}{2\tau_{RL}}\right) \mathrm{sh}(\underline{\omega} t + \varphi), & \delta > \omega_0 \\ q_0 \dfrac{\omega_0}{\underline{\omega}} \exp\left(-\dfrac{t}{2\tau_{RL}}\right) \sin(\underline{\omega} t + \varphi), & \delta < \omega_0. \end{cases}$$

The respective graphs of transient of the capacitor discharge are shown in Fig. 4.12.

$q_0 := 2 \cdot 10^{-4}$ $\omega_0 := \frac{1}{\sqrt{L \cdot C}}$ $\delta := \frac{R}{2 \cdot L}$ $\omega_1 := \sqrt{\delta^2 - (\omega_0)^2}$ $R := 2 \cdot 10^4$

$\tau := \frac{L}{R}$ $\phi := \operatorname{atanh}\left(\frac{\omega_1}{\delta}\right)$ $q(t) := q_0 \frac{\omega_0}{\omega_1} \cdot \exp\left(\frac{-t}{2 \cdot \tau}\right) \cdot \sinh(\omega_1 \cdot t + \phi)$

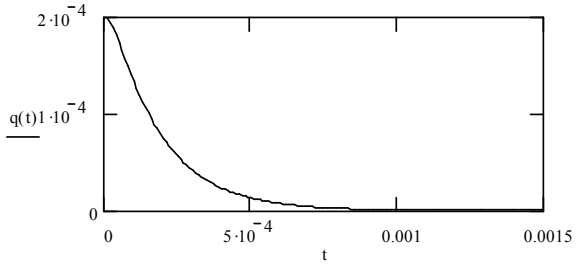

Case1: $\delta > \omega_0$
a

$R := 2 \cdot 10^3$ $L := 5 \cdot 10^{-1}$ $C := 10^{-8}$ $q_0 := 2 \cdot 10^{-4}$ $t := 0, 0.00001 .. 0.0015$

$\tau := \frac{L}{R}$ $\omega_0 := \frac{1}{\sqrt{L \cdot C}}$ $\delta := \frac{R}{2 \cdot L}$ $\omega_1 := \sqrt{(\omega_0)^2 - \delta^2}$ $\phi := \operatorname{atan}\left(\frac{\omega_1}{\delta}\right)$

$q(t) := q_0 \frac{\omega_0}{\omega_1} \cdot \exp\left(\frac{-t}{2 \cdot \tau}\right) \cdot \sin(\omega_1 \cdot t + \phi)$

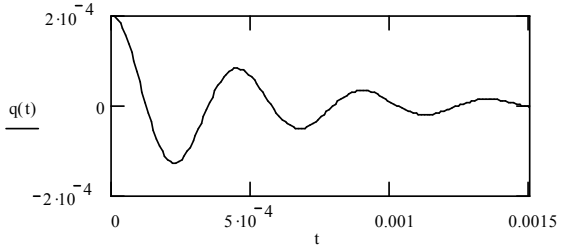

Case2: $\delta < \omega_0$
b

Fig. 4.12. The transients of the capacitor discharge

The first graph corresponds to the value of the resistance R which is great than R_0 defined as

$$R_0 = R_{\text{on}} \frac{w}{D} + R_{\text{off}} \left(1 - \frac{w}{D}\right).$$

The second graph corresponds to the case when $R << R_0$.

The nonlinear equation describing the *MLC*-circuit is written in the form:

$$L\frac{di}{dt} + M[q(t)]i(t) + \frac{q(t)}{C} = 0$$

under the condition that $q(0) = q_0$ and the external voltage source is absent. Such equation may not solve analytically because the memristance M depends on the charge q.

Let's carry out the numerical solution of the nonlinear equation. In this case we have to use the following approximations of the respective derivatives:

$$L\frac{di}{dt} \to L\frac{i_{j+1} - i_j}{\Delta t}, \quad \frac{q}{C} \to \frac{q_j}{C}, \quad \frac{dq}{dt} = i \to \frac{q_{j+1} - q_j}{\Delta t} = i_{j+1},$$

$$q_{j+1} = q_j + i_{j+1}\Delta t,$$

where the value Δt is the step of discretization.

The solution of the equation is given by the following algorithm:

$$w_{j+1} + \eta \frac{D}{Q_0}\left(1 - \left(\frac{2w_j}{D} - 1\right)^{2p}\right) i_j \Delta t,$$

$$i_{j+1} = i_j + \frac{\Delta t}{L}\left[-\frac{q_j}{C} - \left[\frac{w_{j+1}}{D} R_{\text{on}} + \left[1 - \frac{w_{j+1}}{D}\right] R_{\text{off}}\right] i_j\right],$$

$$q_{j+1} = q_j + i_j \Delta t.$$

The graph obtained for the parameter p = 40 of the window function is shown in Fig. 4.13.

formula1_all :=

$P \leftarrow 40$

$\delta \leftarrow 10^{-6}$

$D \leftarrow 1 \cdot 10^{-8}$

$q_0 \leftarrow 2 \cdot 10^{-4}$

$Q_0 \leftarrow 10^{-4}$

$C \leftarrow 1 \cdot 10^{-8}$

$L \leftarrow 5 \cdot 10^{-1}$

$w_0 \leftarrow 0.5 \cdot D$

$i_0 \leftarrow 0$

$R_{on} \leftarrow 100$

$R_{off} \leftarrow 2000$

$n \leftarrow 1$

$t_0 \leftarrow 0$

for $j \in 0 .. 1498$

$t_{j+1} \leftarrow j \cdot \delta$

$w_{j+1} \leftarrow w_j + n \cdot \frac{D}{Q_0} \cdot \left[1 - \left(\frac{2 \cdot w_j}{D} - 1 \right)^{2P} \right] \cdot i_j \cdot \delta$

$i_{j+1} \leftarrow i_j + \frac{\delta}{L} \cdot \left[-1 \cdot \frac{q_j}{C} - \left[\frac{w_{j+1}}{D} \cdot R_{on} + \left(1 - \frac{w_{j+1}}{D} \right) \cdot R_{off} \right] \cdot i_j \right]$

$q_{j+1} \leftarrow q_j + i_{j+1} \cdot \delta$

t

i

q

s ← augment (t, i, q, w)

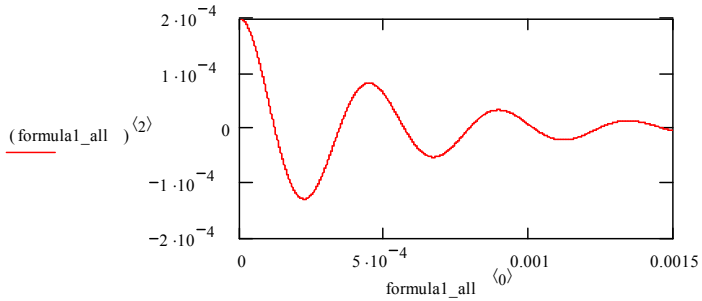

Fig. 4.13. The solution of the nonlinear equation with the window function

For value $\eta = 1$ the damped oscillatory process of the capacitor discharge occurs in the considered circuit. The capacitor discharges through the memristor. The memristance of the memristor determined by the expression:

$$M = R_0 - \eta \frac{\Delta R q(t)}{Q_0}$$

decreases from its initial value R_0.

For $\eta = -1$ the discharge of the capacitor increases the value of the memristance and the process becomes as aperiodical one. It means that if we change the plates of the capacitor (with "$\pm$" on "$\mp$") in the *MLC*-circuit then the discharge of the capacitor will be aperiodical and vice versa. This property corresponds only to the *MLC*-circuit and is defined by the memristive effect.

In conclusion we will consider the transients in the *MLC*-circuit which is connected to the sinusoidal voltage source $u(t) = U_m \sin \omega t$ with the initial value of the charge on the capacitor equaled $q_0 = 0$.

At first we consider the ideal *RLC*-circuit, [102].

The steady-state component of the transient current is defined by the expression:

$$i_{ss} = \frac{U_m \sin \omega t}{Z} = I_0 \sin(\omega t - \varphi),$$

where

$$I_0 = \frac{U_m}{Z}, \quad Z = \sqrt{R^2 + \left(\omega L - \frac{1}{\omega C}\right)^2}, \quad \varphi = \operatorname{arctg} \frac{\omega L - \frac{1}{\omega C}}{R}.$$

The transient current flowing through the capacitor is:

$$i(t) = I_0 \sin(\omega t - \varphi) + A_1 \exp(p_1 t) + A_2 \exp(p_2 t).$$

As before to determine the constants of integration A_1 and A_2 we write the system of equation taking into account initial values of the current:

$$A_1 + A_2 - I_0 \sin \varphi = 0, \qquad p_1 A_1 + p_2 A_2 = -\omega I_0 \cos \varphi,$$

from which it follows:

$$A_1 = -I_0 \frac{\omega\cos\varphi + p_2 \sin\varphi}{p_1 - p_2}, \qquad A_2 = I_0 \frac{\omega\cos\varphi + p_1 \sin\varphi}{p_1 - p_2}.$$

The transient current in the circuit is given by the expression:

$$\begin{aligned} i(t) &= I_0 \sin(\omega t - \varphi) - \frac{I_0}{p_1 - p_2}(\omega\cos\varphi + p_2 \sin\varphi)e^{p_1 t} \\ &\quad + \frac{I_0}{p_1 - p_2}(\omega\cos\varphi + p_1 \sin\varphi)e^{p_2 t} \\ &= I_0 \sin(\omega t - \varphi) + \frac{I_0}{p_1 - p_2}\sin\varphi\left(p_1 e^{p_2 t} - p_2 e^{p_1 t}\right) \\ &\quad - \frac{I_0}{p_1 - p_2}\omega\cos\varphi\left(-e^{p_1 t} + e^{p_2 t}\right). \end{aligned}$$

Many practical applications show that the most interest is the study of the oscillatory type transients. In this case, as shown above, we may assume that:

$$p_1 - p_2 = 2j\underline{\omega}, \qquad -e^{p_1 t} + e^{p_2 t} = -2je^{-\delta t}\sin\underline{\omega} t,$$
$$p_1 e^{p_2 t} - p_2 e^{p_1 t} = 2j\underline{\omega}\, e^{-\delta t}\sin(\underline{\omega} t - \nu),$$

where

$$\nu = \operatorname{arctg}\frac{\omega}{\underline{\delta}}.$$

The final expression for the transient current can be written as:

$$i(t) = I_0 \sin(\omega t - \varphi) - I_0 \frac{\omega_0}{\underline{\omega}} e^{-\delta t}\sin(\underline{\omega} t - \nu)\sin\varphi - I_0 \frac{\omega_0}{\underline{\omega}} e^{-\delta t}\cos\varphi\sin\underline{\omega} t$$

The obtained result shows that the transient current contains two components in the *RLC*-circuit under the action of the sinusoidal voltage of the frequency ω. The first component represents an undamped oscillation with the frequency ω of the external source; the second component is the damped oscillations with frequency of the natural oscillations $\underline{\omega}$ of the considered circuit.

The amplitude of both the natural and the steady-state oscillations depends on the degree of damping δ. Besides, the amplitude of oscillation depends on the frequency ratio ω and $\underline{\omega}$ (for small losses in the circuit, that is $\delta << \omega_0$ we can assume that $\underline{\omega} \approx \omega_0$, $\nu = \frac{\pi}{2}$). When $\omega = \omega_0$ there is the phenomenon of resonance, when the current amplitude reaches a maximum value.

The graphs of the transient current show in Fig. 4.14 for the cases $\underline{\omega} < \omega_0$ and $\underline{\omega} \approx \omega_0$.

Obviously, when the values of the frequencies $\underline{\omega}$ and ω_0 do not coincide the interaction is more complex way.

When the frequencies are sufficiently close, but the amplitudes are almost the same, the addition of the oscillations leads to appearance of the oscillations of the frequency equaled $\omega - \omega_0$, and the so-called beating current appears in the circuit:

$$i(t) = I_0 \sin(\omega t - \varphi) + I_0 \sin(\omega_0 t - \varphi)$$

$$= -2I_0 \sin\left(\frac{\omega - \omega_0}{2} t\right) \cos\left(\frac{\omega + \omega_0}{2} t\right).$$

From this expression it follows that the current amplitude changes slowly over time according to the law $\left|\sin\frac{\omega - \omega_0}{2} t\right|$, and the oscillation frequency is $\frac{\omega + \omega_0}{2} \approx \omega$.

If the losses are very small ($\delta \approx 0$) in the circuit, the transient current has the form which is shown in Fig. 4.14 (lower graph).

Let's consider the circuit behavior under the action of the source of sinusoidal voltage $u(t) = U_m \sin \omega t$ with zero initial charge on the capacitor.

The numerical solution of the differential equation

$$L\frac{di}{dt} + M[q(t)]i(t) + \frac{q(t)}{C} = u(t)$$

may be obtained by means of the following algorithm:

$$w_{j+1} + \eta \frac{D}{Q_0}\left(1 - \left(\frac{2w_j}{D} - 1\right)^{2p}\right) i_j \Delta t,$$

$R := 550 \quad L := 0.5 \quad C := 5 \cdot 10^{-6} \quad d := \frac{R}{2 \cdot L} \quad w0 := \frac{1}{\sqrt{L \cdot C}} \quad w1 := \sqrt{w0^2 - d^2} \quad I0 := 4 \cdot 10^{-3} \quad w := 500($

$\phi := \operatorname{atan}\left(\frac{w \cdot L - \frac{1}{w \cdot C}}{R}\right) \quad \nu := \operatorname{atan}\left(\frac{w1}{d}\right) \quad t := 0, 0.00001 .. 0.01$

$i(t) := I0 \cdot \sin(w \cdot t - f) - I0 \cdot \frac{w0}{w1} \cdot \exp(-d \cdot t) \cdot \sin(\phi) \cdot \sin(w1 \cdot t - \nu) - I0 \cdot \frac{w0}{w1} \cdot \exp(-d \cdot t) \cdot \cos(\phi) \cdot \sin(w1 \cdot t)$

$R := 550 \quad L := 0.5 \quad C := 8 \cdot 10^{-8} \quad d := \frac{R}{2 \cdot L}$

$\phi := \operatorname{atan}\left(\frac{w \cdot L - \frac{1}{w \cdot C}}{R}\right) \quad \nu := \operatorname{atan}\left(\frac{w1}{d}\right) \quad w0 := \frac{1}{\sqrt{L \cdot C}} \quad w1 := \sqrt{w0^2 - d^2}$

$i1(t) := I0 \cdot \sin(w \cdot t - \phi) - I0 \cdot \frac{w0}{w1} \cdot \exp(-d \cdot t) \cdot \sin(\phi) \cdot \sin(w1 \cdot t - \nu) - I0 \cdot \frac{w0}{w1} \cdot \exp(-d \cdot t) \cdot \cos(\phi) \cdot \sin(w1 \cdot t)$

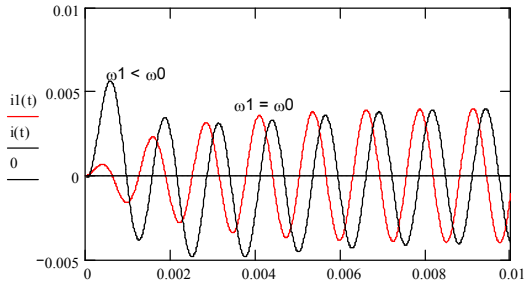

$R := 0 \quad L := 0.5 \quad C := 1 \cdot 10^{-7} \quad d := \frac{R}{2 \cdot L} \quad w0 := \frac{1}{\sqrt{L \cdot C}} \quad w1 := \sqrt{w0^2 - d^2}$

$\phi := \operatorname{atan}\left(\frac{2400}{550}\right) \quad \nu := \operatorname{atan}\left(\frac{835}{550}\right) \quad t := 0, 0.0000001 .. 0.025$

$i2(t) := I0 \cdot \sin(w \cdot t - \phi) - I0 \cdot \frac{w0}{w1} \cdot \exp(-d \cdot t) \cdot \sin(\phi) \cdot \sin(w1 \cdot t - \nu) - I0 \cdot \frac{w0}{w1} \cdot \exp(-d \cdot t) \cdot \cos(\phi) \cdot \sin(w1 \cdot t)$

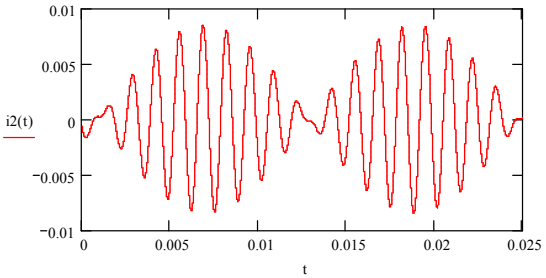

Fig. 4.14. Transient processes in *RLC*-circuit

$$i_{j+1} = i_j + \frac{\Delta t}{L}\left[u_j - \frac{q_j}{C} - \left[\frac{w_{j+1}}{D} R_{\text{on}} + \left[1 - \frac{w_{j+1}}{D} \right] R_{\text{off}} \right] i_j \right],$$

$$q_{j+1} = q_j + i_j \Delta t.$$

The dependencies $q(t)$ and $i(t)$ for ideal *MLC*-circuit are shown in Fig. 4.15 and 4.16 for $\eta = 1$ and different frequencies $\underline{\omega}$ and ω_0. It is seen from graphs the memristive effect is in the transient region only and does not depend on the memristor polarity.

In conclusion, the electrical circuits containing memristors and discussed in this section supplement the standard *RC*, *RL*, *LC* and *RLC*-circuits studied in the courses of physics, electrical engineering and electronics in accordance with the respective programs.

Significant differences of the memristive circuits were indicated, in particular, the change in the discharge rate of the capacitor, when changing the polarity of the plates, and changing the value of the current in a circuit when switching the voltage source terminals.

The idea of the realization of the memristor is relatively simple, but its nanosizes yet restrict the possibility to create and experimental study real samples of the memristors and memristive devices in the laboratories of educational institutions due to the expensive equipment, using advanced nanotechnologies.

Therefore, in many cases it is possible to simulate the behavior of such devices by creating various emulators and the respective software taking into account the physical properties of the memristors.

formula1_all :=

$P \leftarrow 40$

$\delta \leftarrow 10^{-6}$

$\omega \leftarrow 5 \cdot 10^{3}$

$D \leftarrow 1 \cdot 10^{-8}$

$q_0 \leftarrow 0$

$Q_0 \leftarrow 10^{-4}$

$C \leftarrow 5 \cdot 10^{-6}$

$L \leftarrow 5 \cdot 10^{-1}$

$w_0 \leftarrow 0.5 \cdot D$

$i_0 \leftarrow 0$

$R_{on} \leftarrow 100$

$R_{off} \leftarrow 1000$

$n \leftarrow 1$

$t_0 \leftarrow 0$

for $j \in 0 .. 14998$

$t_{j+1} \leftarrow j \cdot \delta$

$w_{j+1} \leftarrow w_j + n \cdot \frac{D}{Q_0} \cdot \left[1 - \left(\frac{2 \cdot w_j}{D} - 1 \right)^{2 \cdot P} \right] \cdot i_j \cdot \delta$

$i_{j+1} \leftarrow i_j + \frac{\delta}{L} \cdot \left[1 \cdot \sin(\omega \cdot t_j) - 1 \cdot \frac{q_j}{C} - \left[\frac{w_{j+1}}{D} \cdot R_{on} + \left(1 - \frac{w_{j+1}}{D} \right) \cdot R_{off} \right] \cdot i_j \right]$

$q_{j+1} \leftarrow q_j + i_{j+1} \cdot \delta$

t

i

q

$s \leftarrow \text{augment}(t, i, q, w)$

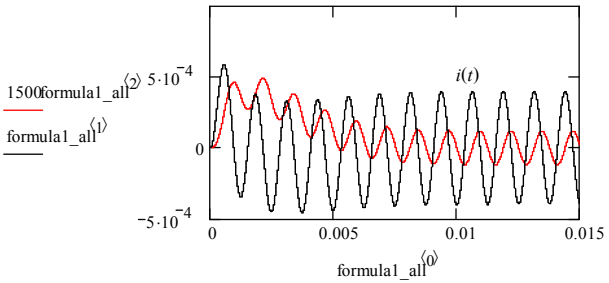

Fig. 4.15. Transient process in the *MLC* -circuit for $\omega > \omega_0$

formula1_all:=

$P \leftarrow 40$

$\delta \leftarrow 10^{-6}$

$\omega \leftarrow 5 \cdot 10^{3}$

$D \leftarrow 1 \cdot 10^{-8}$

$q_0 \leftarrow 0$

$Q_0 \leftarrow 10^{-4}$

$C \leftarrow 8 \cdot 10^{-8}$

$L \leftarrow 5 \cdot 10^{-1}$

$w_0 \leftarrow 0.5 \cdot D$

$i_0 \leftarrow 0$

$R_{on} \leftarrow 100$

$R_{off} \leftarrow 1000$

$n \leftarrow 1$

$t_0 \leftarrow 0$

for $j \in 0 .. 14998$

$t_{j+1} \leftarrow j \cdot \delta$

$w_{j+1} \leftarrow w_j + n \cdot \frac{D}{Q_0} \cdot \left[1 - \left(\frac{2 \cdot w_j}{D} - 1 \right)^{2 \cdot P} \right] \cdot i_j \cdot \delta$

$i_{j+1} \leftarrow i_j + \frac{\delta}{L} \cdot \left[1 \cdot \sin(\omega \cdot t_j) - 1 \cdot \frac{q_j}{C} - \left[\frac{w_{j+1}}{D} \cdot R_{on} + \left(1 - \frac{w_{j+1}}{D} \right) \cdot R_{off} \right] \cdot i_j \right]$

$q_{j+1} \leftarrow q_j + i_{j+1} \cdot \delta$

t

i

q

$s \leftarrow \text{augment}(t, i, q, w)$

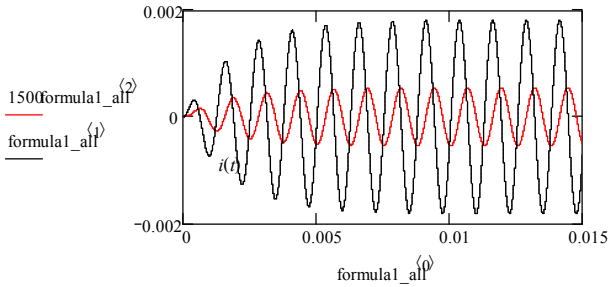

Fig. 4.16. Transient process in the *MLC*-circuit for $\omega \approx \omega_0$

EFFECT OF THE RESISTIVE SWITCHING IN THE MEMRISTOR

- Processes of the binary resistive switching in the memristor
- Functional region of the resistive switching
- Effect of the resistive switching in multi-component oxides of transition metals
- Examples of the resistive switching of the memristor
- Reading binary data from the memristor

5.1 Processes of the binary resistive switching in the memristor

The memristor may be used in the digital computer if it provides two states R_0 and R_1, where $R_0 >> R_1$. The state with a high resistance R_0 can be easily switched to a low resistance state R_1 and vice versa with the greatest possible speed and the least possible consumption of the energy [24].

In the case of a digital computer, requiring only two memory states (0 and 1), it is enough to provide two memristor state and where. In this state with a high resistance can be easily switched to a low resistance state and vice versa, with the greatest possible speed and the least possible expenditure of energy [24]. Unlike main memory, memristors not dissipate any power except that which is necessary in the short time of switching, because:

$$u(t) = \frac{d\Phi(t)}{dt} = 0, \qquad i(t) = \frac{dq(t)}{dt} = 0$$

in both equilibrium states R_0 and R_1.

At first we will consider the processes occurring in the memristor, which is controlled by the charge.

Let's assume that the veber-coulomb characteristic $\Phi(q)$ which describe the memristor controlled by the charge is represented by the three segment polyline curve (in general the dependency $\Phi(q)$ is the nonlinear function), Fig. 5.1.

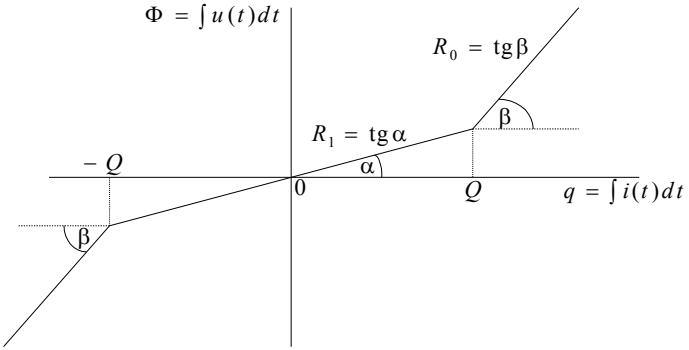

Fig. 5.1. The veber-coulomb characteristic of the memristor

The given veber-coulomb characteristic may be described by the following equation:

$$\Phi(q) = R_0 q + \frac{1}{2}[R_1 - R_0]\left[|q+Q| - |q-Q|\right],$$

where R_1 represents the slope of the middle segment $\left(\operatorname{tg}\alpha = \dfrac{\Delta\Phi}{\Delta q} = R_1\right)$, R_0 represents the slope of the external segments, the value $q = -Q$ defines the left point of the bend of the characteristic and the value $q = Q$ defined the right point.

Obviously, the memristance can be determined in accordance with the general expression:

$$M(q) = \frac{d\Phi(q)}{dq} = R_0 + \frac{1}{2}[R_1 - R_0][\operatorname{sgn}(q+Q) - \operatorname{sgn}(q-Q)],$$

where

$$\operatorname{sgn}(x) = \begin{cases} 1, & x > 0, \\ -1, & x < 0. \end{cases}$$

The graph of the function $M(q)$ is shown in Fig. 5.2. As an example, we choose values of the parameters $R_0 = 6000\ \Omega$ and $R_1 = 2500\ \Omega$.

Let the current source feeding the memristor is

$$i(t) = I_m \sin \omega t, \quad I_m = 2Q\omega.$$

$$Q := 10^{-4} \qquad R_0 := 6000 \qquad R_1 := 2500$$

$$M(q) := R_0 + \frac{1}{2}\cdot\left(R_1 - R_0\right)\cdot(\text{signum}\ (q + Q) - \text{signum}\ (q - Q))$$

$$q := 0, 0.000001 .. 0.0002 \qquad q1 := 0, -0.000001 .. -0.0002$$

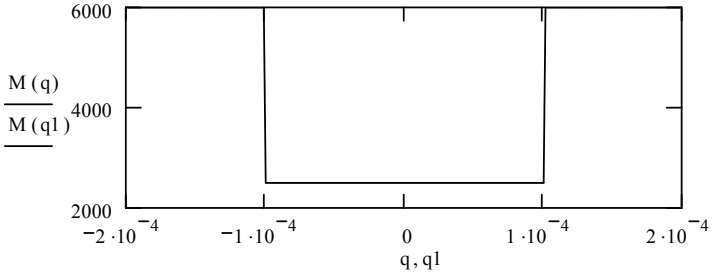

Fig. 5.2. The dependency of the memristance from the charge

Then the charge passing through the memristor is equal to:

$$q(t) = \int_0^t I_m \sin \omega\tau d\tau = -\frac{I_m}{\omega} \sin \omega\tau \Big|_0^t = \frac{I_m}{\omega}(1 - \cos \omega t) = 2Q(1 - \cos \omega t).$$

The magnitude of charge changes from $q = 0$ (at $t = 0$) to $q = 4Q$ (at $t = \frac{\pi}{\omega}$), Fig. 5.3*b*.

The value of the memristance is constant and equal to R_1 until the amount of charge reaches the value $q = Q$. The value of the memristance changes abruptly to the value R_0. The charge continues to increase ($q > Q$) and the value of the memristance does not change and remains the value R_0.

After that, when the charge reaches the maximum value $4Q$ (at time $t = \frac{\pi}{\omega}$ that corresponds to the end of the input current half period in the memristor), the process of reducing the charge quantity begins.

In the next half period the input current of the memristor changes sign, respectively, and the voltage across the memristor changes sign as well, Fig. 5.3*a*. The process passes back along the path traversed from

the maximum value $q = 4Q$ with a constant value of the memristance R_0 to the bend point Q at the left, where the value of the memristance is changed to the value R_1. The magnitude of the charge continues to decrease until it returns to the starting point, where $q = 0$ (at the time $t = \frac{2\pi}{\omega}$).

$Q := 10^{-4}$ $w := 1$ $i(t) := 2 \cdot Q \cdot w \cdot \sin(w \cdot t)$ $R_0 := 6000$ $R_1 := 2500$ $t := 0, 0.001 .. 10$ $q(t) := 2 \cdot Q \cdot (1 - \cos(w \cdot t))$

$M(t) := R_0 + \frac{1}{2} \cdot (R_1 - R_0) \cdot (\text{signum}(q(t) + Q) - \text{signum}(q(t) - Q))$ $u(t) := M(t) \cdot i(t)$

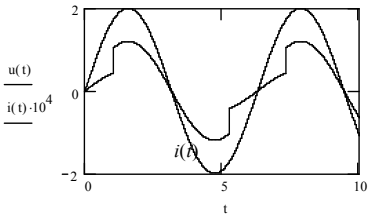

a

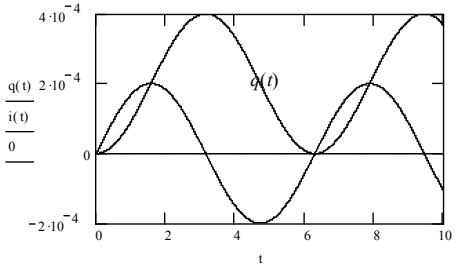

b

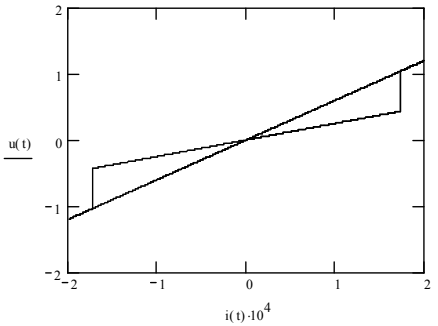

c

Fig. 5.3. Basic dependencies of the memristor controlled by the charge

Since $u(t)$ and $i(t)$ have a negative sign in the reverse pass, the current-voltage characteristic is odd "pinched" hysteresis loop as shown in Fig. 5.3*c*.

Note that the loop consists of two inclined branches, corresponding to two values of the memristances: R_1 for the lower and R_0 for upper branches.

We note also that the switching occur instantly in both directions. If we "rewritten" the voltage-current characteristic obtained in a plane $u - i$ in the plane $M - i$, then we obtain a square hysteresis loop of the memristance (rectangular resistance hysteresis loop), as shown in Fig. 5.2.

Consider processes in the memristor, which is controlled by the magnetic flux and is characterized by a piecewise-linear dependency $q(\Phi)$, Fig. 5.4.

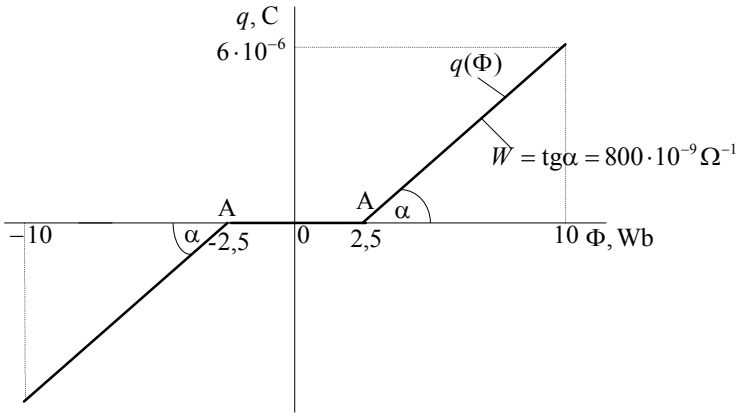

Fig. 5.4. Coulomb-weber characteristic of the memristor

The charge q is measured in nanocoulomb, and the magnetic flow is measured in the weber. By analogy with the considered above case, the analytical expression for the symmetric odd function can be written as:

$$q(\Phi) = \frac{1}{2} W_1 \left[2\Phi + |\Phi - A| - |\Phi + A| \right],$$

where as the numerical example the values W and A are chosen as $W_1 = 800 \cdot 10^{-9}\ \Omega^{-1}$ and $A = 2.5$ Wb respectively.

It is obvious that the considered device is not controlled by charge memristor because its memristance is infinite at all points of the horizontal segment of the piecewise-linear function $q(\Phi)$ where the memconductance W_0 is equal to zero.

Thus, the horizontal segment has the memconductance $W_0 = 0$ and two parallel outer segments of the characteristics have the memconductance equaled $W_1 = 800 \cdot 10^{-9}\ \Omega^{-1}$.

Let the sinusoidal voltage of the source (for simplicity we assume $\omega = 1,\ U_m = 5$ V) is applied to the memristor, Fig. 5.5*a*:

$$u(t) = \begin{cases} U_m \sin \omega t = 5 \sin t, & t > 0 \\ 0, & t < 0. \end{cases}$$

We determine the magnetic flux $\Phi(t)$ by the integration $u(t)$ over time (Fig. 5.5*b*):

$$\Phi(t) = \int_0^t 5 \sin \tau d\tau = -5 \cos \tau \Big|_0^t = 5(1 - \cos t), \quad t > 0.$$

Substituting this expression into the expression for the charge $q(t)$, we get, Fig. 5.5*c*:

$$q(t) = 400 \cdot 10^{-9} \left[10(1 - \cos t) + \left| 5(1 - \cos t) - 2.5 \right| - \left| 5(1 - \cos t) + 2.5 \right| \right].$$

Obviously, the value of the charge $q(t) = 0$ if $\left| \Phi(t) \right| < 2.5$ and $q(t) = 800 \cdot 10^{-9} [\Phi(t) - 2.5]$ when $\Phi(t) \geq 2.5$. The maximum value of the charge is reached for $\omega t = \pi$ and equals:

$$q_{\max}(\omega t = \pi) = 800 \cdot 10^{-9} (10 - 2{,}5) = 6 \cdot 10^{-6}\ \text{Cl}.$$

Differentiating with respect to time the expression for the expression we find the expression for the current $i(t)$, Fig. 5.5*d*:

$$i(t) = \frac{dq(t)}{dt} = 4 \cdot 10^{-6} \sin t \left\{ 1 + \theta[5(1 - \cos t) - 2.5] - \theta[5(1 - \cos t) + 2.5] \right\},$$

where $\theta(z) = \begin{cases} 1, & z \geq 0, \\ 0, & z < 0. \end{cases}$

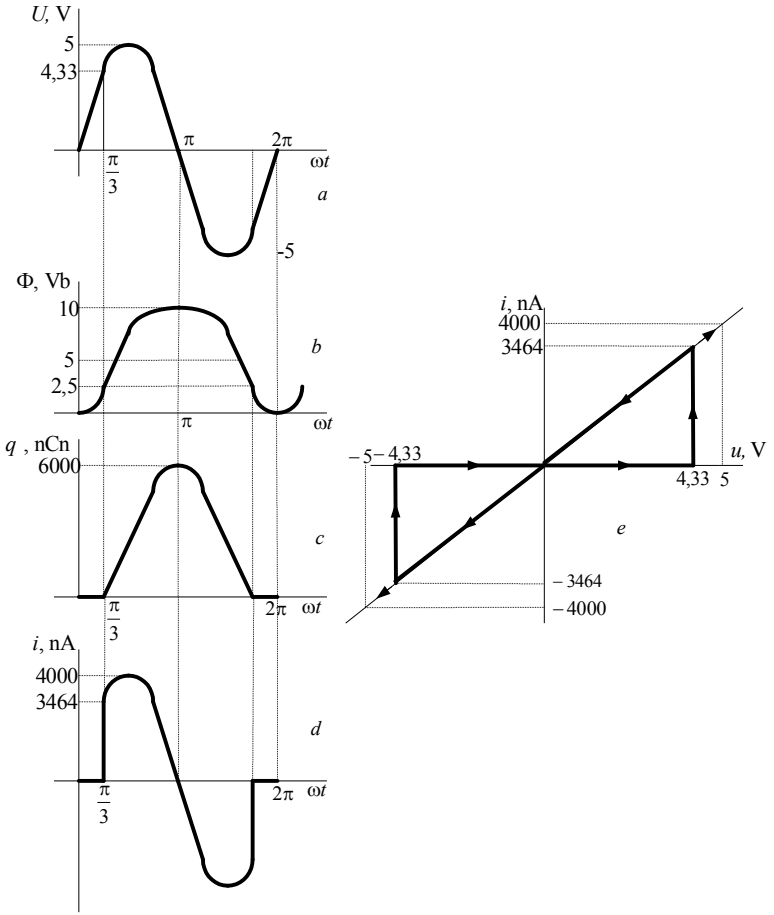

Fig. 5.5. Theoretical graphs of the basic dependencies

To calculate the current $i(t)$ the unity function $\theta(z)$ was approximated by the expression:

$$\theta(z) = \frac{1}{1 + \exp\left(-\frac{z}{b}\right)},$$

where the coefficient b defines the slope of the jump of the current from 1 to 0.

Next we define the voltage values that correspond to the two break point of the characteristics $q(\Phi)$ when $|A| =$ 2.5 Wb, Fig. 5.4. In this case:

$$u(t) = 5(1 - \cos t) = 2{,}5 \quad \rightarrow \quad \cos t = \frac{1}{2} \quad \rightarrow \quad \omega t = \frac{\pi}{3},$$

from which it follows $u\left(\omega t = \frac{\pi}{3}\right) = 5 \cdot 0{,}866 = 4{,}33$ V.

Knowing the expressions for the current $i(t)$ and the voltage $u(t)$ we may construct the memristor current-voltage characteristic in the plane $i - u$, Fig. 5.5*e*. Note that memconductance in Fig. 5.5*e* is switched abruptly from $W_0 = 0$ (the horizontal segment) at two points corresponding to the voltages of 4.33 V and minus 4.33 V. Switching is instantaneous due to the break of the characteristics $q(\Phi)$ at the points $\Phi = \pm$ 2,5 Wb, respectively, Fig. 5.4.

The results of the mathematical modeling are shown in Fig. 5.6.

5.2 Functional region of the resistive switching

Existing materials and technologies in the semiconductor industry are approaching to their physical limitations and the major scientific achievements in this field lead to continuous reduction of the size of devices within the nanoscale. The phenomenon of the resistive switching was the precondition for the creation of an entirely new class of devices with functional properties that are not available in traditional electronics. In particular, the nanoscale memory cell was designed for computer systems such as ReRAM (Resistive Random Access Memory), [65], [67], and [69].

Improvement of memory cells having nanosizes is one of the most important technological steps in the near future to create a nonvolatile random access memory (NVRAM).

Resistive switching in the structure of metal/oxide/metal having nanosizes, have great potential to transform the types of nonvolatile memory, and may lead to new forms of computing and new structures of the computer engineering. To successfully develop new achievements in this field we have to understand the interconnected electronic and ionic

phenomena that occur in nanoscale devices that are the dynamics of the electron-ion, which today explains the behavior of the devices based on the memristor.

$$t := 0, 0.01 .. 15 \qquad w := 1 \qquad u(t) := 5 \cdot \sin(w \cdot t) \qquad \Phi(t) := 5(1 - \cos(w \cdot t))$$

$$q(t) := 400 \cdot 10^{-9} [\, 10 \cdot (1 - \cos(w \cdot t)) + |5 \cdot (1 - \cos(w \cdot t)) - 2.5| - |5 \cdot (1 - \cos(w \cdot t)) + 2.5| \,]$$

$$i(t) := 4 \cdot 10^{-6} \sin(w \cdot t) \left[1 + \frac{1}{1 + \exp[-100 \cdot [5 \cdot (1 - \cos(w \cdot t)) - 2.5]]} - \frac{1}{1 + \exp[-100 \cdot [5 \cdot (1 - \cos(w \cdot t)) + 2.5]]} \right]$$

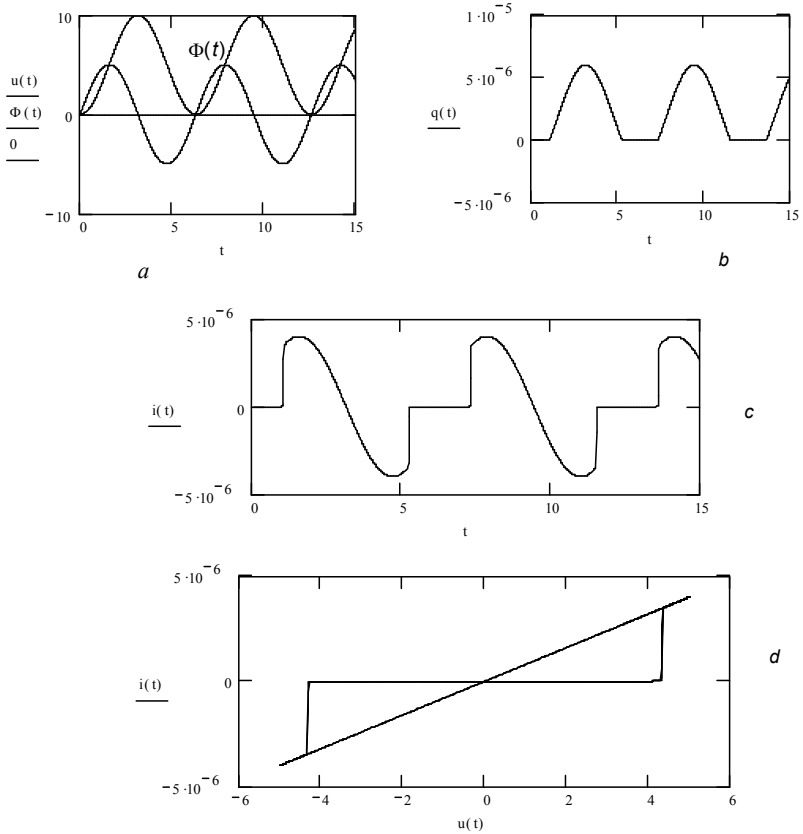

Fig. 5.6. Basic dependencies of the resistive switching

There are various mechanisms of the resistive switching. The main difficulties lie in the fact that the active regions of devices have extremely small sizes and are the "hidden" under the metal contact.

To describe the processes of the resistive switching some physical models have been proposed, the main ones are models that describe:

- mechanism of oxidation/reduction;
- formation of the conductive channels.

A reversible effect of the change of the conductivity memristor is called the resistive switching effect. The main structure with the considered effect is the structure of metal/dielectric/metal (MDM), which is sometimes called the structure of metal/insulator/metal (MIM).

The effect of the resistive switching of MDM structure is based on the change of the dielectric resistance by several orders under the action of the electric field generated by the applied voltage in the dielectric, Fig. 5.7.

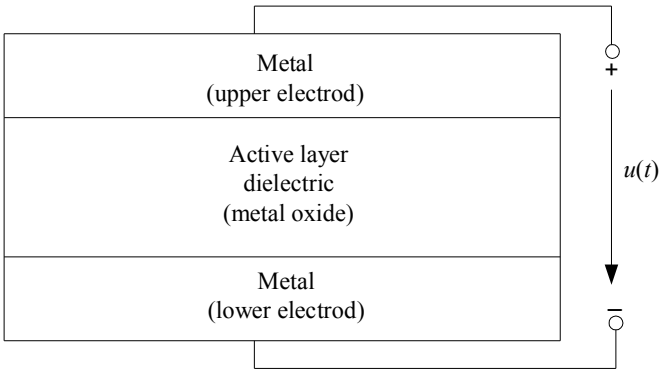

Fig. 5.7. MDM structure of the memristor

The number of resistive switching from one value to another value of the resistance is theoretically unlimited. However, it should be noted that the obtaining of the stable element, which is able to stand a large number of cyclic switching without changing the stated resistance values (for example R_{on} and R_{off}), is a complex task today.

Uneven distribution of electrons between atoms in the compounds is called the oxidation. Element, the electrons of which are displaced to atoms of other element, shows a positive oxidation unlike the other element which shows a negative oxidation. The number of electrons which are offset from one atom of the given element (positive oxidation state), or to one atom of the given element (negative oxidation state), is called the degree of oxidation of the element.

For example, the degree of oxidation of oxygen, usually equals –2. The most important exceptions are peroxide compounds, for which it is -1.For elements with variable oxidation state it is always possible to calculate the degree of oxidation, knowing the formula of the compound and the fact that the sum of the oxidation degree of all atoms in the molecule is zero.

Let's define as an example the oxidation of the titanium and the tantalum in the compounds TiO_2 and Ta_2O_5, assuming that the degree of oxidation of the oxygen equals –2:

$$TiO_2 \qquad x + 2(-2) = 0 \qquad x = +4,$$

$$Ta_2O_5 \qquad 2x + 5(-2) = 0 \qquad x = +5.$$

All chemical reactions can be divided into two groups. In the reactions of the first group the oxidation of all elements included in the composition of the reactants, remains unchanged; in the reactions of the second group the oxidation of one or more elements changes.

The reactions in which the degrees of oxidation of elements change, called **oxidation / reduction** reactions.

Return of the electrons which is accompanied by an increase of the degree of oxidation is called **oxidation.**

Joining of the elements, accompanied by a decrease of the degree of oxidation is called the **reduction.**

The substance, which includes acescent element, is called a reducing agent and a substance containing a recovering element is called the **oxidant.**

As shown by numerous researches, the memristor characteristics are determined primarily by the architecture of the layers and the element material. In particular, the complex poorly studied the effect of resistive switching depends on the material of the metal contacts, which define the interface between the metal and the dielectric.

As already noted, the drift of the oxygen ions (oxygen vacancies) accompanies to the reaction of the reduction/oxidation. Oxygen vacancies have a high mobility on the depth of oxide and are the "traps" for electrons in which the charge is transferred from one metal electrode to the

other. Depending on the concentration of oxygen vacancies and their diffusion in the oxide MDM structure can be in the high resistance state (HRS) with the designation R_{off} or the low resistance state (LRS) with the designation R_{on}.

In order to effect of the resistive switching was stable it is necessary to control the concentration of oxygen vacancies in the oxide layer.

As the active layer of the memristor (except for the active layer $TiO_2 - TiO_{2-x}$, which has been used to realize the first memristor) was proposed a several of alternative materials that can be easily integrated in silicon technology. In particular, the metal oxides such as: $ZrO_2 - ZrO_{2-x}$, $HfO_2 - HfO_{2-x}$, $Ta_2O_5 - TaO_2$, $WO_3 - WO_{3-x}$, $Nb_2O_5 - NbO_2$ and others may be used for the realization of the memristors. Elements Hf, Zr and Ti are the elements of the fourth group of the periodic table and Ta is the element of the fifth group.

One approach to improving the functional properties of the memristors based on transition metal oxides (TiO_2, HfO_2, ZrO_2) is the doping of the oxides by the trivalent impurity, for example Al.

As was shown in [94] the addition of the aluminum Al into the zirconium dioxide ZrO_2 reduces the energy of formation of the oxygen vacancies is almost doubled. Experimental researches have also shown improved performance MDM structures on the base of three-component metal oxide, for example $HfAlO_x$ and $TiAlO_x$ in comparison with classical structures $TiO_2 - TiO_{2-x}$ and $HfO_2 - HfO_{2-x}$.

Switching resistive effect can be observed at the same applied voltage polarity of certain amplitude. In this case the switching is called unipolar switching (switch via amplitude).

Typical unipolar switching cycle is shown in Fig. 5.8 *a*. If the device is in a state HRS (off), then the relatively large voltage U_{on} must be applied to the memristor in order to initiate the increase of the current and the switching of the memristor into the state LRS (on). In order to switch the device back in the condition HRS, it is necessary to apply the voltage of the same polarity, but of smaller magnitude U_{off}. It is necessary to note that both the positive (U_{on} and U_{off}) and the negative values can be used with unipolar switching.

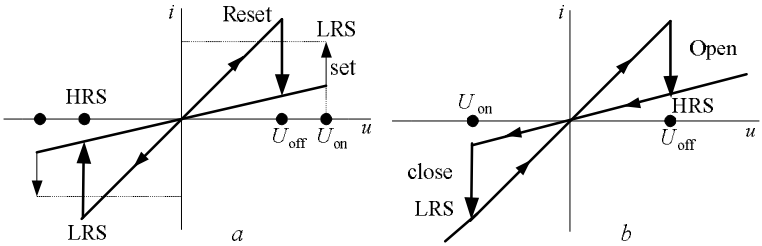

Fig. 5.8. Unipolar (*a*) and bipolar (*b*) the memristor switching

Thus, unipolar effect does not depend on the polarity of the applied voltage. This fact shows that in this case the major role belongs to the thermal processes that create the so-called conducting channels in the middle of the active layer between the metal electrodes.

The second variant of the resistive switching at the polarity change may be used. This variant is called the bipolar switching when certain voltage amplitude is applied to the memristor, Fig. 5.8*b*. In this case, a positive voltage U_{off} is used to switch from the state LRS to state HRS and a negative voltage U_{on} to switch from the state HRS to the state LRS.

Consider the MDM structure of the type $\text{Pt} / \text{TiO}_2 / \text{Pt}$. The process of oxidation – reduction in such structure is schematically shown in Fig. 5.9. During initial application of the voltage (the so-called process of "forming") the dielectric is divided into two layers defined by the generation of oxygen vacancies. The positively charged oxygen vacancies drift toward the negatively charged electrode, reducing the layer TiO_2 to TiO_{2-x} and decreasing it (TiO_2) resistance. The oxidation process takes place on the positive electrode (anode).

The boundary between the insulating layer TiO_2 and the conductive layer TiO_{2-x} (the virtual cathode or the virtual boundary) moves to the left until it reaches the anode, which is positively charged. The resistance across the MDM structure is substantially reduced reaching the value R_{on}.

As a rule, the considered process is indicated by the symbol SET (switch on). Thus, for the given polarity of the applied voltage MDM structure has the state LRS (low resistance state).

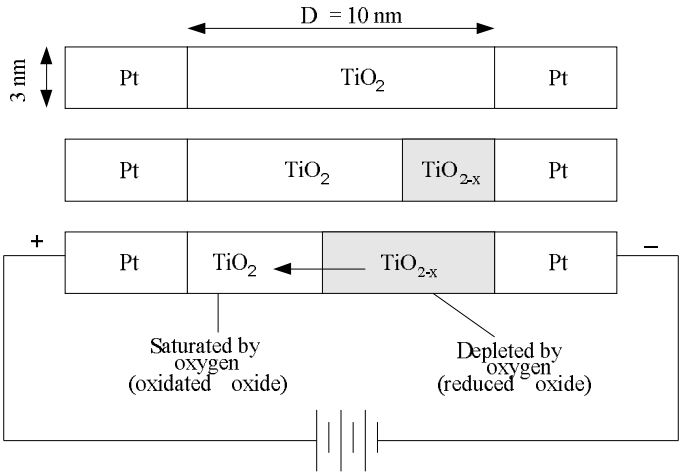

Fig. 5.9. Process of the oxidation | reduction in the MDM structure

The applied voltage of the negative polarity leads to the reverse procedure: the resistance across the MDM structure is substantially increased reaching the value R_{off}.

This process is referred to RESET (switch off). As already mentioned, such switching is called the bipolar one.

It should be noted that the states with the intermediate resistance value (intermediate resistance state – IRS) may be realized in the memristor.

The described resistive switching process in oxides of the transition metals is called the mechanism of the oxidation / reduction or the valence change mechanism (VCM).

In the laboratory (HP – Hewlett-Packard) were researched the resistive switching processes in the structure $\text{Pt}/\text{TiO}_2/\text{Pt}$ with the ratio $\frac{R_{\text{off}}}{R_{\text{on}}} = 10^3$ [86], [94], and [95]. The image of the nanodevices in the nodes of the matrix structure obtained by using an atomic force microscope is shown in Fig. 5.10.

Nanowires were produced by means of the nanoprint lithography method from the platinum of 50 nm thick. Between them in the nodes the thin film of 50 nm thick, having two layers TiO_2 and the layer of the oxygen-depleted oxide TiO_{2-x} is located. When testing the voltage

is applied to the two electrodes (the lower electrode is grounded) for all measurements. Multiple switches showed a high degree of repeatability (see also Fig. 5.15). Memristor switched in the state LRS(on) at a negative voltage and in the state HRS(off) at a positive voltage (in essence the bipolar switch has been realized). Reached switching speed was less than 50 ns.

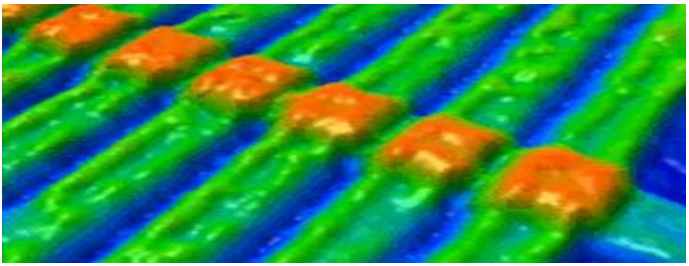

Fig. 5.10. The image of the memristors in the nodes of the matrix structure

It is known [99] that the dependencies of the resistances of the MDM structures in the HRS and LRS states from the area of the metal electrodes are substantially different for the different transition metal oxides. For some structures values of these resistances are inversely proportional to the area (for example, for the structure on the base $SrTiO_3$ alloyed by the niobium Nb), and for other structures (for example the structures on the base NiO) almost do not depend on the area of the structure.

Experiments have shown that in the first case the resistive switching occurs across the all area of the structure, and in the second case the switching occurs locally through the formation of the so-called filiform conducting channels. Local resistive switching mechanism is called the filamentary one.

Both variants of the resistive switches are schematically shown in Fig. 5.11.

The experimental data confirm the possibility of local resistive switching, whereby the models of the switching on the base of formation of the local conductive channels have been developed (Fig. 5.12) in addition to the models based on the mechanism of changing the valence of the dielectric material over the entire area of the structure. In particular, the process of the filament formation in the structure $Ag/SiO_2/Pt$ is shown in Fig. 5.13.

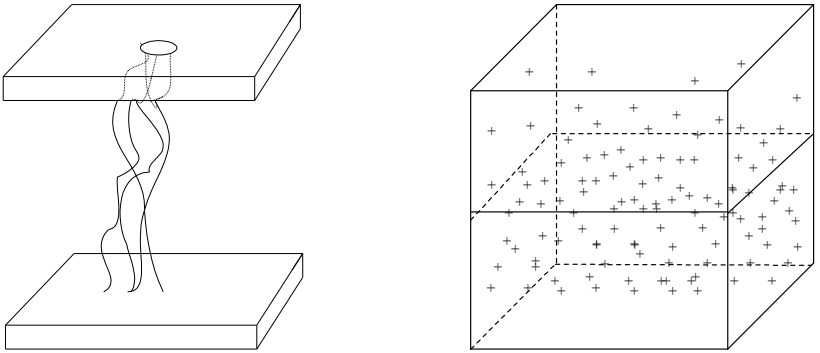

Fig. 5.11. The methods of the resistive switching: *a*: filamentary switching process in which the conductivity of the active region is limited by the thread (threads) and the switching occurs within that thread; *b*: uniform switching process (VCM), for which the entire active region located under the metal electrode, participates in the process of switching

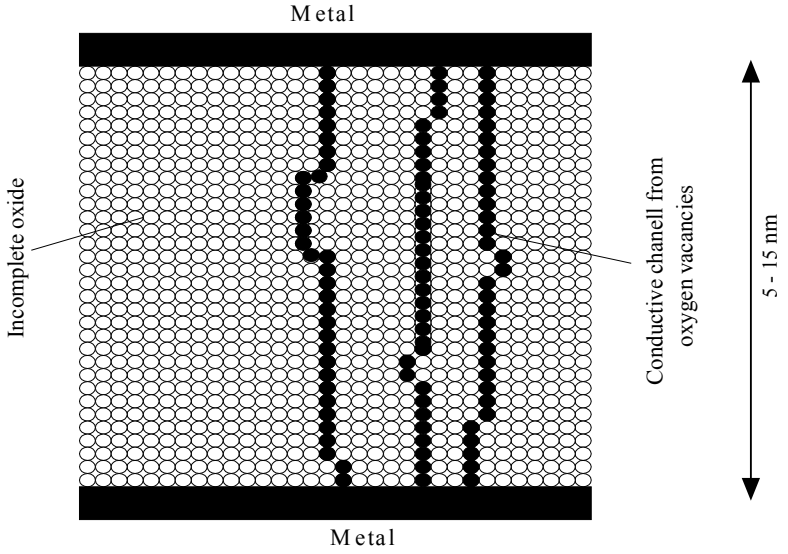

Fig. 5.12. Formation of the filaments in the resistive switching process

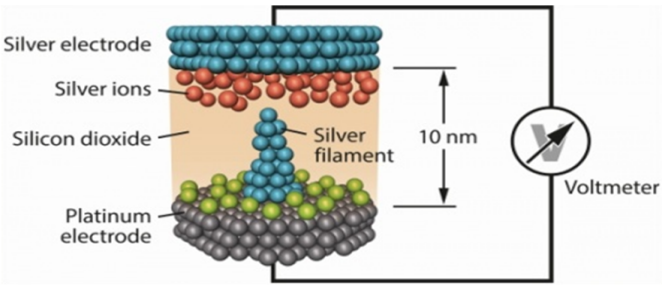

Fig. 5.13. Formation of the filament in the structure $Ag/SiO_2/Pt$

Taking into account the importance of the generation of oxygen vacancies for the resistive switching process the respective model of the switching was developed that explains the possibility of obtaining a set of intermediate resistances (IR-states) of the MDM structure depending on the applied voltage to it. This is the main memristive effect, Fig. 5.14.

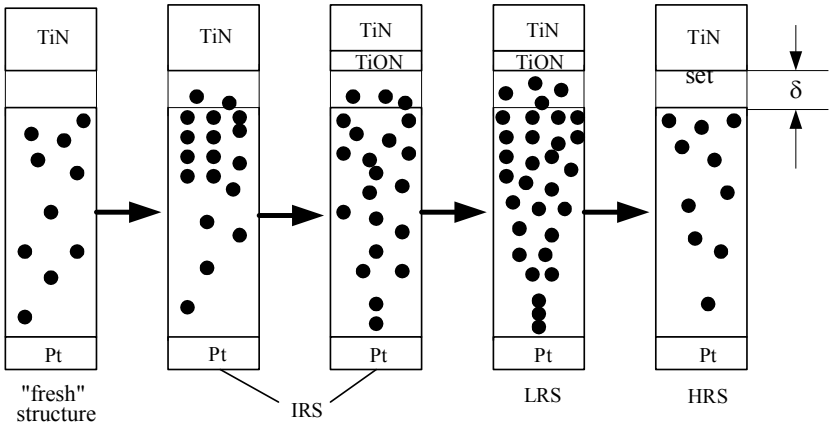

Fig. 5.14. Formation of the intermediate states of the structure

The state with the lowest resistance (LRS) is explained by the presence of conductive filaments with the highest density of the positively charged oxygen vacancies.

To realize the switching processes of the structure in the state with a high resistance value it is necessary to take into account important physical processes of change of the filaments structure, as well as the

processes of so-called reverse anodic oxidation of the filament area near the interface with the upper Pt electrode.

Indeed, the increase of the positive potential applied to the electrode Pt, activates increasing oxygen vacancies drift from the anode deep into the material. As a result, it becomes possible to obtain a set of different resistances (IR1, IR2 ....) due to the gradual change of the density of oxygen vacancies which act as the dopants in the insulating layer of the thickness δ, Fig. 5.14.

Thus, there are two types of resistive switching which are used in memristors and the memory elements on their basis (ReRAM). The first type is called the interface switching (VCM). The second type is called the filamentary switching, in which the oxygen vacancies are aligned along the "conductive track", the presence of which is determined by their migration. This creates cross-arrays with a very high density, which use a programming voltage for the migration of oxygen vacancies. It allows to change the resistance of the bit cell by the nonvolatile manner.

As reported in the scientific journals using filamentary switching allows to reduce programming time (writing) to fractions of nanoseconds, and to reduce the operating current to a few hundred nanoamperes.

5.3 Effect of the resistive switching in multicomponent oxides of the transition metals

The most stable effect of the resistive switching is observed in multicomponent oxides of the transition metals. One of the mechanisms to control by the concentration of oxygen vacancies in the memristor manufacturing stage is the doping of the metal oxide with the oxidation level +4 by the metal ions with the oxidation level +3 (three valence electrons are in the outer electron shell). As mentioned above, the doping of ZrO_2 by the impurity Al^{+3} allows to decrease the formation of energy of oxygen vacancies by 1.7 times [8].

The similar method of controlling the concentration of oxygen vacancies is possible for the hafnium oxide HfO_2, which is most convenient to introduce in the industry. It is explained by close structural and electronic properties of the zirconium and the hafnium oxides (both elements are in the group IV).

One of the electrodes of the memristor (for example the electrode from titanium nitride TiN is effective "reservoir" of the oxygen) is an additional source of oxygen vacancies. The combination of both approaches (the doping of the oxide layer and the use of the electrode from the active material with respect to the oxygen) is an effective means of controlling the concentration of oxygen vacancies in the oxide layer to achieve a stable effect of the resistive switching of the memristor. To obtain long-term stability and reliability of the memristor it is necessary to provide the spatial limitation of areas where the origin and movement of the oxygen vacancies take place. In particular, for this purpose the concentration of the impurity of aluminum Al changes throughout the depth of the oxide, for example in the memristor based on the thin film of the ternary oxide $Hf_xAl_{1-x}O_y$ with varying content of Al throughout the depth of the oxide.

The layer adjacent to the TiN electrode has the highest Al content and, respectively, has the lowest dielectric constant (which increases the electric field at the interface) and simultaneously has the greatest number of the oxygen vacancies. When voltage is applied to the structure a conductive channel is formed in the corresponding dielectric layer $Hf_xAl_{1-x}O_y$. Smooth switching stage corresponds to the process of expansion of the conductive channel in accordance with the profile of Al content in the oxide layer due to the oxygen diffusion to the layer TiN and the formation at the boundary TiN / $Hf_xAl_{1-x}O_y$ of the TiON layer of some thickness. This results to partial reduction of oxide $Hf_xAl_{1-x}O_y$, which is accompanied by the generation and diffusion of the oxygen vacancies in the oxide layer. In this case the structure has a set of intermediate resistances (IRS). The experimental current-voltage characteristics of the memristor with several intermediate states, which are determined by the respective voltage levels, are shown in Fig. 5.15.

As already mentioned, positively charged oxygen vacancies are traps for electrons, so the mechanism of the charge transport in the channel formed by the oxygen vacancies associated with the tunneling of electrons through the traps.

Unlike the most metals which are active with respect to oxygen, (such as Ti, Zr) the nitride of titanium TiN is capable to absorb and release the oxygen ions. It was shown experimentally that the TiN elec-

trode is effectively oxidized in the process of diffusion of oxygen ions from the oxide under the influence of an electric field, so memristors with TiN electrode have highly reproducible effect of the resistive switching. The platinum electrode (Pt) provides an inert boundary with the dielectric.

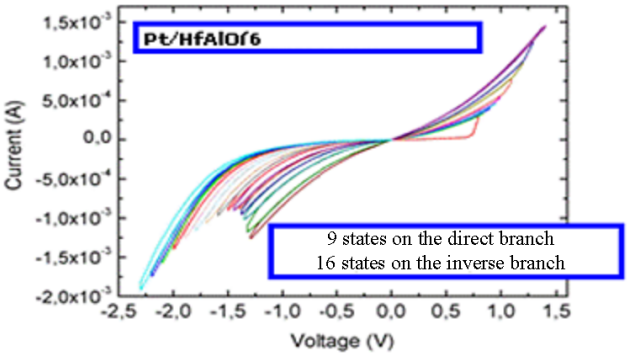

Fig. 5.15. The experimental current-voltage characteristics of the memristor with several intermediate states

The structure with platinum contacts which were used in the memristor based on the titanium oxide was researched by the worldwide centers, [99]. The researches have shown that at a relatively high ratio of the maximum to the minimum values of the resistance (about 100) the samples with platinum contacts are degraded relatively rapidly, that is the samples degenerated into the usual resistors with the resistance. R_{on}.

In conclusion, the following should be noted.

Recently, considerable attention is paid to the creation of devices-of the nonvolatile resistive memory (ReRAM) based on the MDM structures, including devices using the oxides with high mobility of oxygen vacancies as dielectric.

In these researches, generally the non-stoichiometric single-layer or multilayer oxide structures with ionic bonds were used as dielectric. Experiments show that the conductivity in the low resistance state is determined by conducting channels (filaments) that occur during the so-called forming [86], [87].

The concentration of oxygen vacancies in the oxide and the state of the interface dielectric / electrode may be the most significant factors

controlling the resistive switching in oxides under an applied electric field.

Switching leads to the formation and destruction of the conductive channels in the process of the reduction / oxidation (redox) and depends on the electrode material. The stages of the formation and destruction of the filaments in the process of the resistive switching are shown in Fig. 5.16.

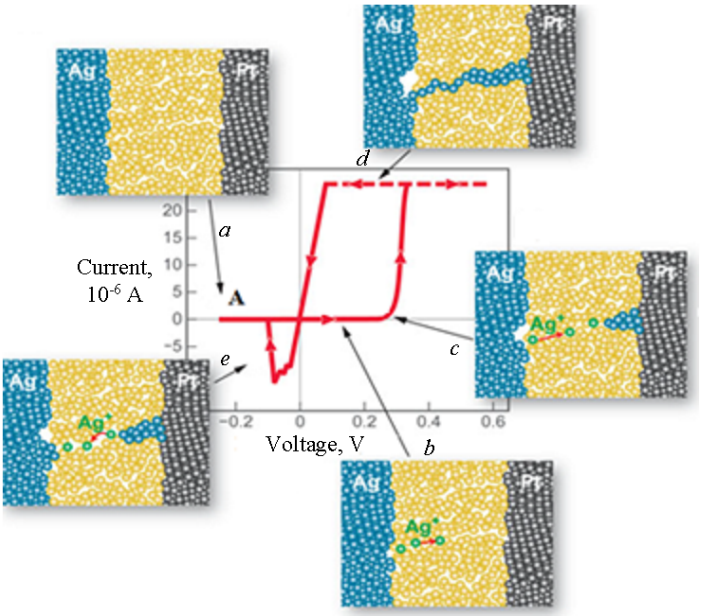

Fig.5.16. The stages of the formation and destruction of the filaments

The resistive switching in the active region consisting of the metal and the oxide was proposed in [8], [9]. In this case the oxide is both the second electrode and the active region, the change of the resistance of which leads to the resistive switching of the entire device. It is proposed to use a four-component oxide, which is a conductor instead of the poorly conducting binary structure of the transition metal with the oxygen.

A composite oxide is a compound of three or more simple oxides with similar chemical properties. For these compounds the range of physical properties it is considerably broader than for the simple oxides from which these compounds are made.

Thus, the problems related to the choice of the most perspective materials to create the memristors and the non-volatile memory devices remain relevant today. The particular interest is the MDM structures in which the materials and the technology of the formation of the structures are compatible with the silicon technology.

5.4 Examples of the resistive switching of the memristor

Let's consider two examples with bipolar and unipolar ways of the resistive switching of the memristor taking into account it's the weber-coulomb and the coulomb-weber characteristics.

Let weber-coulomb characteristic of the memristor controlled by the charge, has the form shown in Fig. 5.17*a*.

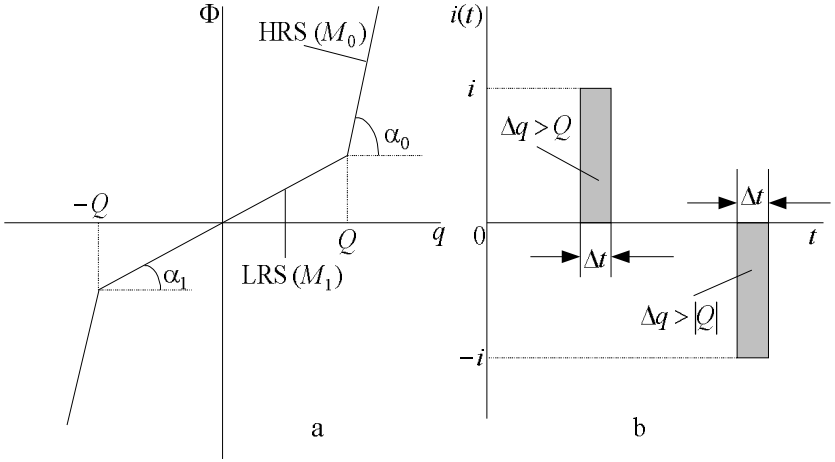

Fig. 5.17. The signals of the bipolar switching of the memristor

It is obvious that the memristor has two states: a low resistance ($\mathrm{LRS} \to M_1$) and a high resistance ($\mathrm{HRS} \to M_0$), which are defined as:

$$M_1 = \frac{d\Phi}{dq} \approx \frac{\Delta\Phi}{\Delta q} = \mathrm{tg}\alpha_1, \quad M_0 = \frac{d\Phi}{dq} \approx \frac{\Delta\Phi}{\Delta q} = \mathrm{tg}\alpha_2,$$

where M_0 and M_1 are the respective values of the memristance M.

Thus, the value M_1 corresponds to the average segment of the characteristics $\Phi(q)$ having a smaller slope, and the value M_0 corresponds to the extreme segments having greater slope.

To switch the memristor from the state $\mathrm{LRS}(M_1)$ to the state $\mathrm{HRS}(M_0)$, it is necessary to apply a current pulse of such magnitude and duration that the corresponding amount of the charge $\Delta q = i\Delta t$ exceeds the value Q, defining the bend point of the characteristics $\Phi(q)$, that is $\Delta q > Q$, Fig. 5.17*b*.

To switch the memristor back from the state $\mathrm{HRS}(M_0)$ to the state $\mathrm{LRS}(M_1)$ it is necessary to apply the same current pulse of the negative polarity. It is obvious that in this case the method of the bipolar resistive switching is used.

The following example illustrates the method of the unipolar resistive switching. In this case we consider the memristor controlled by the flux Φ with the characteristic $q(\Phi)$, Fig. 5.18*a*.

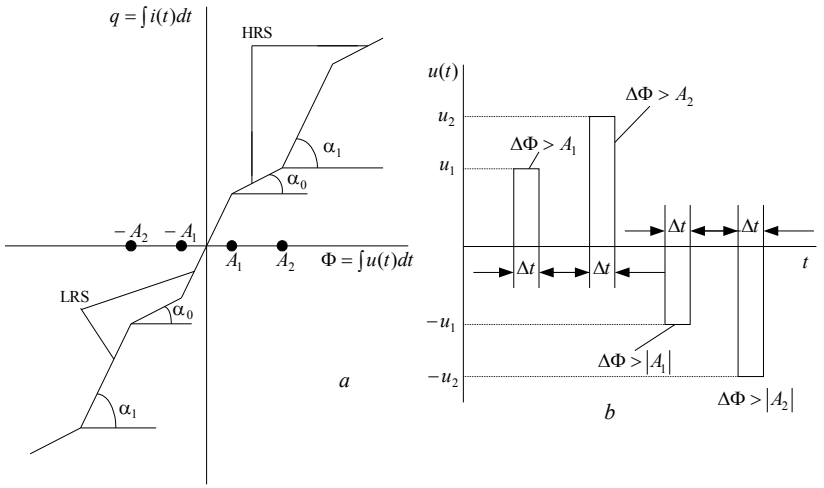

Fig.5.18. The signals of the unipolar switching of the memristor

The characteristic $q(\Phi)$ is represented by a seven-segment piecewise linear characteristic. Three parallel segment with the greatest slope

determine the state LRS with the high conductivity value W_1, while the remaining four parallel segments with the lower slope determine the state HRS with low conductivity value W_0, which are defined as

$$W_0 \approx \frac{\Delta q}{\Delta \Phi} = \mathrm{tg}\alpha_0, \quad W_1 \approx \frac{\Delta q}{\Delta \Phi} = \mathrm{tg}\alpha_1.$$

To switch the memristor from the LRS state to the HRS state (state of the low conductivity) it is necessary to apply a relatively low amplitude impulse voltage because a small value of the increment $\Delta\Phi$ is required in order to exceed the value A_1 which determines the bend point of the curve $q(\Phi)$, that is $\Delta\Phi_1 = u_1\Delta t > A_1$, Fig. 5.18*b*. To switch back the memristor in the state LRS (the state of high conductivity) it is necessary to apply a voltage pulse of the same duration and the same polarity, but of greater amplitude to exceed the value A_2 which determines the second bend point of the characteristics $q(\Phi)$, Fig. 5.18*b*.

To switch the states LRS-HRS-LRS the same switching sequence, but of the opposite sign can be used, Fig. 5.18*b*.

To prevent the excessive current jump from a small value to a sufficiently large value it is necessary to limit the value of the current to the maximum safe level which is called the agreed current level (compliance current level). It is explained by the possible damage of the device.

5.5 Reading binary data from the memristor

Any electronic device having two electrical terminals (one-port network) is a nonvolatile resistive memory device if it "remembers" one of the two resistance values for a long time without consuming any energy, and can be switched from the state of the low resistance (LRS) into the state with the high resistance (HRS) and vice versa by applying to his terminals or a short voltage pulse or a short current pulse.

The state of the memory in which the binary information is encoded, for example, as "0" (high resistance) and "1" (low resistance) can be read at any time. It is necessary to make the following note. The information reading mode relatively small in magnitude signals memristor should be a conventional linear resistor, which is described by Ohm's

law. The linear properties of this element imply that both the read signal and the response signal of the memristor should be identical in shape. This means that the voltage-current characteristic of the memristor in a plane $u - i$ must be represented by a straight line passing through the origin in process of reading information (in the mode of small signal). Its slope must be sufficiently small ($\mathrm{tg}\alpha_0 = R_{\mathrm{on}}$) if the readable resistance is small value (R_{on}), or enough large ($\mathrm{tg}\alpha_1 = R_{\mathrm{off}}$) if the readable resistance has the maximum value R_{off}, Fig. 5.19.

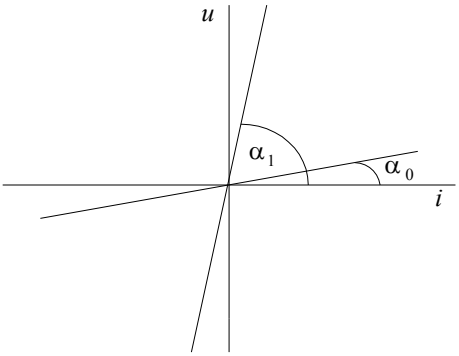

Fig. 5.19. The slope of the characteristic at the reading of the information

It should be noted that today the widespread adoption of the memristors in nanoelectronics is limited by the following problems [8], [12]. One of them is the need to reduce energy consumption of the memory cell. The existing method of reading information in the memristor, considered above, is based on feeding a constant voltage across its terminals, which is less than the critical value, initiating a change in its resistance. Then the resistance value of the memristor is determined by passing through it a direct electric current [74]. This method has significant shortcomings:

• a limited number of reading cycles of the information stored in the memristor without rewriting it,

• increased power consumption in the reading of the information,

• a small temperature range, in which the resistive random access memory can work [74].

The first shortcoming is due to the possibility of distortion of information stored in the memristor, because that the current flowing through

it (even short-term) changes the dimensions of the spatial region in which the oxygen vacancies are concentrated. Then the value of the contact resistance of the metal / oxide change as well (this resistance is an informative parameter).

Increased consumption occurs due to the relatively large value of the voltage (approximately one volt or slightly higher), which must be applied to the memristor to rewrite the information in the traditional method. Insufficient temperature range is associated with significant temperature dependence of the voltage applied to the memristor to write and / or read the information [8], [12].

The change of the temperature, as shown in [8], [12], does not lead practically to a change of the critical currents that change the resistive state. Therefore, application of the current instead of the voltage decreases the sensitivity to the temperature. Then, the current pulse applied to the memristor allows to determine the stored information by means of the measuring of the voltage across the memristor.

To read the information two pulses of current of the different polarity are used. These pulses have the area smaller than the area of the current pulse which is used to preserve it (that is $i\Delta t = q < Q$, as was considered above, Fig. 5.17).

To read the information the memristor must be connected through the address bus to a power source that generates the pulse $i\Delta t_{\text{read}}$.

Then the memristor must be connected through the another address bus to another power source connected to another power source, which generates a current pulse of opposite polarity $i\Delta t_{\text{supp}}$ which is called "support pulse". In this case $i\Delta t_{\text{read}} \approx i\Delta t_{\text{supp}}$. As a result, the distorted distribution of oxygen vacancies due to pulse $i\Delta t_{\text{read}}$ will be restored. It allows significantly to increase the number of the readings of the information until it is complete loss [12].

It should be noted that to provide high-speed of the resistive memory the thickness D of the oxide active area should be nano-sized and consistent with the other parameters, in particular with the average mobility of oxygen vacancies μ_D, with the device resistance in the low-resistance state R_{on}, with the duration of the write current and its value.

In accordance with the expression for the speed of the displacement of the virtual boundary separating the conducting and isolated parts of the oxide, we may write:

$$\frac{dw}{dt} = \mu_D E = \frac{\mu_D i(t) R_{\text{on}}}{D} \quad \Rightarrow \quad dw = \frac{\mu_D i(t) dt R_{\text{on}}}{D},$$

from which it follows the general expression for the value of D:

– for $\Delta w \approx 0{,}2D$

$$D = \sqrt{5\mu_D i(t) \Delta t R_{\text{on}}};$$

– for $\Delta w \approx D$

$$D = \sqrt{\mu_D i(t) \Delta t R_{\text{on}}}.$$

For example, let's assume the relatively high mobility of oxygen vacancies is $\mu_D = 10^{-8} \dfrac{\text{m}^2}{\text{V} \cdot \text{s}}$, the recording current value is $i_{\text{wr}} = 10^{-2}$ A, the oxide thickness D equals 10 nm, a resistance of the structure in a state LRS equals 100 ohms and $w \approx D$. Then the write pulse duration should be less than

$$\Delta t_{\text{wr}} = \frac{D^2}{\mu_D i_{\text{wr}} R_{\text{on}}} = \frac{10^{-16}}{10^{-8} 10^{-2} 10^{2}} = 10^{-8} = 10 \text{ ns}.$$

PHYSICAL REALIZATION OF THE MEMRISTOR ON THE BASE OF THE MULTILAYER STRUCTURES

- Main stages of the physical realization of the memristor
- Main stages of the manufacture of the memristor
- Measurement of the memristor characteristics in the laboratorial conditions

6.1 Main stages of the physical realization of the memristor

At the present level of the development of production technology of the memristors functional element has a standard lateral dimension of 100 nm x 100 nm or less. The image of the matrix $Pt/TaO_x/TiO_{2-x}/Pt$ in the atomic force microscope is shown in Fig. 6.1.

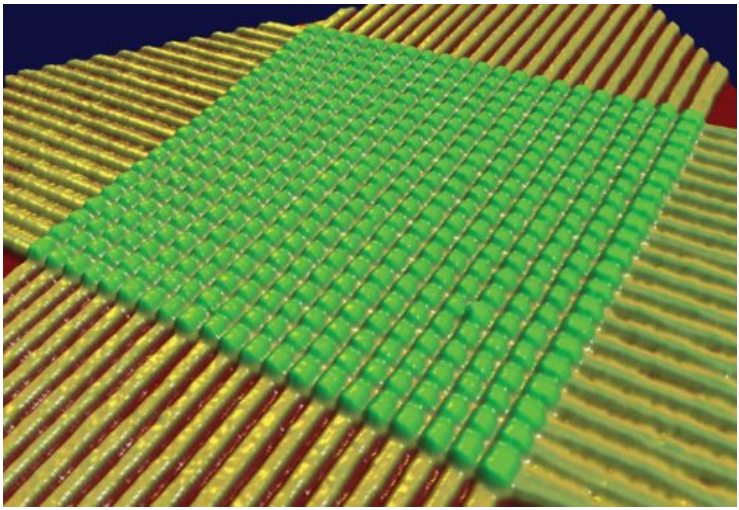

Fig. 6.1. The image of the matrix of the memristors in the atomic force microscope

Atomic force microscope (AFM) is a scanning probe microscope of the high resolution. It uses to determine the surface topography with a resolution from tens of angstroms up to atomic sizes. Unlike a scanning tunneling microscope, AFM can be used for the research both of conductive and nonconductive surfaces. The microscope is called the power one because it has not only the ability to scan, but also to manipulate atoms.

The principle of the AFM is based on registration of the power interaction between the sample surface and the probe. The nanoscale tip (cantilever) is used as the probe, located on the end of the elastic console, Fig. 6.2.

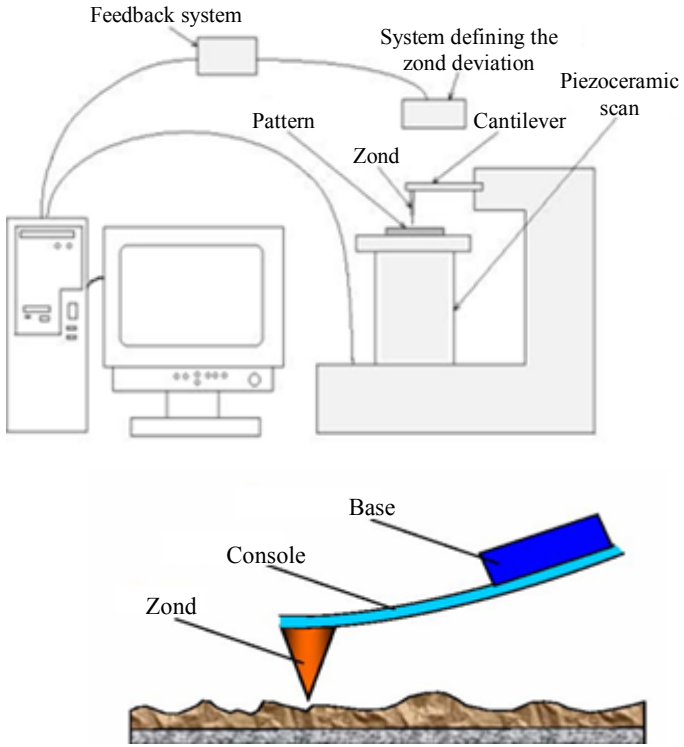

Fig. 6.2. Principle of operation of the atomic force microscope

The force acting on the probe from the surface leads to the bend of the console. The forces acting between the probe and the sample represent, primarily the long-distance Van der Waals forces (intermolecular forces, which are based on the electrostatic interaction of the dipoles), which at first are the forces of attraction, and with the further rapprochement these forces are transformed into the repulsive forces, Fig. 6.3.

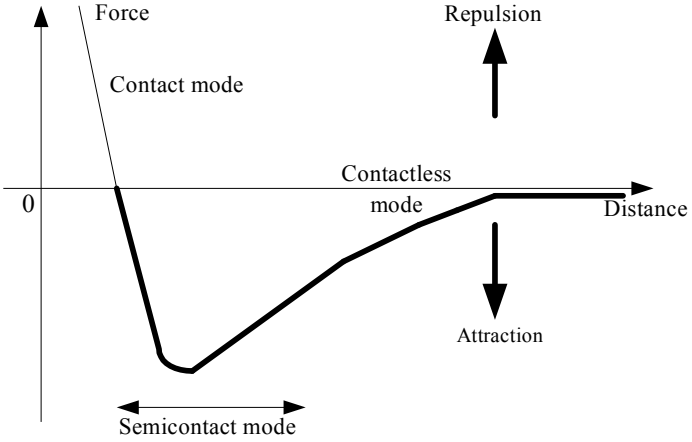

Fig. 6.3. The graph of the dependency of the Van der Waals force from the distance between the console and the sample surface

The appearance of heights or hollows under the edge leads to a change of the force acting on the probe, and hence to a change in the bending of the console. Thus, we may do the conclusion about the relief surface by registering the bending.

Depending on the acting of the force we may consider three modes of AFM operation:

- contact mode;
- "semi-contact" mode (tapping mode);
- noncontact mode.

Atomic force microscope provides a true three-dimensional topography, Fig. 6.4. Besides, non-conductive surface, viewed from the AFM does not require a metal coating, which often leads to a significant surface deformation.

Atomic force microscope is able to provide real atomic resolution in ultra-high vacuum conditions. The minimum vertical drop during scanning is a few microns, and a maximum scan field is 150 x 150 squared microns.

To get the AFM images it is required from several minutes to several hours.

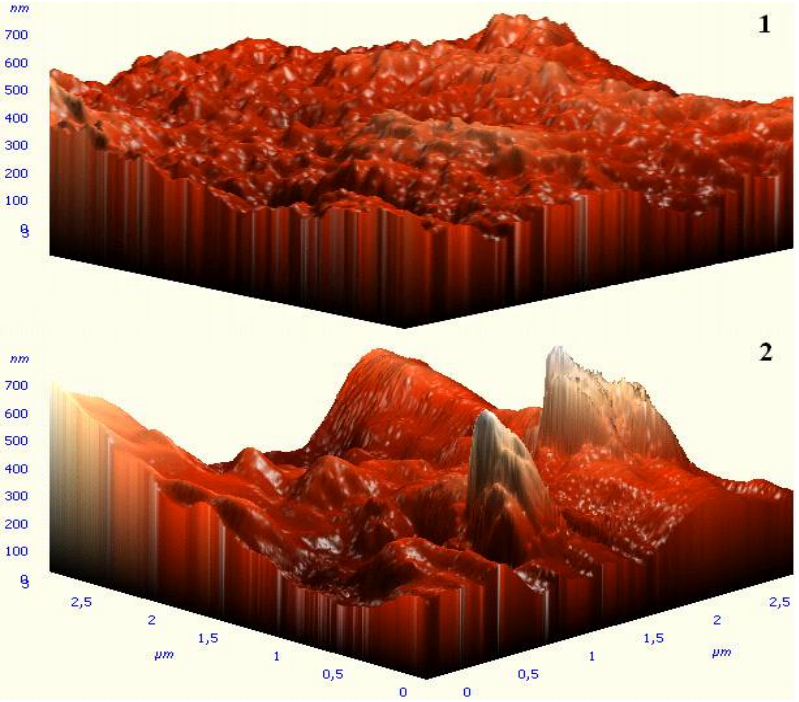

Fig. 6.4. The image of the surface in AFM

To increase the operating speed probe it is offered to use the microscope called video AFM, which provides a satisfactory quality of the image of the surfaces with television scanning frequency. Almost always, the results of the initial scan are subjected to mathematical processing. Usually it is used the respective software.

The thickness of the dielectric layers in the functional elements is typically 5-20 nm. The manufacture of the array of the memristors and the electrical contacts to the memristors, which are used for the research

their electrical characteristics, is achieved through several cycles of electron-beam lithography and photolithography.

Electronic lithography is the nanolithography method using an electron beam. The sharply focused electron beam deflected by a magnetic system draws the desired configuration on the surface of the resist which is sensitive to the electron radiation.

The resist is sprayed on the substrate (the surface). Management electron beam is produced by varying the current in the deflection magnetic systems, which are controlled by the computer.

Sections of the resist illuminated by the radiation are polymerized, and acquire the insolubility.

Further, not illuminated sections are washed by the chosen solvent. Through these windows the vacuum deposition of the respective material (for example, titanium nitride TiN or metals Pt, Au, and others) is produced.

Polymerized resist is washed with another solvent. After removal of the substrate the mask is finally formed for the use in photolithography.

E-lithography allows, at the current level of the technology development, to obtain the structures with a resolution of less than 1 nm, unattainable for the tough ultraviolet radiation due to a more short de Broglie wavelength of the electrons (in accordance with the wave character of the electron), in comparison with the light.

Electronic lithography is the main method of obtaining masks for subsequent photolithography.

The systems that use lasers are an alternative method of creating masks, but they have a lower resolution.

One of the main companies supplying the electronic lithography system is the company Mapper Lithography (Netherlands).

A block diagram of one of the modern electronic lithography systems is shown in Fig. 6.5.

The complex consists of an electron-optical column 1, the working chamber 2, the computer and a several of electronic components.

The structure of the electron-optical column includes:

- cathode-ray gun consisting of a cathode 4 and an anode 3;
- power supply of the cathode-ray gun 5;

- control unit of the electron beam intensity 6;
- adjustable rectangular diaphragm 7 and its control unit 8;
- electro-optical system 9 and its power block 10;
- coils of the precise deflection of the electron beam (*X*) and (*Y*) and the deflection control unit 11;
- system of the dynamic focusing 12.

The working chamber 2 includes:

- precision coordinate table 13 with precise electromechanical drive 14;
- photomask blank 15;
- laser diode 16 and a high-precision interferometer 17;
- secondary electrons sensor 18.

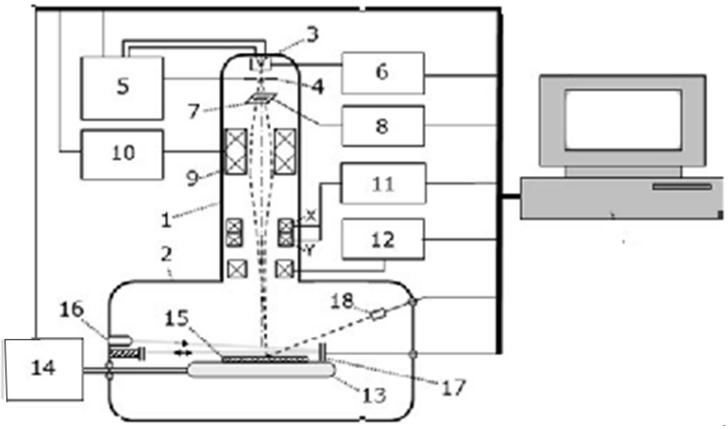

Fig. 6. 5. Block diagram of the electronic lithography system

Electron-optical system 9 projects on the surface of the photomask blank 15, a reduced image of the rectangular diaphragm 7, the size of which may vary from 1–5 nm to about 1–5 microns.

By means of the deflection coils and the block 11 the electron beam of the rectangular section can be quickly positioned in any point with the given coordinates within the region of 2x2 or 5x5 mm.

The coordinate table 13 and the drive 14 allow accurately to move the following section of the photomask 15 under the electron beam.

Photolithography is a method of obtaining a certain pattern on the surface of the material, widely used in micro and nanoelectronics.

It is one of the basic and expensive methods of the planar technology, used in the manufacture of the respective semiconductor devices.

The process of the photolithography contains the following steps.

The photoresist is sprayed on the treated surface and is exposed by the light through the photomask with the given pattern obtained on the electronic lithography step, Fig. 6.6.

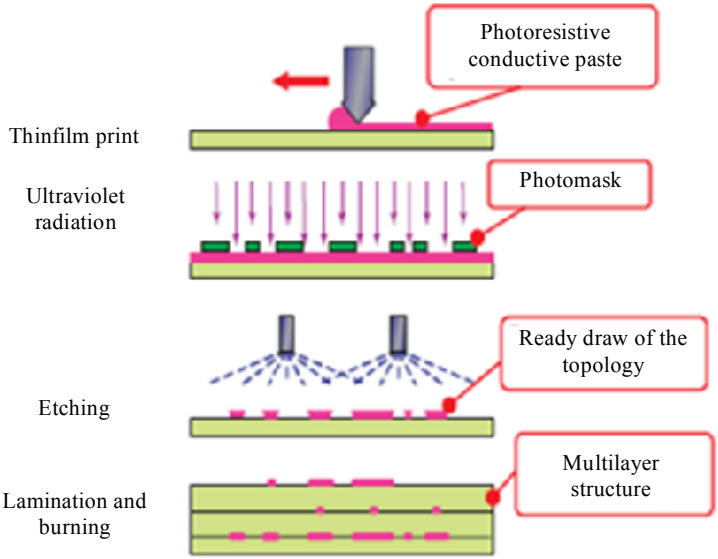

Fig. 6.6. The process of the photolithography

Next the exposed areas of the photoresist are removed in the developer. The pattern obtained on the photoresist is used for such processing steps as etching, electrodeposition, vacuum deposition, and others.

After one of these processes, the remainders of the photoresist are removed by the special substance. The basic stages of the photolithography process are shown in Fig. 6.7.

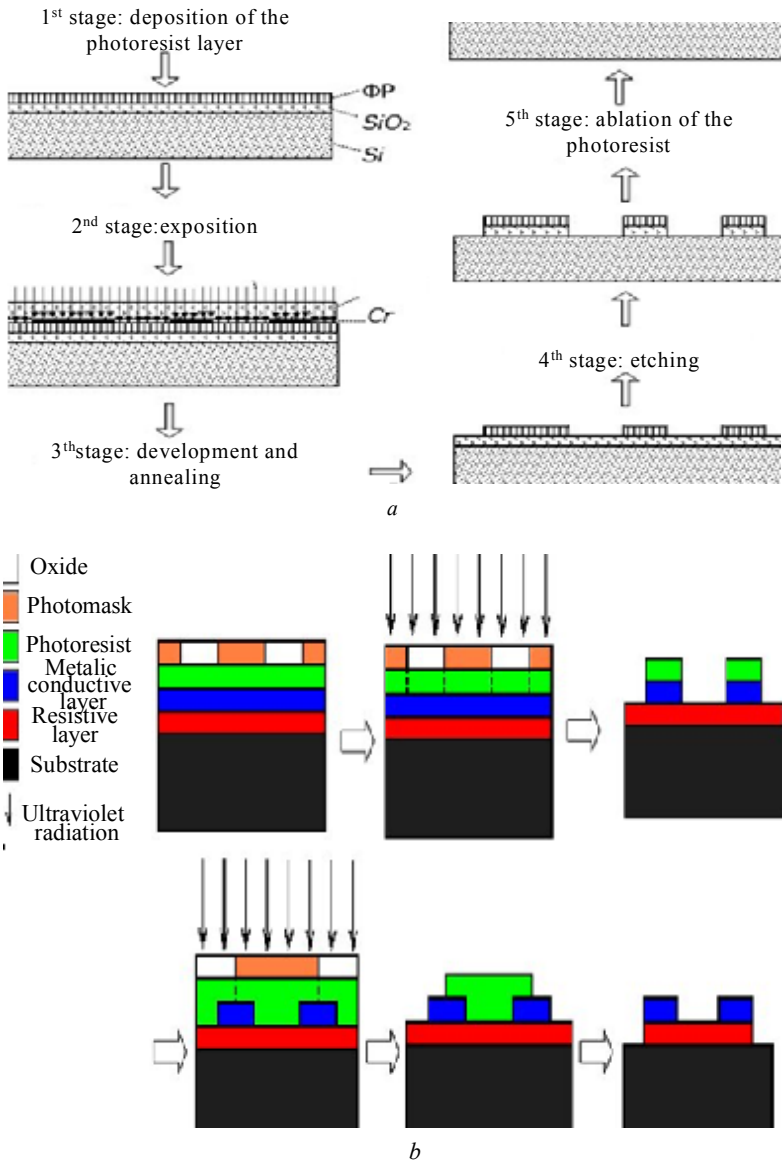

Fig. 6.7. The basic stages of the photolithography process (*a*) and their realization (*b*)

The principal difference of the photolithography from other types of the lithography is that the exposure is made by the visible or the ultraviolet light, whereas in other types of lithography the stream of ions, the electron stream, X-rays and other are used for this purposes.

The memristor represents the MDM structure and may be manufactured on a silicon substrate. As an example, we will consider the structure with the three-component oxide, Fig. 6.8.

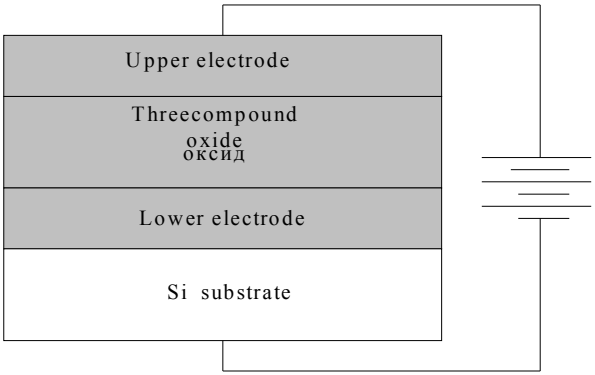

Fig. 6.8. MDM structure of the memristor

As already noted, for the first time the effect of the memristance has been experimentally demonstrated in 2008 for the structure of the type $Pt/TiO_2/TiO_{2-x}Pt$. It is shown that the memristive effect occurs in the MDM nanostructures by means of the movement of charges in the ultrafine dielectric layer upon application of an electric field, particularly at movement of the oxygen vacancies in the layer of the titanium dioxide.

In recent years it has been proposed a set of alternative materials for the use as the active layer of the memristor in order to integrate in silicon technology.

One approach to improving the functional properties of the memristors based on the transition metal oxides (in particular TiO_2, HfO_2, ZrO_2) is the doping of the oxides by the trivalent impurity, such as Al.

In the traditional system of layers TiO_2/TiO_{2-x} the distribution of the charge carriers (oxygen vacancies) in the film thickness is random.

Therefore it is necessary to create the controlled profile of the distribution of impurities in the volume of the active layer to effectively control by the charge carriers in the memristor.

In particular, the widely used technique of the ion implantation of the elements having a large number of the valence electrons in the volume of the active layer is not optimal for the formation of a homogeneous distribution of the impurities.

It means that this method does not improve the stability of the memristor characteristics thereof its active layer almost always has a small thickness of 5–20 nm.

Consequently, a resistive switch (for example, in the memory elements) in most cases will be unstable: the switching parameters, such as the value of the current in the high-resistance and low-resistance states, the threshold voltage of transitions from one state to another state may vary from cycle to cycle.

In addition, there is heterogeneity of the electric field distribution in the active layer and accordingly, a low stability and repeatability of the memristor characteristics, the total number of switchings is small. Then, as a rule, there is a degradation of the structure, after that it irreversible passes to the low-impedance state.

Ion implantation is the way of the inclusion of the impurity atoms into the surface layer of the plate or the film by means of bombardment of its surface by the ion beam with high energy (10–2000 keV).

This method is used as the way of metal doping to modify their properties.

Ion implantation is widely used to manufacture the semiconductor devices by means of the planar technology.

The technology of implantation is applied to form in the surface layer of the semiconductor the regions containing donor or acceptor impurities to create $p-n$ transitions and the low-resistance contacts.

Ion implanting technology allows to introduce a given amount of almost any chemical element into a needed depth, and thus to alloy the one substance by other in proportions which can not be achieved even when the high temperatures are used.

Ion implantation leads to a significant change of the surface

properties throughout the depth, Fig. 6.9.

A block diagram of an ion implantation is shown in Fig. 6.10.

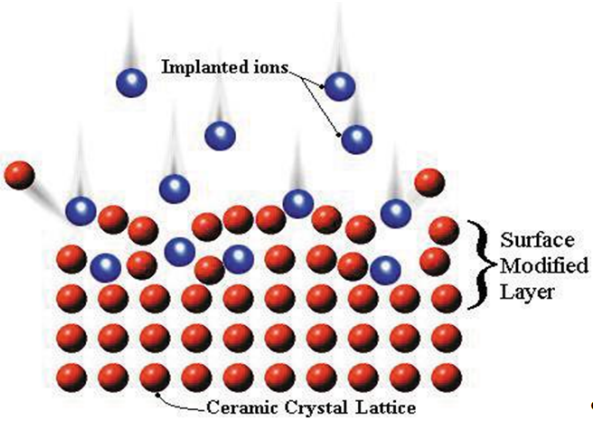

Fig. 6.9. The ion implantation process

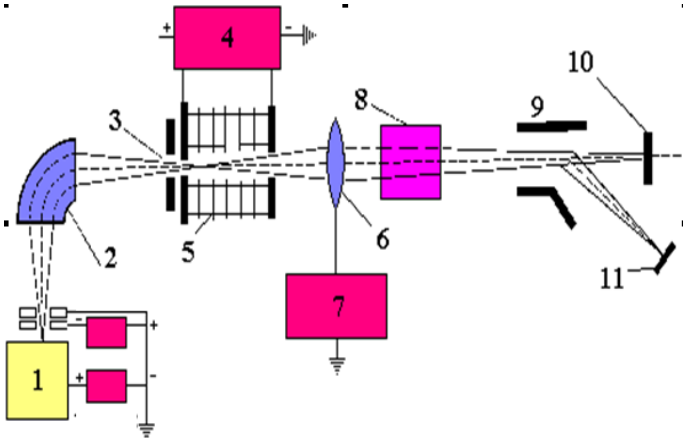

Fig. 6.10. A block diagram of an ion implantation

The considered plant includes:

- ion source 1;
- mass-spectrometer 2 and the diaphragm 3;
- high voltage source 4, accelerating tube 5, the lens 6 and the power source 7;
- system of the beam deflection on vertical line 8 and horizon-

tal line 9;
• target for absorption of the neutral particles 10;
• substrate 11 and the electrometer 12.

Magnetic mass spectrometer is used to separate unwanted ions from alloying ions, the electrometer is required for measuring the flow of implanted ions.

To eliminate these shortcomings the different variants for realization of the memristor active layer are offered, one of which is to provide a spatial limitation of areas where the origin and movement of oxygen vacancies exist, which will lead to long-term stability and reliability of the memristor.

The structural separation into two areas is realized in the active layer: the region containing a large concentration of oxygen vacancies which is the source and the accumulator of these vacancies, and the region in which the increase of the vacancy concentration due to their drift from the first region leads to the condensation of these vacancies.

A layer accumulating the vacancies should have a high solubility of the vacancies and a high equilibrium their concentration. The layer where condensation of the vacancies occurs should have a low solubility.

Thus, the active layer having the property of the resistive switching is a two-layer structure of an oxide, arranged between two electrically conductive layers.

The materials for the conductive layers must have a high output work (work function).

The work function. The electrons of conduction in the metal are in a chaotic thermal motion. Most fast-moving electrons, which have a sufficiently high kinetic energy, can escape from the metal into the medium. In this case they do work against the force of gravity from the excess positive charge, which occurs in the metal as a result of their emission, and against the forces of repulsion from the part of the previously emitted electrons, which form near the surface of the conductor the electronic "cloud". Between the electronic gas in the metal and the electronic "cloud" the dynamic equilibrium is set.

The work, which is necessary to make to remove the electron from the metal in a vacuum, is called the work function. The work

is always done by decreasing their kinetic energy. Therefore it is evident that the slow-moving electrons can not escape from the metal.

The work function depends on the chemical nature of the metal and the state of its surface (pollution changes its value). For pure metals, the work function ranges from a few electronvolts.

Deficiency of electrons in a metal conductor and their excess in the environment that is formed as a result of the emission of the electrons from the metal, are shown only in a very thin layer on both sides of the conductor surface. The thickness of this layer is equal to a few interatomic distances in the metal.

As a first approximation we can assume that the metal surface is a double electric layer like very thin capacitor. The potential difference $\Delta\varphi$ between the plates of such capacitor depends on the work function A of the electron from the metal:

$$\Delta\varphi = \frac{A}{e},$$

where e is the absolute value of the electron charge.

Electron emitted outside the metal, has to overcome the delay of its electric field of the double layer which delays its movement. This field is characterized by the potential difference $\Delta\phi$ which is called the contact potential difference between the metal and the environment.

The electric field does not exist outside of the double layer, and the potential of the environment is equal to zero. Consequently, the potential within the metal is a positive and equals $\Delta\varphi$. The potential energy of the conduction electrons is negative and equals $-e\Delta\varphi = -A$. In other words, we can assume that the entire volume of the metal represents the "potential well" for conduction electrons, the "depth" of which is equal to the output work A.

As a rule, one of the noble metal (Pt, Au, Pd) is used as a material with a high work function. However, the use of these metals in silicon chip manufacturing technology is extremely undesirable. The most commonly the titanium nitrate TiN (or tungsten nitride WN) is used for the manufacture of electrodes. Besides, as was noted above, the elec-

trode of titanium nitride is an effective oxygen tank, that is an additional source of the oxygen vacancies.

The combination of both approaches: the doping of the oxide layer and the use of the electrode from the material which is active with respect to the oxygen must be an effective means of controlling the concentration of oxygen vacancies in the oxide layer. In this case a stable effect of the resistive switching of the memristor may be achieved.

To increase the effective work function of the electrode made from TiN it is sufficient to place the ultrathin layer of the conductive ruthenium oxide RuO of 1–2 nm thickness on the interface between TiN/HfO2. It was shown by many experiments.

The general structure of the memristor is shown in Fig. 6.11.

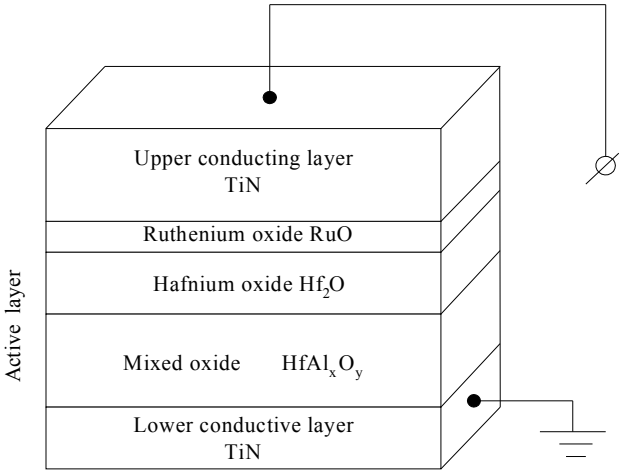

Fig. 6.11. The general structure of the memristor

6.2. Main stages of the manufacture of the memristor

To get acquaintance with the basic principles of the physical realization of the memristor, some elements of nanotechnology we will consider below the main stages of its creation.

- **Manufacturing of the lower electrode**. To form the lower electrode as the metallic TiN layer the method of magnetron sputtering of the target (for example, the plant BOC Edwards AUTO 500) can be applied.

Vacuum deposition (physical vapor deposition – PVD) is represented by the group of the covering deposition techniques (thin films) in the vacuum. The covering is obtained by the direct condensation of the vapor of the deposited material. There are several groups of sputtering methods, in particular, a magnetron sputtering method which belongs to the group of the ion sputtering

Vacuum deposition is used to create the functional covering in the form of a thin layer of some metal or compound on a some surface. It is one of the fundamental processes of micro and nanoelectronics, which is used for creation of the conductive layers (metallization). Vacuum deposition can be used to obtain the optical coverings such as reflective and filtering.

Materials for sputtering are the targets made of the different materials, metals (titanium, aluminum, tungsten, molybdenum, iron, nickel, copper and others). Besides, the alloys and compounds (SiO_2, TiO_2 and Al_2O_3) may be used. A reactive gas (for example, nitrogen or oxygen) can be added in the technological process. The coverings with a thickness from a few angstroms to a few microns may be obtained with the help of a vacuum deposition method as well. As a rule, after the covering the surface does not require additional processing. Magnetron sputtering process is shown schematically in Fig. 6.12.

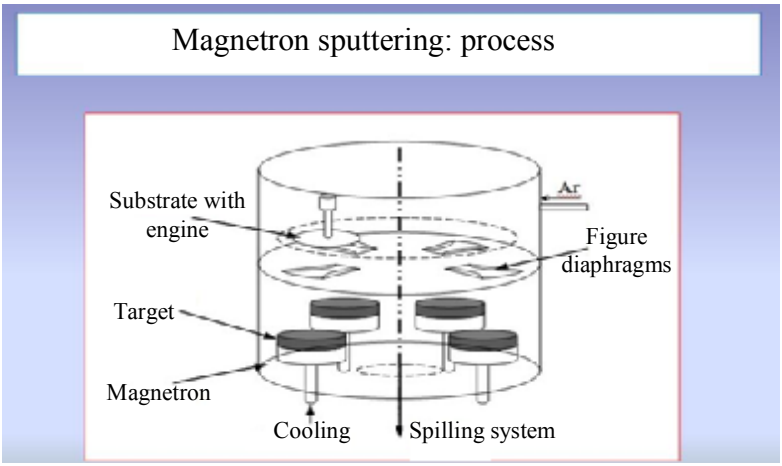

Fig. 6.12. Magnetron sputtering process

The plant BOC Edwards AUTO 500 is widely used for the vacuum deposition. It has a high-frequency magnetron, DC magnetron and sputtering electron beam system.

Materials of the targets for the magnetron sputtering (target diameter equals 100 mm) are: Al, Ti, Cu, W, SiO2, Cr, Zr, V, Nb, Ta.

The working gases for the magnetron sputtering are: Ar, N, O_2 and their mixtures.

The use of oxygen and nitrogen allows to deposit the chemical compounds of metals such as titanium nitride (TiN) or tantalum oxide (TaO_x).

The block diagram and the general photo of the plant for the magnetron deposition are shown in Figs 6.13 and 6.14.

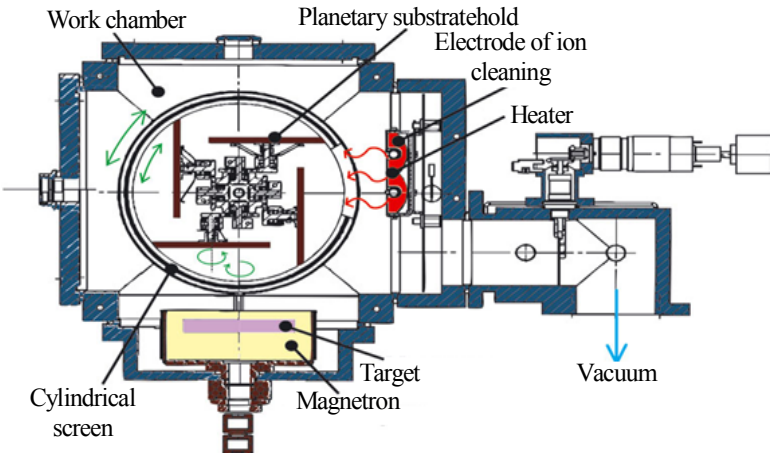

Fig. 6.13. Block diagram of the magnetron deposition plant

Control of the film thickness in magnetron sputtering is carried out by measuring the material deposition time.

The metallic layer is usually applied over the entire area of the silicon substrate $Si - SiO_2$. Directly before sputtering the silicon substrate is processed (for at least 30 seconds in a 1% aqueous solution of hydrofluoric acid HF) to eliminate a natural silicon oxide SiO_2 from the Si wafer. The thickness of the lower electrode is 50–100 nm.

Fig. 6.14. General photos of the plants

• **Manufacturing the dielectric layer**. The active layer deposits on the substrate with the formed lower electrode. This layer consists of the two sublayers: Hf $Al_{0,4}O_x$ of the thickness 4–5 nm, and HfO_2 of 3–4 nm thick.

The film may be grown by atomic layer deposition technique (ALD) at a temperature of 240° C, for example, in a reactor Sunale R-150 Picosun *OY*.

The plants for atomic layer deposition (ALD) are designed to produce the free of defects thin films based on nitrides, metal oxides, pure metals.

The equipment allows alternate the layers of the metal and the non-metal to form a sandwich structure and can be used in the respective nanotechnologies.

Atomic layer deposition method is used due to its unique ability to obtain homogeneous thin films (a few nm) of a given thickness and to control their composition. With the help of ALD the functional layer of the dielectric is formed in the MDM (MIM) structure.

Besides ALD is used in particular in the manufacture of electrodes on the base of titanium nitride TiN, tantalum nitride Ta_3N_5, on the base of the platinum Pt, iridium Ir, ruthenium Ru, and for the manufacture of the active layer by sputtering titanium dioxide TiO_2, zirconium dioxide ZrO_2 and hafnium dioxide HfO_2.

In addition, the ALD also is used during the deposition of the mixed oxides $HfAl_xO_y$, $Ti_xZr_yHf_zO_2$, $ZrTiO_3$ for deposition of the precision multi-layer structures.

The general principle of the formation of the thin films using atomic layer deposition is shown in Fig. 6.15.

One of the main ALD systems is the plant of the company Picosun of the type Sunale R-150, Fig. 6.16.

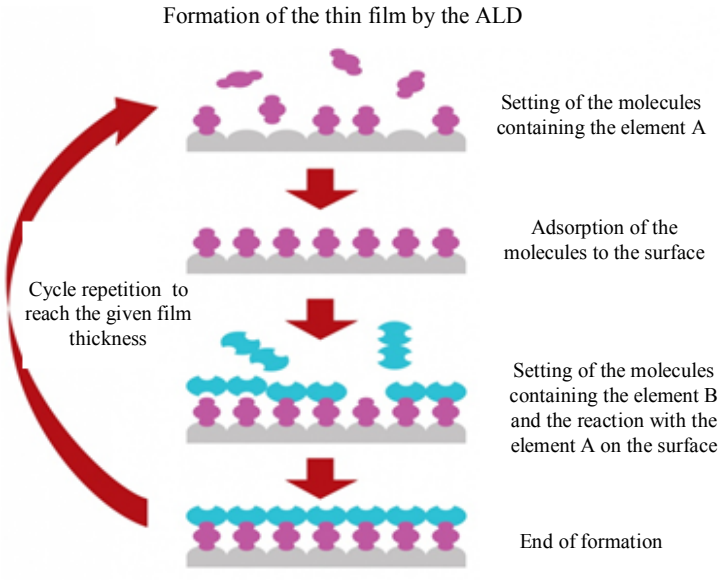

Fig. 6.15. Formation of the thin films by the ALD

Fig. 6.16. Photo of the ALD plant

To form the functional layer of the dielectric in the MDM (MIM) structure the atomic-layer deposition method is used because it has unique ability to obtain the homogeneous thin films of a given thickness (a few nanometers) and to control their composition. As already noted, the oxygen vacancies play a key role in the effect of the resistive switching.

In order to the active layer does not cover the contact areas of the lower electrodes their surface is covered by the so-called electronic resist, which is removed after forming the active layer. It should be noted that in order to obtain a variable concentration of Al through the film depth, the atomic layer deposition, usually is carried out within a few cycles according to the special recipe.

• **Production of the upper electrode**. The layer of the ruthenium oxide of 2 nm thickness is sprayed on the surface of already formed the active layer through a shadow mask by the pulsed laser deposition.

Deposition of ruthenium oxide layer is carried out by the laser ablation from the metallic target of Ru in an oxygen atmosphere.

Pulsed laser deposition (PLD) is getting of the films and coverings by the condensation on the surface of the material of the reaction products in a vacuum of the pulsed laser radiation with the target material (at ablation). Laser ablation is the method of removal of substance from the surface of the material (for example, the target material) be the laser pulse.

Recently, several techniques of the deposition of thin films have evolved in parallel. Each of them has found its proper application. The method of PLD gets especially rapid development due to the ability to control by the parameters of the process by the simple means.

In comparison with continuous methods of deposition of the thin films the PLD method has the ability to modify the energy spectrum of the deposited particles in a wide range and, therefore, is one of the most promising tools of modern nanotechnologies to improve the devices of the quantum electronics.

Implementation of laser ablation in a deep vacuum leads to the formation of a narrow plume of products in which are a high proportion of charged particles. Scheme of implementation of the laser ablation is shown in Fig. 6.17.

Pulsed laser deposition is getting of the films and coverings by the condensation on the surface of the material of the reaction products in a vacuum of the pulsed laser radiation with the target material (at ablation). Laser ablation is the method of removal of substance from the surface of the material (for example, the target material) be the laser pulse.

Recently, several techniques of the deposition of thin films have evolved in parallel. Each of them has found its proper application. The method of PLD gets especially rapid development due to the ability to control by the parameters of the process by the simple means.

In comparison with continuous methods of deposition of the thin films the PLD method has the ability to modify the energy spectrum of the deposited particles in a wide range and, therefore, is one of the most promising tools of modern nanotechnologies to improve the devices of the quantum electronics, optoelectronics and spintronics in computing.

Implementation of laser ablation in a deep vacuum leads to the formation of a narrow plume of products in which are a high proportion of charged particles. Scheme of implementation of the laser ablation is shown in Fig. 6.17.

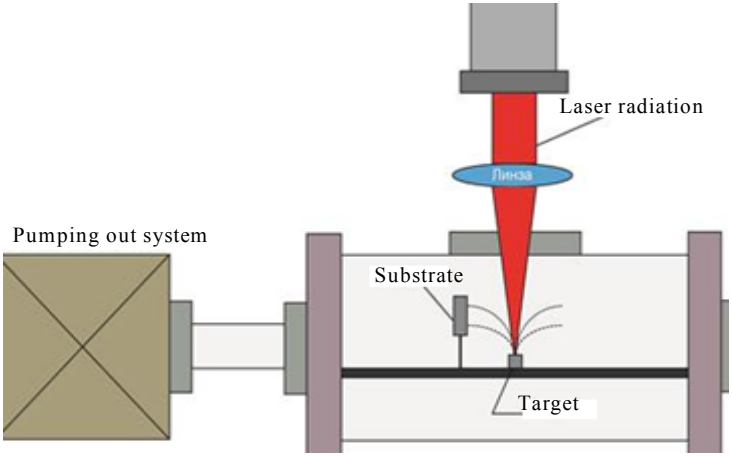

Fig. 6.17. Laser ablation of the target material

TiN layer of 50 nm thickness is sprayed by magnetron sputtering method, using the same shadow mask as in the pulsed laser deposition.

It should be noted that to measure the characteristics of the memristor in the laboratorial conditions the Al additional layer thickness of about 100 nm is deposited for subsequent better contact of the needle of the probe station with the upper electrode. This is due to the fact that the structures obtained by magnetron sputtering method through a shadow mask have degraded edges with a gradient of film thickness and is slightly distinguished in the microscope. Therefore, the Al sublayer plays a supporting role.

6.3. Measurement of the memristor characteristics in the laboratory

In general, for laboratory researches the array of the memristors is made with lateral dimensions 100–1000 μ, but the thickness of the functional dielectric layer (active layer) must correspond to modern international practice (5–15 nm). The sample of the memristors usually is manufactured on a silicon substrate.

The required amount of the upper electrodes with different sizes in diameter is sprayed on the one sample.

To measure the required characteristics of the memristors measuring device is connected in pairs between the lower and upper electrodes (for example, the device Agilent E4980 A, containing the power source and ammeter). Measurement of the current-voltage characteristics in the range from minus 2.5 V to 2.5 V and switching memristors from a high-resistance state to a low-resistance state, and vice versa is carried out by means of the standard control program of the plant.

As a result of the measurement the values of resistances of the low-resistance R_{on} and high-resistance R_{off} states of the memristors are defined over N cycles of switching from one state to another state and back. Similarly the threshold voltage of switching is averaged.

The probe station can be used in the laboratory conditions to obtain the characteristics of a memristor. In this case, the corresponding probes of the station are set over respective contacts by means of the microscrews. Adjustment of these probes is carried out by means of the optical microscope, Fig. 6.18.

The measurement process of the volt-ampere characteristics of complete cycle of the memristor resistive switching usually contains the following steps.

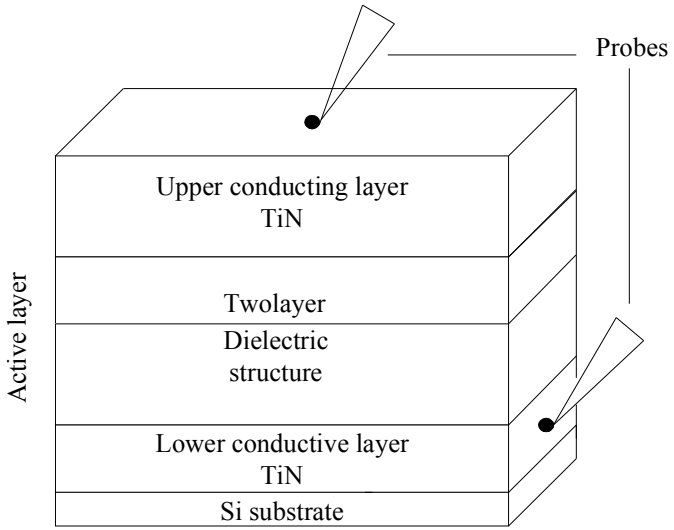

Fig. 6.18. Position of the probes with respect to the sample

• **Forming memristor**. Generally, the "fresh" MDM structures do not show the resistance switching effect. To effect was shown the structures must be formed (so-called "forming" process). In this case, it is necessary to apply the respective voltage V_{form} which will form a conductive filament from the oxygen vacancies or the metal ions. Then the whole system goes into the state with low resistance R_{on} (switch on), [97].

To switch the system into the state with high impedance R_{off}, it is necessary to apply the voltage of the respective value of the reverse polarity (switch off voltage). In this case the conductive filament is broken. Next, to return the system into the state with low resistance, it is necessary to apply the switch on voltage (U_{on}), which is less than the forming voltage [97].

The process begins with the measurement of current-voltage characteristics in the range from 0 to 1 V, and then in the opposite direction from 1 V to 0. If the characteristic does not show the hysteresis, then it is necessary to increase the range, for example, on 0.2 V (0 – 1,2 V $\rightarrow$ 1.2 V – 0). The process of gradually increasing the voltage continues until the occurrence of the forming process. In this case the value U_{form} is determined.

• **Measurement of the CVC of the RESET process**. In this case, the current-voltage characteristic is measured in the range from 0 to minus 1 V and from minus 1 V to 0. If the CVC does not show the hysteresis, it is necessary to increase the range on 0.2 V in the negative voltage region. The process of gradually increasing the voltage continues until the RESET voltage characteristic will not come to the stable branch. In this case the resistance reaches the value R_{off} (HRS), Fig. 6.19 and the value U_{off} (U_{RESET}) is determined.

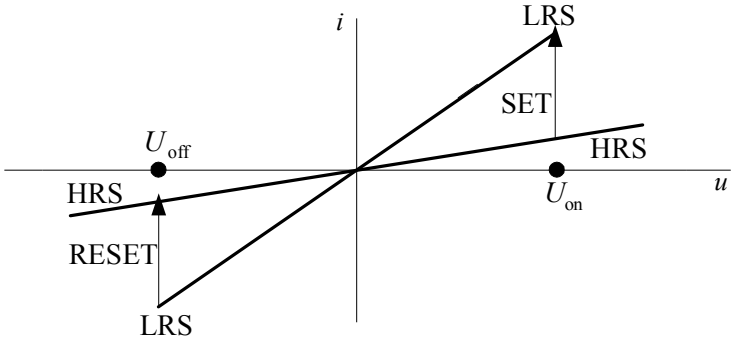

Fig. 6.19. Measurement of the CVC of the RESET and SET processes

• **Measurement of the CVC of the SET process**. The current-voltage characteristic is measured in the range from 0 to U_{form} and from U_{form} to 0. The degree of deviation the form of the CVC of the SET process from the CVC of forming process is set and the value U_{on} (U_{SET}) is determined.

• **Calculation of the resistance values in the states of HRS and LRS.** In this case the values of the respective currents are determined

for a certain value of the voltage, called the read voltage of the information ($U_{read} \approx 0.5\,V$) and the values R_{off} and R_{on} are calculated.

• **Calculation of the intermediate resistance values in the IRS states.** At first the current-voltage characteristic (CVC) is measured in the ranges of 0–1 V and 1 V–0 of the positive CVC branch. Then the measurements of the CVC with increasing values of the "scanning" voltage on 0.1 V with each new cycle are repeated, Fig. 6.20. Next the resistance values R_{IRS} are calculated for each cycle and their number at the read voltage U_{read}.

Similar measurements and calculations are carried out for the negative branch of the CVC.

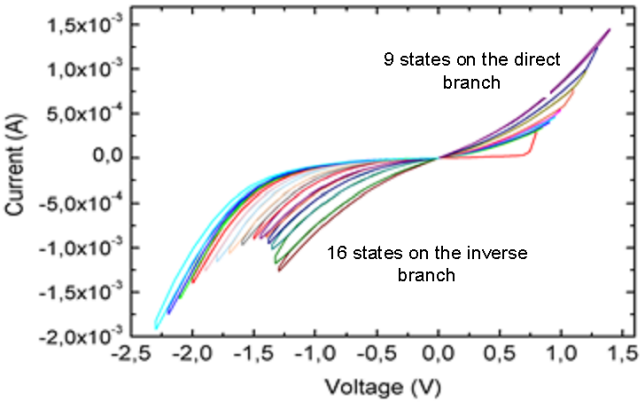

Fig. 6.20. Current-voltage characteristics of the intermediate states of the memristor

• **Determination of the mechanism of the memristor resistive switching**. In this case the current-voltage characteristics of the complete cycle of switching for the memristors with the different diameters of the upper electrodes (with the different areas) are measured. The dependencies R_{off} and R_{on} from the electrode area are constructed and is defined the resistive switching mechanism: the filamentary mechanism (resistive switchings occur locally through the formation of filamentary conductive channels) or mechanism of the valence change (resistive switchings occur throughout the structure area).

NONVOLATILE MEMORY DEVICES

- Memory structure of the modern computers
- Resistive random access memory (ReRAM)
- Magnetoresistive random access memory (MRAM)
- Phase state change random access memory (PCRAM)
- Ferroelectric random access memory (FeRAM & FeTRAM)
- Nonvolatile random access memory of the CeRAM type
- Magnetic track random access memory MRM (DWM)
- Nonvolatile random access memory (NRAM)
- MRAM memory with the use of the spin-transport remagnetization
- Compare and prospects

7.1 Memory structure of the modern computers

Now in the field of micro and nanoelectronics there are several problems associated with the need to increase the degree of integration of chips including the memory devices. It is explained by the need to create a new generation of the memory devices, such as nonvolatile memory devices.

Nonvolatile memory must replace the widely used memory devices, the so-called flash memory, the basic element of which is the field effect transistor (FET): metal-insulator-semiconductor (MIS) with a floating gate.

The development of the nonvolatile, small size and the fast memory requires the new memory concepts. Now existing types of the memory, such as the resistive RAM (ReRAM), with its subclass of the phase RAM (Phase Change RAM - PCRAM), magnetic RAM (Magnetoresistive RAM–MRAM), ferroelectric RAM (FeRAM), the resistive type of the CeRAM (Correlated electron RAM) are well known examples of the emerging concepts of the nonvolatile memory. Each of them has their own strengths and weaknesses.

A field effect transistor with the floating gate is different from the conventional FET by presence of "floating gate" which represents the conducting region over a channel isolated from oth-

er parts of the structure and which can store the electrical charge, Fig. 7.1.

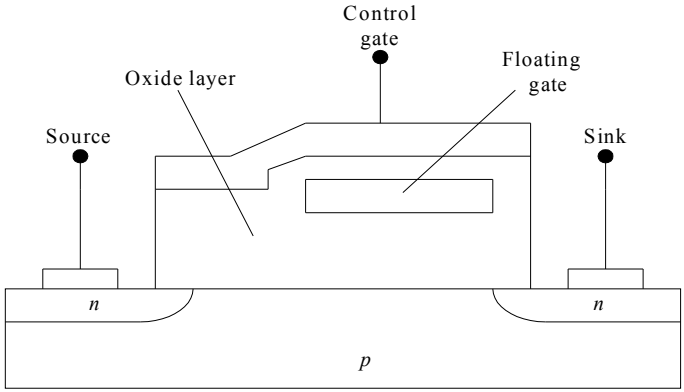

Fig. 7.1. The scheme of the field effect transistor with the floating gate

Changing the charge on the floating gate leads to the shift of the current-voltage characteristic of the transistor. It is used to encode logic states 0 and 1. To transfer the electrons from the substrate to the floating gate the phenomenon of avalanche breakdown of the transition source (sink) - substrate (avalanche charge injection).In general, the change of the electric charge of the internal gate insulated by the dielectric layers is made purely electrically. Changing the charge of the floating gate is due to the tunneling of the electrons and the reversible avalanche breakdown of the superfine (a few nm) dielectric layers, due to the high electric field in the dielectric (recall that the electric field intensity is defined as $E = \frac{U}{d}$ where d is the thickness of the dielectric layer). Since the charge of the floating gate, isolated from all electrical circuits is retained (if not very strong electric fields act in the dielectric layers) then the chips built on these structures retain the information without power supply.

One of the most perspective approaches to create the nonvolatile memory devices, which considerably exceed the flash memory characteristics, is the use of the resistive switching effect in the thin films, in particular in the oxide films.

Such the integrated chips of the random access memory (ReRAM on the base of the memristors) are simpler in the technology and inexpensive to manufacture. The advantage of the ReRAM is also the fast switching (nanoseconds) and low energy of switching (pJ), which is two orders less than in the flash memory elements. It must lead to the increase of recording density.

7.2 Resistive random access memory (ReRAM)

As already mentioned, the recording and the information storage systems (memory devices) are very important components of the modern nanoelectronics.

Traditional memory based on classical principles (static and dynamic random access memory), in its development tends to the limit above all because of problems with its further scaling. In the research of new types of the memory the concept of the universal memory has been proposed which may replace all existing today forms of memory.

This memory must have such important characteristics: nonvolatile properties, recording and rewriting speed (~ ns), the period of the data storage is greater than 10 years, low power consumption (about 10 pJ), scalability and the ability of the 3D integration, Fig. 7.2.

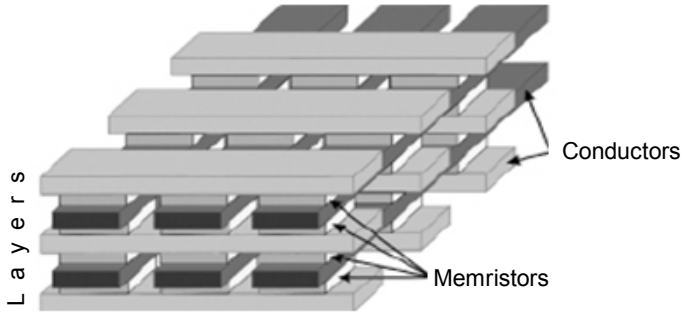

Fig.7.2. Forming 3D structure of the ReRAM memory

Now, the memory based on the resistive switching is one of the most perspective among the new types of memory based on new physical principles.

The basic elements of the ReRAM are the memristors the resistive switchings of which are used to store the information. It can be said that the memristor is a resistor, which stores the acting applied to it in the past, and therefore it allows to store information in itself.

Thus, the fundamental difference between the memory based on the memristors from the most types of the modern semiconductor memory is the fact that it is not afraid of the charge leakage, which must be combated in the transition to the chips of nanometer scale. It means that such memory is completely nonvolatile, [1], [8], [18], and [74].

Universal memristor memory can replace the two lower pyramid memory elements (DRAM, Flash, and HDD) and is able to eliminate the difference between the memory RAM and the external drives, so that the hard drives is not needed, because all the information is stored directly in the memory of the computer.

As noted above, the effect of the resistive switching in the MDM (MIM) structures is the reversible change in electrical conductivity of the dielectric layer under the action of the applied to the electrodes the electrical potential difference which is greater than a certain threshold value.

The dielectric layer may be formed from a single layer of a simple or a complex oxide or of several sublayers of simple or complex oxides or other dielectric materials.

The base of the resistive switching processes are the reduction / oxidation processes (redox processes), which can be described as the migration of the oxygen ions (oxygen vacancies) in the presence of the electric field.

Since the oxygen vacancies act as the donors within the oxide, the change of their local concentration leads to a significant change of the conductivity of the active layer. This is the basis of the effect of the full resistive switching. In other words, when the relatively high voltage is applied to the crystal then the bonds that hold the oxygen atoms, begins to destroy.

Oxygen retains the "hole" and the free electrons after itself which are able to become by the charge carriers. The "holes" tend to form the conductive channels in the crystal. The reverse voltage returns the oxygen, again turning the material into the dielectric. Such transitions create the stable memory states, which vary only under the action of relatively high voltage values of a certain polarity.

As a rule, two variants of the switching process are considered.

The first of them is that the dielectric which normally has a very high resistance value can form inside the conductive channels of the low resistance and change from the dielectric into the conductor after the voltage application of the respective value.

These conductive channels can be produced by the different mechanisms. The conductive channels may be either destroyed (and the material becomes an insulator again) and formed (and the material becomes a conductor again) if the respective levels of the voltage are applied to the memristor. Such processes are the reversible and are called the filamentary processes [38], [93].

The essence of the second variant is that the effects of switching are formed by the homogeneous zones of the dielectric that is the resistive switching processes act in all dielectric area.

There are three main problems in creating resistive nonvolatile memory devices [30], [58], and [99]:

- the problem of improving the stability of the parameters of the memory cells;
- the problem of increasing the resistance ratio in the high-resistance and the low-resistance states of the resistive memory element;
- the problem of improving the reliability of controlling the operation of forming the memristor (cell).

To design the memory chip the respective cells can be connected to the data lines in the crystal by the three ways: directly, through the diodes and through the transistors, forming the so-called crossbar, [46] and [96].

The memory cells form the classic matrix with rows and columns (and layers for multi-layer memory). The control by each individual cell is carried out with the help of applying the voltage to a certain column, and a certain line, the point of intersection of which is the respective cell.

Crossbar is a matrix, the rows which are formed by the conductors connected to the inputs, and columns are connected to the outputs, so that at the intersection of lines and columns of the matrix are switches that can either close the connection the row to the column, or, on the contrary, disconnect it, Fig. 7.3.

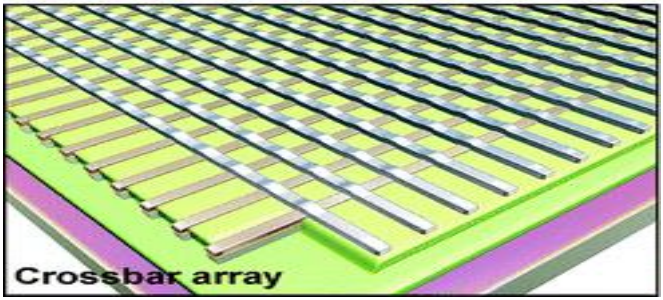

Fig. 7.3. Structure of the matrix of the crossbar type

To control by the switches, located at the intersection of rows and columns of the switching matrix, crossbar must have the controller, which controls by the state of switches

Crossbar $n \times l$ connects the n input and l output terminal nodes (for example, processors), and so that the exchange of information at the same time can exist $\min(n, l)$ of pairs of terminal nodes, so that conflicts do not arise in this case. The new connection may be set at any time, under the condition that the input and the output ports are available (free).

The main advantage of the topology is that the device provides the less delay in the transmission of the signals, in comparison with other topologies, since any path contains only one switch.

The switching mechanism (selector of the rows, the columns, and the layers) may be multi-dimensional and multi-channel, and operate with several layers simultaneously and independently.

The functional multilayer structures of the ReRAM memory cells on the different oxides are shown in Fig. 7.4, [63].

As an example, let's consider the main characteristics of the developed version of the nonvolatile ReRAM memory of the company Crossbar. According to the developers, the memory can store up to 1 TB of data in the chip of 200 mm^2 area, and provides access to the data 20 times faster than the best examples of the modern NAND flash memory. At the same time the chip has the size smaller by half, extremely high rate of the information storage density and high read-write speed, which is about 140 MB/s. The new memory chips have low power consumption.

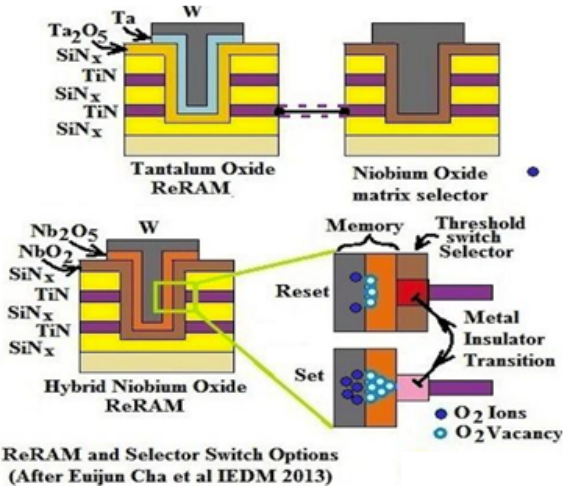

Fig. 7.4. Multilayer structures of the ReRAM memory cells

The main peculiarity of the memory cell is its special structure, which provides ultra low leakage currents.

The multilayer stack contains the metal platinum electrode on top of the insulating silicon dioxide layer SiO_2, which in turn is located on the standard silicon wafer. The metal electrode is covered by very pure tantalum with the nano-porous layer of tantalum oxide Ta_2O_5.

Ten atomic layers of the graphene (the so-called multi-layer graphene MLG) are sprayed on the top of the tantalum oxide. The stack has another (upper) platinum electrode, Fig. 7.5.

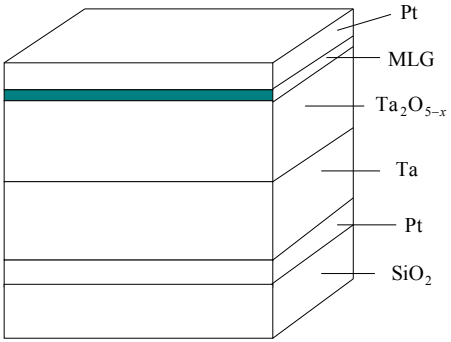

Fig. 7.5. Memory cell structure of the ReRAM type

Graphene is the first known true two-dimensional crystal. In contrast to earlier attempts to create two-dimensional conductive layers (for example, two-dimensional electron gas), the electrons in the graphene are localized in the plane much more. Graphene is a two-dimensional crystal consisting of a single layer of the carbon atoms collected in a hexagonal lattice. Its theoretical research began long before the appearance of the real samples of the material.

Graphene can be a substitute for the silicon semiconductors. The most urgent problem of the construction of the computer chips is to increase the power and decrease the size of chips without significantly increasing the temperature. In theory, the graphene transistors can provide a much higher speed, without increase of the temperature at the microscopic level.

It is not only the thinnest material but it is also about 200 times stronger than the steel. Researchers at Columbia University have proven that the graphene is the strongest material that has ever been measured. In addition, the graphene conducts the electricity at the room temperature better than any other material known to mankind.

Extensive study of the material in the universities and the research laboratories is explained by the availability and simplicity of its manufacture with the use of the mechanical splitting of the graphite crystals.

The principle of operation of the graphene transistors is substantially different from the principle of operation of the traditional silicon field effect transistors, as graphene is a forbidden zone of zero thickness, and the current flows in the graphene channel at any applied gate voltage. That's why other approaches are developed to the creation of the transistors. The high mobility of the charge carriers makes the graphene as the perspective material for use in various applications such as nanoelectronics with the possible substitution of the silicon in the integrated circuits. Such mobility (maximum mobility of the electrons among all known materials) is one of the main parameters needed to create high-speed high-frequency transistors. The concern IBM demonstrated a 100 GHz transistor using graphene, and stated that the processor of 1 THz can be created in principle.

The perfect graphene consists exclusively of hexagonal cells. The presence of five and heptagonal cells will lead to different kinds of defects. Availability of the pentagonal cells leads to a curls of the atomic planes in the cone. The thickness of the graphene layer can be determined by using an atomic force or by using the combination dispersion (Fig. 7.6).

From a long list of possible applications of the graphene we choose the following:

- replacing silicon in transistors;
- the introduction in the plastic in order to obtain electrical conductivity to it;
- optoelectronics;
- transparent conductive recovering for the solar panels.

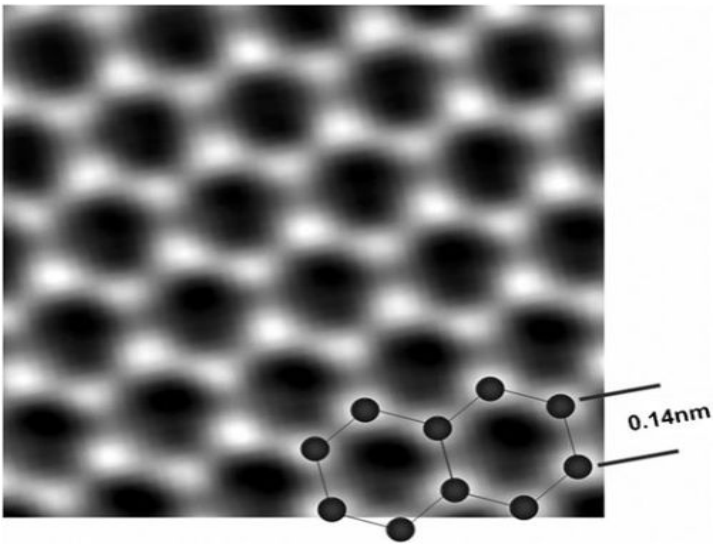

Fig. 7.6. Image of the graphene structure obtained by the atomic force microscope

Crossbar technology provides a simple three-layer structure, which allows to create 3D-chips of the multi-terabyte capacity, Fig. 7.7*a*. The entire array of the memory cells is placed in three layers, composed as the "sandwich". From the advantages of this development the company indicates on compatibility with CMOS manufacturing technology.

Now, leading companies developed technologies to design the 3D memory as a classic version of the cross-memory (cross-point memory). Most often, such a structure is associated with the structure of the resistive memory ReRAM, Fig. 7.7*b*.

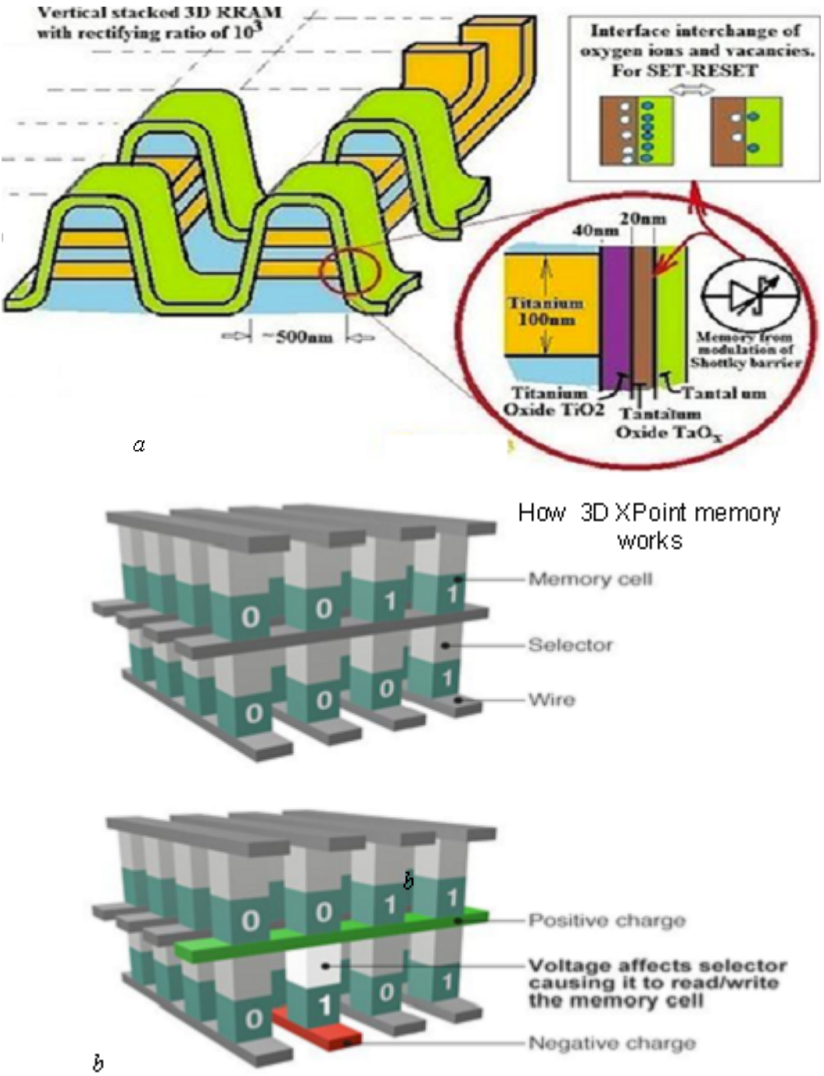

Fig. 7.7. The structure of the 3D memory of the ReRAM type

In particular, Intel and Micron companies developed another type of the nonvolatile memory 3D X Point, Fig. 7.8.

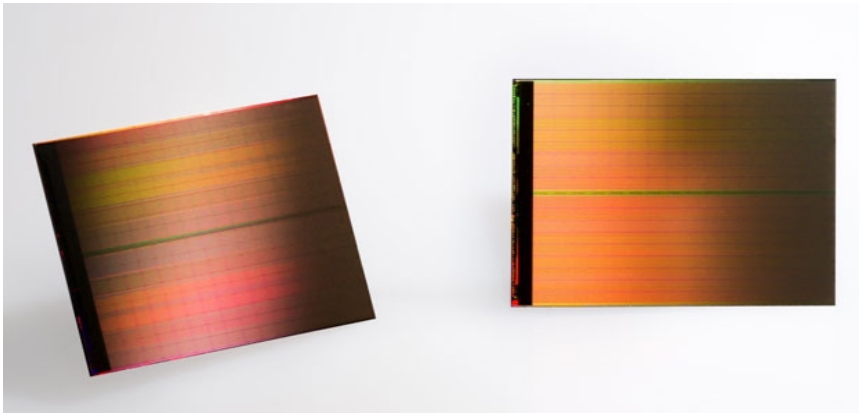

Fig. 7.8. Nonvolatile memory 3D X Point of the ReRAM type

According to the statement of developers with the development of the technology the new layers may be added into the 3D X Point chips. It allows to increase the memory capacity without substantial increasing costs.

7.3 Magnetoresistive random access memory (MRAM)

Another type of the resistive memory is the nonvolatile magnetoresistive random access memory (MRAM), which stores the information using the magnetic moments instead of the electrical charges, [29] and [36].

In the twentieth century, it was known that the electrons creating the current in an electrical circuit, have own magnetic moment, but for practical purposes it is not used. Now, a new branch of the science appears which is called the spintronics.

Spintronics is a branch of science, which is based on the concept of the electron spin. In accordance with this concept the electrons are divided into two types of the current carriers: electrons with spin-up and electrons with spin-down $\left(\frac{1}{2}\right.$ or minus $\left.\frac{1}{2}\right)$ according to the principle of quantization of the spin projection on the chosen axis.

Today the spintronics studies the magnetic and magneto-optical interaction in the different metallic and semiconducting nanoheterostructures as well as the quantum magnetic phenomena in nanometer-sized structures.

Development of the nanotechnologies allows to synthesize the completely new multicomponent materials with the controlled properties, the so-called nanostructures, consisting of alternating layers. The so-called effect of the giant magnetoresistance (GMR) was discovered in the multilayer consisting of the ferromagnetic layers separated by the nonmagnetic layers. This effect is due to the spin-dependent dispersion of the conduction electrons [6], [25], [55], and [60].

In the ferromagnetic metals the conduction electrons divided into the electrons with spin-up (the spin is parallel to the magnetic moment in the ferromagnetic) and spin-down (spin is antiparallel to the magnetic moment). Therefore, the current in the ferromagnetic metal can be represented as the sum of the currents with the two types of spins.

Magnetoresistance defined by these currents depends on the direction of the magnetization in the ferromagnetic layers.

For example, in the multilayers Co/Cu the probability of the dispersion of the electrons with the spin which are parallel to the magnetization direction is smaller than for the electrons with the spin which are antiparallel to the magnetization vector.

The three-layer film in which the GMR effect can be observed is shown in Fig. 7.9.

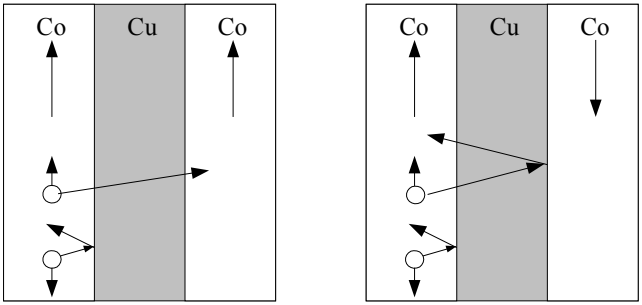

Fig. 7.9. Examples of the magnetic moments of the adjacent ferromagnetic layers

If the magnetic moments of the adjacent ferromagnetic layers are formed up in parallel then the conductivity of the structure is greater than for the antiparallel case. The antiferromagnetic forming up of the magnetic moments of the adjacent layers (with the same value of the coercive force H_c) occurs due to the oblique antiferromagnetic acting (AFM), Fig. 7.10.

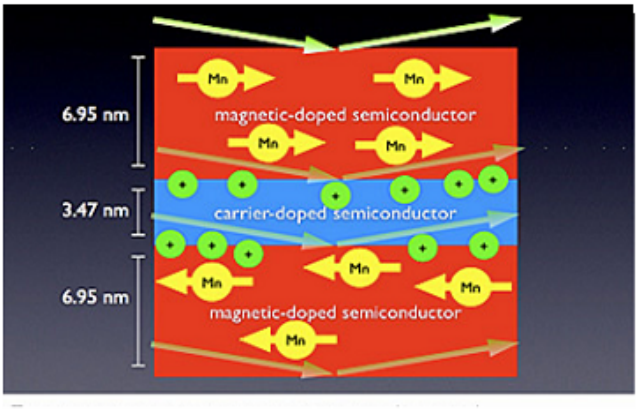

The thin magnetic layers of the semiconductor (red) separated by the nonmagnetic layer(blue) may demonstrate the phenomenon known as the antiferromagnetic relation when the atom of the manganese (Mn) is magnetized in the opposite direction on the adjacent magnetic layer

Fig. 7.10. Illustration of the antiferromagnetic relation

Changes of the magnetic structure caused by the AFM relation, influence not only the magnetoresistive but also on the magnetic properties of the multilayer nanostructures.

One of the main problems of the spintronics is the integration of the magnetic systems in the semiconductor nanoelectronics. Easy control by the electron spins in the semiconductors allows to create two new classes of the hybrid materials: the magnetic semiconductors (hybrid structure of the ferromagnetic / semiconductor) and spin-electronic nanotransistors.

Common to all devices of the spintronics is that they are based on the metal. Obvious metal analogues of the traditional semiconductor transistors (in which flow-out of the electrons from the base of the transistor allows other electrons to come from the emitter to the collector) are yet absent. Finding materials that possess proper-

ties both the ferromagnetics and the semiconductors is the hard problem. It is explained by the great difference in the character of the chemical bonds. Ferromagnetic semiconductors, on the one hand, would be sources of the spin-polarized electrons, and on the other hand they would be easily integrated with the traditional semiconductor devices.

Developing nanoelectronics alloyed to create the three-terminal device, consisting of two ferromagnetic layers separated by the layer of paramagnetic. Such device shows the GMR effect and is called the Johnson transistor, Fig. 7.11. Like the bipolar transistors Johnson transistor contains the base (paramagnetic PM), the emitter and the collector (ferromagnetic FM).

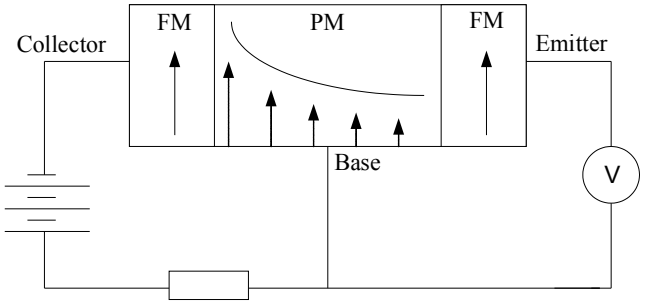

Fig. 7.11. The structure of the Jonson transistor

If the voltage is applied to the collector, then the electrons with the orientation spin -up and spin-down are accumulated in the emitter-base circuit, [55].

The collector current in this case will depend on the direction of its magnetic moment with respect to the magnetization of the emitter. In this case ferromagnetic emitter plays the role of a polarizer for the accumulating spins.

Obviously, to change the potential in the emitter-base circuit it is necessary to apply an external magnetic field, which "switches" the vector of the magnetic moment of the collector or the emitter in the opposite direction. In other words, the electrical characteristics of the transistor can be controlled by changing the magnetic field.

The main shortcoming of the Johnson transistor is that the measured voltage values are very small, and to increase the value of the

voltage it is necessary to apply the additional equipment. To eliminate this shortcoming the Monsma transistors, SPICE-transistors (Spin Polarized Injection Current Emitter transistor) are developed.

Perspective directions of development of the spintronics are:

- high-speed switching of the magnetic state (see below the principle of operation of the MRAM);
- spin-electronic sensors for the different purposes;
- coherent quantum optronics;
- quantum computing (development of the devices in which the information will be transmitted not by the spin of electrons, and using the qubit pairs).

The ability to combine magnetic, semiconducting and dielectric materials has the great perspectives in the control of electrical and magnetic properties of the produced structures. This will allow to get new nanostructure that can find the practical application.

The basic element of the MRAM is the nanoheterostructure with the magnetic tunnel junction (MTJ), [39] and [47].

The magnetic tunnel junction. Nanostructure MTJ consists of two ferromagnetic layers separated by the insulator, as a rule Al_2O_3. The thickness of the insulator is so small (less than 2 nm) that an electron can seep through this barrier. This process is called tunneling, and is explained by the wave nature of the electron. The wave-particle duality de Broglie applies on the particles with the rest mass. The so-called de Broglie wavelength corresponding to the particle depends on its mass and the velocity.

According to Planck, any radiation is determined by the energy

$$w = h\nu,$$

where ν is the frequency of the radiation, h is Planck's constant, equaled $6{,}62 \cdot 10^{-34}$ J·s. In accordance with the teachings of Einstein between energy and mass of any substance there is the relationship:

$$w = mc^2$$

where c is the speed of light in vacuum equaled

$$c = \lambda\nu,$$

and λ is the wavelength. Then we can write that the relativistic mass of the particle is determined by the following equation:

$$m = \frac{w}{c^2} = \frac{h\nu}{c^2} = \left|c = \lambda\nu\right| = \frac{h}{c\lambda}.$$

If the velocity of the particle is less than 20% of the speed of light in vacuum, the relativistic mass with sufficiently good approximation can be defined as the rest mass. Then, the de Broglie wavelength is

$$\lambda = \frac{h}{mv} = \frac{h}{p},$$

where p is the momentum of the particle.

It should be noted that the other particles having the mass m and moving with the speed v have the wave properties (not only electrons). However, due to the large mass of certain particles and their small velocity de Broglie wavelength becomes extremely small and can not be displayed in any diffraction researches. For example, a particle of the mass 1g, which is moving at a speed of 1 cm/s, has a de Broglie wave length just $6{,}62 \cdot 10^{-27}$ sm. The diffraction of the wave of such length can not be detected. The wave properties of the electrons (protons) are taken into account for low mass of the particles and high speed of their movement.

Thus, the respective de Broglie wavelength λ characterizes the stream of any identical particles moving at the same speed. The probability of tunneling depends on the wavelength and the energy of the electron.

In the ferromagnetic material the energy of the electrons with spin orientation up or down is different. This leads to a spin-dependent tunnel effect. If the magnetic moments of the adjacent layers are parallel, then the magnetic tunnel junction conductance is large, and if the magnetizations are antiparallel, the tunneling probability is small, Fig. 7.12. The maximum value of the magnetoresistive effect observed in such structures is about 50 %.

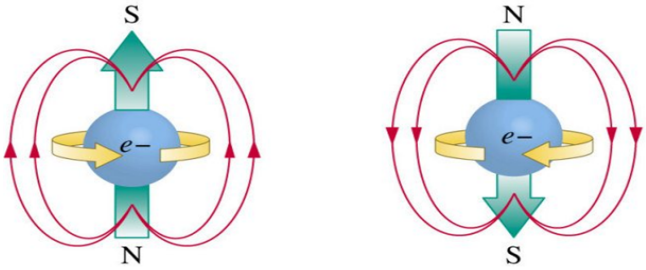

Fig. 7.12. Illustration of the spin-dependent tunneling effect

Now high quality MTJ structures with a barrier layer AlO_x are already developed. We explore The potential possibilities of other materials, such as Ta_3O_5, GaAs, ZnS, MgO are already researched.

The unit cell of this memory is a multi-layer structure, which combines a ferromagnetic storage layer (sometimes referred to as "free" layer), a ferromagnetic fixed layer and the dielectric, Fig. 7.13.

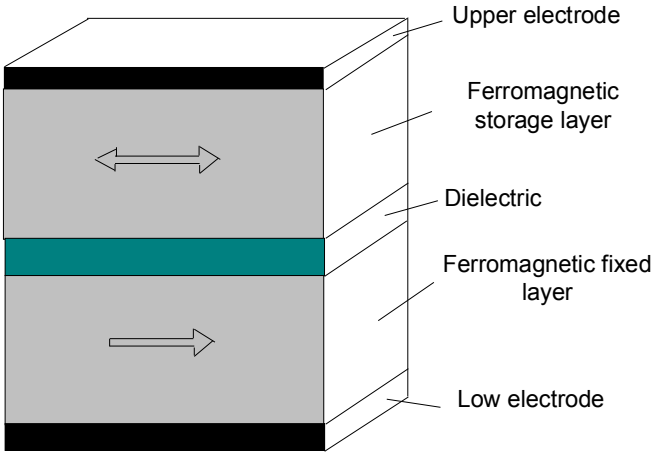

Fig. 7.13. The structure of the elementary cell

The ferromagnetic of the storage layer has a coercive force which is sufficient to keep the recorded information for a long time, but it can be remagnetized by the strong enough external magnetic field (*m*-metal magnetic layer).

A fixed ferromagnetic layer acts as a permanent magnet (hard magnetic layer), that is its coercive force is sufficiently large, and the magnetization direction is unchanged even in strong fields.

The electrical resistance of the cell is sufficiently large if the storage layer is magnetized oppositely to the fixed layer. When the external magnetic field exceeds the coercive force of the storage element, it is remagnetized and the electrical resistance of the cell decreases abruptly, remaining the same low value after the disappearance of an external magnetic field, Fig. 7.14. Obviously, at any given time we can check the state ("0" or "1") of the storage cell of the element.

The random access memory based on such cells is called magnetoresistive memory, although the information (magnetization direction) is stored and saved in the ferromagnetic storage layer.

The memory cells are the sufficiently small sizes (about 10 nm) and can be densely packed, although this is the difficult task. This is due to the necessity of a random access to each cell for reading and writing of the information. As a rule, a matrix organization of the memory is used. In this case, the memory cells are placed at the intersection of bit and address lines with the respective register and the decoder.

The orientation of the easy magnetization axis of the storage layer with respect to the bus system is important for the address matrix sample of memory cells. This axis is at an angle 45° to each bus system, Fig. 7.15*a*.

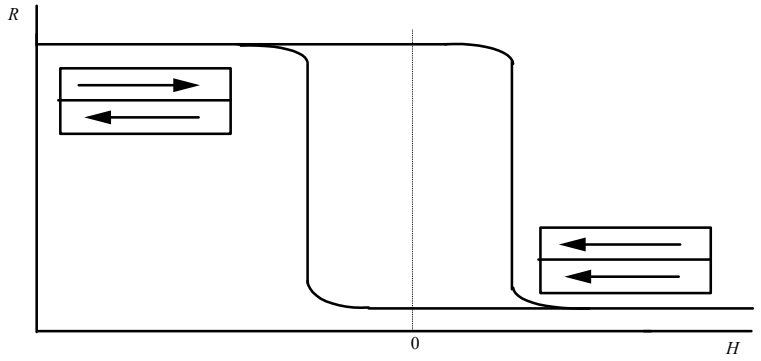

Fig. 7.14. The switching of the states in the MRAM cell

The reading circuit is shown in Fig. 7.15*b*. The reading voltage is applied to the selected address bus. In this case the value of the current

that flows in each bit line depends on the information written in the corresponding bit. If the memory cell has a high resistance, the current has the relatively small value, and it has a large value if the cell has a small resistance.

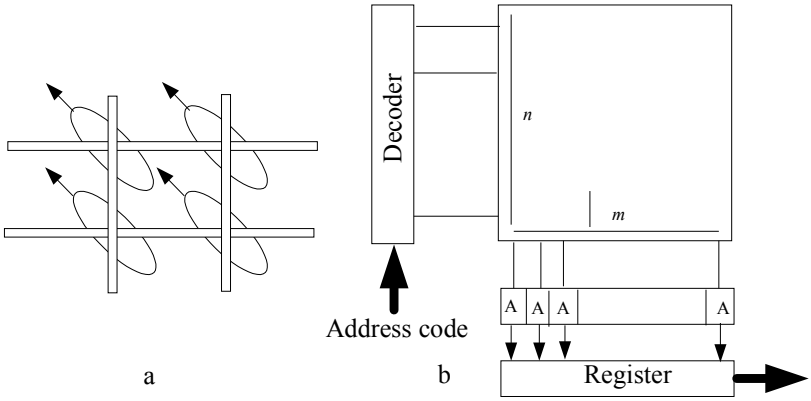

Fig. 7.15. The reading circuit

Each bit line is connected to the amplification and formation circuit of the reading signal. The written in the memory the *m*-digit binary number is reading from the outputs of these circuits.

The writing of the information is carried out on the digits.

Data recording is made on discharge. In accordance with the given address the decoder selects one of the buses and opens the respective valve (for example, the MIS transistor). The current pulse from the writing current source is given to the selected word bus through the valve. The direction of this current is determined by a bit ("0" or "1") which must be written, Fig. 7.16*a*.

The directions of the electric current through the selected buses are shown by the arrows. The magnetic field lines of the respective currents are shown by the dashed lines. These fields act simultaneously on the selected memory cell. The vectors of the intensities $\vec{H}_{\text{bit}}$ and $\vec{H}_{\text{addr}}$ are mutually perpendicular. The result of the addition of the magnetic fields $\vec{H}_{\Sigma}$ in the storage layer at the writing "0" and "1" is shown in Fig. 7.16, *b*. The direction of the magnetization of the fixed layer of the memory cell is designated as $\vec{B}$. In one case the electric currents magnetize the

storage layer in parallel $\vec{B}$ and on the other case the opposite directed currents magnetize antiparallel $\vec{B}$.

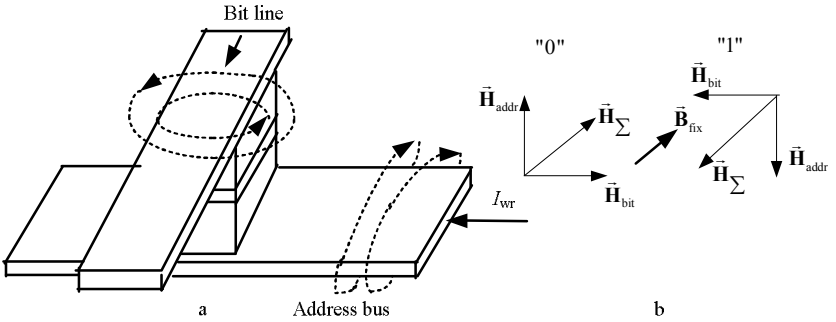

Fig. 7.16. The writing of the information into the chosen cell

The magnitude of the writing current is selected in such a way that the magnetic field of any current was not sufficient to reverse the magnetization of the cells which are adjacent to the respective bus. If these currents act together on the selected memory cell then they must create a total magnetic field $\vec{H}_{\Sigma}$ that exceeds the coercive force $\vec{H}_c$ and remagnetizes the storage layer in the needed direction.

Obviously, the sizes of the elements and buses of the matrix depend on manufacturing technology level, Fig. 7.17.

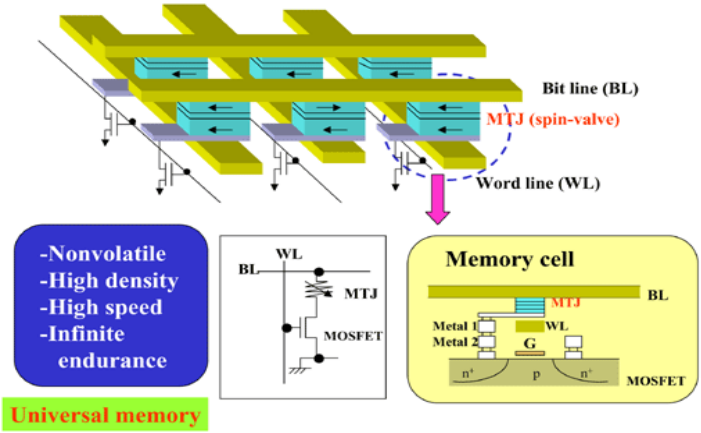

Fig. 7.17. The technology of manufacturing the memory matrix

The scheme of the memory cell MRAM is shown in Fig. 7.18.

The memory cell is formed at the intersection of the bit (BL) and the word (WL) lines and represents the magnetic element.

The magnetic element is formed from two ferromagnetic layers separated by a thin dielectric layer. One of the layers, as already mentioned, is a permanent magnet magnetized in a certain direction, and the magnetization of the other layer changes under the influence of an external field. The memory device is organized on the principle of a grid consisting of individual cells each of which contains the memory element and the transistor.

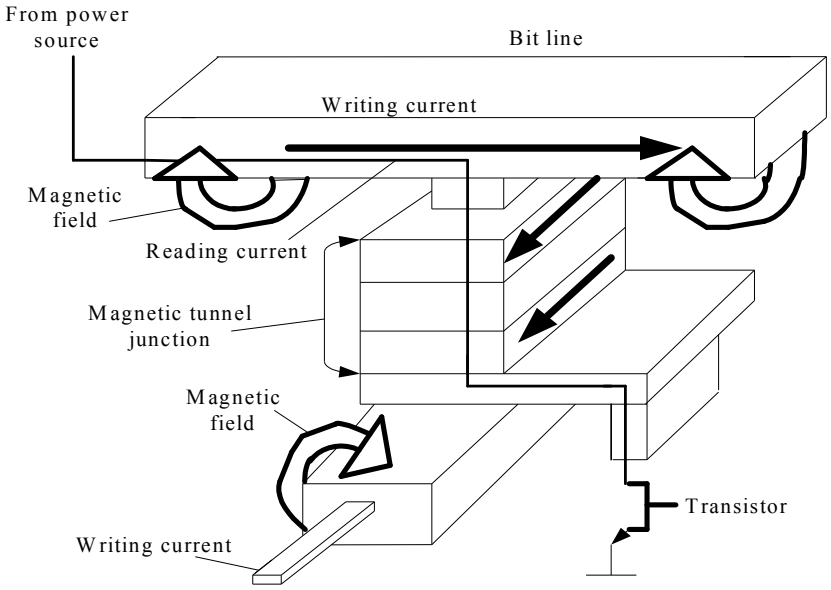

Fig. 7.18. Elementary cell of the MRAM memory

The information is read by measuring the electrical resistance of the cell. To choose single cell the feed is applied to the corresponding transistor which supplies a current from the power supply through the memory cell on the common ground of the whole device.

Due to the tunneling magnetoresistance effect, the electrical resistance of the cell varies depending on the mutual orientation of the magnetization in the layers. The resistance of the cell can be determined by measuring the value of the flowing current, and as a result, the "polari-

ty" of the rewritable layer. Thus, the magnitude of this current depends on the orientation of the magnetization vectors of the magnetic layers of the structure. The resistance of the junction is a minimum if the configuration is parallel and the tunneling current is large. This corresponds to a logical "0".

When the orientation of the magnetizations is antiparallel the resistance is large and the tunneling current has a small value, which corresponds to a logical "1".

The writing of the information into the cell can be carried out by the different ways. In the simplest case, each cell is located between two lines of writing which are placed at right angle to each other, one is placed above the cell and the other is placed below the cell, Fig. 7.19. The current passes through them and the cross magnetic field is induced in the intersection of the writing lines, which changes the magnetic state of the rewriting layer.

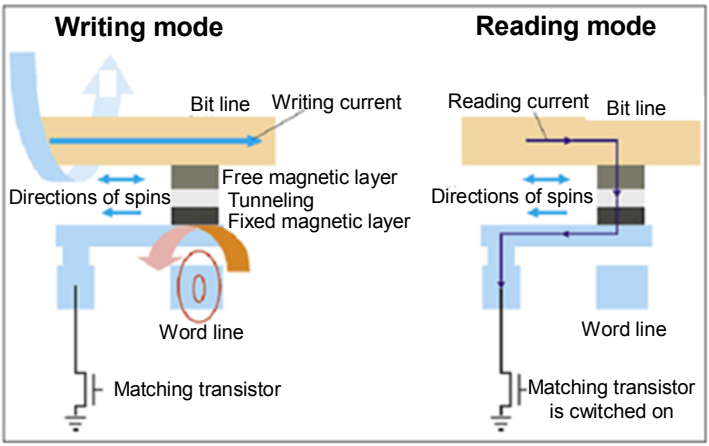

Fig. 7.19. Principle of writing and reading information

This method requires a sufficiently large value of the current to create the magnetic field. It is the main disadvantage of the MRAM.

Moreover, with decreasing sizes of the cell the induced field overlaps the adjacent cells on a small area. It leads to possible errors in the writing.

The access time of the data from the MRAM can be less than 10 ns, which is 5 times less than that for the flash memory, and the writing time is less than 2 ns (on three orders is less than that for the flash memory). In

this case the consumption of the magnetoresistive memory is two times less than for the flash memory and the memory of the DRAM type.

Further improvement of the MRAM cell concerns the structure of the storage and the tunnel elements. For example, the storage layer contains the three layers, Fig. 7.20.

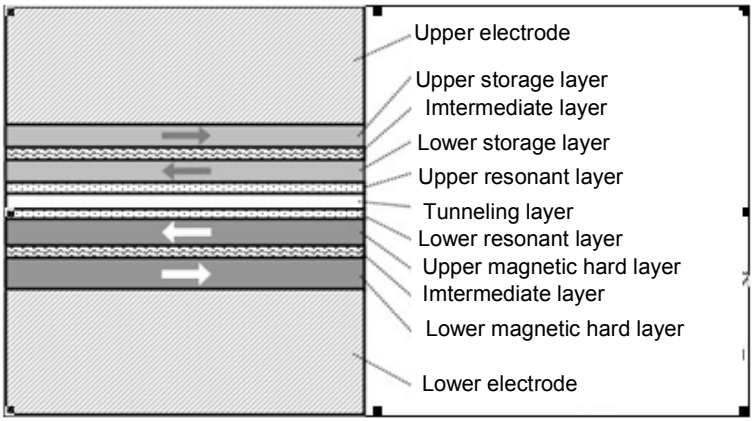

Fig. 7.20. Multilayer architecture of the MRAM cell

Such structure with an intermediate layer is called "synthetic antiferromagnetic" (SAF). In this case the magnetic field of writing suppresses the so-called precession of the magnetic moments around the direction of this field [104] ("spin echo"), which significantly reduces the write time.

In the nanometer-sized elements the turns of the magnetic moments occur very quickly (tens of picoseconds).

The electrical resistance of the magnetoresistive element depends on the direction of the only lower layer of the memory element. The phenomenon of the "resonant tunneling junction" is used to improve the tunneling layer. With this end, both sides of the tunnel dielectric layer (for example, MgO of 1 nm thick) are sprayed by the same thin "resonant" layers (for example, 1 nm layer from CoFeB). In this case the sensitivity of the magnetoresistive element considerably increases and the reliable operation is possible even with a substantial decrease of the area of the memory cells. Then the probability of tunneling of electrons through the dielectric layer (tunnel layer) from one to another resonance level increases.

The great advantage of the MRAM is theoretically unlimited term of the data storage, an unlimited number of the write cycles and essentially lower consumption of the energy for the writing.

The factor which limits the development of the magnetic memory technology is that the magnetic fields are required to switch the magnetic states in the magnetic memory devices. This limits the productivity of the devices and confines their miniaturization. It is explained by the fact that to generate the field which is sufficient for switching device it is necessary to create large currents and use the large diameter conductors.

Now, scientists are studying a new generation of the magnetic devices which can write the information without the help of the magnetic fields. These devices use a mechanism called "spin torque" concerned with the presence of the spin (Spin MRAM type memory). When the electrons interact with the magnets in the tunnel junctions, they transfer them some part of own momentum. This may lead to appearance of a very large torque per unit current, which is at least 500 times more efficient than the momentum occurring when the magnetic field for writing information is used, [98].

Particular interest represents one of new developments of the magnetic memory, which is still at the research stage.

As it is known, in the modern solid-state memory (SSD – Solid State Driver) to store one bit of the information the surface region having about $3 \cdot 10^6$ atoms of the magnetic substance is used.

German and Japanese researchers have jointly developed a new type of the memristor magnetic memory that can store one bit of the information within one molecule of the magnetic substance, which is called the "molecular magnet".

It is known that reduction of the size of one bit on the surface of the hard disk plates is limited by the super paramagnetic effect, the essence of which is that when the crystals of the magnetic substance are reduced in the sizes, they are susceptible to the heat, which causes a spontaneous switch their magnetic state.

Researchers have proposed a completely another way and placed a single magnetic iron atom at the center of the organic molecule consisting of 51 atoms, Fig. 7.21. The organic shell protects the information stored in the central iron atom from external influences.

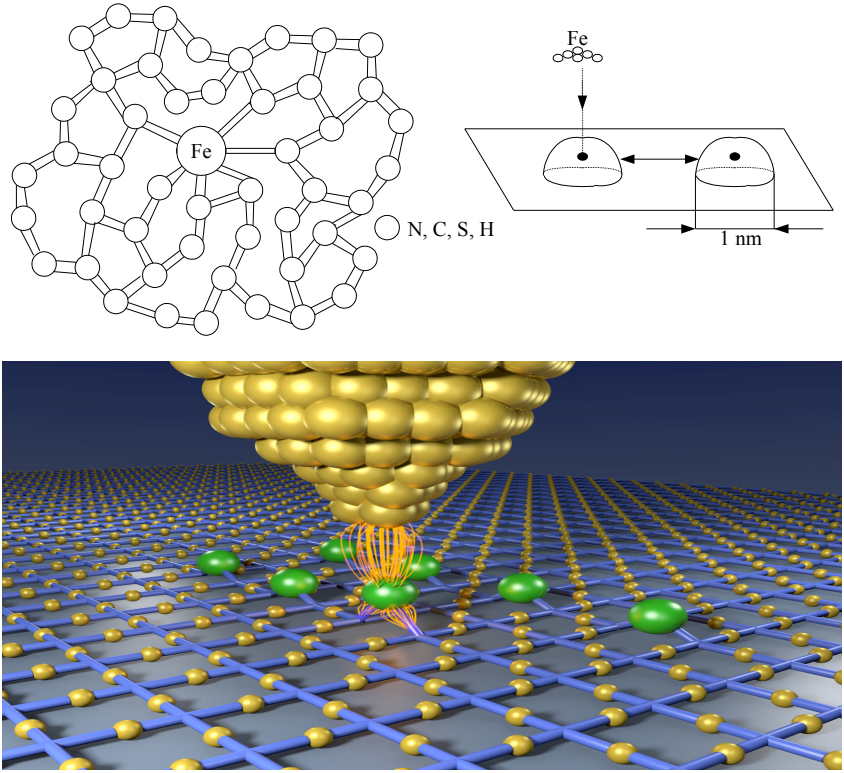

Fig. 7.21.The organic molecule with the iron atom

Besides the highest data storage density equaled one bit per molecule, a new type of the memory (according to the terminology of researchers this type of the memory is based on the effect of the "rotation of intersecting molecules" (spin crossover molecules)) has a simple procedure for writing and reading information. Using the electric current pulse of the given form and size, the metal-organic magnetic molecule can be switched into the conducting magnetic state and into the nonconductive, nonmagnetic state.

Using a scanning tunneling microscope, it is possible to act by the electric pulse with the defined characteristics exactly on the molecule of about 1 nm size. Studies have shown that the electrical pulse changes not only the magnetic state of the iron atom, and the electrical properties of the molecule as a whole.

Scanning tunneling microscope (STM) allows to view the individual atoms, using the so-called quantum effect of the tunneling. Microscope as if "feels" the studied surface: a very thin needle-probe with a tip thickness of one atom is moved over the surface of an object at a distance of about one nanometer.

At the same time, according to the laws of quantum mechanics, the electrons overcome the vacuum barrier between the subject and the needle that is they tunnel, and the current begins to flow between the probe and the object. The current value is highly dependent on the distance between the needle tip and the sample surface.

The change of the gap on few tenths of a nanometer the current can be increased or decreased by an order. By moving the probe along the surface with the help of the piezoelectric elements, we can explore its terrain by the measuring of the current.

To lead to the tip of the probe to the sample at the distance equaled several angstroms and to scan along the surface the piezomotor based on piezoelectrics.

Piezoelectric is the material which changes its sizes under the acting of the control voltage. The image of the surface structure on the atomic level can be obtain by scanning the sample surface in the direction of the axes *X* and / or *Y* with simultaneous measurement of the output signal in the circuit of *Z* coordinate, Fig. 7.22.

The studied structure can be displayed in two modes:

- tunnel current measurement with maintaining the distance from the tip to the sample surface;
- • measurement of the distance to the sample surface under the condition of the constant tunneling current (this mode is used more often).

The microscope allows to see the details of the surface with a resolution of hundredths and even thousandths of a nanometer (corresponds to an increase of about 100 million times), Fig. 7.23.

However, it should be noted that the resulting image is not a photo in the ordinary sense. This is only a graphical representation of how the gap between the probe and the surface is changed to maintain a constant current.

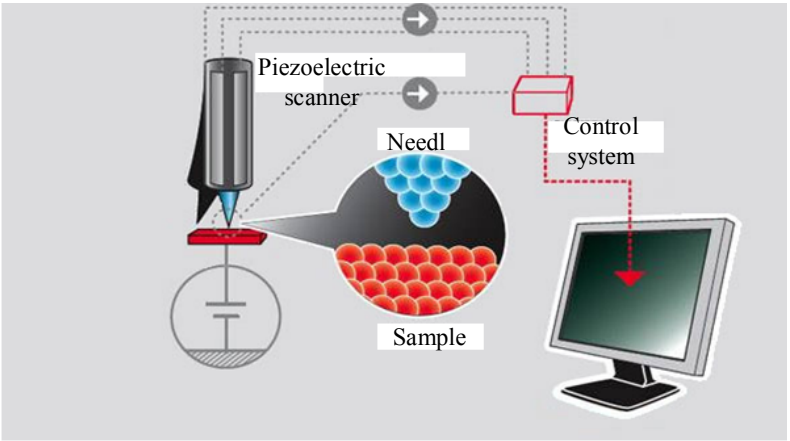

Fig. 7.22. The structure of the scanning tunneling microscope

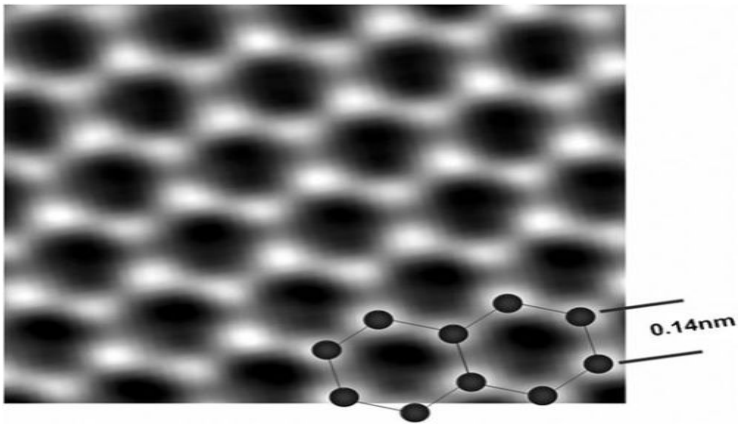

Fig. 7.23. Resolution of the scanning tunneling microscope

The scanning tunneling microscope has no lenses, so the image is not distorted due to aberrations. The energy of electrons, forming the image does not exceed a few electron volts. It allows to carry out the non-destructive inspection of the object.

Creation of the STM was a significant step in the research of the nanoworld.

Design and manufacture of the scanning tunneling microscopes and today represent a hard problem. There are few laboratories

possessing these devices, which would work with true atomic resolution. General view of the microscope is shown in Fig. 7.24.

Fig. 7.24. Scanning tunneling microscope

Thus, the two magnetic states of the iron atoms leads to the different electronic conductivity of the whole molecule, which can be measured relatively simply by measuring the electrical resistance.

According to scientists, the memristor and the spintronic properties, realized within a single molecule, opens up the new fields for further researches in order to introduce in the production process.

7.4 Phase state change random access memory (PCRAM)

The memory on the basis of the phase transition (phase change memory (PCRAM)) is a nonvolatile memory based on the unique behavior of the material under the name "chalcogenide". This material can be switched between two states: crystalline and amorphous when it is heated.

The information is stored in the atomic structure of the material, while the amorphous state has a similarity to the window glass with the unordered atoms, Fig. 7.25.

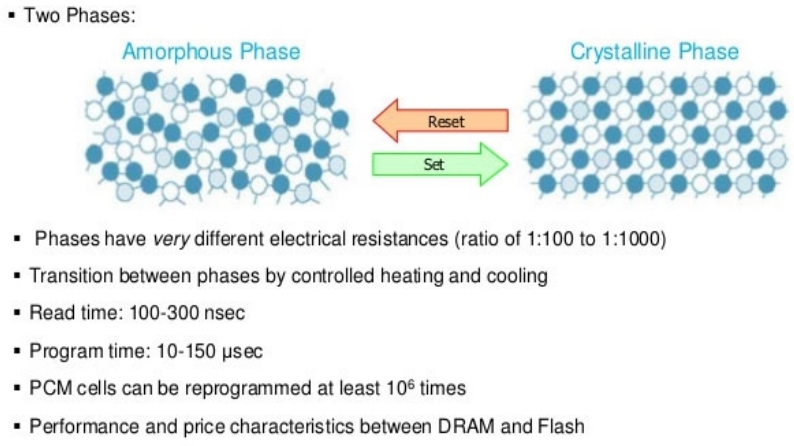

Fig. 7.25. Two phases of the material state

Essentially, PCRAM is one of the forms of the resistive memory ReRAM [26].

Chalcogenide is enclosed in the PCRAM between two electrodes, and to switch the phases (states) it is necessary to apply the laser pulse or the electric current to melt the material and to convert it into an amorphous state.

The prolonged acting the voltage pulse of the certain amplitude leads to the formation of the crystal lattice, and under the action of the short pulse of greater amplitude the material is cooled to an amorphous phase.

Each substance normally forms the crystals of the defined shape. For example, sodium chloride is crystallized in the form of cubes, sodium nitrate in the form of prisms, etc. The internal structure of the **crystals** is presented in the form of a crystal lattice which represents the spatial frame formed by intersecting straight lines. At the points of intersection of the lines (lattice nodes) are the particle centers.

Many of the physical properties of the crystal are not always the same in different directions within the crystal. This important feature of crystalline materials is known as anisotropy.

Depending on the nature of the particles and on which the forces of the interaction between them prevail it is necessary to distinguish atomic, molecular, ionic and metallic crystal lattices.

The number of materials that have the atomic lattice is relatively small (diamond, silicon). The number of substances with a molecular lattice is so many (non-metals, with the exception of the carbon and the silicon).

Substances with ionic lattice include most of salts and small number oxides. Substances with metal lattice are the metals and their alloys.

The molecules are in the nodes of the molecular lattice. In the nodes of the atomic lattice there are the atoms which are connected between each other by a covalent bond. In the nodes of the ionic lattice there are alternately positive and negative ions, which are connected between each other by the forces of the electrostatic attraction. In the nodes of the metal lattice there are atoms of the metal. The electrons which are mutual for these atoms move freely between them.

Each lattice can be characterized by an elementary cell which is the smallest part of the crystal and has all the features of the structure of the given lattice.

For example, in the crystal NaCl each sodium (natrium) ion Na^+ is surrounded by six nearest ions of opposite sign (Cl^- ions), and in the CsCl crystal the Cl^- ion is surrounded by eight ions of Cs^+, Fig. 7.26.

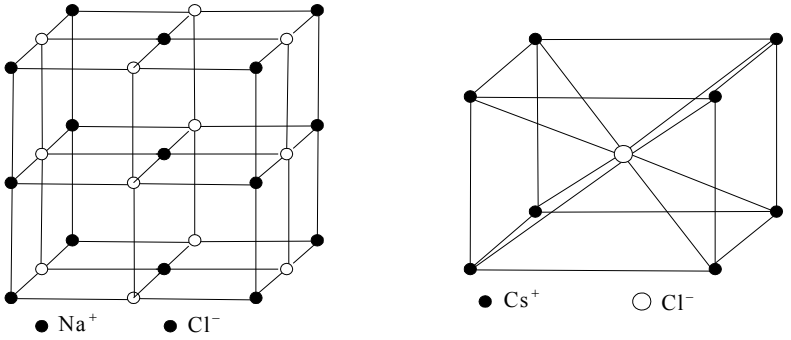

Fig. 7.26. The elementary cells of the lattices

Defects in the structure of real crystals are varied. The simplest and at the same time a very important point defects are unoccupied lattice nodes (vacancies), and the atoms which are between the

nodes. The existence of such defects is due to the fact that the individual lattice atoms or ions have the energy higher than its average value at the given temperature. These atoms can move from the lattice node.

Released from the node the atom forms the unfilled place called the vacancy. At any time moment adjacent to the vacancy atom can move in the place of the vacancy, releasing a new one. Thus, the vacancies pass from one place to another, forming a drift of vacancies (see Shapter 2).

The difference between the crystals and the amorphous substances is sharply shown in their attitude towards heating. The crystals of each substance melt at a strictly defined temperature and at the same temperature crystals pass from the liquid to the solid state. The amorphous substances have no constant melting point. When heating, the amorphous substance gradually softens and begins to flow and finally becomes entirely liquid. Upon cooling, it solidifies gradually. As for the internal structure, the orderly arrangement of the particles in the crystal is preserved in large sections of the crystal, and in the case of well-formed crystals this arrangement is preserved in all volume of the crystal. In the amorphous substances the orderly arrangement of the particles is observed only in very small areas.

Some substances may be both crystalline and amorphous. So the silicon dioxide SiO_2 is encountered in nature as the well formed quartz crystals and also as the amorphous substance (mineral, flint). This crystalline state is always more stable. Spontaneous transition of a substance from a crystalline to amorphous state is impossible.

Spontaneous transition from the amorphous to the crystalline state is possible.

The mechanism of the change of the memory cell resistance is based on the creation or the destruction of the conductive channel within the amorphous substance using the applied pulse voltage. Now the memory cells which include the active layer between the electrodes containing the so-called amorphous silicon are developed. If the pulses of the fixed shape, of the potential and the duration are applied to the electrodes then the conducting filament from the metal silicon is formed in the volume of the amorphous silicon, Fig. 7.27*a*. The pulses with the different characteristics are used for the inverse transformation of the metallic silicon into the amorphous one, Fig. 7.27*b*.

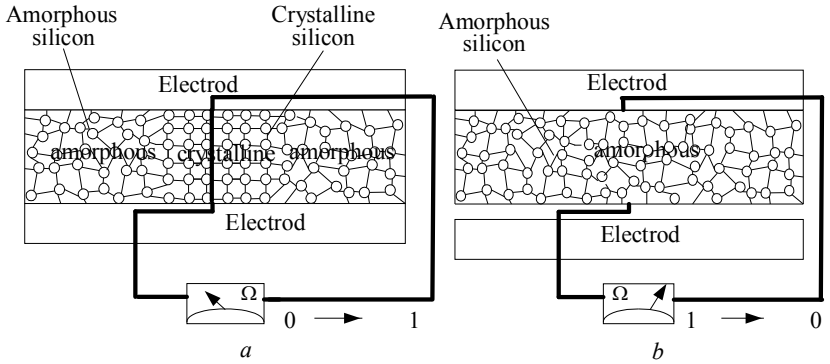

Fig. 7.27. Crystalline and amorphous states of the PCRAM memory cell

It should be noted that the chalcogenides for the active layer are used in the combination with germanium, antimony and tellurium (GeSbTe), referred to GST. The stoichiometric composition of Ge:Sb:Te equals 2:2:5. When GST is heated to a high temperature its chalcogenide component loses the crystalline structure. On cooling it turns into the amorphous glassy form and its electrical resistance increases. When it is heated to a temperature above its crystallization point, but below the melting point, it passes into the crystalline state with a much lower resistance. The time to complete this phase transition depends on the temperature [66].

In terms of the memristive approach the PCRAM cell can be described as the second-order unipolar memristive system which is controlled by the voltage or the current.

In particular, the simple model of the PCRAM cell is based on the equations that describe the process of change of the temperature and the phase state of the material [79], [91] The temperature T and the coefficient of the crystallization (crystalline fraction) C_x are used as the internal state variables:

$$I = \frac{U}{R(C_x, U)},$$

$$\frac{dT}{dt} = \frac{U^2}{C_h R(C_x, U)} + \frac{\delta}{C_h}(T_r - T),$$

$$\frac{dC_x}{dt} = \alpha(1 - C_x)\theta(T - T_x)\theta(T_m - T) - \beta C_x \theta(T - T_m),$$

where

$$R(C_x, U) = R_{\text{on}} + (1 - C_x)\frac{R_{\text{off}} - R_{\text{on}}}{\exp\left[\dfrac{V - U_t}{V_0}\right] + 1},$$

C_h is heat capacitance, δ is the heat dissipation constant, T_{r} is the environment temperature, T_m is the melting temperature (melting point), T_x is the transition temperature into the glass state (glass transition point), α and β are the constants, determining the rate of crystallization and amorphization (the transition to the amorphous state), U_t is the threshold voltage, V_0 is the parameter that determines the shape of the ($i - u$) dependence.

This model takes into account the crystallization ($T > T_m$) and amorphization ($T_m > T > T_x$) processes. The region of the negative differential resistance, adjacent to the threshold voltage U_t is not taken into account. It is not specific meaning when the read / write operations are carried out (the voltage of these operations are outside this region).

Recent researches from Intel and ST Microelectronics have shown the ability of the more close controlling the state of the material and to add two additional states, which allow the material to turn into one of four states: two previous states (amorphous and crystalline) and two new states (semi-crystalline states).

Each of these states has its own electrical properties that can be measured when the information is read. In this case, one cell can store two bits, thereby doubling the density of the memory.

The density of the placement of the storage elements can be very high: only a few atoms are needed to create a cell that can change the state from the crystalline to the amorphous one. Experts believe that the real value is 5 nm, which is almost 10 times less than in the flash memory.

The disadvantages of this type of the memory should include the following:

- The need to transfer energy to heat the memory elements to several hundred °C (slightly more 330° for crystallization phase and higher 730° to pass into the amorphous state), which takes a significant amount of the power; although level of power consumption will decrease with a decrease of the devices based on the PCRAM.
- With a decrease of the time switch PCRAM (theoretically, the switching from one state to another state can be up to 1 ns) the stability of the state of the material is also decreased.

7.5 Ferroelectric random access memory (FeRAM & FeTRAM)

Fundamental researches in the field of physics of nanostructures in recent years have opened up new physical effects that allow to propose new mechanisms for realization of the memory nanodevices, and to take away the physical limitations on their scaling, processing speed and the power consumption. To implement the new physical concepts of writing and storage of the information the synthesis of new materials and detailed research of their properties, including, the multilayer structures are very important. In particular, the property of the ferroelectrics to store the residual polarization when the external electrical acting is disconnected is already being used to write and store the information.

Ultra-thin ferroelectrics are represent a great interest, both from a scientific point of view and from the point of view of possible applications, because their use may allow to observe effects of control by the electron tunneling in the structures metal / ferroelectric / metal by means of the external electric fields. Realization of these effects was predicted theoretically and experimentally implemented recently.

In the research laboratories and the respective enterprises the ultra-thin ferroelectric layers (for example, on the basis of barium titanate $BaTiO_3$) are grown and studied using the pulsed laser deposition method. The research of the properties of these materials is carried out with the help of the atomic force microscopy. The possibilities of their use in the ferroelectric tunnel junctions are researched. The mechanism of the control by the tunneling current through the ferroelectric layer is realized in the junctions by means of the external electric fields.

Successful realization of the ferroelectric tunnel junction opens up the possibility to create a fundamentally new technology of manufacturing the nonvolatile memory devices.

In recent years, the research laboratories actively explore the solid substances having both the magnetic and the electric ordering. Such substances show the magnetoelectric effect, which changes the electric polarization P of the sample by means of the external magnetic field H (direct effect) or changes the magnetization M of the sample under the acting of the electric field E (inverse effect), [5], [17].

An alternative concept of the nonvolatile memory can be based on the electrostatic and the electronic effects in the ultrathin insulating layers of the ferroelectric material (for example, $BaTiO_3$) on the base of which in the structures metal / ferroelectric / metal the so-called ferroelectric tunnel junctions (similar to the magnetic tunnel junctions) can be created. The "resistive" switching (tunneling current control) is achieved by changing the direction of polarization of the ferroelectric by the external electric field that is changing the potential barrier.

Thus, the change of the polarization of the ferroelectric by the external electric field influences on the tunneling conductance of the entire structure. The conductance is changed when the magnitude of the applied electric field is equal to the coercive force of the ferroelectric and is directed opposite to the direction of polarization.

The materials used in the creation of such structures must have the close lattice parameters to realize the epitaxial growth, because the ferroelectric layer shows its functional properties in the ultrathin layers only if the structural orientation exists.

For this purpose, the use of such composite materials as $Fe/BaTiO_3$ and $Fe_3O_4/BaTiO_3$ may be possible.

The word **epitaxy** formed from the Greek words *epi* (on) and *taxis* (order) means the controlled growing of the thin layers with an ordered structure on a flat monocrystal substrate. Significantly, that the crystal structure of the epitaxial layers repeats the structure of the substrate. The chemical composition of the epitaxial layer and the substrate may be different, but the proximity of the values of the lattice constant is a indispensable condition of the epitaxial growth. Epitaxial structures have the following characteristic properties:

• the level of structural perfection, absence of defects and impurities of the epitaxial layers exceed the volumetric materials (including the substrate material);

• the chemical composition of the grown layers can be changed by means of the control, allowing to obtain materials with the given properties. The technology also has the ability to control by the doping of the layers directly in the growth process;

• epitaxy allows to grow the alternating layers of different composition, and, due to the presence of atomic-sharp edges, the layer thickness can be reduced down to atomic sizes;

• the quality of the surface of the epitaxial layer greatly exceeds the quality of the original substrate surface. It is allow you to create the structures with the almost atomically flat boundaries;

• high structural perfection of the epitaxial layers can significantly decrease the dispersion of the free carriers and increase thereby the electric mobility in the material.

• the semiconductor epitaxial structures are characterized by extremely rapid electrical and optical dynamics. This is the important characteristic for creating the high-speed electronic and computing devices.

The main aspects of the ferroelectric nonvolatile memory will be considered in this section.

The ferroelectric random access memory (ferroelectric RAM – FeRAM) is one of relatively new and perspective technologies of the memory devices [70]. The unique properties of the FeRAM allow to use it instead of the RAM and ROM simultaneously. With the development of technology the considered memory may gradually to replace the most widespread types of the memory (Flash, SRAM, DRAM) in many applications.

The properties of the ferroelectrics have been known for a long time and were first discovered in the crystals of Rochelle salt in 1920. The analogy of the electrical properties of this substance with the ferromagnetic properties of the iron led to the fact that in the foreign literature the class of like substances is called the ferroelectrics.

The ferroelectrics are the materials which have a spontaneous polarization in a certain temperature range and have the hysteresis of the dependency of the electric dipole moment from the applied electric field.

The temperature at which the spontaneous polarization of the ferroelectric disappears is called the Curie temperature. These properties make this class of the materials like the ferromagnetics.

Microscopic cause of the ferroelectricity is the presence within the substance of the atomic (or molecular) dipoles. These dipoles are oriented in an external electric field and remain in this state after his removal. The switching of the direction of the field to the opposite direction leads to the reverse orientation of the dipoles. In the ferroelectrics the dipole is formed by the displacement in the elementary cell of the atoms of one kind having two stable positions in the lattice, with respect to the atoms of the other kind.

So the positive ion Ti^{+} has two equivalent stable positions in the lattice with respect to the barium and the oxygen ions in the barium titanate $BaTiO_3$, Fig. 7.28.

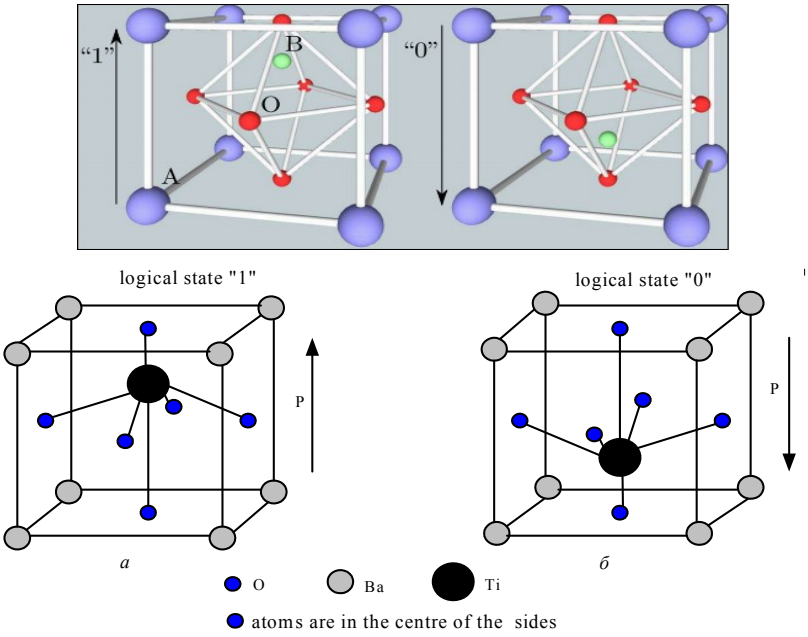

Fig. 7.28. The elementary cell of the barium titanate

Thus, the elementary dipole is formed and oriented in one direction or another. If the ferroelectric is placed in the electric field, the most of

dipoles are arranged advantageously in the same direction, keeping it after removal of the external electric field.

It is necessary to note that piezoelectricity is a necessary but not sufficient condition of the ferroelectricity. To display the ferroelectric properties of the material the more strict conditions put on the symmetry of its crystal lattice.

Intermediate class of the materials between the piezoelectrics and the ferroelectrics are the pyroelectrics in which there is the dependence of the dipole moment from the temperature. The diagram of their mutual properties is shown in Fig. 7.29.

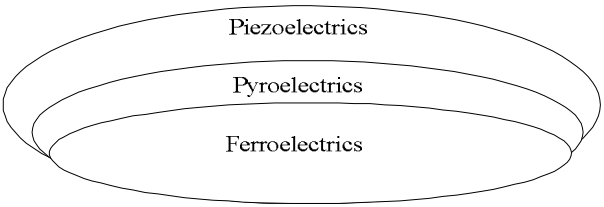

Fig. 7.29. The diagram of the mutual properties of the materials

The physical principle of storing information in the FeRAM cell is the prolonged nonvolatile storage by the ferroelectric material of the polarization obtained in the electric field at the writing.

Under the action of a positive electric charge takes place the positive polarization of the ferroelectric, the result of which is transition in the state corresponding to the logical "1", Fig. 7.28*a*.

Under the action of a negative electric charge takes place the reverse transition corresponding to the logical "0", Fig. 7.28*b*.

In these transitions the ferroelectric material changes its physical properties, and the element, which consists of this material, changes its properties as well. There is a hysteresis loop and as result the states "0" and "1" are far separated on the energy value. It allows to make their an unambiguous identification.

Schematic view of the hysteresis loop for a ferromagnetic ferroelectric capacitor and its symbol are shown in Fig. 7.30.

Here, Q_r is the residual charge, Q_s is the charge of saturation, U_C is the coercive voltage and C_{FE} is the designation of the capacitor in the circuit diagram. Standard FeRAM cell consist of the pair transistor - capacitor like in the dynamic memory, but in a capacitor the ferroelectric is used as a dielectric.

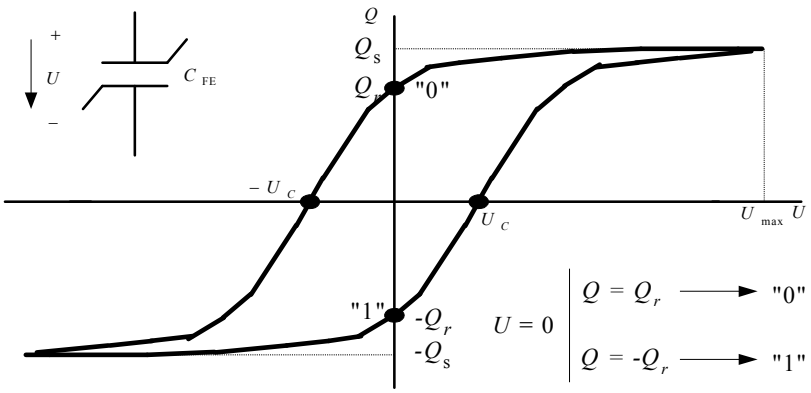

Fig. 7.30. The hysteresis loop of the ferroelectric capacitor

As a result, there is no need for frequent regeneration; the power consumption is significantly reduced.

Now the companies carry out active searches to select the materials that have the best properties to create the capacitors and transistors on the basis of the ferromagnetic ferroelectrics, [72].

As is known, in the DRAM memory type the information is represented by the electric charges in millions of the microcapacitors, each of which encodes one bit. Common DRAM-capacitor consists of two parallel conductive plates separated by a thin layer of the silicon oxide SiO_2 (or a combined layer of the oxide and the nitride of the silicon SiN_2). But this technology has fundamental limitations on the density of the information writing, since it requires the large area of the plates in order to reach the capacity of the capacitor at least 25 femtofarad ($25 \cdot 10^{-15}$ F) per bit. The area may be reduced, for example, increasing the dielectric constant and decreasing the thickness of the layers of the dielectric (in accordance with the known relationship $C = \frac{\varepsilon_a S}{d}$).

Then it is obvious that the ferroelectric materials having the dielectric constants in the range from 300 to 1500 are perspective in this approach. For comparison, the dielectric constants of the silicon and the nitride oxide are respectively 4 and 6. That is why the ferroelectric thin films are used in the FeRAM memory cells.

At the moment there are a huge number of the possible combinations of the basic elements from which the memory cell is constructed namely

the ferromagnetic ferroelectric transistor and the same capacitor. Four main types are considered from these combinations.

Using the ferroelectrics of the latest generation, such as a composite oxide SBT ($SrBi_2Ta_2O_9$) with the addition of hafnium Hf and a modification of the ferroelectric field effect transistor structure allow to significantly increase the information capacity of the memory.

The scheme of the 1TFeRAM cell type (the cell contains one transistor) is shown in Fig. 7.31*a*. The memory type 1SFeRAM (SFRAM) consists of 1C cells, that is each cell contains one ferroelectric capacitor, Fig. 7.31*b*.

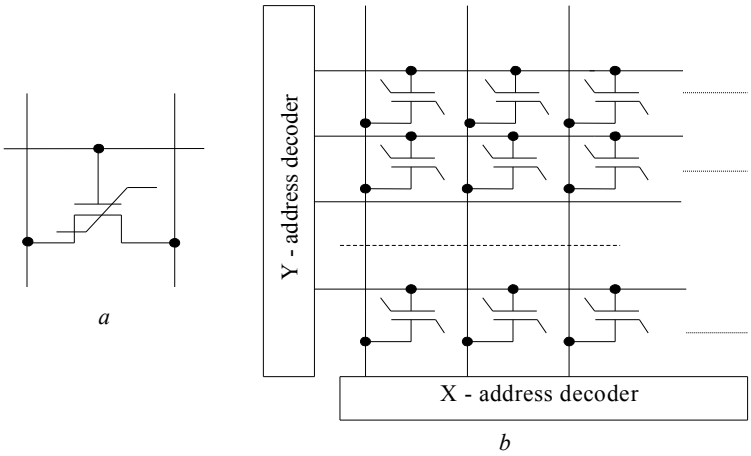

Fig. 7.31. (*a*) is the scheme of the 1TFeRAM cell type; (*b*) isthe memory type 1SFeRAM (each cell contains one ferroelectric capacitor)

The key positions of this technology are very small cell size and, consequently, a higher information capacity per unit area of the chip in comparison with the SRAM, low power consumption in the reading mode, high speed and low price. This type of memory most is closer in structure to a long-forgotten memory on the ferromagnetic cores.

Memory Type 1T-1C FeRAM is very close in structure to the ordinary DRAM, as it is easily seen from the concepts of both types of the memory, Fig. 7.32 *a*, *b*.

The main difference from the DRAM type memory besides the ferroelectric capacitor and the transistor includes is the method of connecting the cell to the common structure.

The negative plate of the DRAM capacitor is connected to the chip ground, and in the case of the FeRAM there is a connection to additional conductor called the transmission line (drive line). This connection completely changes the principle of the data writing into the cell.

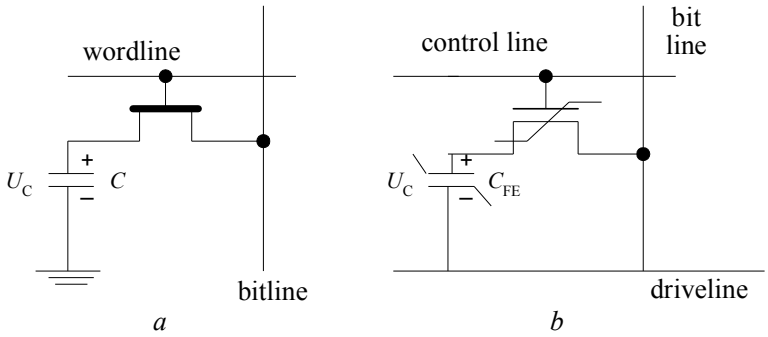

Fig. 7.32. Memory cell DRAM type (*a*) and 1T-1C FeRAM type (*б*)

To write a binary "1" in the DRAM cell the positive voltage is applied to the data line (bit line) and the signal, which opens the FET is applied to the control line (word line), then the capacitor is charged and the cell assumes the state of "1". Writing a binary zero is as follows: the data line is grounded, the signal, which opens the transistor, is applied to the control line, and the capacitor is discharged, and the cell takes the state of "0".

In the case of the FeRAM, to write a binary "1" the positive voltage is applied to the transmission line (driveline), the data line is grounded, the signal which opens the transistor is applied to the control line, as the result the negative polarization of the capacitor occurs and the cell takes the state of "1". To write “0” the positive voltage is applied to the data line, and the transmission line is grounded, and the signal which opens the transistor is applied to the control line, as a result the positive polarization of the capacitor occurs and the cell takes the state of "0". In both cases, the positive voltage is used but applied from the different directions.

The main circuit element respondent for data writing is the capacitor. Writing takes place after the opening of the transistor. Consequently, there is a certain time constant, including the transistor response time plus the time capacitor polarization. This constant is responsible for the speed of the memory of the FeRAM type. Obviously, for each ferroelec-

tric this constant will be different; therefore, it is necessary to find the materials and dopants for which the time constant is smallest.

Memory type 2T-2C FeRAM represents double cells 1T-1C type. These cells can be combined in the different ways, so several variants may correspond to the general formula 2T-2C, one of which is shown in Fig. 7.33.

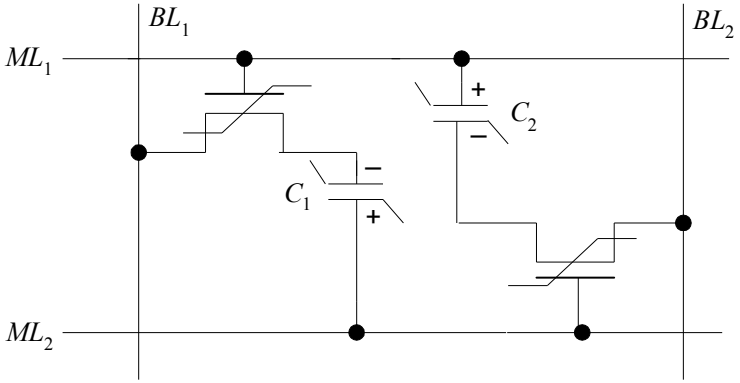

Fig. 7.33. Memory cell 2T-2C FeRAM type

The memory cell is connected to two control lines, combined with the transmission lines (ML – merged word line / plate line), and the two data lines (BL). It corresponds to WL/PL architecture. This arrangement raises the integration of the components on a chip.

Some modernization of the FeRAM memory was existed by researchers from Purdue University (USA), which create a pre-production model of the nonvolatile memory with the name FeTRAM (Ferroelectric Transistor RAM).

FeTRAM memory technology is based on the combination of the silicon nanowires with the ferroelectric polymer material, which changes its polarization when the electric field of the respective polarity is applied. As in FeRAM memory type the polarization may be read as "0" and "1" without difficulty.

However, the new technology uses the ferroelectric transistor instead of the capacitor (Fig. 7.34). It means that the information from the cell can be read without destruction of this information.

According to the calculations the FeTRAM memory will consume only one percent of the amount of energy consumed by the modern flash

memory. But thanks to its organization the FeTRAM memory will approach the memory SRAM with respect to operating speed.

Now, the manufacture of the memory FeTRAM can be organized with the use of the modern industrial technological processes of the semiconductor manufacturing (complementary metal oxide semiconductor, CMOS).

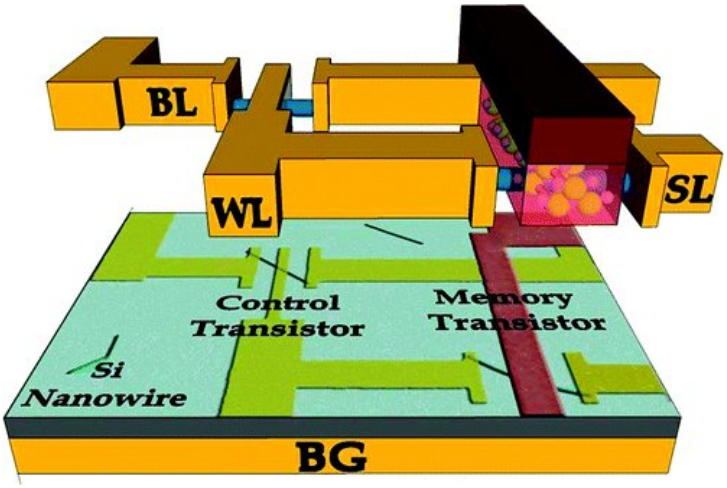

a

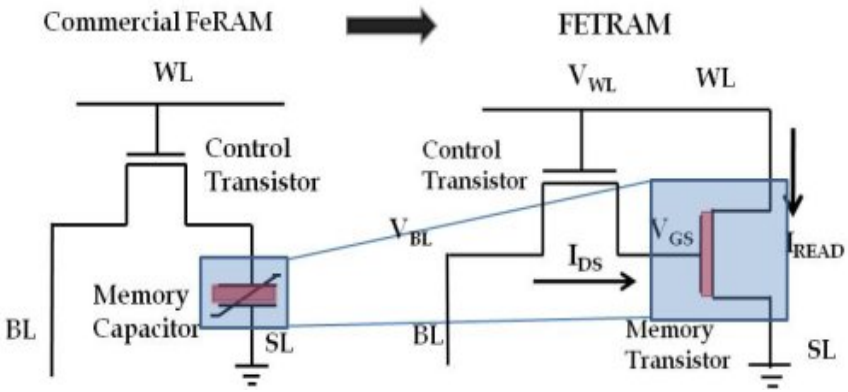

b

Fig. 7.34. (*a*) is the structure of the FeTRAM cell; (*b*) is the scheme of the cell

The main advantages of the FeRAM (FeTRAM) technology include.

- **The operating speed is the same as in the static memory (SRAM) but this memory is nonvolatile.** Reading and writing the information in the FeRAM memory can be carried out with the frequency of the processor bus, like the SRAM type memory. However, unlike SRAM, the written information is not lost after switching of the power. Data are stored more than 10 years without the need for regeneration or standby power in the temperature range from minus 40 to + 85° C.
- **Unlimited downloads resource cycles**. The best flash memory samples provide no more than 10^6 the data modification cycles. The FeRAM memory, used on three volt supply voltage range, can provide an almost unlimited number of circulations.
- **Low power consumption**. The FeRAM components are more economical not only in comparison with the static type of the memory, but also excel in this the flash memory. Economy of the FeRAM is based on the efficient architecture of the matrix array, the features of the technology and the process of circulation to the cell.
- **Energy consumption is the same in the reading and writing cycles.** In essence, it mince that the definition (reading) or modification (writing) of the polarity of the capacitor charge in a very short intervals of time (about 1 ns). In the storage mode the array of the FeRAM does not require the energy. It is consumed by only the control circuits of the framing and interface. The level of consumption by the FeRAM components with the series interface in the standby mode (waiting mode) is less than 1 mA. With the parallel interface the FeRAM is also more economical than the other technologies (15–20 mA).
- **High stability in operation mode**. The physical principle of storing information in electrically polarized material with a sufficiently wide hysteresis loop FeRAM provides high stability to external noises (first of all to the electromagnetic fields).

Thus the main advantages of the of nonvolatile memory of the FeRAM type used for many applications (the computer and office equipment, measuring equipment, motor transport, appliance electronics, telecommunication and communication) are low power, consumption, speed and nonvolatility. For example, the most mass measuring devices, which use the FeRAM memory, are electricity meters. The more than 30 million domestic and industrial electricity meters have produced in the world.

7.6 Nonvolatile random access memory CeRAM

The memory of the CeRAM type, which is also the resistive memory, uses the same transition metal oxide (TMO), for example, nickel oxide NiO, but unlike the ReRAM memory the conductive filaments do not use. In the CeRAM memory the quantum effects of the correlation of the electron position are observed from which it follows its name (CeRAM is the correlated electron RAM that is the memory with correlated electrons).

The active region of TMO, which separates the two conductive layers, is formed in the CeRAM structure. In the ReRAM memory the transition metal oxide takes up entirely all area between the metal layers

As is well known, the predominant model for describing ReRAM memory is the model of the conductive filaments whereby the thin oxide films obtained from the deposition, are insulators. According to this model (see section 1.3) the pulse of high voltage U_{set} is applied to the film and causes the formation of the filaments (electroforming). Then the transition metal oxide becomes the metal conducting the current through these filaments. If the voltage of the defined level U_{reset} is applied to the film, the filaments are destroyed by Joule heat caused by a large current and the oxide becomes an insulator again.

This process of the electroforming justifies the filamentary model.

Recently, researches consider some transition metal oxides which also exhibit the reliable resistance switching effect. In particular, it was shown that the nickel oxide NiO exhibits the stable unipolar properties at the switching from the state "setting" (SET) into the state "reset" (RESET), wherein the operating current is smallest.

In research laboratories the different physical mechanism of the formation of conducting and nonconducting states are researched. According to this approach the nickel oxide NiO can be produced in the primary state as the metal, which is achieved by means of alloying by the nickel carbonyl ligands.

Metal carbonyls are formed in the process when the carbon oxide combines with the metals, for example, the nickel carbonyl $Ni(CO)_4$. The chemical bonds in the molecules of the metal carbonyls are formed according to the donor-acceptor method by means of the unpaired electron pairs of CO molecule and free orbitals of

the excited metal atom. For example, the excited atom of the nickel has 4 unoccupied orbits, so the nickel carbonyl molecule has a composition corresponding to the $Ni(CO)_4$, Fig. 7.35.

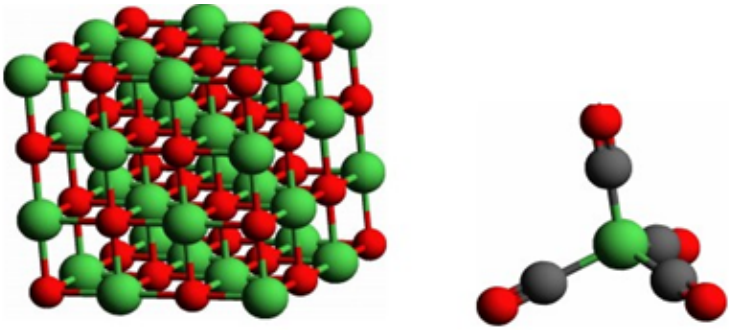

Fig. 7.35. The crystal structure of the nickel oxide $Ni(CO)_4$

According to the coordination theory explaining the properties and the structure of the complex compounds in the molecule of any such compound one of the ions, usually positively charged, occupies a central place and is called the central ion. Some number of the oppositely charged ions or electrically neutral molecules, called the ligands and forming the inner coordination sphere of the connection are located around the central ion in direct proximity (coordinately).

The rest ions, which do not place in the inner sphere, are at a more remote distance from the central ion, and form the outer coordination sphere. The number of ligands surrounding the central ion, is called the coordination number.

Thin films of NiO exhibit the reliable bistable resistive states in the absence of the electroforming and therefore a new model for the theoretical description, which differs from the filamentary model, is required.

The main states of the new model are based on the so-called Mott transitions, [53], [54].

The so-called Mott insulators that do not conduct electricity despite the band theory of solids exist among the crystalline dielectrics.

For example, the compound of NiO has one external electron on the nickel atom, but it is an insulator. In the proposed model it is explained by correlated arrangement of the electrons in the nodes of the crystal lattice.

Some Mott insulators with increasing the temperature become the conductive substances. This phenomenon is called the Mott transition.

The simplest theoretical justification for the behavior of Mott insulators and Mott transition was given in [54]. The behavior of the electrons is determined by two mechanisms:

- conductivity of the crystal is determined by the tunneling of the electron from the orbital of one atom on the orbital of another atom (the so-called "jump");
- coulomb repulsion of electrons prevents the electrical current and creates a high resistance of the crystal.

Depending on the external conditions one or the other mechanism prevails. It provides the respective transitions conductor-insulator and insulator-conductor.

Mott insulators are the crystals with the dielectric properties, the formation of which is not due to the influence of the periodic field of the crystal lattice (as in the conventional dielectrics or semiconductors such as Ge and Si), but with a strong electron-electron interaction. This state is realized if the characteristic energy of such interaction $U = \frac{e^2}{r_{\text{av}}}$ (r_{av} is the average distance between the electrons) will be greater than the average kinetic energy of the electrons which is defined by the width of the permitted band $W_{\text{k}} = \frac{h^2}{mr^2}$ (m is effective electron mass; r is the distance from the nucleus; h is Plank constant).

When $U < W_{\text{c}}$ then the simple band diagram of solid is suitable. The situation changes cardinally if $U > W_{\text{k}}$. The bond can be partially filled by the electrons, as in the metals, but the motion of the electrons needed for the charge transport, is weaken by the other electrons which are located on adjacent atoms. They repulse and "lock up" (localize) each electron on its atom and do the substance by the insulator. This is the case if the average distance between the electrons r_{av} more than the so-called Bohr radius, that is $r_{\text{av}} > r_0$. Bohr radius r_0 is the radius of the first (closest to the nucleus) Bohr orbit in the hydrogen atom, $r_0 = 0{,}53 \cdot 10^{-10}\,\text{m} = 0{,}53\,\overset{0}{\text{A}}$.

From a modern point of view Bohr's orbits had lost their original meaning, since, according to quantum mechanics the motion of an electron in an atom can not be regarded as a movement on the trajectory. Bohr's orbits characterize the region of space where the probability of finding an electron is a maximum.

A more precise analysis gives a criterion $\sqrt[3]{n}\, r_0 \approx 0{,}02$ where n is the electron concentration. At low concentration ($\sqrt[3]{n}\, r_0 < 0{,}02$) in an electrically neutral system the electrons and holes form bound states (the so-called excitons) and the substance deprived of the charge carriers, becomes nonconductive (an insulator). For larger concentration of the electrons ($\sqrt[3]{n}\, r_0 >> 0{,}02$) screening of the Coulomb interaction leads to the disappearance of the bound states and the transition insulator-metal (Mott transition) occurs.

It should be noted that there is another interpretation of the Mott insulator, which is based on the discrete model, describing the electrons moving from one lattice node to another one during the repulsion of two electrons at one node (the Hubbard model). Many compounds of the transition and rare-earth metals with partially filled internal *d*- or *f*-shells belong to Mott insulators.

Due to the small radius *d*- and *f*-orbitals their overlap is a little, and for them are easy carried out the condition $U > W_k$. In substances that are in the insulator phase the transition to the metallic state can occur at changing external conditions (pressure, temperature).

Thus, previously known more general band theories (the valence band and the conduction band) of the solid state did not take into account the interaction between the electrons that is the electrons are not correlated. This fact distinguishes a new type of the CeRAM memory, which takes into account the electron correlation, from the well-known the ReRAM memory.

One of the unique features of the CeRAM operation is the possibility of the oxidation and reduction reactions (losses and gains of the electron) at one lattice node. Let's consider current-voltage characteristic of the CeRAM memory cell, which shows a SET/RESET cycle, Fig. 7.36 (the theory is completely described in [28], [51]).

The work starts from the state of conductivity at low values of the voltages. If the voltage is increased (the current changes on the SET

curve) to 0.8 V, then the characteristic makes an instant jump to the insulator state, so that the structure has a high resistance (RESET).

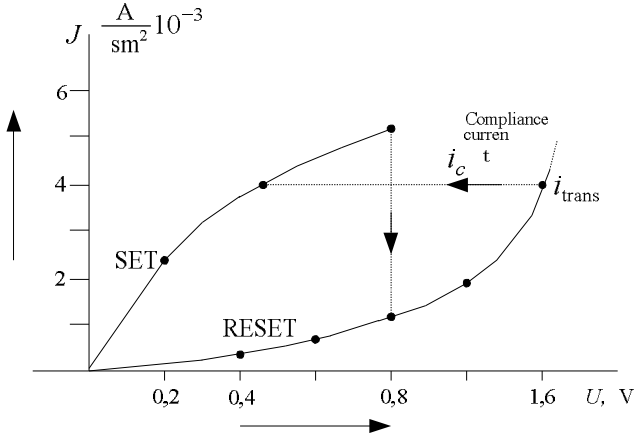

Fig. 7.36. Current-voltage characteristic of the CeRAM cell

To carry out the reading operation the current decreases to low values when the voltage decreases from 0.8 V in the insulator state. In this case the current is changed according to the RESET curve.

When the voltage increases from 1.6 V (RESET curve) the current begins to rise sharply to a value at which the transition occurs to the conducting state.

Thus, in order to write the isolated state (R_{Off} similar to the ReRAM) the voltage of 0.8 V is applied to the structure on NiO base. To write the conductive state (R_{On}) the voltage 1.6 V is applied to the structure. It does not require the electroforming operation and the thermodynamic phase transitions, as in conventional ReRAM. The switching speed of the CeRAM cells can reach several tens of femtoseconds (10^{-15} s), and the reading voltage is only about 0.1 – 0,2 V (see Fig. 7.36.). The memory state remains stable state even when it is heated up $400°\,\text{C}$.

The structure of the CeRAM memory contains three layers of the doped nickel oxide $Ni(CO)_4$, placed between two electrodes, Fig. 7.37.

The active region lies between two doped oxide films which are the buffer electrode. These two buffer films are heavily doped to obtain high conductivity and act as the matching electrodes.

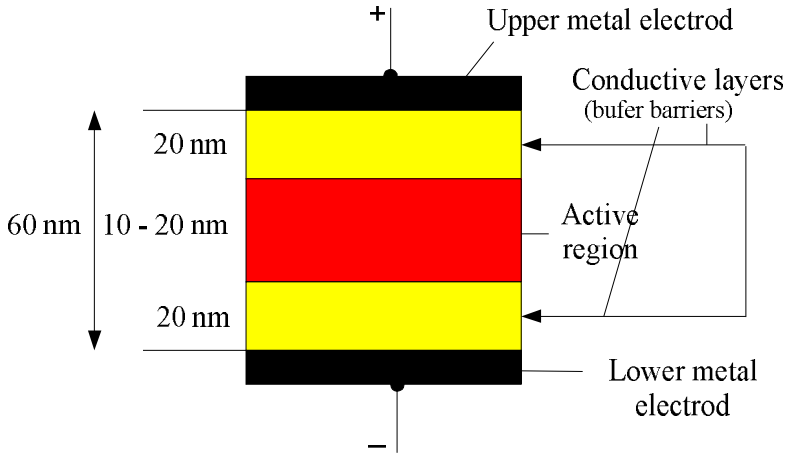

Fig. 7.37 The structure of the CeRAM memory cell

It is interest to compare the structures of the ReRAM and CeRAM, Fig. 7.38.

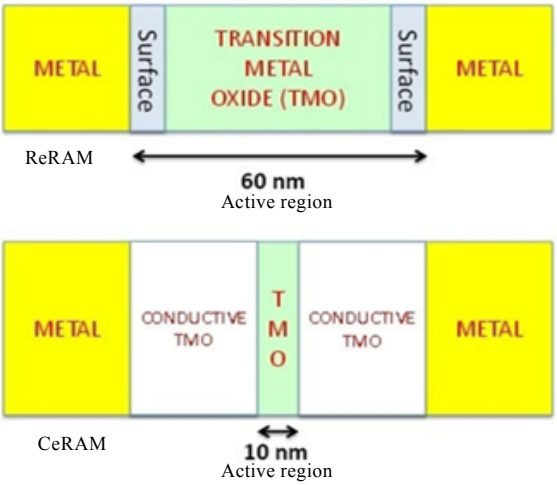

Fig. 7.38. Structures of the ReRAM and CeRAM

Active area also contains the nickel oxide, but with a lower level of the same doping. The transition metal-insulator-metal is carried out in the active region. In the active region each nickel ion can be regarded as a local switch "On" or "Off". In the buffer layer such switches are always in the state "On", Fig. 7.39.

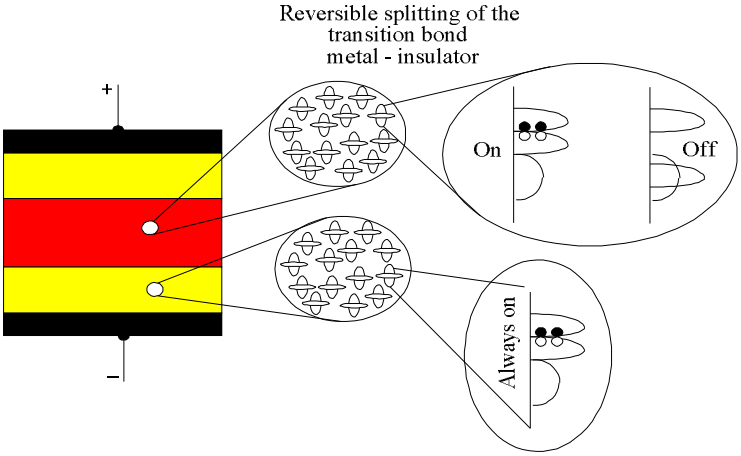

Fig. 7.39. The local zone structures for different states of the conductance

The functioning of the CeRAM memory cell is provided by the reversible splitting of the transition zone metal-insulator. In this case the band structure is a localized effect and should not be mixed up with the band structure of single-crystal silicon which is determined by the periodic structure of the lattice, a density of states of which can not be manipulated, [16].

The transition metal oxides have incomplete atomic shells 3*d* and 4*d*, which pass through the metal-insulator transition. The basis of operation of the cell is the splitting of the zone 3*d*8 of the conduction state on the zones 3*d*7 and 3*d*9 zone of the insulator state.

Let us consider the state of an electron in the many-electron atoms in more detail.

In many-electron systems not only the nucleus, but all the other electrons act on each electron. In this case the electron clouds of the individual electrons as if merge into one common many-electron “cloud”. The exact solution of the Schrödinger equation for such complex systems is usually unattainable.

If we assume that the electrons have the wave properties then **Schrodinger** suggested that the state of the moving electron should be described by the equation of the standing electromagnetic wave known in physics and electrical engineering:

$$\nabla\psi(x,y,z)+\left(\frac{2c}{r}-\lambda^2\right)\psi(x,y,z)=0.$$

Substituting in this equation instead of the wavelength of its value from the equation of de Broglie

$$\lambda=\frac{h}{mv},$$

we can get a new equation relating the energy of the electron with the spatial coordinates and the so-called wave function ψ. The function ψ corresponds to the amplitude of the three-dimensional wave process (ways of solving this complicated equation are considered in the courses of physics and physical chemistry).

Like amplitude of any wave process, it can assume both positive and negative values. The value ψ^2 is always positive, and the larger value ψ^2 in the area of the space, the higher the probability of finding an electron at this part of the space, defined as

$$\Delta P=\psi^2\Delta V,$$

where ΔV is some small volume (by analogy with the mathematical definition of probability

$$P\{a\le x\le b\}=F(a)-F(b)=\int_a^b f(x)dx,$$

where $f(x)$ is the probability density of the random variable (in the one-dimensional case)).

The study of the spectrums of the many-electron atoms has shown that in this case, the energy state of the electrons depends not only on the principal quantum number *n*, but also on the orbital quantum number *l*. This is due to the fact that the electron in the atom is attracted by the

nucleus and also feels the repulsion from the electrons located between this electron and the nucleus. The internal electronic layers as if form a screen that weakens the attraction of the electron to the nucleus (shielding the outer electron from the nuclear charge). The electrons with the different values of the orbital quantum number *l* are shielded inequality.

So in the nickel atom (ordinal (atomic) number is 28 with the electronic formula $1s^2 2s^2 2p^6 3s^2 3p^6 3d^8 4s^2$) closest to the nucleus *K*-and *L*-layers are occupied by 10 electrons. The *M*-layer has 16 electrons, while sublayers *s* and *p* are filled, and sublayer *d* has 8 electrons and not completely filled, and finally in the *N* layer ($n = 4$) sublayer *s* is filled by 2 electrons. The maximum number of the electrons in the sublayer *d*, which consists of 5 orbitals ($2l + 1$) is equal to $n = 2(2l + 1) = 10$.

In accordance with the radial distribution of the probability $4\pi r^2 \psi^2$ (*r* is the distance from the nucleus) we can determine the extent of shielding. For example, for a natrium atom (formula $1s^2 2s^2 2p^6 3s^1$), the probability distribution is shown in Fig. 7.40.

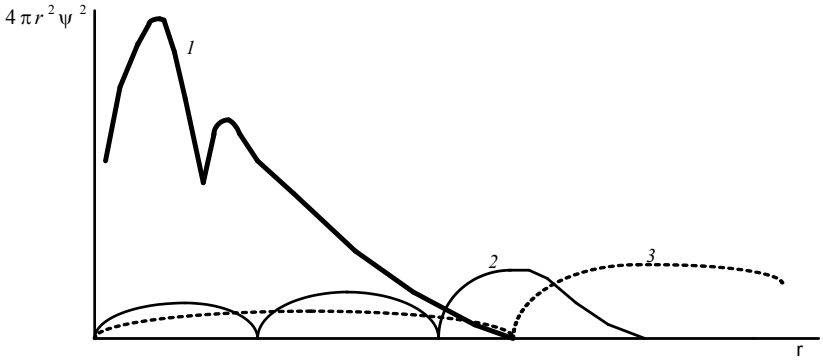

Fig. 7.40. The probability distribution of the electron "clouds"

The curve *1* corresponds to a probability distribution for the total electron "cloud" of ten "inner" electrons of the natrium atom. The first maximum corresponds to *K*-layer, and the second one corresponds to *L*-layer. The curve *2* corresponds to 3*s*-electron, and the curve *3* corresponds to 3*p*-electron.

It is obvious that prevalent part of the outer electron cloud of the natrium atom is located outside the area occupied by the inner electrons,

and therefore is shielded weaker. As it follows from Fig. 7.39, the electron cloud of the 3*s*-electron in the greater extent penetrates into the area occupied by electrons *K*-and *L*-layers, and therefore it is shielded weaker than the electrons of the area of 3*p*-electron. Consequently, the electron in the state 3*s* will be more attracted to the nucleus and have a lower energy than the electron in the state $3p$.

The electron cloud of the 3*d*-orbital is almost entirely located outside the area occupied by the internal electrons is shielded in the greatest extent and most weakly attracted to the nucleus. That is why the stable state of the natrium atom corresponds to the placement of a single outer electron on the orbital 3*s*.

Thus, in many-electron atoms, the electron energy depends not only on the principal quantum number, but also on the orbital quantum number. The principal quantum number determines only a certain energy band within which the precise value of the electron energy is determined by the value *l*. As a result the increase of the energy according to the energy sublevels occurs in the following order:

$$1s < 2s < 2p < 3s < 3p < 4s < 3d < 4p < 5s < 4d < 5p < 6s < 5d$$

$$4f < 6p < 7s < 6d$$

$$5f < 7p.$$

Thus, the relationship between the energy of the Coulomb interaction $U = \frac{e^2}{r_{\text{av}}}$ and the kinetic energy of electrons $W_{\text{k}} = \frac{h^2}{mr^2}$, where r_{av} is the average distance between the electrons and *r* is the distance from the nucleus of the atom (radius of the orbit). The relationship between these energies determines the respective transitions metal-insulator-metal.

The schematic difference between the states metal-insulator at the level of the nickel ions is shown in.Fig. 7.41.

If the inequality $U < W_{\text{k}}$ is fulfilled, then the material has the conducting state. The charge carriers can move freely in the local conducting zone of the material, Fig. 7.41*a*. If the inequality $U > W_{\text{k}}$ is fulfilled then the charge carriers are localized, that is the Coulomb forces of the repulsion prevail. These forces inhibit the movement of the carriers, and the material becomes an insulator (electrons as if "frozen" in the crystal lattice), Fig. 7.41*b*.

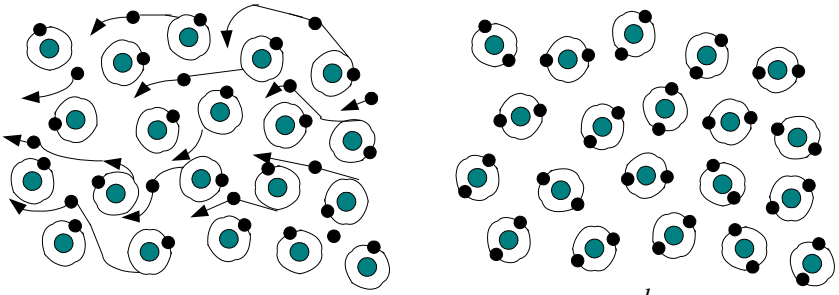

Fig. 7.41. The schematic difference between the states metal-insulator at the level of the nickel ions

7.7 Magnetic track random access memory MRM (DWM)

As noted in section 7.1, now the digital information is stored on the two main types of the storage devices: the magnetic disks (hard disk drive, HDD) and the solid state drives (solid state drive, SDD). Since the basis of the HDD mechanism is the rotating magnetic disk, then it decreases the data storage reliability and the access to them is rather slow (about 5 ms).

The SDD devices do not have moving parts (they include RAM and the flash memory) and the data access time is decreased to 5 ns (10^6 times less), but the cost of the storage of one bit is 100 times higher than for the HDD. Both types of the drives are constructed according to a two-dimensional technology, so that the increase their capacity can only take place by decreasing the size of the elementary cells.

In addition to the data storage technologies considered above, the new technology, which is based on spintronic effects is tested now in one of the research laboratories (Almaden Research Center of IBM, USA). This technology uses the spin current to move the nanoscale magnetic objects, namely the domain walls along some the conductive structure (for example, nanowires). The nanowire is made from the iron-nickel alloy of about 10 microns length and 150 nanometers width.

Under the influence of the spin current the domain walls are moved the one after the other on the fixed conductive structure (as the runners move on the sprint track). Hence the name of this technology is the magnetic racetrack memory, MRM (Track Memory). In the periodicals another name is encountered, namely the domain-wall memory (DWM), [59].

It is obvious that a single magnetic domain can be used as an elementary carrier of the information. Thus it is possible to achieve a very high density of its placement.

Ferromagnetics are the substances having a very high relative permeability ($\mu \approx 10^2 - 10^5$) of the fact that the magnetic moments of atoms and electrons spontaneously tend to orient in the same direction as it is energetically favorably for them

The random thermal motion of the particles counteracts this orientation, but such spontaneous magnetization is "frozen" at a temperature lower than the so-called "Curie point". In this case the domains re formed as the microscopic regions of the uniform magnetization, which under the influence of the external magnetic field are remagnetized as a whole.

The domain sizes depend on many factors and are in the range from 10 nm to 100 μm. The magnetic domains which are greater than 1 micron can be observed with an optical microscope. To observe and study the behavior of the nanosize domains the electron microscopy, the atomic force and raster tunnel microscopes are used.

The neighboring magnetic domains are separated by the **domain walls** which are represented by the ultrathin intermediate layers in which the magnetization vector smoothly changes its direction from the orientation in one neighboring domain to the orientation in other one (the electron spins smoothly rotate).

In the absence of an external magnetic field ($H = 0$), the domain magnetization directions are random so that the total magnetic moment of the ferromagnetic material consisting of a large number of microcrystals (crystal "grain") and domains is equal to zero.

When the external magnetic field H is present then the forces act on the magnetic moments of the domains tending to rotate them in the direction of the field, which leads to a considerable increase of the total magnetic field.

If a weak magnetic field acts then the magnetic moments of the domains are only partially rotated in the direction of an external magnetic field, and this change is a reversible process, that is if the external magnetic field is taken off, then the magnetic moments of the domains are returned into reset state. In this range, the relationship between B and H is proportional, that is $B = \mu H$.

In stronger magnetic fields the domain walls begin to shift, thereby the domains whose magnetic moments are oriented in the direction of the external field, increase in volume, some domains are combined and the volume of the other domains is reduced. The process becomes irreversible: if the external magnetic field is turned off, then in the ferromagnetic material is observed the residual magnetization. The increase of the magnetic induction B with increasing H becomes slower, the linearity of the dependency is no observed. In a sufficiently strong external magnetic field, the magnetic moments of all domains are oriented in one direction and a further increase of the magnetic induction B is stopped (is saturated). When the intensity of the external magnetic field decreases and falls down to zero, the ferromagnetic material remains magnetization in the same direction with a residual induction value B_r. When the external magnetic field H increases in the opposite direction then the value of the former magnetization decreases to zero, and then ferromagnetic is remagnetized.

The intensity of the external magnetic field needed to demagnetize the ferromagnetic material is called the coercive force.

In the cyclic variation of the external magnetic field, the magnetization curve is represented by the closed line which is symmetrical about the origin. Such curve is called the hysteresis loop.

The main requirements to the ferromagnetic material of the thin films are the following. These materials must provide high induction of the saturation B_s and a large coercive force H_c. The induction of the saturation depends on the composition of the ferromagnetic and influences on the signal that is read. The great coercive force prevents the demagnetization of the elements under the action of writing and reading currents which flow in the neighboring cells. The coercive force depends on the composition of the film and its thickness, and also on the deposition conditions, which define the size of the grain.

The peculiarity of the magnetic properties of thin films is determined primarily by the fact that their linear dimensions in the plane of the film are much greater than the thickness. Consequently, the demagnetizing factor in the direction of the normal to the plane of the film is much higher (about 10^5 times) than in its plane.

The domain boundaries in thin films substantially differ from the so-called Bloch walls, which are formed in the massive materials. The simplest type of the wall in the thin film is the wall of Noel, in the middle of which the spins are smoothly rotate around the axis (from the direction in the given domain to the direction in the neighboring domain), which lies in the plane of the wall.

The sizes and the shape of the domains in the plane of the film depend on the deposition conditions and the film thickness. If the constant magnetic field is applied to the film in the process of deposition in the substrate plane then the large domains are formed and located along the field. The magnetic properties of the film get the respective anisotropy. This means that the film has a predominant direction of magnetization (the axis of easy magnetization). This direction is in the plane of the film and coincides with the direction of the external field.

In particular, the thin films of the permalloy (an alloy of the nickel and iron with a small amount of copper, chromium and molybdenum) can be manufactured so that their magnetic properties will differ in the different directions. In the direction of the hard magnetization axis (HMA) the hysteresis loop is almost entirely absent, and under the right angle to it the hysteresis loop is almost complete in the direction of the easy magnetization axis (EMA).

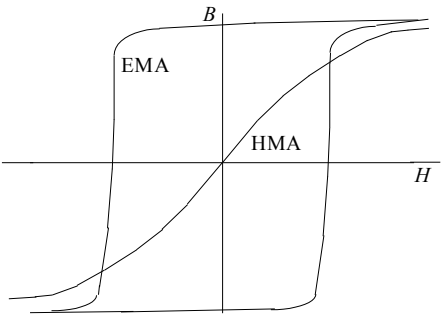

When the film thickness decreases to a few hundred Angstroms the magnetic film becomes the single-domain magnetic film with respect to its thickness. In this case a little time switching films ($\sim 10^{-9}$ s) and high operation speed of the magnetic elements may be provided.

Let's consider the processes of the spin-transport magnetization reversal (STMR) in the long ferromagnetic nanowire with a small cross-section (for example, 30 x 10 nm), in which the region of spontaneous magnetization (domains) with different orientations are formed, Fig. 7.42.

The arrows indicate the direction of local magnetization of the material. Domains are separated by the walls in which the magnetization is reconstructed from the one direction to another. Three domains separated by two domain walls of the opposite polarity are shown in Fig. 7.42. The current passing through the magnetized material becomes the spin-polarized current and begins to turn out the "small magnets" in one direction or another. As a result of such turn the domain wall as if shifts and the direction of the shift of all walls is the same.

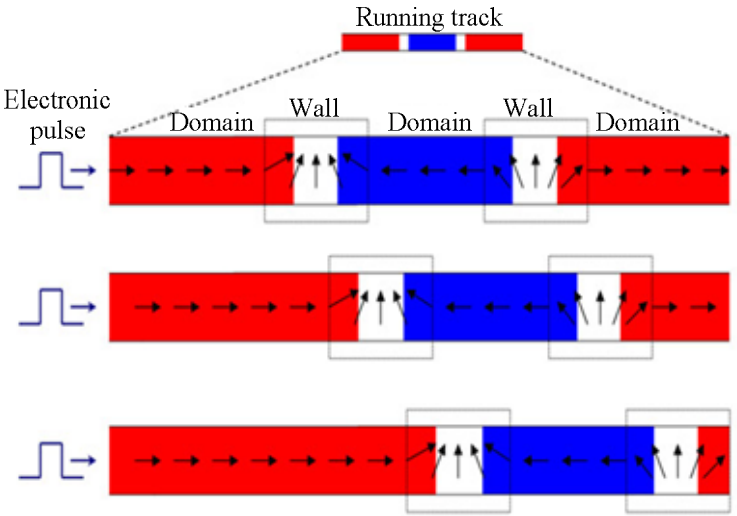

Fig. 7.42. Movement of the domain walls under the acting of the spin-polarized electric current

If the conductor has a sequence of the domain walls, then under the acting of the spin-polarized current, these walls will move, but the conductor remains in the place.

The spin-polarized electrical current is a current when both the electric charge and the spin are transferred through the conductor simultaneously. This current is characterized by the "degree of the spin polarization" (or simply "degree of the polarization") P:

$$P = \frac{i_\uparrow - i_\downarrow}{i_\uparrow + i_\downarrow} 100,$$

where $i_\uparrow$ is the component of the electric current that transports the electrons with the spin oriented "up" (in the direction of the existing magnetic field), $i_\downarrow$ is the component of the electric current that transports electrons with the spin "down" (opposite to the magnetic field), $i = i_\uparrow + i_\downarrow$ is the total electric current.

Obviously, the degree of the polarization may be either positive or negative. In the ferromagnetic metals such as the iron, the cobalt and the nickel the degree of the polarization is positive and at the room temperature equals 10 – 15 %. The high degree of the polarization allows more precisely to determine the value of the spin current in order to avoid errors in subsequent processing of information [31] and [32].

Over 100 years the electronics dealt only with the non-polarized electrical currents, for which $P = 0$.

To obtain a sufficiently a great value of the current is necessary to polarize the spins that is to put in order in one direction. It is important that also the spin lifetime (the time during which the spin direction does not change) was large enough to transfer the spin on the needed distance. For example, the flux of the electrons at the input of the ferromagnetic is not polarized, but it becomes polarized after passing through the ferromagnetic layer that is it becomes by the spin current.

Spin-transport magnetization reversal. When the spin-polarized electric current flows then the transfer of the spins occurs at the same time. It means that then the transfer of the magnetization

occurs as well. Then it is possible to exist the magnetization reversal of the ferromagnetic layer by means of the transmission of the spin-polarized current.

The scheme of such magnetization reversal is shown in Fig. 7.43.

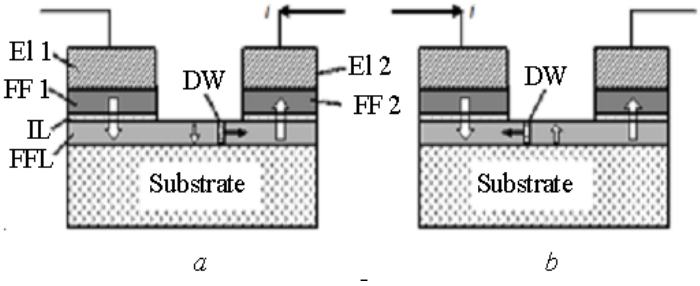

Fig. 7.43. Process of the spin-transport magnetization reversal

The region of the fixed ferromagnetic layer (FF1) is permanently magnetized vertically downward and to the right the region (FF2) is magnetized vertically upward (directions of magnetization are indicated by arrows). The areas of the free ferromagnetic layer (FFL) are located beneath and magnetized respectively. Between the free and the fixed layers is located the intermediate layer (IL). All layers are electrically conductive. Above the regions of the fixed layers the electrodes are formed (El1 and El2).

If the electric current *i* flows from the right to the left from the electrode El2 (see Fig. 7.43*a*), then the electrons in the free layer move from the right to the left.

Because most of them, leaving the layer FF1 has the spin down, then they carry downward magnetic moment, as a result, the area of the free layer between FF1 and FF2 is magnetized downward. Physically, it looks like the movement to the right of the domain wall DW.

If the electric current i flows from the left to the right from the electrode El1 (see Fig. 7.43*b*), then the electrons in the free layer move from the right to the left.

Because most of them has the spin up, then they carry upward magnetic moment, as a result, the area of the free layer is magnetized upward as well. Physically, it looks like the movement to the left of the domain wall DW.

This method of writing the information in the magnetic memory cell is called the spin-transport magnetization reversal (STMR). Such way allows to essentially decrease the write current in the MRAM memory and significantly reduce the area of the magnetoresistive cells.

In general, the motionless conductor represents a memory cell that can be installed either vertically or horizontally, Fig. 7.44.

The individual reading and writing elements that are based on the magnetic tunnel junction (see MRAM-memory), which is one of the basic elements of spintronics are set for each cell. The current due to the quantum phenomenon of the tunneling is very sensitive to the direction of the magnetization of the running track area.

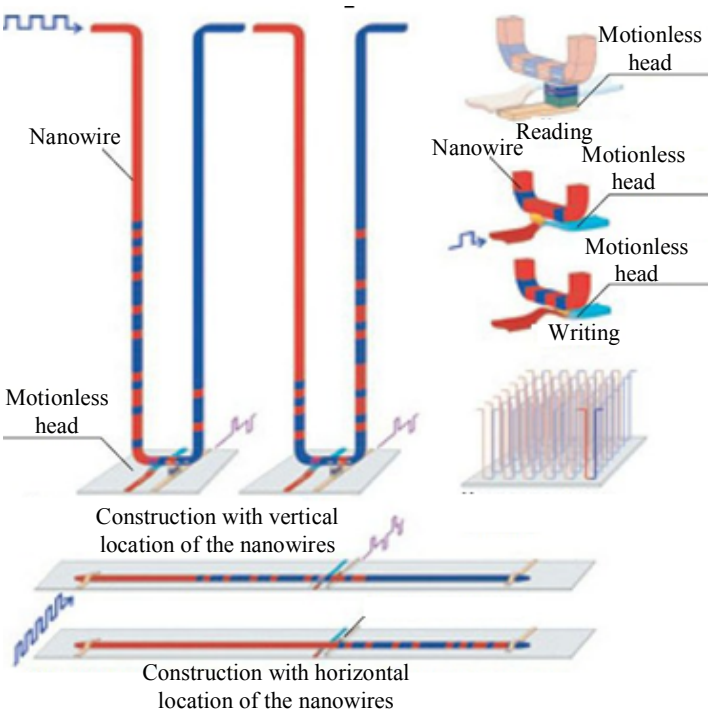

Fig. 7.44. The ways of the nanowire location

If the sequence of the pulses of the spin polarized current is applied to the running track then the domains will come in motion, and the read-

ing element defines the sequence of "0" and "1" measuring the tunnel junction resistance change

The writing of the information is carried out using the nanowire located across the running track, Figs 7.45 and 7.46.

The pulses of the current of the writing element at certain time moments generate and shift the domain walls on the running track in the needed place, in other words rebuild the domain structure.

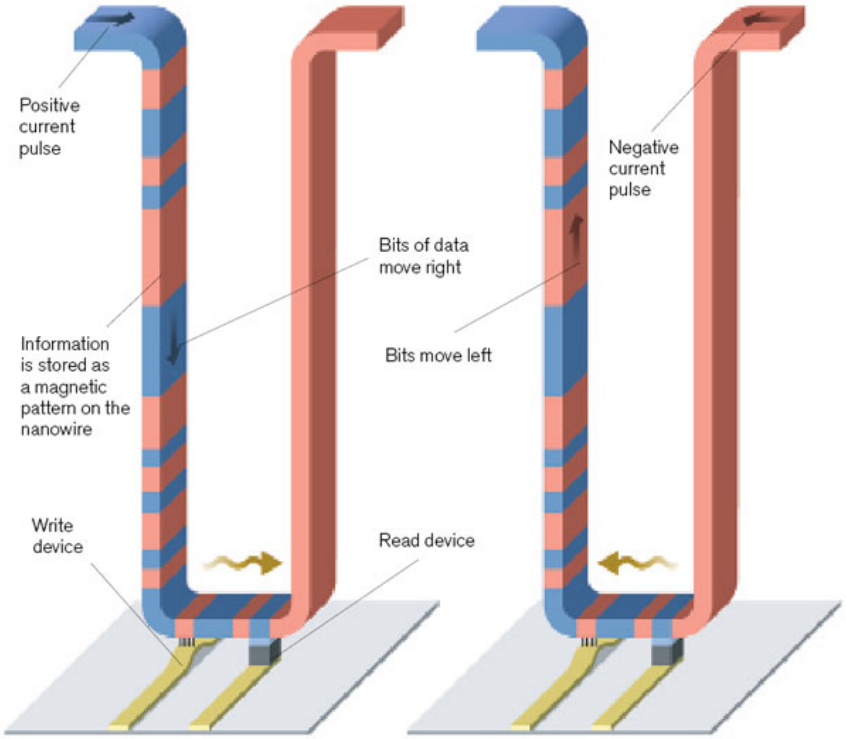

Fig. 7.45. Writing and reading operations used in the vertical location of the nanowires

Let's consider in more detail the writing and reading units of the information in / from the ferromagnetic nanowire, in which the magnetic domains are moved, Fig. 7.47 *b* and *c*.

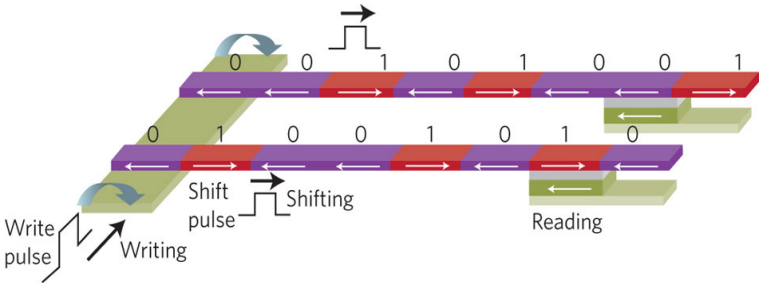

Fig. 7.46. Writing and reading operations used in the horizontal location of the nanowires

The ferromagnetic nanowire *2* is formed on the surface of the wafer *1*. To write the information (Fig. 7.47*b*) the conductive nanowire *3* (for example, from the gold) or the carbon nanotube is laid across the ferromagnetic conductor. If the pulse of the electric current passes through it, then the strong enough magnetic field *4* occurs to magnetize the region of the ferromagnetic conductor in one direction or another (depending on the direction of the writing current).

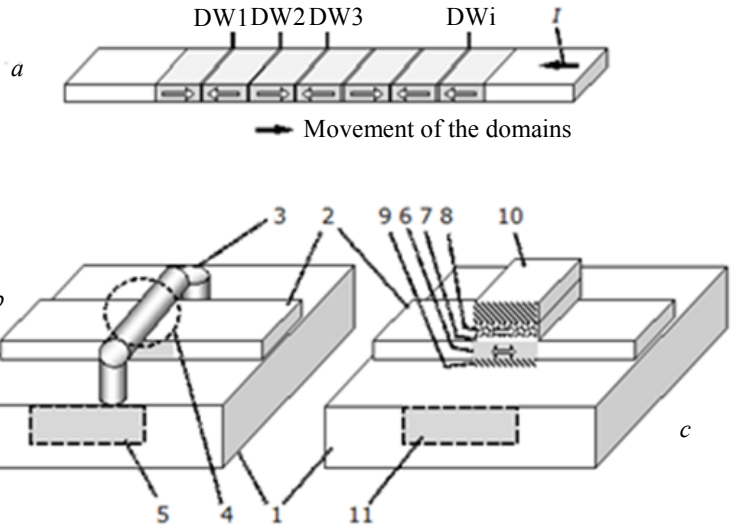

Fig. 7.47. Movement of the domains (*a*), writing (*b*) and reading units (*c*)

The electronic scheme *5* is beforehand formed inside the semiconductor wafer *1*. This scheme generates and feeds the required current pulse of the given direction into nanowire *3* in a certain time moment.

To read the written information (Fig. 7.47*c*) the magnetoresistive reading element is formed above the nanowire 2 which consists of the superthin tunnel layer *7*, the fixed ferromagnetic layer *8* and the metal electrodes *9* and *10*. Depending on the direction of the magnetization of the domain *6*, the electrical resistance of the element (structure with the magnetic tunnel junction) will be smaller or larger. The electronic circuit *11* generates the respective reading signals. This scheme is beforehand formed within the semiconductor wafer *2*.

The memory with the three-dimensional storage of data may be created with a vertical arrangement of the nanowires (cells). In particular, the researchers have demonstrated the functionality of reading and writing of the data on the array containing 256 nanowire columns.

If few bits of the information (no one bit) will be written on each vertical nanowire (cell) then the memory, created using this technology can surpass all known information carriers with respect to the writing density. IBM's developers have proposed such three-dimensional organization of the track memory, Fig. 7.48.

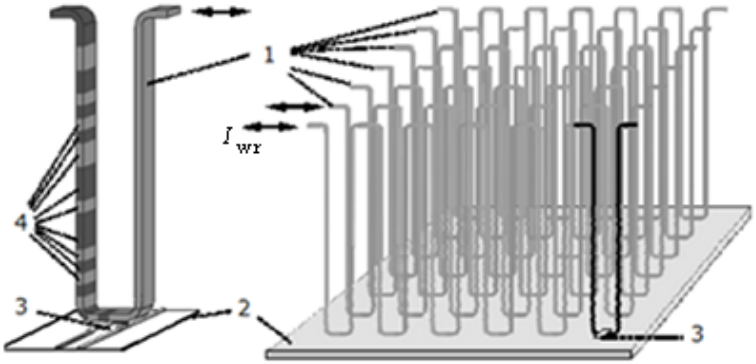

Fig. 7.48. The organization of the three-dimensional memory

The nanowires *1* from the ferromagnetic (for example, the permalloy or the alloy FeCo) of the *U*-shaped form of the thickness less than 100 nm and the height of 20–40 micrometers are vertically set on the surface of the silicon wafer *2*, in which the electronic schemes of the

memory control are formed. The components of writing and reading information *3* are formed near the "bottom" of each nanowire. In the half of each nanowire 75–280 domains *4*, which store 64–256 bits of the information, can be written.

The electrical current pulses of the overwriting I_{wr} of the respective direction shift the written domains from one half to the other and vice versa during 100–200 ns. The electronic control circuits allow to address to any nanowire and to read from it or write to it all 64–256 bits of the information during 150–300 ns.

The vertical arrangement of the ferromagnetic nanowires provides the information writing density which is much higher than in other types of the nonvolatile semiconductor memory.

The most important shortcoming of the track memory is that the electric current I_{wr} required for moving the domains has a sufficiently great value. Due to the Joule heat the ferromagnetic nanowire is quite strongly heated and as a result the reliability of the storage of the information in the domain of small size decreases.

Thus, under the influence of the electric current, all magnetic domains in the ferromagnetic nanowire are moved synchronously from the left to the right, if the electric current flows from the right to the left along the conductor (conduction electrons in this case will move from the left to the right). Accordingly, when the current is passed from the left to the right, all the magnetic domains are moved synchronously from the right to the left. This means that magnetic domains can be moved along the ferromagnetic nanowire forward and backward. It allows to send certain data area just under the writing or the reading elements.

It should be noted that the nanowire and all atoms therein remain motionless. The state of the magnetization moves only. At the same time the atomic structure of the nanowire does not change, all manipulations are made at the level of the elementary particles.

One of the serious shortcomings in the development of the tracking technology was very high current density. The studies have shown that the critical current density and the speed of the movement of the domain walls and therefore the speed of the movement of the domains depend on the material from which the nanowire is made, on its geometry and on the conditions at the boundaries. The critical current density is 10^{11}–10^{14} A/m^2, that is 0,1–100 μA/nm^2.

The domain movement speed in this case is 5–500 m/s. In particular, to move the domains in the nanowire made from the permalloy of 30 x 10 nm section it is required to pass the electric current of about 30 microamperes (which is quite a large quantity in order to "push" the domain walls). In this case the movement speed is 100–500 m/s. This difficulty could be avoided by replacing one powerful energy pulse by the series of weaker pulses, the duration of which corresponds to the frequency domain oscillations in the nanowire (resonant amplification).

7.8 Nonvolatile random access memory NRAM

The nonvolatile memory NRAM type (Nantero RAM, Nantero is a company engaged in the development of the electronic devices and the respective technologies) is based on the use of the thin films from the so-called carbon nanotubes (Carbon NanoTube, CNT), Fig. 7.49.

Carbon nanotubes have the unique structural and electrical properties, which make the created memory by one of the main contenders for the next generation of the super operating speed devices of the information storage having ultra-high density of the placement with very low energy consumption.

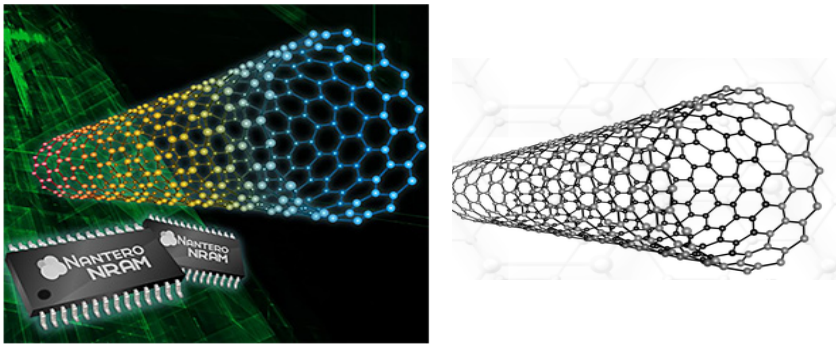

Fig. 7.49. The carbon nanotubes obtained with the help of the respective nanotechnologies

A carbon nanotube is a tiny cylinder of about 2 nm in the diameter, which is 50 times stronger than the steel and has the best thermal and electrical properties compared in comparison with other materials used for these purposes.

The image of the film from the carbon nanotubes (in the cross-section from up to down), obtained with the help of the scanning electron microscope is shown in Fig. 7.50.

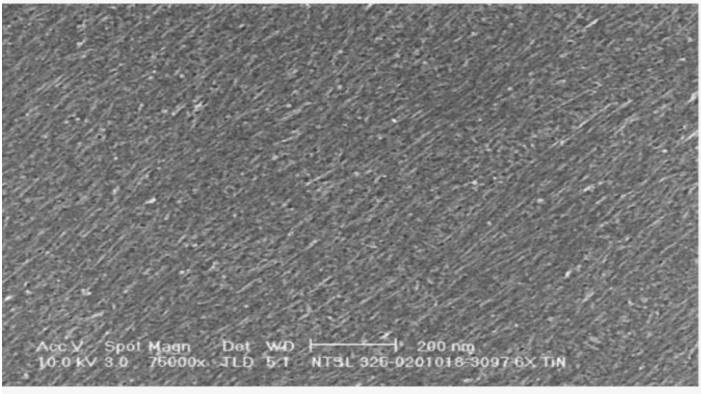

Fig. 7.50. The image of the film from the carbon nanotubes

The researchers from the Nantero Company consider that the NRAM can be used as a universal memory for storing information replacing DRAM and SRAM memory and a solid-state flash memory (SSD) as well.

The NRAM memory cell consists of the thin film of the matrix of the carbon nanotubes and two metal electrodes between which it is placed.

The recent studies have shown that the basic operation of the SET and RESET are possible under the action of the voltage pulses with the duration which is less than 20 picoseconds (20×10^{-12} s) with the current consumption below 20 microamperes, Fig. 7.51.

According to the Nantero Company, the memory cell can potentially store multiple bits of the information. The number of the overwriting cycles (SET / RESET) reaches 10^{11}, which significantly exceeds the possibility of other memory types (for example, the number of cycles for the DRAM corresponds to from 10^4 to 10^6).

Besides, the NRAM cells do not consume the energy in the "stand-by" mode and in the writing mode they consume the energy per bit 160 times less than the flash memory, have high resistibility to the environmental factors (they sustain heating up to 300° C, can operate at a radiation , vibration and in the strong magnetic fields without loss of the information).

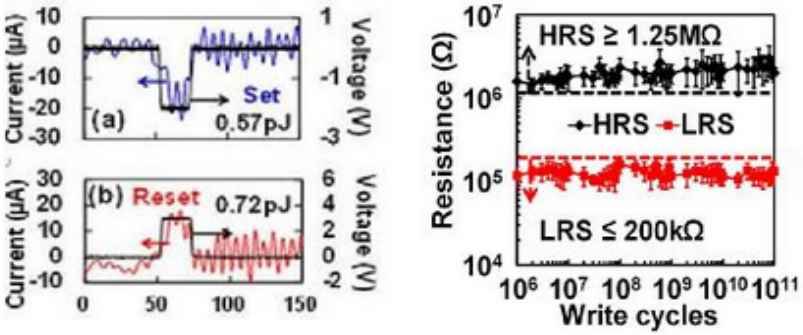

Fig. 7.51. The dependency of the consumed current from the applied voltage (*a*); the dependency of the memory cell resistance in the states with high resistance (HRS) and low resistance (LRS) from the number of the overwriting cycles (*b*)

Further improvement of the memory will be based on 10 nm - technology to create the superdense terabit arrays.

Operation of the NRAM cell is as follows.

When the voltage is applied to the cell, a great number of the rod-shaped carbon nanotubes which are separated from each other in the initial state, make contact, as Van der Waals forces cause them to "stick" to each other. Consequently, the number of conductive paths between the electrodes increases (the nanotubes are conductors) and the resistance of the structure significantly decreases (some analogy with the formation of the filamentary channels in the ReRAM memory). The pulse of the voltage RESET of other polarity is used to break the bonds and return the matrix of the nanotubes to the state with high resistance (HRS), Fig. 7.52.

Obviously, the NRAM memory type acts as the resistive nonvolatile random access memory. In both states, the nanotubes are stable. It allows to use this mechanism as the memory. In the disconnected state the mechanical deformation of the tubes is low, so they naturally remain the open state, thereby "memorizing" the state "0". When the tubes are attracted by applying to the upper electrode of the respective voltage pulse, then the nanotubes get the mechanical deformation due to the Van der Waals forces and remain this state thereby "memorizing" the state "1". Both states, as already was noted, are quite stable to the external

influences, such as radiation, which can erase or damage the data in the conventional DRAM memory.

The carbon nanotubes of high purity with a very small amount of the impurities are created by the use of the special nanotechnology, but the cost of this process is not much more expensive than in the production of the semiconductors. It means that the basic process of creating NRAM is not too complicated and does not require any additional equipment to that which is used in manufacturing CMOS devices.

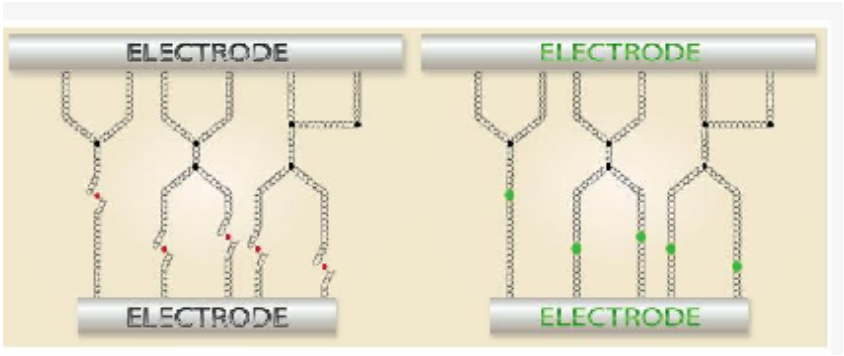

a *b*

Fig. 7.52. The functioning diagram of the NRAM memory cell for the disconnection of the nanotubes (*a*) and their connection (*b*)

The scheme of the NRAM cell with the corresponding CMOS transistors of the choice and the image of the cell in cross section, obtained with a scanning electron microscope are shown in Fig. 7.53.

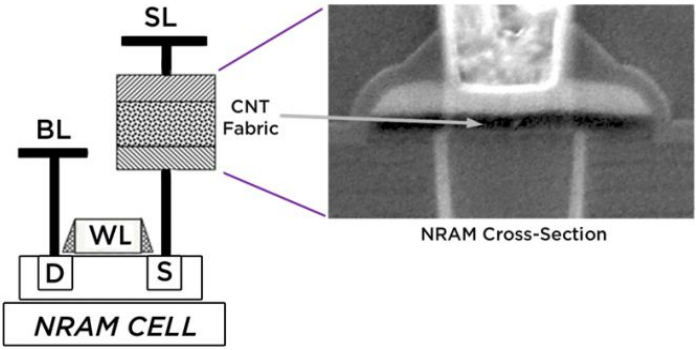

Fig. 7.53. The structure of the NRAM cell and the image of its cross-section

Note that NRAM memory has a density of the cell placement which is not less than for the DRAM memory. However, there is a minimum size at which the DRAM chips can be created, below which the charge will have enough small value and the cell will not be able to save it for reading.

Obviously, the NRAM memory is limited only by the modern technological achievements in the lithography. In future the NRAM memory can reach higher density in comparison with DRAM memory.

Unlike the DRAM memory type the considered memory type does not require the energy for updating the data. The additional power required for writing information is much lower than for the DRAM memory, which accumulates the charge that on the plates of the capacitor. Theoretically the NRAM memory can achieve productivity of the SRAM memory, which is faster than DRAM, but has a much lower density of the placement.

7.9 MRAM memory with the use of the spin-transport remagnetization

To improve the characteristics of the magnetoresistive memory the vertical magnetization of the ferromagnetic layers with writing information by the spin-transport magnetization reversal (STMR) was proposed. The structural diagram of the memory cell is shown in Fig. 7.54.

Operation of the cell is carried out as following.

Let the "free" (storage element) ferromagnetic element (FFE) is magnetized downwards (shown by the arrow), the electric resistance of the magnetoresistive cell is sufficiently large (the state "1").

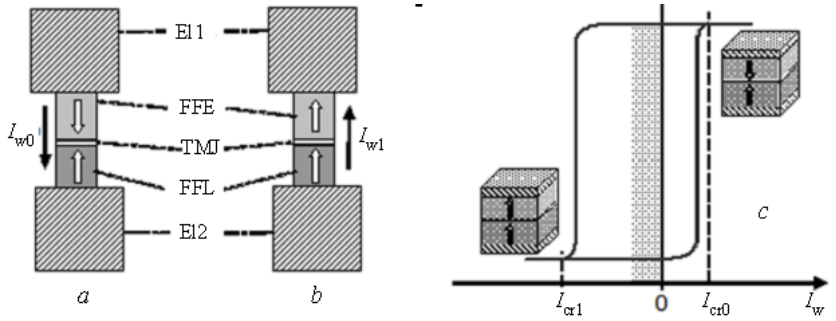

Fig. 7.54. The structural diagram of the memory cell

If the electric current I_{w0} exceeding a certain critical value I_{cr0} (Fig. 7.54*a*), flows through the cell then the electrons leaving from the "fixed" ferromagnetic element (FFL), carry up the magnetic moment oriented upwards. As a result, FFE is magnetized reversal in the state "0". When the value of the current is sufficient magnetization reversal occurs at the time of the order of 1ns.

The current I_{w0} flowing through the cell, which is already in the "0" state, does not change the state of the cell, since the magnetic moments in the FFE is already oriented upward.

To write "1" in the memory cell which is in the "0" state, it is necessary to pass the current I_{w1} through it, (Fig. 7.54*b*). The electrons leaving from the metal electrode El1 have the magnetic moments oriented both upward and downward. The electrons with the magnetic moment oriented upwards, easily pass through the magnetic tunnel junction (TMJ), and the electrons with the magnetic moment oriented downward, are accumulated. If their concentration is sufficient, the FFE is remagnetized in the state "1".

The current I_{w1} flowing through the cell, which is already in the "1" state, does not change the state of the cell.

The dependence of the electrical resistance value of the magnetoresistive cells from the electric current passing through it is shown in Fig. 7.54*c*.

As can be seen from the graph, the dependency is asymmetrical. It is explained by the following fact. The electrons with the magnetic moment oriented upwards are used for remagnetization of the cell in the state of "1". The number of these electrons constitutes the majority in the FFL, and to reverse the magnetization in the state "0" the electrons with a magnetic moment oriented downward are used. Such electrons are a minority in the FFE.

Thus, the critical current value of the remagnetization I_{cr1} of the cell in the state of "1" is several times greater than the critical current value of the remagnetization I_{cr0} in the state of "0".

It should be noted that the critical current value for the remagnetization by STMR relatively rapidly decreases with decreasing cell sizes. In particular, when the cell sizes are less than 300 nm, the critical current value becomes smaller than the electric current to be supplied to the address and the data buses to remagnetize the storage element by the total magnetic field of the mentioned currents.

The area of the current values used for reading information from the memory cell is shown in Fig. 7.54*c*.

The values of these currents are sufficient to determine the resistance of the cell (great or low for reading states "1" and "0"). However, it is not enough for the remagnetization.

The transition to the vertical magnetization (see Fig. 7.54) to write the information by the method STMR allows significantly to decrease the memory cell area and therefore to increase the amount of the information in a single chip. In this case the write time of the information is decreased and the costs of the energy on the writing are reduced to the value of about 1 pJ/bit.

The considered variant of the writing of the information by the method of the STMR is considered as the "second generation" of the magnetoresistive memory. In the periodicals such memory is called STT MRAM (spin-torque-transfer MRAM, spin-MRAM).

In some ways of the MRAM construction the local momentary heating of the memory cell during writing is used. In this case the size of such cell can be reduced up to 10 nm, so that the cell area is determined only by the switch transistor.

The time reading information in the ultra fast variants is reduced to 300 ps (0.3 ns). This memory is referred to as STT + TA MRAM (STT + Thermally assisted MRAM) or TA + STT MRAM.

7.10 Comparison and perspectives

Very significant changes in the field of the data storage technology have been occurred during just a few decades, especially with the development of the flash memory. The next generation of the memory devices technology will use the new materials to provide the access time of a few nanoseconds or less. And today we have many contenders on the title of "next generation technologies".

• **MRAM memory**. This is the random-access memory that does not store the information in the form of the electric charges or currents. The information stores in the form of the magnetic moments by means of the respective memory magnetic element. The reading of the information is carried out by measuring the electrical resistance of the cell. Due to the effect of the tunnel magnetoresistance, the electrical resistance of the cell varies depending on the mutual orientation of the magnetizations in

the layers. The resistance of the cell is determined by measuring the magnitude of the flowing current. As a rule, the same orientation of the magnetization in the layers of the element is interpreted as "0", and the opposite direction of the magnetization of the layers, characterized by a high resistance of the element is interpreted as "1".

One of the shortcomings of the memory is that the induced magnetic field may overlap the adjacent cells on the small area if the sizes of the chips will reduce. As a result it leads to the possible errors of the writing. But IBM researchers have demonstrated the MRAM devices with the access time about 2 ns, what is much better than most "advanced" DRAM, built on the latest technological processes. The advantages in comparison with the flash memory are more significant.

• **FeRAM memory**. This type of memory is similar to the DRAM, but it uses the ferroelectric layer instead of the dielectric layer to provide the energy independence and have the same functionality as the flash memory.

Among the advantages of the FeRAM with respect to the flash memory we may note the low power consumption, more fast the writing of the information and the more great maximum number of the rewrite cycles.

The main determining factor of the cost of the memory system is the density of the component placement. The limitation from below in the process of scaling is one of the basic points of the comparison, what is typical for all technologies in general.

For DRAM memory it is the problem even at 55 nm technology because at this size the amount of the charge stored by the capacitor becomes too small. For the FeRAM memory the additional restriction on the size is that the material loses its ferroelectric properties with a strong decrease.

• **PCRAM memory**. This type of memory is based on the change of the phase states of the active region. The information is stored in the atomic structures of the materials having two possible states: amorphous and crystal. To switch the phase states it is necessary to use the voltage pulse or the electric current to melt the material.

The main shortcoming is the necessity of the energy transfer to heat the memory elements to several hundred °C, but with the size reduction the level of the power consumption will decrease.

The density of the placement of the elements is very high: only a few atoms are needed to create the cell that can change the state from crystalline to amorphous.

Experts believe that the real value is 5 nm. This is almost 10 times less than in the flash memory. The PCRAM switching time can be up to 1ns. However, the decrease of this parameter leads to the decrease of the stability of the material state. The optimum ratio of the speed and stability is the main task of engineers.

• **ReRAM memory**. This memory type is comparable to the PCRAM with respect to the scale of the bit storage elements. Unlike the PCRAM in the ReRAM the electrochemical reaction is used instead of changing the phase state under the acting of the heat.

When the high voltage is applied to the crystal then the bonds holding the oxygen atoms begin to break down. The oxygen generates the "holes" and the free electrons which become by carriers. The "holes" tend to form narrow rows of the conductive channels in the crystal.

The reverse voltage returns the oxygen and the material again becomes by the dielectric. Such transitions create the stable memory states, which vary only under the action of the corresponding values of the defined voltage polarity.

The ReRAM memory is a high-speed technology with low power consumption. The memory chip with an area of one square centimeter can storage 500 GB of the information, in the future the amount of the data of one chip can be extended up to 1.5 TB.

• **MRM-memory**. In the track memory the bits are stored in the form of very small size of the magnetization domains (almost like a hard drive). The electric current moves the domains passing through the fixed reading and writing elements.

The process speed reaches 200 m/s, what is equivalent to the reading time about tens of nanoseconds. This may be compared with the current types of the memory, but the advantage of the track memory is its capacity.

The use of the three-dimensional configuration of the nanowires will allows to store the number of bits which is hundred times more in comparison with the flash memory on the same area.

The increasing of the level of the integration and the operating speed, the decreasing of the price and the reduction of the energy consumption

are the stable tendencies in the development of the memory devices with the use of the modern nanotechnology.

However, the achievement by the elements of the nanoelectronic devices of the dimensions which are compared with the molecular, sizes is constrained by a set of the physical and technological limitations.

The proposed table compares the characteristics of the existing types of the memory and the information storage technologies with the characteristics of the MRM memory type and other relatively new technologies expected in the coming years.

TABLE 7.1 COMPARISON TABLE

Memory type	Capacity	Productivity			Power consumption	Reliability		
	Number of bits per cell	Reading time at random access	Writing time at random access	Transfer of data at reading information,Mb/s	Writing one bit, pJ	Reading cycle number	Writing cycle number	Keeping time, years
SRAM	1	2–100	2–100	500	2	10^{15}	10^{15}	–
DRAM	1	6–40	6–40	800	2	10^{15}	10^{15}	–
NOR FLASH	2	70	2×10^{4}	80	160	10^{15}	10^{5}	10
NAND FLASH	2	10^{4}	10^{5}	30	65	10^{15}	10^{5}	10
HDD	–	$>2\times10^{6}$	2×10^{6}	1000	–	–	–	4–6
Field MRAM	1	3–30	3–30	200	50	10^{15}	10^{15}	10
Spin MRAM	1	10–20	3–30	100	2	10^{15}	10^{15}	10
PCRAM	>1	50	100	50	100	10^{15}	10^{12}	10

CONTINUED TABLE 7.1

FeRAM	1	50	50	20	2	10^8–10^{14}	10^8–10^{14}	10
Vertical MRM	up to 128	9.5	9.5	400–670	2	10^{15}	10^{15}	10
Horizontal MRM	>1	9.5	9.5	400–670	2	10^{15}	10^{15}	10

Therefore, the basic concept is changed: instead of the transport of the electron and hole charges, having the properties of the classical particles, the use of the state changes and regularities determined by the wave nature of the electrons (spin state of the electrons, tunneling, the interaction of the wave functions, and so forth.).

1. *Akinaga H.* Resistive Random Access Memory (ReRAM) Based on Metal Oxides / H.Akinaga, H.Shima // Proceeding of the IEEE, 2010.- N98(12).- pp. 2237-2251.
2. *Albo-Canals J.* How to Teach Memristors in EE Undergraduate Courses / J. Albo-Canals, G.E.Pazienza // Circuits and Systems (ISCAS), IEEE International Symposium on. 2011.- pp. 345-348.
3. *Appelbaum I.* Electronic Measurement and Control of Spin transport in Silicon / I.Appelbaum, B.Huang, D.J.Monsma // Nature.-2007. Vol. 447.- p. 205.
4. *Argall F.* Switching Phenomena in Titanium Oxide Thin Films / F.Argall // Solid-state Electronics.- 1967.- Vol. 11, N5.- pp. 535-541.
5. *Auciello O.* The Physics of Ferroelectric Memories / O.Auciello, J.F.Scott, R.Ramesh // Physics Today.- 1998.- N51(7).- p.22.
6. *Baibich M.N.* Giant Magnetoresistance of (001) Fe / (001) Cr Magnetic Superlattices / M.N.Baibich, J.M.Brito, A.Fert. et.al. // Physics Review Letters.- 1998.- Vol. 61.- pp. 2472-2476.
7. *Beck A.* Reproducible Switching effect in Thin Oxide Films for Memory Applications / A.Beck, J.G.Bednorz, Ch.Gerber, C.Rossel, D.Widmer // Applied Physics Letters.- 2000.- Vol. 77, N11.- pp. 139-141.
8. *Belogolovsky M.A.* Nanoelectronic devices with the memory based on the electromigration effect of the oxygen vacancies in the complex oxide of the transition metals. M.A.Belogolovsky, S.Y.Larkin // Electronics and communication. - 2013.- N2.- pp. 9-15, (in Russian).
9. *Belogolovsky M.A.* Memristor is a new nanosized element of the electronic microcircuitry / M.A.Belogolovsky // Bulletin of the Science National Academy of Ukraine. - 2014, N2.- pp. 32-39, (in Ukrainian).
10. *Biolek D.* Reliable Spice Simulations of Memristors, Memcapacitors and Meminductors / D.Biolek, M.Di Ventra, Y.V.Pershin // Radioengineering.- 2013.- Vol. 22, N4.- pp. 1-33.

11. *Biolec Z.* Spice Model of Memristor with Nonlinear Dopant Drift / Z.Biolec, D.Biolec, V.Biolkova // Radioengineering.- 2009.- Vol. 18, N2.- pp. 210-214.
12. *Bloschitsky V.P.* Nanosized resistive switches based on contact of the conductor with the complex oxide of the transition metal // V.P. Bloschitsky, S.Y.Larkin, M.A.Belogolovsky. Science art. of Donetsk Univer. "Comp. tech. and automatization".- 2013, N2(25).- pp. 28-36, (in Russian).
13. *Borghetti J.* Memristive Switches Enable Stateful Logic Operations via Material Implication / J.Borghetti, G.S.Snider, R.S.Kuekes, J.J.Yang, D.R.Stewart, R.S.Williams // Nature Letters.- 2012.- Vol. 464.- pp. 873-876.
14. *Burr G.W.* Phase Change Memory Technology / G.W.Burr, M.J.Breitwisch, M.Franceschim, D.Garetto, K.Gopalakrishnan, B.Jackson, B.Kurdi, C.Lam, L.A.Lastras, A.Padilla // Journal of Vacuum Science & Technology B: Microelectronics and Nanometer Structures.- 2010.- Vol. 28, N2.- pp. 223-262.
15. *Bugaev A.A.* The phase transition metal-semiconductor and its application / A.A.Bugaev, B.P.Zaharchenya, F.A.Chudnovsky // St-Peter.., Energy.- 1979.- 424 p, (in Russian).
16. *Celinska J.* Material and Process Optimization of Correlated Electron Random Access Memories / J.Celinska, C.McWilliams, CP.De Araujo, KH. Xue // Journal of Applied Physics 109(9).- 2011.- pp. 091603(6).
17. *Chandra S.* On the Discovery of a Polarity-Dependent Memory Switch and/or Memristor / S.Chandra // IEEE Technical Review.- 2010.- N27.- pp. 179-180.
18. *Choi B.J.* Resistive Switching Mechanism of TiO_2 Thin Films Grown by Atomic-layer Deposition / B.J.Choi, D.S.Jeong, S.K.Kim, C.Rohde, S.Choi, J.H.Oh, H.J.Kim, C.S.Hwang, K.Szot, R.Waser, B.Reichenberg, S.Tiedke // Journal of Applied Physics.- 2005.- Vol. 98, N3.- pp. 033715 (1-10).
19. *Chua L.O.* Memristor – the Missing Circuit Element /L.O.Chua // IEEE Trans. On Circuit Theory. – 1971.- Vol. 18, N5.- pp. 507-519.
20. *Chua L.O.* Memristive Devices and Systems /L.O.Chua, S.M.Kang // Proc. IEEE. – 1976.- Vol. 64, N2.- pp. 209-223

21. *Chua L.O.* Nonlinear Circuit Foundations for Nanodevices. Part 1: The Four-dimensional Torus / L.O.Chua // Pros. IEEE.- 2003.- Vol. 91 (11).- pp. 1830-1859.
22. *Chua L.O.* The Fourth Element / L.O.Chua // Proceeding IEEE.- 2012.- Vol. 100.- pp. 1920-1927.
23. *Chua L.O.* Introduction to Memristors / L.O.Chua // IEEE Expert Now.- 2009. Educational Course.
24. *Chua L.O.* Resistance Switching Memories are Memristors / L.O.Chua // Applied Physics A.- 2011.- Vol. 102.- pp. 765-783.
25. *Dieny B.* Giaht Magnetoresistance in Spin-valve Multilayers / B.Dieny // J. Magn. Magn. Mater. – 1994.- Vol. 136.- pp. 335-339.
26. *Driscoll T.* Phase-transition Driven Memristive System / T.Driscoll, H.T.Kim, B.G.Chae, M.Di Ventra, D.N.Basov // Applied Physics Letters.- 2009.- Vol. 95.- pp. 503-506.
27. *Emelyanov AV.* The influence of the layers thick TiO_x/TiO_2 on their memristive properties / A.V.Emelyanov, V.A.Demin, I.M.Antropov, G.I.Tscelikov, Z.V.Lavrushina, P.K.Kashkarov // Journal of Technical physics.- 2015б Т.85б issue.1.- pp. 114-117, (in Russian).
28. *Habbard J.* Electron Correlations in Narrow Energy Bands / J.Habbard // Proceeding of the Royal Society of London, Series A. Mathematical and Physical Sciences.- 1963.- N276(1365).- pp. 238-257.
29. *HO Y.* Nonvolatile Memristor Memory: Devices Characteristics and Design Implications / Y. Ho, G.M.Huang, P.Li // IEEE/CAM International Conference.- 2009.- pp. 485-490.
30. *Honda K.* Pulsed Laser Deposition and Analysis for Structural and Electrical Properties of $HfO_2 - TiO_2$ Composite Films / K.Honda, A.Sakai, M.Sakashita, H.Ikeda, S.Zaima, Y,Yasuda // Jpn. Journal Applied Physics.- 2004.- Vol. 43.- pp. 1571-1576.
31. *Huang B.* Coherent Spin Transport through a 350 Micron Thick Silicon Wafer / B.Huang, D.J. Monsma, I.Appelbaum // Physical Review Letters 99.- 2007.- pp. 177209.

32. *Huang B*. Experimental Realization of a Silicon Spin Field-Effect transistor / B.Huang, D.J.Monsma, I.Appelbaum // Applied Physics Letters 91.- 2007.- p.072501.
33. *Jameson J.R.* Field Programmable Rectification in Rutile TiO_2 Crystals / J.R.Jameson, Y.Fukusumi, Z.Wang, P.Griffin, K.Tsunoda, G.I.Meijer, Y.Nishi // Applied Physics Letters.- 2007.- Vol. 91.- pp. 112101-1 – 112101-3.
34. *Joglecar Y.* The Elusive Memristor: Properties of Basic Electrical Circuits / Y.Joglecar, S.Wolf // Eur. Journal hysics.- 2009.- Vol. 30.- pp. 661-675.
35. *Johnsen G.K.* An Introduction to the Memristor – a Valuable Circuit Element in Bioelectricity and Bioimpedance / G.K. Johnsen // Journal of Electrical Bioimpedance.- 2012.- Vol. 3.- pp. 20-28.
36. *Johnson M.* Bipolar Spin Switch / M. Johnson // Science.- 1993.- Vol. 260.- pp. 320-323.
37. *Kavehei O.* The Fourth Element: Characteristics, Modeling and Electromagnetic Theory of the Memristor / O.Kavehei, A.Iqbal, Y.S.Kim, R. Esraghian, S.F. Al-Sarawi, D.Abbot // Proceeding of the Royal Society a Mathematical Physical and Engineering Sciences.- 2010.- Vol. 466.- pp. 2175-2202.
38. *Kim K.M.* Anode-interface Localized Filamentary Mechanism in Resistive Switching of TiO_2 Thin Films / K.M.Kim, B.J.Choi, Y.C.Shin, C.Choi, C.S.Hwang // Applied Physics Letters.- 2007.- Vol. 91.- pp. 012907 (1-6).
39. *Krzysteczko P.* Memristive Switching of MgO Based Magnetic Tunnel Junctions / P. Krzysteczko, G.Reiss, A.Thomas // Journal of Magnetism and Magnetic Materials.- 2011.- Vol. 321.- pp. 144-147.
40. *Kumar M.J.* Memristor – Why do We Have to Know All about it? / M.J.Kumar // IEEE Tech. Rev..- 2009.- Vol. 26, N1.- pp. 3-6.
41. *Kvatinsky S.* MAGIC-Memristor Aided Logic / S.Kvatinsky, D.Belousov, S,Liman, G.Satat, N.Wald, E.Friedman, A.Kolodny, U.Weiser // IEEE Transactions on Circuits and Systems –II: Express Briefs, Vol. XXX, NXXX.- 2014.- pp. 1-5.
42. *Kvatinsky S.* TEAM: ThrEshold Adaptive Memristor Model / S.Kvatinsky, E.Friedman, A.Kolodny, U.Weiser // IEEE Transac-

tions on Circuits and Systems –I: Regular Papers.- 2013.- Vol. 60, N1.- pp. 211-221.

43. *Kvatinsky S.* Memristor-based IMPLY Logic Gate Design Procedure / S.Kvatinsky, E.Friedman, A.Kolodny, U.Weiser // Proceeding of IEEE International Conference on Computer Design.- 2011.- pp. 142-147.
44. *Lehtonen E.* Applications and Limitations of Memristive Implication Logic / E/Lehtonen, J.Poikonen, M.Laiho // Proceeding of the International Workshop on Cellular Nanoscale Networks and their Applicationss (CNNA).- 2012.- pp. 1-6.
45. *Lehtonen E.* Two Memristors Suffice to Compute All Boolean Functions / E.Lehtonen, J.Poikonen, M.Laiho // Electronics Letters.- 2010.- Vol. 46, N3.- pp. 239-240.
46. *Linn E.* Complementary Resistive Switches for Passive Nanocrossbar Memories / E.Linn, R.Rosezin, C.Kugelar, R.Waser // Nature Materials.- 2010.- Vol. 9, N5.- pp. 403-406.
47. *Lodder J.C.* The Spin-valve Transistor: Technologies and Progress / J.C.Lodder, D.J.Monsma, R.Vlutters, T.J.Shimatsu // Journal Magn. Materials.- 1999.- Vol. 198.- pp. 119-124.
48. *Mahmoudi H.* Compact Modeling of Memristive IMP Gates for Reliable Statefull Logic Design / H.Mahmoudi, T.Windbacher, V.Sverdlov, S.Selberherr // 21st International Conference "MIXDES 2014", June 19-21, 2014, Lublin, Poland.- pp. 58-61.
49. *Mahvash M.* A Memristors Spice Model for Designing Memristor Circuits / M.Mahvash, A.Parker // Aug.2010.- pp. 989-992.
50. *McDonald N.R.* Analysis of Dynamic Linear and Non-linear Memristor Device Models for Emerging Neuromorphic Computering Hardware Design / N/R/McDonald, R.E.Pino, P.J.Rozwood, B.T.Wysocki //
51. *McWilliams C.R.* Device Characterization of Correlated Electron Random Access Memories / C.R.McWilliams, J.Celinska, CP.De Araujo, KH.Xue // Journal of Applied Physics 109(9).- 2011.- pp. 091608(5).
52. *Moutett B.* The Mythology of the Memristors / B.Moutett // Circuits and Systems (ISCAS), Proceeding of 2010 IEEE International Symposium on, May 2010.

53. *Mott N.F.* Transitions metal-insulator / N.F.Mott // M.: Science.- 1979.- 342 p, (in Russian).

54. *Mott N.F.* The Basic of the Electron Theory of Metals, with Special Reference to the Transition Metals / N.F.Mott // Proceeding of the Physical Society. Section A.- 1949.- N62(7).- p. 416.

55. *Ognev A.V.* Spintronics: physical principles, devices, perspectives // A.V.Ognev, A.S. Samardak. Bulletin of LED RAS.- 2006.- N4.- pp. 70-80, (in Russian).

56. *Oster G.F.* A Note on Memristors / G.F.Oster // IEEE Transactions on Circuits and Systems.- 1974.- p. 152.

57. *Oster G.F.* The Memristor: A New Bond Graph Element / G.F.Oster, D.Auslander // ASME trans. Dyn. Syst. Meas. Contr.- 1972.- Vol. 94, N3.- pp. 249-252.

58. *Pan X.* Defective TiO_2 with Oxygen Vacancies: Synthesis, Properties and Photocatalytic Applications / X.Pan, M.Yang, X.Fu, N.Zhang, Y.Xu // Nanoscale.- 2013.- Vol. 5, N9.- pp. 3601-3614.

59. *Parkin S.* Magnetic Domain-Wall Racetrack Memory / S.Parkin, M.Hayashi, L.Thomas // Science. – 2008. - Vol. 320. – pp. 190 – 194.

60. *Pershin Y.V.* Spin Memristive Systems: Spin Memory Effects in Semiconductor Spintronics / Y.V.Pershin, M.Di.Ventra // Phys. Rev.- 2008.- B78.- pp. 113309 (4).

61. *Pershin Y.V.* Memory Circuit Elements: from Systems to Applications /Y.V.Pershin, J.M.Rincon, M.Di. Ventra // Journal of Computational and Theoretical Nanoscience.- 2011.- Vol. 8.- pp. 441-448.

62. *Pershin Y.V.* Experimental Demonstration of Associative Memory with Memristive Neural Networks / Y.V.Pershin, M.Di Ventra // Neural Networks.- 2010.- Vol. 23.- pp. 881-886.

63. *Pershin Y.V.* Memory Effects in Complex Materials and Nanoscale Systems / Y.V.Pershin, M.Di Ventra // Advances in Physics.- 2011.- Vol. 60, N2.- pp. 145-227.

64. *Pershin Y.V.* Practical Approach to Programmable Analog Circuits with Memristors / Y.V.Pershin, M.Di Ventra // IEEE Transactions on Circuits and Systems: regular Papers.- 2010.- Vol. 57, N8.- pp. 1857-1864.

65. *Pickett M.* Switching Dynamics in Titanium Dioxide Memristive Devices / M.Pickett, D. Strukov, J.Borghetti, J.Yang, G.Snider, D.Steward, R.Williams // Journal Applied Physics.-2009.- Vol. 106, N7.- pp. 074508 (1-6).
66. *Plecenik T.* Effect of Crystallographic Anisotropy on the Resistance Switching Phenomenon in Perovskites /T.Plecenik, M.Tomasek, M.Belogolovskii // Journal Applied Physics.- 2012.- Vol. 111, N5.- pp. 056106(1-3).
67. *Plecenik A.* Studies of Resistance Switching Effects in Metal/ $YBa_2Cu_3O_{7-x}$ Interface Junctions / A.Plecenik, M.Tomasek, T.Plecenik // Applied Surf. Science.- 2010.- Vol. 256, N18.- pp. 5684-5687.
68. *Prodromakis T.* Two Centuries of Memristors / T.Prodromakis, C.Toumazou, L.Chua // Nature Materials.- 2012.- Vol. 11.- pp. 478-481.
69. *Prodromakis T.* Switching Mechanism in Microscale Memristors / T.Prodromakis, K.Michelakis, C.Toumazou // Electronics Letters.- 2010.- Vol. 46, N1.- pp. 63-65.
70. *Prodromakis T. A* review on Memristive Devices and Applications / T. Prodromakis, C. Toumazou // Electronics, Circuits and Systems (ICECS), 17th IEEE International Conference on.- 12-15 Dec. 2010.- pp. 934-937.
71. *Prodromakis T.* A Versatible Memristor Model with Non-linear Dopant Kinetics / T.Prodromakis, B.P.Peh, C.Papavassilion, C.Toumazou // IEEE Transactions on Electron Devices
72. *Ren T.L.* Model and Key Fabrication Technologies for FeRAM / T.L.Ren, M.M.Zhang, Z.Jia, L.K. Wang, C.C.Wei, KH Xue, Y.J.Zhang, H.Hu, D.Xie, L.T.Liu // Journal ECS Transactions.- 2009.- Vol. 22(1).- pp. 217-225.
73. *Rozenberg M.J.* Nonvolative Memory with Multilevel Switching: a Basic model / M.J.Rozenberg, I.H.Inoue, M.J.Sanchez // Phys. Rev. Lett.- 2004.- Vol. 92.- pp. 178302 (1-5).
74. *Sawa A.* Resistive Switching in Transition Metal Oxides / A.Sawa // Materials Today /- 2008.- Vol. 11, N6.- pp. 28-36.

75. *Scott J.E.* Ferroelectric Memories / J.F.Scott, CP. De Araujo // Science.- 1989.- N246(4936).- pp. 1400-1405.

76. *Shin S.* Compact Models for Memristors Based on Charge-flux Constitutive relationships / S.Shin, K.Kim, S.M.Kang // IEEE Transactions on Computer-Aided Design of Integrated Circuits and Systems.- 2010.- Vol. 29 (4).- pp. 590-598.

77. *Strukov D.B.* The Missing Memristor Found / D.B.Strukov, G.S.Snider, D.R. Stewart, R.S. Williams // Nature.- 2008.- Vol. 453.- pp. 80-83.

78. *Strukov D.B.* Coupled Ionic and Electronic Transport Model of Thin-Film Semiconductor Memristive Behavior // D.B.Strukov.- 2009.-Small 5, (9).- pp. 1058-1063.

79. *Szot K.* Microscopic Nature of the Metal to Insulator Phase Transition Induced Through Electroreduction in Single-crystal $KNbO_3$ / K.Szot, W.Speier, W.Eberhardt // Applied Physics Letters.- 1992.- Vol. 60.- pp. 1190-1192.

80. *Thakoor S.* Solid-state Thin-film Memistor for Electronic Neural Networks / S.Thakoor, A.Moopenn, T.Daud, A.P, Thaloor // Journal of Applied Physics.- 1990.- Vol. 67.- pp. 3132-3135.

81. *Tour J.M.* The Fourth Element / J.M. Tour, T.He // Nature/- 2008.- Vol. 453, N9.- pp. 42-43.

82. *Umul Y.Z.* Electric Charges that Behave as magnetic monopoles / Y.Z.Umul // Progress in Electromagnetics Research Letters.- 2010.- Vol. 18.- pp. 19-28.

83. *Ventra M.Di.* Circuit Elements with Memory: Memristors, Memcapasitors and Meminductors / M.Di.Ventra, Y.V.Pershin, L.O.Chua // Proceedings of the IEEE.- 2009.- N97.- pp. 171-176.

84. *Vongehr S.* The Missing Memristor: Novel Nanotechnology or Rather New Case Study for the Philosophy and Sociology of Science / S/Vongehr // Advanced Science Letters.- 2012.- Vol. 17, N1.- pp. 285-296.

85. *Wang F.Y.* Memristor for Introductory Physics / F.Y.Wang // [Online]. Available: http:// arxiv.org/abs/0808.0286, [physics.class-ph], 4 August 2008.- pp. 1-4.

86. *Waser R.* Nanoionic-Based resistive Switching Memories / R.Waser, Aono M. // Nature Materials.- 2007.- N6.- pp. 833-840.

87. *Waser R.* Redox-Based Resistive Switching Memories – Nanoionic Mechanism / R.Waser, R. Dittman, G.Staikov, K.Szot // Prospects, and Challenges, Adv.Mater.- 2009.- Vol. 21.- pp. 2632-2663.

88. *Widrow B.* Birth, Life and Death in Microelectronic Systems / B.Widrow, W.H.Pierce, J.B. Angell // Office of Naval Research Technical Report (1552-2/1851-1).- 1961.- pp. 362-368.

89. *Williams R.S.* Reply to – On the Discovery of a Polarity-Dependent Memory Switch and/or Memristor (Memory Resistor)/ R.S.Williams // IEEE Tech. Rev.- 2010.-N27.- pp. 181-182.

90. *Williams R.S.* How We Found the Missing Memristor / R.S.Williams // IEEE Spectrum.- 2008.- Vol. 45, N12.- pp. 28-35.

91. *Wong H.-S.P.* Phase Change Memory / H.-S.P.Wong, S.Raoux, SB.Kim, J,Liang, J,P,Reifenberg, B.Rajendran, M.Asheghi, K.E.Goodson // Proceeding of the IEEE.- N98(12).- pp. 2201-2227.

92. *Xue KH.* A Non-filamentary Model for Unipolar Switching Transition Metal Oxide Resistance Random Access Memories / KH Xue, C.P.de Araujo, J,Celinska, C.M.Williams // Journal of Applied Physics 109(9).- 2011.- pp. 091602(6).

93. *Xue KH.* A Combined Ab Initio and Experimental Study on the Nature of Conductive Filaments in $Pt/HfO_2/Pt$ Resistive Random Access Memory // KH Xue, B.Traore, P.Blaise, LRC Fonseca, E.Vianello, G.Molas, B.De Salvo, G.Ghibando, B.Magyari-Kope, Y.Nishi // IEEE Transactions.- 2014.- pp. 1-1.

94. *Yang J.J.* Memristive Switching Mechanism for Metal/Oxide/Metal Nanodevices / J.J.Yang, M.D.Pickett, L.Xuema, A.A. Douglas, A.Ohlberg, D.R.Stewart, R.S.Williams // Nature Nanotechnology.- 2008.- N3.- pp. 429-433.

95. *Yang J.J.* Memristive Devices for Computing / J.J.Yang, D.B.Strukov, D.R.Stewart // Nature Nanotechnology.- 2013.- Vol. 8.- pp. 13-24.

96. *Yang J.J.* Engineering Nonlinearity into Memristors for Passive Crossbar Applications / J.J.Yang, M.X. Zhang, M.Pickett, F.Miao, J.P.Strachan, W.D.Li, W.Yi, D.A.A.Ohlberg, B.J.Choi, W.Wu,

J.H.Nickel, G.Medeiros-Ribeiro, R.S.Williams // Applied Physics Letters.- 2012.- Vol. 100, N11.- pp. 113501-113503.

97. *Yang J.J.* The Mechanism of Electroforming of Metal Oxide Memristive Switches / J.J.Yang, F.Miao, M.D.Pickett, D.A.A.Ohlberg, D.R.Stewart, C.N.Lau, R.S.Williams // Nanotechnology.- 2009.- N20.- pp. 215201 (9).
98. *Yihong Wu.* Nano Spintronics for Data Storage / Wu.Yihong // Encyclopedia of Nanoscience and Nanotechnology // Ed. Nalva S.H.ACP.USA.- 2004.- Vol. 10.- pp. 1-50.
99. *Hrapovitskaya Y.V.* Researching influence of the material of the memristor contact on its stability to degradation under the cyclic switching // Y.V.Hrapovitskaya, N.E.Maslova, Y.V.Grischenko, V.A.Demin, M.L.Zanaveskin // Letters in JTP.- 2014.- Vol. 40, issue. 7.- pp. 87-94, (in Russian).
100. *Shevirtalov S.N.* Resistibe bipolar switching in the thin film resistive structures on the base of Si – Ag // S.N.Shevirtalov, D.A.Koiva, A.Y.Goisman // Bulletin of Balt. Federal. Univers..- 2014.- Issue. 4.- pp. 24-28, (in Russian).
101. *Zelenkov A.A*. Linear and nonlinear electric circuits: manual / A.A.Zelenkov, V.P.Shahov, A.A.Bunchuk – Kyiv: NAU, 2003. – 168 p., (in Ukrainian).
102. *Zelenkov A.A*. Transients in the linear circuits: manual / A.A.Zelenkov, V.P.Shahov, A.A.Bunchuk – Kyiv: NAU, 2003. – 132 p., (in Ukrainian).
103. *Zelenkov A.A*. Fundamentals of Electrical Engineering. Electric circuits with the distributed parameters. Theory of the electromagnetic field: manual / A.A.Zelenkov, A.A.Bunchuk – Kyiv: NAU, 2014. – 312 p., (in Ukrainen).
104. *Sineglazov V.M*. Quantum electronics: manual / V.M.Sineglazov, A.A.Zelenkov, S.I.Askerov. – Kyiv: “Education of Ukraine”, 2015. – 342 p., (in Russian).

GLOSSARY

Atomic electronic orbital	State of an electron in an atom, characterized by certain values quantum numbers n, l and m, that is a certain size, shape, and the orientation in space of the electron clouds.
Diamagnetics	Each electron creates its own magnetic field due to its spin. The direction of this field is determined by the direction of the spin, so that the magnetic fields formed by two paired electrons cancel each other. This is due to the fact that according to the Pauli principle the atom can not have two electrons whose four quantum numbers would be equal. From this it follows that each atomic orbital, which is characterized by defined values *n*, *l* and *m*, may be occupied by no more than two electrons whose spins have opposite directions (such electrons are called paired), unlike the single (unpaired) electron occupying any orbital. Substance, the atoms or molecules of which do not have a permanent magnetic moment under the acting of the external magnetic field, is called the diamagnetic. The diamagnetics do not create their own magnetic field, since they contain only the paired electrons. In particular, this occurs in the atoms, ions and molecules with the completely filled electron shells, such as the inert gases.For the diamagnetics $\mu < 1, \chi < 0$ (for example, silver, copper, bismuth), so that they do not significantly weaken the magnetic field (see Ferromagnetic).
Dioxides	Dioxides are the compounds of the elements with the oxygen. For the elements with variable valence it is shown in parentheses by the Roman numerals and defines the valence of the element in this oxide. For example CaO according to the International nomenclature is called the calcium oxide, and the compounds Cu_2O and CuO are respectively called copper oxide (1) and copper oxide (II). The oxides EO_2 or EO_3 are also called the dioxides and trioxides respectively (E – chemical element).

Electron formula	The electron formula defines the electron construction of the atom in which at first all states with the given value n are written in series and then it is necessary to write the states with higher value of n. The stable state of the atom is characterized by the least energy and consequently the electrons fill in the orbitals according to the order of increase their energy. The electrons fill in its sublevels according to Klechkovskii and Gunda rules. The scheme of the series infill of the electron energy sublevels in the atom is shown in Fig. A1.1. As an example we consider the electron formula of the titanium (Ti (Z = 22)): $$1s^2 2s^2 2p^6 3s^2 3p^6 3d^2 4s^2$$ To characterize the electron construction the electron-graphical schemes are used. For example: 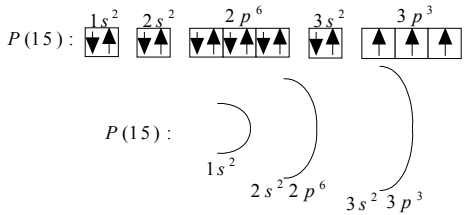 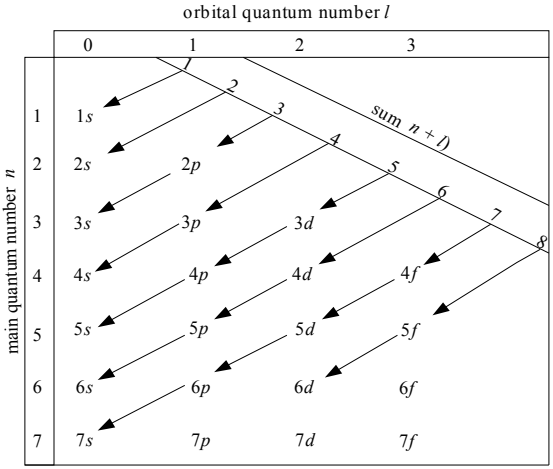 Fig. A1.1. Electron-graphical schemes

Electron layer	The electron layer is the aggregate of the electrons placed on the one energy level which are characterized by the same value of the main quantum number and form in the atom the electron clouds of approximately same sizes.
Electron shell	The atom consists of the nucleus and electron shell. The electron shell is the aggregate of all electrons in the given atom. The chemical properties of the given element depend on the construction of the electron shell.
Energy band (zone)	The successive increase of the number of the acting atoms leads to the forming of the energy levels. The total number of levels will be equal to the number of acting atoms, Fig. A1.2. 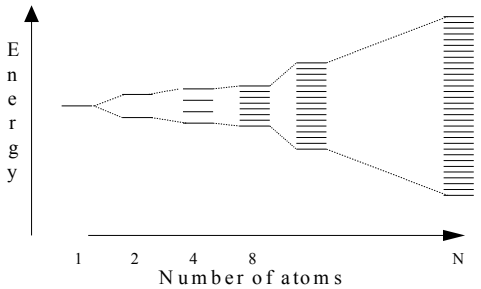 Fig. A1.2. Distribution of the energy levels Thus the growth of the number of the atoms leads to the increase of the number of the permitted energy states. The distance between the neighbor energy levels decreases. If the number of the interacting atoms is not great then to transfer the electron from some energy level on the nearest higher level it is necessary to spend relatively great energy. If the number of the interacting atoms N is great then the neighbor energy levels are little differ so that the continuous energy band is formed. It means that the transfer of the electron on the nearest higher level may be realized by means of insignificantly energy. If such nearest level is not occupied by the electrons then the electron which is placed on the previous level may move on the crystal under indefinitely small energy acting.

Energy level	According to the quantum mechanic laws the energy of the electron bounded up in the atom, and consequently the energy of the atom as a whole is not arbitrary. It has the defined discontinuous row of values called the energy levels. This set of the "permitted" energy values is called the energy spectrum of the atom. The bottommost energy level for which the energy of the atom is the least is called the basic level. The rest of levels corresponding to higher energy of atom are called the excited levels. From the quantum physics it follows that the energy level is the aggregate of the orbitals having the same value of the main quantum number n. The energy levels are designated by the capital letters of the Roman alphabet: K, L, M, N, O, P and Q (sometimes the numbers are used: 1, 2, . . . , 7. The energy of orbitals increase if the number increase as well. Thus, the orbitals having the same values of n, near energy values and sizes form one energy level. The electron clouds having the various geometrical shapes may be placed on the one energy level. The total number of orbitals on the one energy level equals $2n^2$.
Energy sublevel	The energy of orbitals which are placed on the one energy level and have the various shape is not the same: $W_s < W_p < W_d < W_f$. That is why on the one level the different energy sublevels are chosen. The energy sublevel is the aggregate of orbitals which are placed on the one energy level and have the same shape. The orbitals of one sublevel have the same values of the main n and the orbital l quantum numbers but differ by the orientation (direction) in the space. It means that they differ by the values of the magnetic quantum number m. The sublevels are designated by the small letters: • s – sublevel ($l = 0$, $m = 0$) has one orbital; • p – sublevel ($l = 1$, $m = -1, 0, +1$) has three orbitals;

	,
	• d – sublevel ($l = 2, m = -2, -1, 0, +1, +2$) has five orbitals; • f – sublevel (l = 3, m = –3, –2, –1, 0, +1, +2, +3) has seven orbitals. Thus, the number of orbitals on the sublevel equals $2l + 1$.
Ferroelectrics	Ferroelectrics are the substances which have the spontaneous polarization in the certain temperature range and the hysteresis of the dependency of the dipole electric moment from the electric field intensity. Microscopical cause of the ferroelectric phenomenons is the presence of the atomic or molecular dipoles within substance which are oriented according to the external electric field and remain oriented after its switching off. Switching over to the opposite direction of the electric field leads to the inverse orientation of the dipoles. In the ferroelectrics the dipole is formed by displacement in the elementary cell of the atoms of the one kind having two stable positions with respect to the atoms of another kind (see section 7.5). So the positively charged ion Ti^+ in the barium titanate has two equivalent stable positions in the lattice with respect to the ions of the barium and oxygen. Thus the elementary dipole oriented in the respective direction is formed. In the case of spontaneous polarization the dipoles in all cells have the random direction. When the ferroelectric is placed in the electric field then most of dipoles are formed up mainly in one direction which is kept after switch off the external electric field. Ferroelectrics are used in the ferroelectric transitions to create the devices of the nonvolatile memory.
Ferromagnetics	Under the action of the external magnetic field the dipoles are oriented in the field direction and increase the magnetic induction from B_0 to B_1 and the magnetic

flux from Φ_0 to Φ_1. The increment of the induction ΔB is called the magnetization J.

In all substances (with the exception of ferromagnetics) the magnetization is directly proportional to the field intensity:

$$J = \chi \mu_0 H .$$

Here χ is the magnetic susceptibility; μ_0 is the magnetic constant equaled $4\pi \cdot 10^{-7}$ H/m.

The magnetization J of the ferromagnetics is not proportional to the magnetic field intensity H and at its great values tends to the maximum value. The considered above formula is not correct because in this case the magnetic susceptibility and the magnetic permeability are not the constant values.

The dependency between the magnetic induction B and the magnetic field intensity H is described by means of the normal magnetization curve, Fig. A1.3.

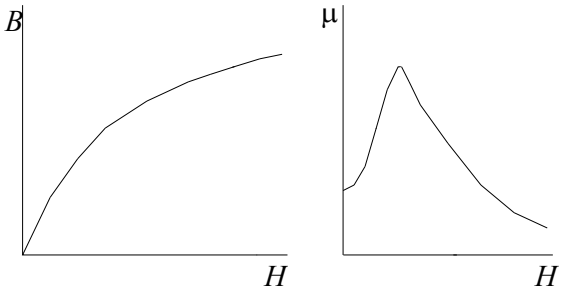

Fig. A1.3. The dependencies of the magnetic induction B and the magnetic permeability μ from the magnetic field intensity H

In general case the magnetization curve of the ferromagnetic represents the hysteresis loop for which two values of the magnetic induction correspond each value of the magnetic intensity/ It depends on the increase or decrease of the magnetic field intensity, Fig. A1.4.

	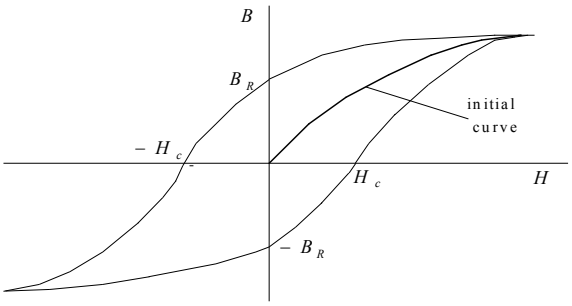 Fig. A1.4. The normal magnetization curve of the ferromagnetic The value of the induction B_R which is retained at $H = 0$ is called the residual induction. The magnetic field intensity H_c for which the induction equals zero is called the coercive force. There are the ferromagnetics with the narrow and wide hysteresis loop. In the first case the value of the coercive force is less than in the second one. The substances with $\mu >> 1$, $\chi > 0$ (for example the iron, cobalt, nickel) are the ferromagnetics because the magnetic field in these substances essentially increases unlike the diamagnetics for which $\mu < 1, \chi < 0$.
Filamentary model of switching	The filamentary model of the memristor represents the model of the structure metal/ dielectric (insulator)/ metal (MDM or MIM) for which the resistive switchings in the active layer from the high resistance state (HRS) into the low resistance state (LRS) are realized by means of the forming of the filament channels consisting of the oxygen vacancies and providing the current flow. In this case the conductance of the active region is confined by the filament(s). It means that the switching occurs locally within the filament. The value of the resistances R_{On} and R_{Off} in this case practically not depends on the area of the MDM structure.

Forbidden band	Crystals of some substances (not metals) do not have the noticeable electronic conductivity and are the dielectrics (insulators). In this case too, the formation of the continuous energy bands is possible, but the conduction band is separated from the valence band by means of the so-called forbidden band, having the significant energy gap ΔW, Fig. A1.5 *a*. The energy of the thermal motion (or the weak electric field) is insufficient to overcome this gap, and the electrons do not pass from the valence band to the conduction band. Thus, in the dielectrics the electrons can not move freely through the crystal and serve as the carriers of the electric current. The **semiconductors** have the specific properties because they are distinguished from both the metals and the dielectrics. At low temperatures, their resistance is very large, and in these conditions they have the properties of the insulators. However, the electrical conductivity of the semiconductors increases sharply and can reach the values comparable with the conductivity of the metals under the heating or in the presence of a relatively large electric field. Like dielectrics, the valence band is separated from the conduction band by the forbidden zone (Fig. A1.5, *b*), however, the width of the forbidden band ΔW is small in the case of the semiconductors, and in certain cases, the electrons that occupy the upper levels of the valence band can pass on in the conduction band and take part in carrying electric current. When the electrons pass on in the conduction band then not fully occupied by the electrons the energy levels occur in the valence band the so-called electron vacancies or "holes." In the electric field, such holes behave as the positive electric charges. Therefore, the transfer of the current in the semiconductors can be carried out by the electrons of the conduction band (*n*-conduction.) and holes of the valence band (*p*-conductivity).

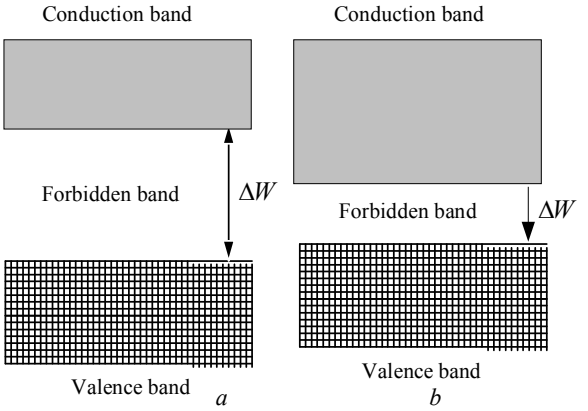

Fig. A1.5. Forbidden band: *a* is the dielectric; *b* is the semiconductor

Giant magneto-resistance

One of the main effects of spintronics is the giant magneto-resistance discovered in the magnetic multilayers (multilayer magnetic films) and the granular magnetic structures.

Magnetoresistance effect δ_H is the relative change of the electrical resistance when a magnetic field is switched:

$$\delta_H = \frac{\rho(H) - \rho(0)}{\rho(H)},$$

where $\rho(0)$ is the electrical resistance in the absence of the field, $\rho(H)$ is the electrical resistance in the field *H*.

Previously the magnetoresistance was studied in massive materials, where the length of the magnetic inhomogeneities greatly exceeded the length of free path of the electrons, that is the distance to the collision.

In the multilayers such as Fe/Cr, the ferromagnetic layers Fe of the thickness ~ $30\,\overset{0}{A}$ ($1\,\overset{0}{A} = 10^{-10}$ m = 0,1 nm) alternated with the non-ferromagnetic layers of the chromium Cr of the

	thickness $9-18\overset{0}{A}$. It was found that the magnetic moments of the Fe atoms within one layer are parallel and the magnetic moments of the adjacent layers Fe are oriented antiparallel. In a magnetic field which is greater than the saturation field H_s and applied in the plane of the layers, the antiferromagnetic exchange coupling is destroyed and all the magnetic moments of the Fe atoms occur parallel each other. As a result, the electrical resistance decreases sharply, that is, there is the colossal magnetoresistance. 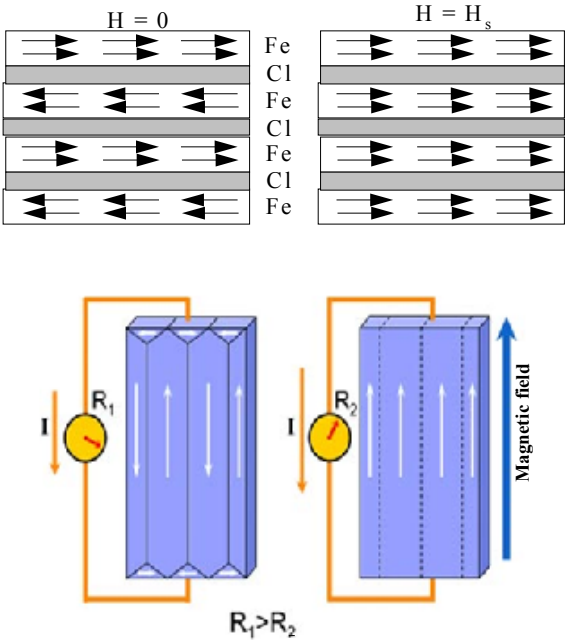
Gunda rule	Gunda rule defines that a stable state of the atom corresponds to such distribution of the electrons within the energy sublevel for which the absolute value of the total spin (the sum of the spin quantum numbers) atoms is a maximum. It should be noted, that the Gunda rule does not forbid the other distribution of the electrons, it merely

	states that the maximum value of the total spin of the atom corresponds to the stable state (unexcited state) in which the atom has the lowest possible energy. For any other distribution of the electrons the energy of the atom will be more value, so it will be excited (unstable) state. For example, for the carbon atom (Z = 6) the electron formula is given by the form $1s^2 2s^2 2p^2$. However, this formula could match any of the three distributions: 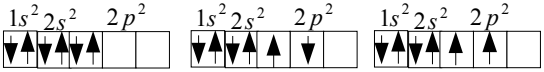 According to the first scheme, the two $2p$-electrons are in the same orbital. It means that their magnetic quantum numbers have the same value, and the spins are oppositely directed. Second circuit means that the two $2p$-electrons are at the different orbitals (they have the different values m) and have oppositely directed spins. From the third scheme it follows the two $2p$-electrons correspond to the different orbitals, but their spins have the same direction. Analysis of the atomic carbon spectrum shows that for the unexcited atom of the carbon the last scheme is correct because the value of the total spin is a maximum and equal to $1\left[\frac{1}{2}+\frac{1}{2}=1\right]$.
Impurity conductance	It is known that the most important semiconductor materials are the germanium and silicon. The atoms of these elements have four electrons on the external orbital which form the valence bond with the electrons of the neighbor atoms. If the thermal energy (as an example) is applied to the material then interatomic bonds in the lattice lose the electrons so that the positive charge is formed. The place in the lattice where the electron is absent is called the “hole”. In the pure semiconductor the conductance of which is defined by the thermal excitation the same number of the electrons and holes moves in the opposite directions.

The electrons lose the energy and are grasped by the holes. This process is called the recombination.

At the constant temperature the recombination speed and the formation speed are the same. It means that the product of the concentration of the electrons $n\_$ and holes n_+ is the constant value equaled

$$n\_n_+ = n_0 \exp\left[-\frac{\Delta W}{kT}\right]$$

where n_0 is the coefficient of proportionality which characterizes the number of the atoms in the lattice per the volume unity, k is Boltzmann constant equaled $1.38 \cdot 10^{-23}$ J/K, ΔW is the distance between the valence and conductance band, T is the temperature in Kelvin (K).

In the germanium the number of carriers equals $n_\pm = 2.5 \cdot 10^{13} \frac{1}{\text{sm}^3}$ at the room temperature and the density of the atoms equals $4.4 \cdot 10^{22} \frac{1}{\text{sm}^3}$

Thus approximately 10^9 atoms account for one pair of the charge carriers.

The conductance of the semiconductor may be increased by the addition of the atoms of other elements (doping process). If the impurities are introduced into the semiconductor lattice then the impurity conduction occurs (unlike the self-conductance).

For example, if the quadrivalent germanium is doped by the quinquivalent arsenic (or the antimony, phosphorus) then the redundant free electron occurs in the location of the impurity atom.

As a rule 10^5 – 10^6 atoms of the semiconductor lattice account for one atom of the impurity.

The impurities which promote to the occurrence of the free electrons are called the donor impurities, energy levels of the donor impurities are located below the conductance band (zone), Fig. A1.6.

The impurity leads to the increase of the electron concentration (approximately 10^3 times) therefore the

concentration of the holes decreases at the same value that is $n_- = 10^6 n_+$.

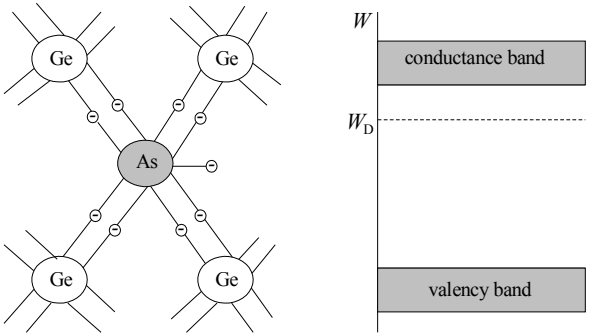

Fig. A1.6. Donor impurity provides the electron conductance of the semiconductor

Since $n_- >> n_+$ then the electrons are called the basic carriers. In this case the germanium is called the semiconductor with electron conductance or the *n*-type semiconductor. The conductance of such semiconductor is provided by the electrons.

The doping of the semiconductor by the elements with smaller valency also increases its conductance (for example the doping by the trivalent indium or gallium). In this case the redundant hole occurs in the location of the impurity atom.

The impurities which decrease the number of the free electrons are called the acceptor impurities. The energy levels of the acceptor impurities are located above the valency band, Fig. A1.7.

Such impurity leads to the increase of the hole concentration therefore the concentration of the electrons decreases.

Since $n_+ >> n_-$ then the holes are called the basic carriers and such semiconductor is called the semiconductor with the hole conductance or the*p*-type semiconductor.

	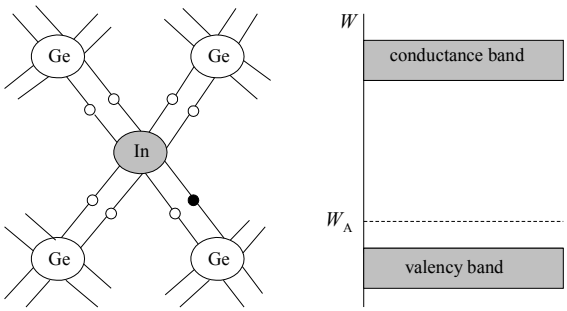 Fig. A1.7. Acceptor impurity provides the hole conductance of the semiconductor
Interface model of switching	In the interface model of the switching of the memristor the conductive part of the active region is the uniform (homogenous) zone across the all area of the structure unlike the filamentary model where the conductive part is formed along the thin filaments.
Ion implantation	Ion implantation is the method of entering the impurity atoms into the surface layer of the film or the plate by means of the bombardment of the surface by the ion beam with the high energy (from 10 to 2000 keV). The ions of the alloying substance at a certain depth come into collision with the electrons and nucleuses of the target lose the energy and stop. If the type and the energy of the ions and the properties of the material are known, then the depth of penetration (or the track length) can be calculated. For the beams with the typical energies from 10 to 500 keV the track length value reaches one micron. Due to many factors, the distribution of the introduced substance in the surface is close to a Gaussian (normal) distribution.
Ionization energy	The energy of the ionization is the energy which is spent to separate the electron from the atom which is turned into the ion in this case. The most typical chemical property of the metals is the ability their atoms easily to send the external electrons and turn into the positive charged ions. The

	non-metals have the ability to join the electrons and turn into the negative ions. The energy of the ionization may be defined by means of the bombardment of the atoms by the electrons accelerated in the electric field. The least voltage of the electric field when the speed of electrons is sufficient to ionize the atoms is called the potential of ionization of the given element atoms and is measured in volts. The energy of electrons is expressed in electron-volts (eV). The value 1 eV is the energy obtained by the electron in the accelerating electric field with the difference of potentials of 1V (1 eV = $1,602 \cdot 10^{-19}$ J). The energy of ionization expressed in electron-volts is numerically equal to the ionization potential expressed in volts. If the sufficient energy is applied to the atom then two, three and more electrons may be separated from the atom. It is said that the separation energy of the first electron from the atom is the first potential of ionization. By analogy the second potential of ionization may be found. The successive moving away of the electrons from the atom leads to the increase of the positive charge of the forming ion. That is why to separate each next electron from the atom it is required the greater value of the energy. As a rule, the element has the greater "metallic" properties in comparison with another element if its potential of ionization is less than the potential of another element.
Klechkovski rules	Klechkovski rules determine the sequence of filling up of the electron orbitals. The first rule states: if the charge of the atomic nucleus increases then the sequential filling up of the electron orbitals begins from the orbitals with the lower value of the sum of principal and orbital quantum numbers ($n + l$) to the orbitals with the great value of this sum (structure of e-formula). The second rule states: if the value of the sum ($n + l$) is the same then the filling up of the orbitals exists consistently in the direction of increasing value of the principal quantum number n.

	For example, in the case of $(n + l) = 5$ at first the sublayer $3d$ ($n = 3$) must be completed, then the sublayer $4p$ ($n = 4$) and finally the sublayer $5s$ ($n = 5$).
Magnetic quantum number	The magnetic quantum number m characterizes the orientation of the electron orbital plane in space and takes $(2l + 1)$ different values, where l is the orbital quantum number. The orbital momentum (impulse) $\vec{M}$ of the electron around the nucleus is represented by the vector the allowed direction of which is determined by the values of the magnetic quantum number m. This means that the projection of the vector $\vec{M}$ on a certain chosen direction z (for example on the direction of the electric or magnetic field) for the given l may assume $2l + 1$ different values: $$M_{lz} = \frac{h}{2\pi} m_l$$ where $m_l = l, l-1, ..., -l$ is the magnetic quantum number. The possible values of the quantum numbers for several levels of the atom energy are shown in Fig. A1.8. 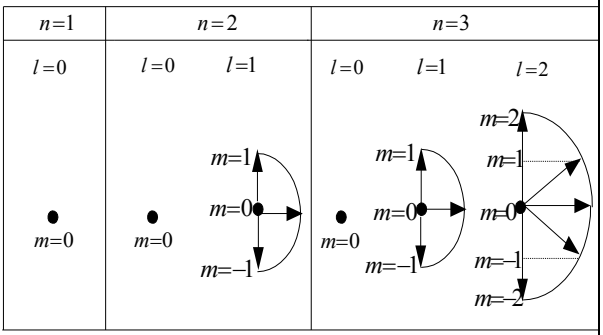 Fig. A1.8. The possible orientations of the electron orbitals
Magnetic tunnel junction	Magnetic tunnel junction (MTJ) consists of a very thin dielectric layer (about 1 nm) sandwiched between two magnetic layers. Each of the magnetic layers has its own magnetic field vector.

	The upper magnetic layer is called the free layer; it may change the vector of its field. The magnetic layer of the base is called the fixed layer, the vector of its magnetic field is blocked and does not change. The direction of the magnetic field vector of the free layer determines the state of the bit as a logical zero or one. If the vectors of the free layer and the fixed layer are oriented in the same direction, then the resistance MTJ structure is a low. If the vectors are antiphase with respect to each other (opposite direction) then the resistance of the MTJ structure is a high. 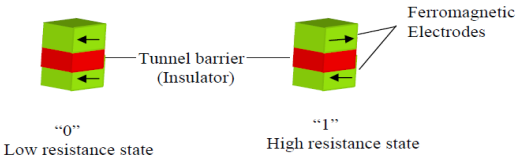 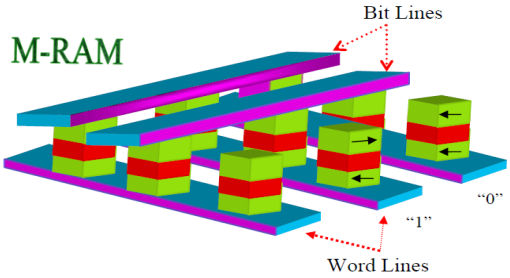 Magnetic tunnel junction is used to create the magnetic random access memory. The value of the MTJ transition resistance determines whether the resistance of the cell will read as "0" or "1", when the read current passes through the cell.
Memristive systems	The concept of the fundamental element, called the memristor [19] is described with the help of such fundamental variables of the electrical circuit as the charge and magnetic flux: $$\Phi(t) = M[q]q(t)\,.$$

Since the values Φ and q may be defined through the time integrals with respect to the voltage $\Phi(t) = \int u(t)dt$ and the currents $q(t) = \int (t)dt$ then we may obtain

$$u(t) = M[q]i(t).$$

In the latter case there is no need for a physical interpretation of the magnetic flux.

Introduced in [20] ratios can be generalized to any class of the two-terminals memristive systems, whose resistance depends on the internal state variables.

Let's assume that $\vec{X}$ is the vector of the state variables describing the internal state of the system:

$$\vec{X} = \left[x_1, x_2, ..., x_n\right]^{\mathrm{T}},$$

$u(t)$ and $y(t)$ are the two main variables (the current, the charge, the voltage or the flux) that define the input and output of the system. Then we can define the generalize class memristive systems of the n-th order, controlled by the voltage:

$$y(t) = g\left\{\vec{X}, u(t), t\right\}u(t), \qquad \frac{d\vec{X}}{dt} = f\left\{\vec{X}, u(t), t\right\},$$

where $g(*)$ and $f(*)$ are the continuous n-dimensional functions.

For the given initial value $u(t = t_0) = u_0$ these equations have a unique solution.

Let's consider the particular case of this system. Let the memristive system of the n-order, controlled by the current, is given by the equations:

$$u(t) = M\left\{\vec{X}, i(t), t\right\}i(t), \qquad \frac{d\vec{X}}{dt} = f\left\{\vec{X}, i(t), t\right\},$$

where, as before, the vector $\vec{X}$ represents n internal state variables, $i(t)$ is the current flowing through the device, $v(t)$ is the voltage at its terminals, M is the memristance of the system.

	A particular case of such memristive system is the device controlled by the charge $q(t)$ when the value M depends on only the charge: $$u(t) = M[q(t)]\,i(t), \qquad \frac{dq}{dt} = i(t).$$ Note that these equations represent one-dimensional case $(x_1 = x = q)$, describing the memristive device.
Mobility of carriers	The electronic conductivity is determined by the presence of the mobile charge carriers that move under the influence of the electric field. The negative charges move from the negative to the positive pole and the positive charges move in the opposite direction, so that the total current is the sum of currents caused by two kinds of carriers: $$I = I_+ + I_-.$$ The ratio of the number of the mobile charge carriers N to the volume V determines the density of the charge carriers n as $$n = \frac{N}{V}.$$ The number of the mobile charge carriers N may be found by the following way. Let's assume that S is the cross-section of the conductor, $\overline{v}$ is the speed of the movement of carriers (drift velocity). Then we can find the value N in the time Δt: $$N = n S \overline{v} \Delta t\,.$$ If each carrier has a single elementary charge (which is not necessarily for the ions), then the carried charge is equal to: $$\Delta Q = Ne = n e \overline{v}\, S \Delta t,$$ where e is the elementary electric charge, equal to $1.602 \cdot 10^{-19}$ Cl.

The current produced by the charge carriers is given by the expression:

$$I = \frac{\Delta Q}{\Delta t} = n e \overline{v} S$$

and the current density is

$$\delta = \frac{I}{S} = n e \overline{v}.$$

Since the magnitude of the current depends on the resistance of the conductor, we can write

$$I = \frac{U}{R} = \left| R = \frac{\rho l}{S} \right| = \frac{US}{\rho l} = \left| E = \frac{U}{l} \right|$$
$$= \frac{ES}{\rho} = \left| \gamma = \frac{1}{\rho} \right| = \gamma ES = \delta S,$$

where γ is the conductivity, E is the electric field intensity, l is the length of the conductor. Thus, the current density δ is proportional to the intensity of the electric field.

Obviously, the drift velocity of the carriers can be defined as

$$\overline{v} = \frac{\delta}{ne} = \frac{\gamma E}{ne}.$$

Then, the mobility of the charge carriers μ is determined by the ratio of the drift velocity to the electric field intensity:

$$\mu = \frac{\overline{v}}{E} = \frac{\gamma}{ne}.$$

The meaning of the product ne can be understood by considering the ratio

$$ne = \frac{N}{V} e = \frac{Q}{V}$$

which determines the spatial charge density.

	Since the dimensions $\bar{v}$ and E are m/s and V/m respectively, then the dimension of the value μ is equal to $\mathrm{m}^2/\mathrm{V}\cdot\mathrm{s}$.
Orbital quantum number	The Orbital quantum number l characterizes the geometric shapes of orbitals and takes the integer values from 0 to $n - 1$. Orbitals, for which $l = 0$ have a spherical shape and are called *s*-orbitals. They are located on all energy levels, and on the first (*K*) level, there is only *s*-orbital. Orbitals, for which $l = 1$ have the shape of an elongated eight and are called *p*-orbitals. They are located on all energy levels, except the first one. Orbitals, for which $l = 2$ are called *d*-orbitals. Their filling up by the electrons begins from the third energy level, etc.
Oxidation / reduction	The process of the return of the electrons, which is accompanied by an increase in the degree of oxidation of the element, is called the oxidation. The process of the joining of the electrons, which is accompanied by a decrease in the degree of oxidation of the element, is called the reduction. The reaction that result of which is the change of the degree of the element oxidation is called the redox reaction. For example, the redox reaction $2\mathrm{Na} + \mathrm{Cl}_2 = 2\mathrm{NaCl},$ passes two stages: • oxidation of sodium $\mathrm{Na} = \mathrm{Na}^+ + e^-, \quad 2\mathrm{Na} = \mathrm{Na}^+ + 2e^-;$ • reduction of the chlorine $\mathrm{Cl}_2 + 2e^- = 2\mathrm{Cl}^-.$ From equations reduction and oxidation processes it can be seen that one chlorine molecule, reducing,

	joins two electrons and the oxidation of two sodium atoms is accompanied by a return of two electrons. In this example, the sodium is a reducing agent (he gives two electrons to reduce the chlorine), and the chlorine is the oxidant (it takes two electrons for the oxidation of the sodium). The number of electrons given by the molecules (atoms, ions) of the reducing agent equals the number of electrons attached by the molecules (atoms, ions) of the oxidant. Obviously, one molecule of the chlorine (Cl_2) can oxidize two sodium atoms.
Pauli principle	According to the Pauli principle the atom can not have two electrons, in which all four quantum numbers n, l, m and s coincide. Using the Pauli principle we can calculate the maximum number of electrons which can be located at different energy levels and sublevels in the atom. The maximum number of electrons in each energy level is equal to $2n^2$. Thus, the K-layer has two electrons ($2 \cdot 1^2 = 2$), the L-layer has eight electrons ($2 \cdot 2^2 = 8$), the M-layer has 18 electrons ($2 \cdot 3^2 = 18$) etc. It should be noted that the obtained numbers coincide with the same number of the elements in the periodic table that is the arrangement of the elements in the periodic table corresponds to the electronic structure of their atoms.
Phase transition	Phase transition is the unique property of some substances: at the heating they may switch between two states: crystalline and amorphous. Crystalline and amorphous states have essentially different values of the resistance/ It property is used to store the information in the respective memory devices. The amorphous state has high resistance unlike the crystalline state which has essentially lower resistance. Such type of the substances is called the chalcogenides. These substances are used in the combination with the germanium, antimony (stibium) and tellurium (GeSbTe) or in the abbreviated form as GST.

Polarization	Polarization is the appearance of the electric dipole moment in the atoms and molecules. In the electric field the centers of the positive and negative charges of the atoms and molecules are displaced and as the result the atoms and molecules have the electric dipole moment which depends on the value and direction of the electric field. The dipole moment occurs as the result of: • displacement of the charges in the atoms (electron polarization); • displacement of the ions (ion polarization); • rotation of the dipole molecules (rotary polarization). There is the linear and nonlinear polarization of the dielectrics. In the first case the dipole moment is proportional to the applied electric field. In the second case the hysteresis of the dependency of the dipole electric moment from the electric field intensity.
Principal (main) quantum number	Spectroscopic measurements show that the energy of the electrons in the same shell ($K, L, M, \ldots$) differs slightly, due to the difference in the shape and location of their orbitals, which can be classified by means of the quantum numbers. The principal quantum number n determines the possible energy states of an electron and assumes the integer values 1, 2, 3, ... When n = 1 the electron has the lowest energy, and with the increase of n the electron energy increases, that is we can say that the quantum number n describes the average distance of the electron from the nucleus. Therefore, the electron state characterized by a defined value of the principal quantum number, is called the energy level of the electron in the atom. At sufficiently great n ($n \to \infty$) the atom energy W_p becomes equal to the potential energy of the electron, infinitely removed from the nucleus: $W_p = U_n$. If $W > W_\infty$ (free movement) the continuous spectrum is obtained which corresponds to the separation of the electron from the nucleus (the ionization of the atom).

	When $W \to W_\infty$ the discrete levels of the energy are highly thickened and their number becomes infinitely large near the ionization boundary. The energy required to remove the electron from the nucleus is determined as $W = W_\infty - W_1$ and represents the ionization energy. The principal quantum number determines the size of the electron "cloud": the large size of the electron cloud corresponds to the more high energy of the electrons in the atom and, therefore, more value of the principal quantum number *n*.
Silicon dioxide	The silicon dioxide SiO_2 is the most stable silicon compound. It occurs in both the crystalline and the amorphous form. The crystalline silicon dioxide exists in nature mostly as the mineral quartz. The transparent colorless crystals have the form of the hexagonal prisms with the hexagonal pyramids at the ends. The crystalline silicon dioxide is very solid and melts at 1728° C, turn into the colorless liquid. If this liquid is cooled then the transparent glassy mass of the amorphous silicon is obtained. The crystals of the high-purity silicon having a minimum number of the structural defects are characterized by very low conductivity. The impurities and violations of the structure sharply increase its conductivity. This property is used in the semiconductor technology, particularly when creating the nonvolatile memory such as PCRAM. The semiconductor silicon-based devices can withstand heating up to 250° C, which expands the area of their application.
Spin quantum number	Spin quantum number *s* characterizes the orientation of the own rotation of the electron with respect to the direction of its orbital rotation. The possible values of *s* are equal to $+1/2$ and minus $1/2$. The positive value corresponds to the same direction of the own and orbital rotation. The negative value corresponds to the opposite their direction.

	The values of the angular moment of the electrons rotating to the left or to the write differ by the value $\Delta M_e = h/2\pi$ according to the bohr quantization condition $M = n\frac{h}{2\pi}$. It means that the angular moment of the electron rotating around the nucleus is divisible by Plank's constant divided by 2π. Thus the own spin angular moment of the electron is equal to $M_e = \pm\frac{1}{2}\frac{h}{2\pi} = s\frac{h}{2\pi}$.
Spintronics	Spintronics is the section of the quantum electronics studying the so called spin polarized transport (spin polarized current) in the solid-state substances (particularly in the heterostructures ferromagnetic-paramagnetic or ferromagnetic- superconductor type). In such structures the source of the spin- polarized electrons is the conductive ferromagnetic which in the magnetized state has the spontaneous spin order of the charge carriers. In the ferromagnetic semiconductors the level of the spin polarization are higher (up to 100%) than in the metals (up to 10%). In the external magnetic field the Zeeman splitting of the conductance band is possible/ In this case two zeeman energy sublevels are formed. If the spin- polarized electrons are injected in such semiconductor then the controlled transitions on both upper and lower levels are possible. In this case it is the possibility to create the population inversion and the generation of the coherent electromagnetic radiation with the control of the frequency by means of the magnetic field.
Standing wave	If two waves spread simultaneously in the same medium in the opposite directions then the standing wave is formed. At the same time it is assumed that these waves have about the same amplitudes, frequencies and wave lengths. For example the standing waves occur at the addition of the incident wave (one-dimensional case is

considered) and the reflected one. The equation of the incident wave in this case may be written in the form:

$$u_{\text{inc}} = U_{\max} \sin 2\pi\left(\frac{t}{T} - \frac{x}{\lambda}\right),$$

and the reflected wave is given by the expression:

$$u_{\text{ref}} = U_{\max} \sin 2\pi\left(\frac{t}{T} + \frac{x}{\lambda}\right),$$

where x is the one-dimensional coordinate of the distance, $\beta = \frac{2\pi}{\lambda}$ is the phase coefficient.

Then the resulting wave is written in the form:

$$\begin{aligned} u(x,t) &= u_{\text{inc}} + u_{\text{ref}} \\ &= U_{\max}[\sin(\omega t - \beta x) + \sin(\omega t + \beta x)] \end{aligned}$$

The sinus addition theorem gives;

$$\begin{aligned} u(x,t) = U_{\max}[&\sin\omega t \cos\beta x - \cos\omega t \sin\beta x \\ &+ \sin\omega t \cos\beta x + \cos\omega t \sin\beta x] \\ &= 2U_{\max} \cos\beta x \sin\omega t \end{aligned}$$

This expression defines the sinusoidal oscillation with the amplitude $2U_{\max}\cos\beta x$ which depends on the distance x.

At the defined values of x (in the several points) the amplitude equals $2U_{\max}$ but at other defined values of x it is equal to zero. These points are the fixed on the x axis and are placed one after another on the distance equaled $\frac{\lambda}{2}$.

The points in which the amplitude always equals zero are called the wave nodes and the points where the amplitude is always equal to $2U_{\max}$ are called the wave loops.

If the medium has the confined size l then the standing wave is formed only in the case when the

	value l is multiple to the integer of the half wave $\frac{\lambda}{2}$, Fig. A1.9. 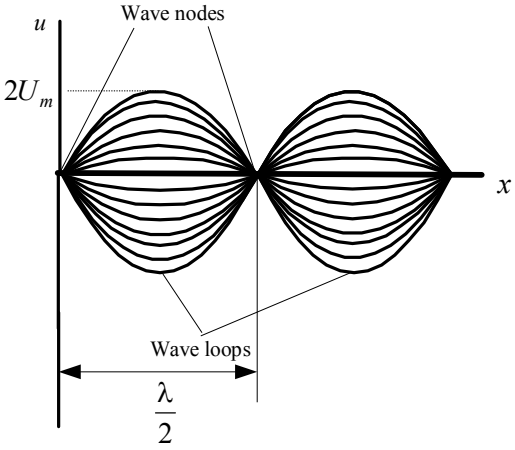 Fig. A1.9. The voltage standing wave (one-dimensional case)
State variable	Any dynamical system is described by the system of differential equations of the first order in the state space. For example, in the two-dimensional case the system of equations is written in the form: $$\frac{dx_1}{dt} = f_1(x_1, x_2), \qquad \frac{dx_2}{dt} = f_2(x_1, x_2),$$ where x_1 and x_2 are the state variables that uniquely characterize the behavior of the dynamic system. As a rule, the variables which are clearly associated with the energy of the system are selected as the state variables. For example, in the electrical and electronic circuits the state variables are the current in the inductive coil $i_L(t)$ associated with the magnetic energy, and the voltage across the capacitor $u_C(t)$ associated with electrical power.

	The number of the state variables determines the number of the first order differential equations the solution of which represents the time functions of change of these variables. To model the processes in the ReRAM memory cell the thickness of the titanium dioxide is used as the state variable which is changed in the time depending on the applied voltage (see section 2.1). In this case the state equation is written in the form: $$\frac{dw}{dt} = f(w).$$ To model the processes in the PCRAM memory cell the temperature T and the crystallization coefficient C_y are used as the state variables and the state equations are written in the form: $$\frac{dT}{dt} = f_1(T, C_x), \qquad \frac{dC_x}{dt} = f_2(T, C_x).$$
Stoichiometry	In the stoichiometric compounds the chemical elements present in the strictly defined ratios (the compounds of the stoichiometric composition). For example the water H_2O is the stoichiometric compound (and practically all organic compounds). If the deviations (infringements) from the stoichiometric law are observed then such substances are called nonstoichiometric ones. So the titanium oxide (II) has the alternate composition in which from 0.65 up to 1.25 oxygen atoms may account for one atom of the titanium.
Titanium dioxide	Titanium atom has two electrons in the outer layer, and in the second outside layer has 10 electrons, the two of which are located on the *d*-sublayer. Therefore, the most characteristic the degree of the oxidation of the titanium is equal to +4. The titanium dioxide TiO_2 (rutile) is the white refractory material, widely used in the industry, particularly in nanoelectronics. The fusion of the TiO_2 with the $BaCO_3$ gives the barium titanate $BaTiO_3$. This salt has a very high

	dielectric constant and, in addition, has the ability to the deform under the action of the electric field. It is also used in nanotechnology.
Transition metals (transition elements)	Transition metals are the elements of the second subgroup of Periodic system of the chemical elements which contain the electrons in atoms on the *d*- and *f*-orbitals. The peculiarities of the transition metals are defined first of all by the electron structure of their atoms which is represented by the following formula: $$(n-1)d^x ns^y ,$$ where n is the main quantum number, *d* and *s* are the energy sublevels which are characterized by the value of the orbital quantum number: $l = 0$ for *s*-electrons and $l = 2$ for *d*-electrons. One or two electrons are located on the *ns*-orbital and the remaining valency electrons are located on the $(n-1)d$ orbital. Since the number of the valency electrons is essentially less than the number of orbitals then the ordinary substances formed by the transition elements are the metals. The basic transition metals are shown in the table. The low values of the ionization energy of the atoms (7–8 eV) indicate on the relatively weak bond of the external electrons with the nucleus. That is why the transition metals in the formed compounds have the positive oxidability and are represented as the metals. However the essential distinction is between the metals of the main and the second subgroups. They are connected with the peculiarities of the electron structure: in the second external layer of their atoms there is *d*-sublevel which is not fully occupied by the electrons. To form the chemical bonds the atoms of the transition metals may use both the external electron layer (it takes place in the elements of the main subgroups) and the free *d*-orbitals of the previous layer. Therefore the alternate valency is more typical for the transition metals unlike the metals of the main subgroups.

Group / Period	III	IV	V	VI	VII	VIII			I	II
4	Sc	Ti	V	Cr	Mn	Fe	Co	Ni	Cu	Zn
5	Y	Zr	Nb	Mo	Tc	Ru	Pd	Rh	Ag	Cd
6	*	Hf	Ta	W	Re	Os	Rt	Ir	Au	Hg
7	* *	Rf	Db	Sg	Bh	Hs	Ds	Mt	Rg	Cn

*lanthanides * *actinium series

Vacancies

Vacancies are the unoccupied nodes of the crystal lattice. The individual atoms or ions of the lattice have the energy which is higher than its average value at the given temperature. Such atoms oscillate more intensively than others and can move from one place to another, for example, from the lattice node into the place between the nodes. The unfilled place where he had previously been is called a **vacancy**. At any time moment the adjacent to the vacancy atom can move in

	the vacancy place, created a new vacancy. Thus, the vacancies move from one place to another and are the carriers of the electric current. The vacancies may be formed by the so-called point defects in the crystal structure of the real crystals, when the spatial periodicity of the internal structure of the crystal is disturbed.
Vacuum deposition	**Vacuum deposition** is the deposition of the thin films in a vacuum by means of condensing from the vapor (gas) phase (physical vapor deposition). In this case the covering is obtained by direct condensation of the vapor of the deposited material. The following stages of the vacuum deposition may be chosen: • creation of the gas (vapor) from the particles that form the covering; • condensation of the vapor on the substrate and forming covering. The group of the vacuum deposition methods includes: • evaporation by means of the electron beam; • evaporation by means of the laser beam (pulsed laser deposition, pulsed laser ablation); • evaporation by means of the vacuum arc (cathode arc deposition, Arc-PVD), in which the material is vaporized in the cathode spot of the electric arc; • molecular beam epitaxy; • sputtering, in which the initial material is sprayed by the ion stream bombardment on the substrate. Magnetron sputtering is one of type of ion sputtering in the nanoelectronics technologies, which is used for obtaining conductive layers (metallization).
Valence	The relation between the valence of the element and its position in the periodic system of elements was set by Mendeleev He also introduced the concept of the variable valence. With the development of the theory of the atomic and molecular structure the concept of the valence get the physical justification. The general definition of the valency is the following. The valency of the element is ability its atoms to join with other atoms in the defined proportions.

Valence band and the conduction band	In the metal crystal (for example, in the crystal of Cu) the atomic orbits of the internal electron layers (K, L, M) are practically overlap. We can assume that in this case, the continuous energy band is created only by the orbitals of the outer electron layer and filled by the electrons of this layer. In the crystal containing N atoms the initial atomic s-orbitals of the outer layer form the energy band consisting of the N levels. In this band N outer s-electrons of the copper atoms are located and occupy $\frac{N}{2}$ energy levels (two electrons are in each level according to the Pauli principle). The totality of these levels occupied by the valence electrons is called the **valence band**. In this case, the valence band occupies only half of the available energy levels. Unfilled levels form the **conduction band**. This means that the free levels, on which the electrons can pass on under acting the electric field are located in the vicinity of the upper occupied levels. This creates the possibility of the current transport by the electrons, providing the electrical conductivity of the metal, Fig. A1.2, *a*. In a crystal, such as titanium, the band consisting of the N levels is formed from the initial atomic $s-$orbitals of the outer layer. But since each atom has two outer $s-$electrons, then in this band the $2N$ electrons must be placed, so that all its levels will be fully occupied. However, under the interaction of the metal atoms not only the external $s-$orbitals, but the external p-orbitals are overlap. As a result, the continuous energy band also is formed, not filled by the electrons. The bands formed s- and p-orbitals are overlap as well, Fig. A 1.2 *b*. In this case, the conduction band containing the free energy levels, which immediately are adjacent to the valence band and therefore the considered crystal must also have high electrical conductivity. Although the Fig. A1.10 shows a sharp boundary between the valence band and the conduction band, in fact, this boundary is blurred, and as a result of the

	thermal motion of the electrons they can pass from the upper levels of the valence band on the lower levels of the conduction band. The ability of these electrons to move freely through the crystal and to transfer the energy from one part of the crystal (heated) to another (cooler) is the cause of the high thermal conductivity of the metal. 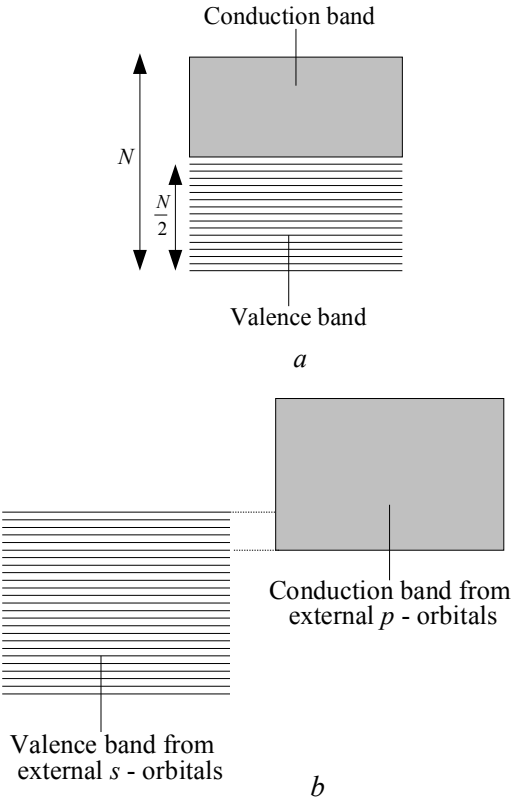 Fig. A1.10. Energy zones
Wave function	In quantum electronics the wave function is determined by the solution of the Schrödinger equation: $$\nabla\psi(x,y,z)+\left(\frac{2c}{r}-\lambda^2\right)\psi(x,y,z)=0.$$

	In the coordinate representation the wave function $\psi(x_1, x_2, ..., x_n, t)$ depends on the coordinates of the system. The wave function has no the physical meaning, but the physical meaning is ascribed to the square of its absolute value $\left|\psi(x_1, x_2, ..., x_n, t)\right|^2$, which is interpreted as the probability density ω (for discrete spectra simply the probability is considered) of finding the system in the position described by the coordinates $x_1 = x_{01}, x_2 = x_{02}, ..., x_n = x_{0n}$ at the time moment *t*: $$\omega = \frac{dp}{dV} = \left|\psi(x_1, x_2, ..., x_n, t)\right|^2 = \overset{*}{\psi}\psi.$$ Then, for the system described by a wave function, we can calculate the probability that the particle will be found in any area of the final volume of the configuration space: $$p = \int dp = \int_V \omega dV = \int_V \overset{*}{\psi}\psi dV$$
ReRAM	The nonvolatile memory based on the switching of the active layer placed between the two metal electrodes from the state with high resistance value (HRS) into the state with low resistance value (LRS) and vice versa by means of the respective voltage levels applied to the active layer. These states are formed due to the reduction-oxidation reactions (redox) in the oxides of the transition metals. The HRS and LRS states are the base of the information storage.
PCRAM	The nonvolatile memory based on the unique property of the chalcogenide which switches between the crystalline and amorphous states at the heating. These states differ by the resistance values which are the base of the information storage. The amorphous state having high level of the resistance is used to store the binary number “0”. The

	crystalline state having low level of the resistance is used to store the binary number "1".
MRAM	The nonvolatile memory stores the information by means of the magnetic moments and is based on the magnetic tunnel junction effect (MTJ) which is provided by the wave character of the electron having the spin. It leads to the spin-depended tunnel effect. The memory cell (magnetic element) consists of the two ferromagnetic layers separated by the insulator. One of the layers is magnetized in the defined direction (permanent magnet) and the magnetization of the second layer is changed under the action of the external magnetic field. The reading of the information ("0" or "1") is carried out by means of the measuring of the cell electric resistance (low or high values).
FeRAM	This type of the nonvolatile memory is based on the property of the ferroelectric to keep the permanent polarization after switching off the external electric field. It is the base of the information storage. The ferromagnetic is the material which has the hysteresis of the dependency of the electric moment from the electric field intensity. If the positive electric charge acts then the positive polarization of the ferroelectric occurs. As a result this state of the ferroelectric corresponds to the logical "0". If the negative electric charge acts then the inverse transition occurs that corresponds to the logical "1". The base of the memory cell is the ferroelectric transistor and capacitor.
CeRAM	This type of the nonvolatile memory is one of the resistive memory type based on the quantum effects of the correlation of electron position (the name "Correlated electron RAM" follows from here that is the memory with the correlated electron). The relationship between the energy of the coulomb interaction U and the kinetic energy of the electrons W defines the transitions metal/insulator/ metal.

	It in one's turn defines the resistance of all structure. If $U > W$ then the structure has the conductive state. If $U < W$ the structure becomes the insulator.
Racetrack Memory	It is one of new technologies of the data storage which is based on the spintronic effects. In particularly the spin current is used to transfer the nanosized magnetic objects within the magnetic nanoconductors which may be placed aflat or upright (3D-architecture). Under acting the spin current the domain walls move along the nanoconductor. If we compare with the well known moving magnetic tape on which the regions of various magnetization are located then the difference is defined by the motionless "tape" (nanoconductor) but the regions of magnetization are moved. When the current passes through the magnetized material it becomes by the spin-polarized current and begins to turn round "small magnets" in some side. As a result the domain wall is shifted at that the direction of the shift for all walls is the same. If the nanoconductor has some order of walls then they will move under the action of the spin-polarized current with the same speed. The memory cells which are the nanoconductors of the fixed length (about 200-300 nm). They are set on the silicon substrate above the individual reading and writing elements. These elements are formed on the base of the magnetic tunnel junctions. One of two possible directions of the magnetization is chosen as "0" then the second direction will correspond "1". If the set of the pulses of the spin-polarized current is applied to the nanoconductor then the domains will move and the change of the resistance on the reading element will fix the sequence of "0" and "1". To write the information in the needed time moments the current pulses are applied to the writing element. They shift the domain walls in the nanoconductor and rearrange the domain structure according to the written information.

	It is necessary to note that in new applications of the spintronics the new concept "skyrmion" is introduced. Skyrmions (topologically nontrivial configuration of the magnetic spin of a vortex-like structure) may be another basis for magnetic storage technology with the use of the Hall skyrmion effect. The modern hard drives for storing information use the magnetic domains whose minimum physical size of up to 100 nm. Skyrmions are more stable structures the size of which can be reduced to a few nanometers. It allows to increase considerably the data storage density. Skyrmion effect will be used in future spintronics applications such as the Racetrack Memory and the logic devices.
NRAM (Nantero RAM)	This type of the nonvolatile memory is one of the resistive memory type based on the use of the thin films as the memory cells on which the matrix of the carbon nanotubes are placed. 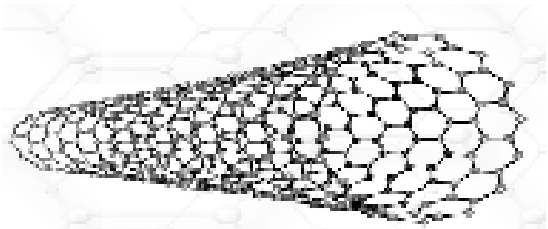 The carbon nanotube is the tiny cylinder of 2nm diameter. In the reset state the stick-like carbon nanotubes are separated from each other. When the voltage pulse of the defined polarity is applied to the cell they create the contact due to the Van-der-Vaals forces. Then the number of conductive ways between the electrodes increases (nanotubes are the conductors) and the resistance of the structure essentially decreases. The voltage pulse of another polarity is used to break the conductive ways and the matrix of nanotubes has the high resistance state (HRS).

	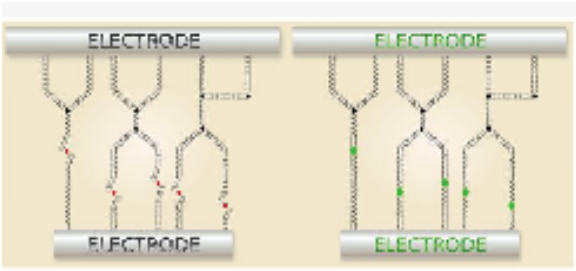 nonconductive state conductive state The mechanical deformation of the nanotubes is low in the off state therefore they keep the nonconductive state and in that way the logical “0”is stored. When the voltage pulse of the respective polarity is applied to the upper electrode the nanotubes are attracted and deformed and in that way the logical “1” is stored.

STATE OF THE ELECTRON IN THE REAL ATOM

The creation of the quantum mechanics occurs in the way of the generalization of the representation about the wave-particle duality of the photon to all objects of a microcosm and, above all, on the electrons.

Corpuscular photon properties are determined by the equation of Planck:

$$E = h\nu ,$$

according to which the photon is indivisible, and exists as a discrete formation. The wave properties of the photon can be expressed by the equation:

$$\lambda\nu = c ,$$

which connects the wave length λ of the electromagnetic wave with its frequency and speed of the propagation c. The concept λ implies that a photon has wave properties.

From these equations we can obtain a relation between the corpuscular characteristic of the photon E with its wave characteristic λ :

$$E = \frac{hc}{\lambda}.$$

It is known that a photon has a certain mass m in accordance with the Einstein equation:

$$E = mc^2 .$$

From the last two equations that

$$\lambda = \frac{h}{mc}.$$

French physicist de Broglie suggested that the obtained equation is valid not only for photons but and for electrons. Consequently, we can write for the electron mass m and speed v:

$$\lambda = \frac{h}{mv}.$$

This equation is called the equation of de Broglie, which says that the electron has the wave properties, and that was confirmed experimentally in studies of the interaction of the electron beam with the gitter (the metal crystals are used as the gitter). The resulting diffraction image was the same as under the action of the X-ray beam on the metal crystal lattice. In these experiments, electrons behave like a wave, the length of which corresponds exactly to the de Broglie equation.

Based on the idea that the electron has the wave properties, Austrian physicist Schrodinger suggested that the state of a moving electron should be described by the equation of the standing electromagnetic wave known in physics and electrical engineering. He get the equation which relates the energy of the electron with the spatial coordinates (x, y, z) with some wave function ψ corresponding in this equation to the amplitude of the three-dimensional wave process, the value ψ^2 is proportional to the probability of finding the electron in a certain region of the space.

From the probabilistic standpoint the location of the electron is "blurred" on the entire volume of the atom in the form of so-called electron cloud (for example, considering the hydrogen atom which has only one electron). The denser the points are located in the some place of the cloud, the higher the probability of finding the electron there.

The electron state can be considered as some cloud of the electrical charge around an atom, which has not exact boundaries. Even at great distances from the nucleus a certain (very small) probability of finding an electron exists. Since the electron can not go beyond the atom (the electron in an atom is stable), it can be assumed that the boundaries of its movement are fixed. Due to the fact that the electron has the wave properties, the electron oscillations form a standing wave (similar to the oscillations of a string fixed at both ends, when we consider as a simple physical analogy, one-dimensional case).

Similarly, if we consider the simplified one-dimensional model of the atom (the electron oscillates between extreme points), then the de Broglie wave must be standing one, and on the boundaries of the atom the wave function ψ (that is the amplitude of the wave) must be

equaled zero. The one-dimensional model of the atom with the standing de Broglie waves, which can be formed in this atom is shown in Fig. A.2.1.

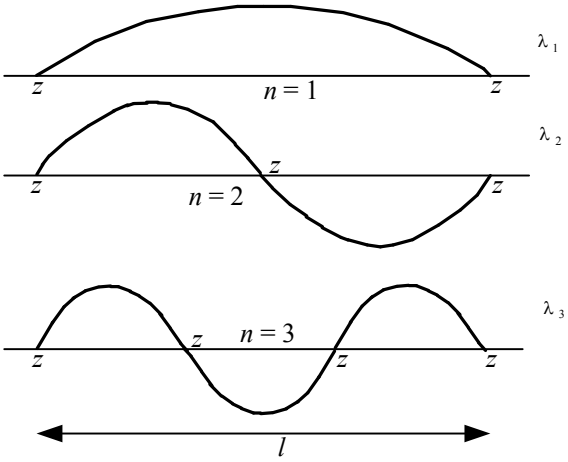

Fig. A2.1. The de Broglie waves for different values n

If the length of the one-dimensional atom is l then for the considered three cases the de Broglie wave length is determined by the following expressions:

$$\lambda_1 = 2l = \frac{2l}{1}, \quad \lambda_1 = l = \frac{2l}{2}, \quad \lambda_1 = \frac{2}{3}l.$$

Consequently, the standing wave can be formed only under the condition

$$\lambda = \frac{2l}{n},$$

where n = 1, 2, 3,… is integer.

On the other hand, according to the equation of de Broglie

$$\lambda = \frac{h}{mv}.$$

Equating the right-hand sides of the last two equations, we obtain for the electron speed the following expression:

$$v = \frac{h}{2ml} n .$$

Knowing the speed of the electron v we can find its kinetic energy E:

$$E = \frac{mv^2}{2} = \frac{h^2}{8ml^2} n^2 .$$

As n is an integer, it is evident that the electron energy in the one-dimensional atom may not have an arbitrary value, it is quantized (when $n = 2$ it is 4 times greater, when $n = 3$ it is 9 times greater, etc.).

Thus, the wave properties of electrons define the quantization of its energy states. This allowed the electron energy levels are determined by the value n of an integer, called the **main quantum number**.

In a one-dimensional model the stationary state of the atom is characterized by the formation of a standing wave of de Broglie. As long as the wavelength is kept constant the state of the electron remains unchanged and the radiation does not occur.

In the process of transition of an electron from one state to another, the de Broglie wavelength will have a variable value does not correspond the condition of the formation of a standing wave. That is why the state of the electron in this period will be unstable and will change as long as the de Broglie wavelength will again correspond the condition of the formation of a standing wave (while the electron will not appear in the new steady state).

In a simplified one-dimensional model the position of the electron relative to the nucleus of an atom is determined by the one coordinate (in this case, the coordinate z), and its state is determined by the value of one the quantum number. In the two-dimensional (flat) model of the atom the electron position is determined by the two coordinates, according to this, its condition is characterized by two quantum numbers.

Similarly, in the three-dimensional model of the atom the electron state is determined by the three quantum numbers. However, the study of the properties of the electrons of the real atoms showed that the electron has one more quantized physical characteristic (spin) is not connected with the spatial position of the electron.

Thus, for a complete description of the state of an electron in a real atom it is necessary to indicate the values of the four quantum numbers.

The energy of an electron in the real atom is the quantized value as well. The possible energy states of an electron in an atom are determined by the value of the main quantum number. The electron has the least energy when $n = 1$. With the increase of n the energy of the electron increases. The condition of the electron is called the electron energy level in the atom (when $n = 1$ the electron is placed on the first energy level, if $n = 2$ the electron is placed on the second level, etc.).

The main quantum number determines the size of the electron cloud. In order to increase the size of the electron cloud, it is necessary to remove the part of the cloud (to expand) on the greater distance from the nucleus. The forces of electrostatic attraction of the electron to the nucleus prevent this process, the overcoming of which requires energy. Therefore, the large size of the electron cloud corresponds to a higher energy of the electron in the atom and, therefore, the greater value of the main quantum number n.

Electrons, which are characterized by the same main quantum number, form in the atom the electron clouds of the same size. Therefore, it is said that the atom contains the electron layers or electron shells which correspond certain values of the main quantum number.

The following symbols are assumed for the energy levels of the electron in the atom (for the electron shells), corresponding to different values n:

n	1	2	3	4	5	6	7
Designation of the energy level	K	L	M	N	O	P	Q

So, the energy of the electron in the atom (and respectively the electron cloud size) can take certain values. However the shape of the electron cloud can not be arbitrary as well. It is determined by the **orbital quantum number** l (the orbital number which can take integer values from 0 to $n - 1$ (the second parameter from the four)). The different number of possible values l corresponds to different values n. So when $n = 1$ it is possible only one value of the orbital quantum number equaled zero ($l = 0$). In general, n different possible values of the orbital quantum number correspond to the given value n.

The physical meaning of the orbital quantum number l is that it defines the value of the orbital angular momentum of the electron $\vec{M}$. This value (as well as the energy) is the quantized physical characteristic of the state of the electron in the atom.

As is known, the orbital angular momentum $\vec{M}$ of the particle, which moves around the center of rotation on some orbit, is given by the relationship:

$$\vec{M} = m[\vec{v}\vec{r}].$$

According to the vector product, the value $\vec{M}$ is a vector quantity, and the direction of the vector $\vec{M}$ is perpendicular to the plane in which the vectors $\vec{v}$ and $\vec{r}$ are located, Fig. A2.2 *a*.

Since the value *l* is the integer, the vector $\vec{M}$ can only take the discrete values; consequently, the shape of the electron clouds can not be arbitrary. This means that a well-defined form of cloud corresponds to respective possible value *l*, Fig. A2.2*b*.

It is evident that *n* shells of the various shape corresponds to the main quantum number *n*: one circular shell and $(n - 1)$ elliptical shells.

In each orbit the electron has a definite energy. The angular momentum of the electron on the orbit is always an integer: $M = l\bar{h}$, where $\bar{h} = h/2\pi$ (Bohr quantization condition). The quantum number *l* can take the values 0, 1, 2, 3. . . $(n - 1)$ .The designation of the orbits the numbers are replaced by the letters:

Orbital quantum number *l*	0	1	2	3	4	5	6	7
Designation of the energy sublevel	*s*	*p*	*d*	*f*	*g*	*h*	*l*	*k*

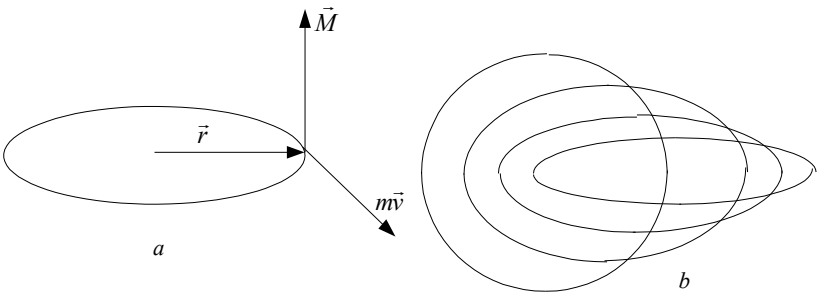

Fig. A2.2. The shapes of the electron cloud

The electron speed changes when it moves on the elliptical orbit, consequently its relativistic mass change as well. This explains the slight difference of the electron energies on the different elliptical orbits. Quantum mechanics leads to a more precise expression for the orbital angular momentum $M = \sqrt{l(l+1)}\ \hbar$.

It is obvious that for a given value of the main quantum number n *s*-electrons have the lowest energy, and then *p*-, *d*-, *f*-, …, *k*-electrons follow. The state of the electron in the atom is denoted as follows: the designation $2p$ refers to the electron, for which $n = 2,\ l = 1$, the designation $3d$ refers to the electron, for which $n = 3, l = 2$, etc.

As mentioned above, the electron cloud is not sharply defined boundaries in space. Let's consider as an example the electron cloud of 1*s*-electron in the hydrogen atom. It is obvious that with increasing distance r from the nucleus the value ψ^2 monotonically decreases. However, this does not mean that the probability of finding the electron is also monotonically decreases with the increase of the distance r.

With the growth of r the value ψ^2 decreases, but at the same time the volume increases, and the probability of finding the electron in a small volume is defined as $\psi^2 \Delta V$. Since $\Delta V = 4\pi r^2 \Delta r$, therefore, the probability of detection of the electron in a spherical layer, and between r and $r + \Delta r$ is proportional to the value $4\pi r^2 \psi^2$. For small values of r the value $4\pi r^2$ increases more rapidly than the value ψ^2 decreases; at large values it occurs on the contrary. The graph of the probability distribution of the 1*s*-electron is shown in Fig. A2.3.

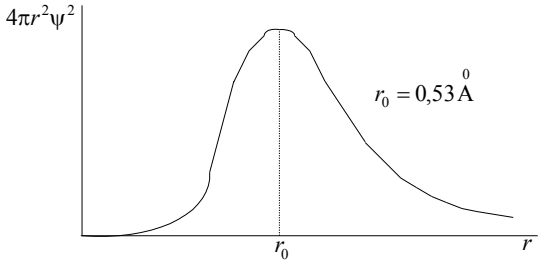

Fig. A2.3 The graph of the probability distribution of finding electron in the hydrogen atom

From the standpoint of quantum mechanics, the distance $r_0 = 0,53\,\text{Å}$ (r_0 is the Bohr radius of the nearest to the nucleus orbit of the electron in the hydrogen atom) corresponds to the maximum probability of finding the electron.

The electron clouds of the *s*-electrons of the second, third and following layers have the spherical symmetry as in the case of 1*s*-electrons. However, in these cases, the wave function on the distance changes more complicated manner. It is not monotonous, and the graphs of the radial probability distribution have several maximums. The electron cloud of 2*s*- and 3*s*-electrons of the hydrogen atom is schematically shown in Fig. A2.4. In this case the main maximum is located farther from the nucleus, the greater the value of the main quantum number *n*.

Consider now the structure of the electron cloud 2*p*-electron (in this case $n = 2$, $l = 0$ and $l = 1$ so that 2*s*- and 2*p*-electrons can be in the cloud). In contrast to the *s*-electron the wave function is not spherically symmetric. In this case the height of the maximums (on the one side of the nucleus) and minimums (on the other side of the nucleus) depends on the chosen direction of the radius-vector $\vec{r}$, Fig. A2.5.

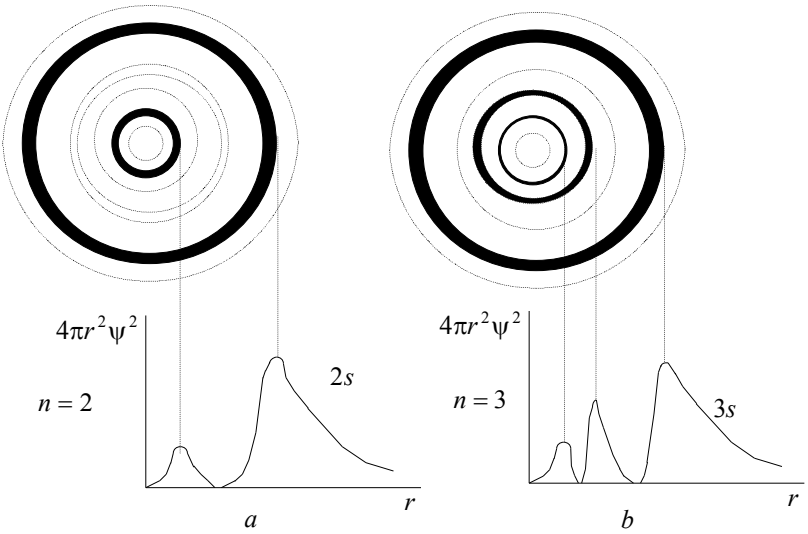

Fig. A2.4. The graphs of the electron cloud of 2*s*- and 3*s*-electrons

In a certain direction (for example let's choose the coordinate x) the height of the maximum is the greatest (Fig. A2.5, curve *1*). In the directions, which make a some angle with the axis x, then the height of the maximum the greater this angle the smaller (curve *2*). If it equals 90°, the value of the function ψ in this direction is equal to zero at all distances from the nucleus.

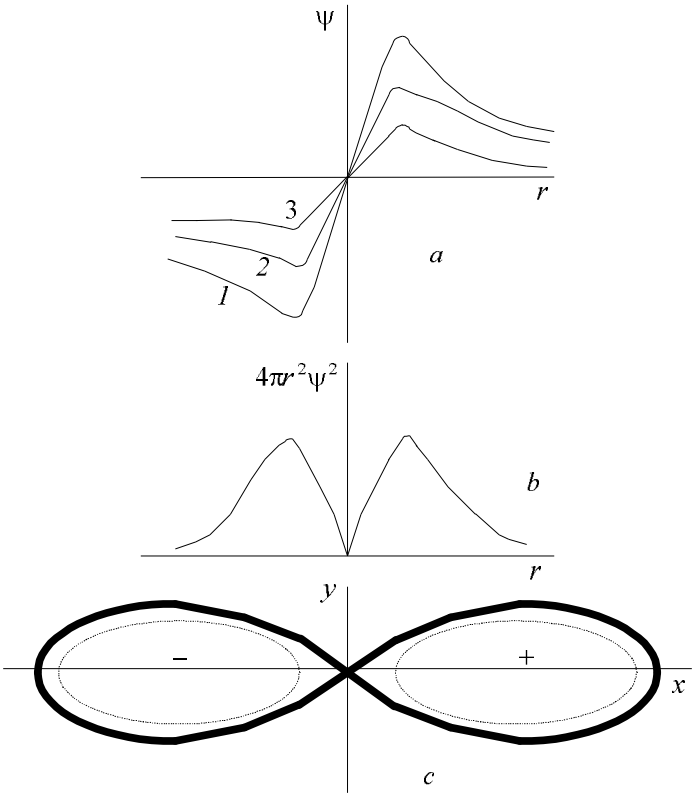

Fig. A2.5. The graphs of the functions ψ and ψ^2 for 2*p*-electrons

The graph of the radial distribution of the probability is shown in Fig. A2.5*b*. The position of the maximum is independent from the choice of the direction. However, the height of this maximum depends on the direction: it is greatest when the direction $\vec{r}$ coincides with the direction of x axis.

The shape of the electron cloud, as shown in Fig. A2.5*c* corresponds to the distribution of the probability of finding the 2*p*-electron. The signs relate to the wave function ψ, which has the different sign in the different parts of the electron cloud. The electron cloud is concentrated near the *x*-axis and in the *xy*-plane which is perpendicular to this axis, the electron cloud is absent: the probability of finding the 2*p*-electron here equals zero.

More complex shapes have 3*p*-, 4*p*-electrons and *d*-electrons as well ($l = 2$).

Thus, the sizes and shapes of the electron clouds in the atom can not be arbitrary, but only those which correspond to the possible values of the quantum numbers *n* and *l*.

It follows from the Schrodinger equation that the orientation of the electron cloud in the space can not be arbitrary as well and is determined by the value of the third quantum number, which is called the **magnetic quantum number** *m*.

The magnetic quantum number can take on both positive and negative integer values in the range from + *l* to minus *l*. In general, a certain value *l* corresponds to $2l + 1$ possible values of the magnetic quantum number that is $2l + 1$ possible locations of the electron cloud in the space. For example, when $l = 2$ (*d*-electrons) the value *m* can take 5 different values: (–2, –1, 0, 1, 2).

As is known, the value of the orbital angular momentum vector $\vec{M}$ of the electron (the length of the vector) is determined by the value of the orbital quantum number *l*. From the Schrödinger equation it follows that the direction of the vector $\vec{M}$, which characterizes the spatial orientation of the electron cloud is also quantized (it can not be arbitrary).

The electron which moves on a closed orbit is equivalent to a circular current, the magnetic field of which interacts with the external magnetic field. The plane of the electron orbit takes certain positions, which are characterized by the magnetic quantum number.

The orientation of the orbit is defined by the angle δ between the magnetic field direction and the axis which is perpendicular to the orbital plane, Fig. A2.6. The angle of the orbit inclination is determined by the condition $\cos\delta = m/l$. Quantum mechanics gives a more precise expression for this angle: $\cos\delta = m/\sqrt{l(l+1)}$.

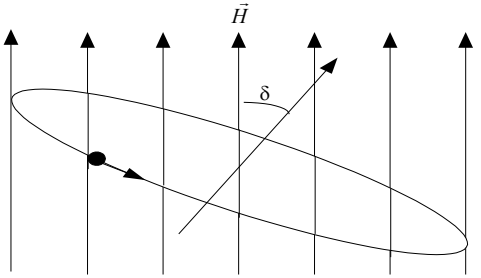

Fig. A2.6. The orientation of the orbit of the electron

If we consider the orbital quantum number as a vector $\vec{l}$ (characterizing the direction of the orbital angular momentum $\vec{M}$), there may be only such orientation of the orbit in space, which corresponds to an integer value m of the projection of the vector $\vec{l}$ on the direction of the magnetic field, Fig. A2.7.

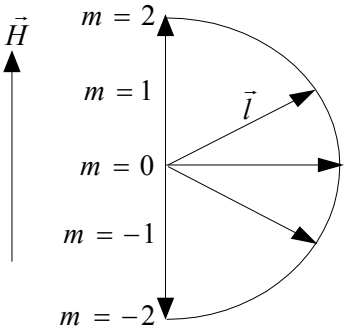

Fig. A2.7. The vector representation of the orbital quantum number

The case when $l = 2$ (the length of the vector $\vec{M}$ is given by the value $l = 2$ and is the same) is shown in Fig. A2.7.

The quantum number m has been called as the magnetic one because its value defines the interaction of the magnetic field generated by the electron in motion with the external magnetic field.

Example. Let's assume that the orbital quantum number $l = 2$. The magnetic quantum number m can take on $2 \cdot 2 + 1 = 5$ different values. As a result, we get:

Magnetic quantum number m	–2	–1	0	+1	+2
Ratio $\frac{m}{l}$	$\frac{-2}{2}$	$\frac{-1}{2}$	$\frac{0}{2}$	$\frac{+1}{2}$	$\frac{+2}{2}$
$\cos\delta$	–1	–0.5	0	0.5	+1
Angle of inclination of orbit δ	180°	120°	90°	60°	0°

If the external magnetic field is absence then the energy of the electron in the atom does not depend on the value *m*, that is the electrons with the same values *n* and *l*, but with the different values *m* have the same energy. However, under the action of the external magnetic field their energies differ for the different values of the number *m*. This means that the interaction energy of the magnetic field of the electron with the external magnetic field depends on the magnitude of the magnetic quantum number. That is why there is a Zeeman effect (splitting of certain atomic spectral lines in the magnetic field), which is used in the quantum electronics [104].

State of the electron in the atom, which is characterized by certain values and quantum numbers *n*, *l* and *m* (the state is determined by the size, shape and orientation in the space of the electron cloud) is called the **atomic electron orbital**.

As an example, Fig. A2.8 shows the shapes and location in the space of the electron clouds which correspond 1*s*-, 2*p*- and some 3*d*-orbitals. Since a single value of the magnetic quantum number ($m = 0$) corresponds to the *s*-state ($l = 0$), then any possible positions of the *s*-electron cloud in the space are the same.

Electron clouds corresponding *p*-orbitals ($l = 1$) may be characterized by three different values *m*, and therefore they may be positioned in the space in three different ways, etc.

The study of the atomic spectrum led to the conclusion that, in addition to the quantum numbers *n*, *l* and *m* electron is characterized by another quantum value which is not related to the motion of the electron around the nucleus. This value determines its own state, and is called the **spin quantum number**, or simply spin (spin-rotation). The electron spin can have only two values, $+1/2$ and $-1/2$. It is evident that the possible values of the spin quantum number differ by one $\left(\frac{1}{2}-\left(-\frac{1}{2}\right)=1\right)$, as for the rest quantum numbers. Moreover, a positive

value corresponds to the same direction the own and orbital rotation, a negative value corresponds to their opposite direction.

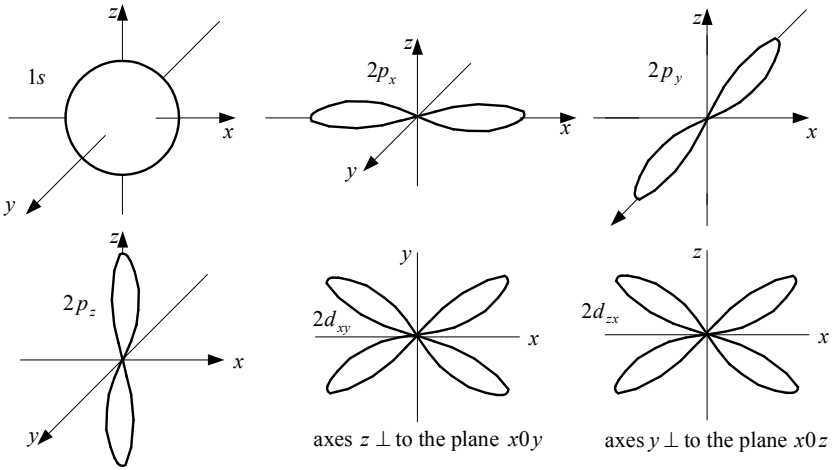

Fig. A2.8. Location of the electron clouds in the space

In addition to the orbital angular momentum which is defined by the value l the electron has the intrinsic angular momentum that we can simplistically consider as a result of the rotation of the electron around its axis. The projection of the intrinsic angular momentum of the electron on the chosen direction is called the spin s.

Thus, the four quantum numbers n, l, m and s completely determine the state of the electron in the atom.

If the electron in the hydrogen atom is in the force field, which is created only by the nucleus, then in many-electron atoms not only the nucleus, but all the other electrons act on each electron. In this case the electron clouds of the individual electrons as if merge into one common many-electron cloud. This means that an electron in the atom is attracted by the nucleus but also tests repulsion from the direction of electrons disposed between the nucleus and this electron. The internal electronic layers as if form the original screen which weakens the attraction of the electron to the nucleus. It is said that the screen shields the outer electron from the nuclear charge. At the same time the electrons, which have the different values of the orbital quantum numbers, have the unequal screening.

Generally, in accordance with the radial probability distribution for the total electron cloud of the "internal" electrons we can make the conclusion about degree of shielding. For example, the outer electron of the sodium (e-formula is $1s^2 2s^2 2p^6 3s^1$) has the possible states 3*s*, 3*p* and s*d*. However, the electron cloud of the 3*s*-electron increasingly penetrates into the region occupied by the first two layers (*K*- and *L*-layers for 1*s*-, 2*s*- and 2*p*-electrons), and therefore is shielded weaker than the electron cloud of the 3*p*-electron. This means that the electron is the state 3*s* will be stronger attracted to the nucleus and have a lower energy than the electron in the 3*p* state.

The electron cloud of the 3*d*-orbital is almost entirely located outside the region occupied by the internal electrons and screened by the greatest degree and most weakly attracted to the nucleus. That is why a stable state of the sodium atom corresponds to the placement of the electron on the 3*s*-orbital, where it has the lowest energy.

Thus, in many-electron atoms, the electron energy depends not only on the main quantum number, but also on the orbital number.

As a result the increase of the energy in the energy sublevels occurs in the following order (see also Fig. A2.9):

$$1s < 2s < 2p < 3s < 3p < 4s < 3d < 4p < 5s < 4d < 5p < 6s < 5d \approx 4f < 6p < 7s < 6d \approx 5f < 7p.$$

To determine the states of the electron in the many-electron atom Pauli principle is used: the atom can not contain more than two electrons, which have the four equaled quantum numbers.

Then it is obvious that each atomic orbital, which is characterized by certain values *n*, *l* and *m* may be occupied by no more than two electrons whose spins have opposite signs.

Two such electrons which are located on the one orbital are called by the paired, as opposed to a single (unpaired) electron occupying any orbital.

The most stable state of the electron in the atom corresponds to the minimum possible value of its energy. Any other its state is called excited, unstable state, from which the electron spontaneously goes into a state of lower energy.

It is easy to calculate the maximum number of the electrons on the atomic energy levels and sublevels, Table A2.1.

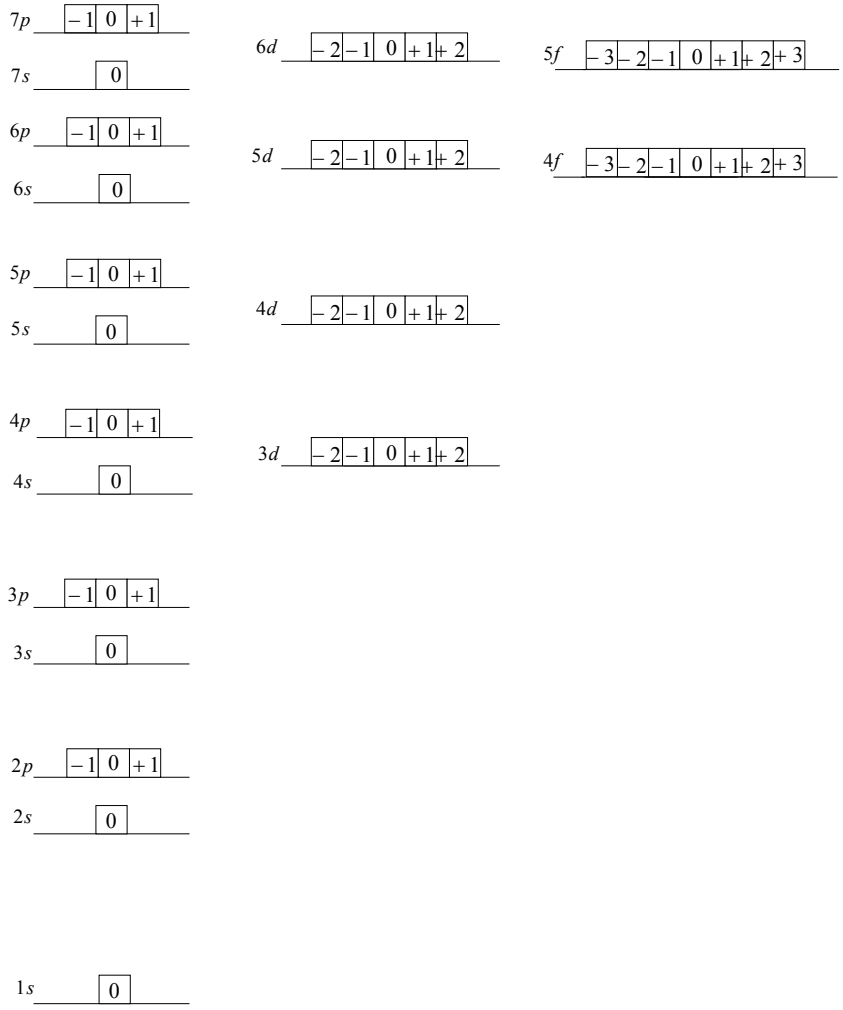

Fig. A2.9. The scheme of mutual arrangement of the energy sublevels in the atom

For example, for $l = 0$ (on the *s*-sublayer) the magnetic quantum number is also equal to zero.

Consequently, the *s*-sublayer contains only one orbital. It is obvious that it can not contain more than two electrons whose spins are directed in opposite directions.

Thus, the maximum number of the electrons on the *s*-sublevel of each electron layer is equal to 2.

TABLE A2.1

MAXIMUM NUMBER OF THE ELECTRONS ON THE ATOMIC ENERGY LEVELS AND SUBLEVELS

Shell	n	l	Designation	m	s	Number of states	Number of states in each shell
K	1	0	$1s$	0	$\pm 1/2$	2	2
L	2	0	$2s$	0	$\pm 1/2$	2	8
		1	$2p$	0	$\pm 1/2$	2	
				± 1	$\pm 1/2$	4	
M	3	0	$3s$	0	$\pm 1/2$	2	18
		1	$3p$	0	$\pm 1/2$	2	
				± 1	$\pm 1/2$	4	
		2	$3d$	0	$\pm 1/2$	2	
				± 1	$\pm 1/2$	4	
				± 2	$\pm 1/2$	4	
N	4	0	$4s$	0	$\pm 1/2$	2	32
		1	$4p$	0	$\pm 1/2$	2	
				± 1	$\pm 1/2$	4	
		2	$4d$	0	$\pm 1/2$	2	
				± 1	$\pm 1/2$	4	
				± 2	$\pm 1/2$	4	
		3	$4f$	0	$\pm 1/2$	2	
				± 1	$\pm 1/2$	4	
				± 2	$\pm 1/2$	4	
				± 3	$\pm 1/2$	4	
and so on							

For $l = 1$ (*p*-sublevel) we have three different values of the magnetic quantum number (–1, 0, +1). Consequently, *p*-sublayer has three orbital,

each of which may be occupied by no more than two electrons. It means that only 6 electrons can be placed on the *p*-sublevel. Obviously, the sublayer *d* ($l = 2$) consists of 5 orbitals on which 10 electrons are placed, on the *f*-sublayer ($l = 3$) 14 electrons may be located. In general, the maximum number of the electrons on the sublevel with the orbital quantum number l is equal to $2(2l+1)$.

The first energy level (*K*-layer, $n = 1$) contains only *s*-sublayer, the second energy level (*L*-layer, $n = 2$) consist of *s*- and *p*-sublevels and etc.

Some possible variants of the placement of the electrons are displayed in the Table.A2.1.

The maximum infill of each shell is determined by how many different values the quantum numbers can make.

If z is the maximum possible number of the electrons on the given shell, n is the main quantum number, then $z = 2n^2$. Then the *K*-layer may contain 2 electrons, the *L*-layer must contain 8 electrons, the *M*-layer contains 18 electrons, the *N*-layer contains 32 electrons etc.

The electronic structure (electronic formula) of the atom is represented by the following way.

Suppose that the *K*-layer ($n = 1$) contains one electron on the *s*-sublayer, then the formula is written as $1s^1$ (reds as "one-s-one"), if the *s*-sublevel contains 2 electrons, it is written as $1s^2$ (reds as "one-s-two").

Suppose, for example, that the *L*-layer ($n = 2$) contains two electrons on the *s*-sublayer, and the *p*-sublayer contains 6 electrons. Then, the electronic formula is written as $1s^2 2p^6$. Similarly, we can construct the electronic formula of the titanium atom Ti: $1s^2 2s^2 2p^6 3s^2 3p^6 3d^2 4s^2$.

To construct the electronic formula it is necessary at first to write in series all states with the given value n and then pass to the state with higher value of n.

However, the order of writing does not always coincide with the order of filling of the energy levels. For example, in the writing of the electronic formula of the scandium atom Sc ($1s^2 2s^2 2p^6 3s^2 3p^6 3d^1 4s^2$) the 3*d*-sublayer is placed previously of the 4*s*-sublayer, although these sublevels are filled in reverse order.

APPENDIX 3

INTRODUCTION TO SPINTRONICS

Physicists and engineers concerned with electronics know that the moving electrons carry their own electrical charge and spin. The own intrinsic magnetic moment and the mechanical moment of the rotation of the electron are connected with the spin. The ignoring of this fact in electronics was due to the fact that the quantity of the conduction electrons with the different random spin orientations moves in ordinary metals (non-ferromagnetics metals) and semiconductors simultaneously. Therefore, the total transfer of the spins is practically equal to zero. And electronics experts could not detect the spin dependence of the electron transfer properties. Even in non-magnetized ferromagnetic metals, in which the magnetic moments of different domains are oriented randomly, spin transfer was not noticeable. For the first time the spin-dependent charge transfer was detected after the discovery of the giant magnetoresistance effect and magnetoresistive memory studies with random access (MRAM). That is why a new electronics section, called spintronics is appeared.

Thus, if the conventional electronics uses the moving electric charges to create the electric current, the spintronics is based on a different physical principle: in the spintronics devices the spins of electrons have moved. The spin is the internal angular momentum, as the electric charge is a fundamental property of the elementary particles. According to the quantum theory, the electrons are divided into two types: the electrons with spin-up (spin direction coincides with the direction of the magnetization of the material) and the electrons with spin-down (spin and the magnetization of the material are in opposite directions).

It should be noted that the electron spin (own angular momentum) is an internal characteristic of the electron, which has a quantum nature and is independent of the motion of the electron.

Recently, in the semiconductor physics perspectives for the creation of the solid-state devices of the spintronics (devices that use both the electric charge and spin) widely discussed.

The electric current is accompanied by the spin transfer when the carriers are polarized, as, for example, under the injection of spin-oriented electrons from the magnetic material into the semiconductor.

In semiconductors, the spin current may be induced in various ways. Basically, the spin current can be caused by the flow of electric current in the structures with the spin-dependent dispersion. In this case, the electrons with the opposite spins are deflected under the dispersion in mainly opposite directions.

Traditional electronic devices are based on the electrical properties of the substance and controlled mainly by the applied voltage. Spintronic devices manipulate by the spin properties (these properties are characterized by the spin direction and the time of its life) with the help of the external magnetic field.

The current generated by the electrons with the spins of the same direction is called the spin-polarized current. To obtain a sufficiently great current it is necessary to polarize the spins by arranging their in one direction. In this case the spin lifetime (the time during which the spin direction does not change) had sufficiently great value to transmit it on the desired distance.

Spintronic devices are fast acting and consume significantly less the energy than traditional electronics devices. This is because the spin overturn (unlike the moving electric charge) does not practically require the energy consumption. It means that in the intervals between the operations the spintronic device may be disconnected from the power source. When the direction of spin changes the kinetic energy of the electron does not change (the spin is independent of the motion of the electron), and therefore no energy is consumed. The rate of the change of the spin direction is very high. The experiments have shown that the spin overturn is done in a few picoseconds (1 picosecond = 10^{-12} s).

In scientific journals the concept of the spin current, called “spin transport” is used. The spin current can be determined by analogy with the electric current as the ratio:

$$i_{sp} = \frac{\Delta Sp}{\Delta t},$$

where ΔSp is the total spin, which is transferred through the cross-section of the conductor at the time Δt. Since the spin is a quantum mechanical dimensionless quantity, the spin-current must be measured in units of "1/s", which coincides with the unit of measurement as "Hertz" and, therefore, is not always convenient to its application.

If we take into account that at the same time with the spin the magnetic moment is transferred (it is very important for spintronics applications), then it is possible to introduce the concept of the magnetic spin current in accordance with the ratio:

$$i_{MS} = \frac{\Delta M}{\Delta t},$$

where ΔM is the magnetic moment carried through a cross-section of the conductor at the time Δt. Since the unit of the magnetic moment of the SI is "J/T", then the unit of the magnetic spin current is "$\frac{\text{J}}{\text{T}\cdot\text{s}} = \frac{\text{W}}{\text{T}}$".

The relationship between the magnetic spin-current i_{MS} and the spin-current i_{Sp} follows from the fact that the magnetic moment carried by the conduction electron is the Bohr magneton:

$$\mu_{\text{B}} = 9{,}274 \cdot 10^{-24} \frac{\text{J}}{\text{T}}.$$

Then

$$\frac{i_{MS}}{i_{Sp}} = 2\mu_{\text{B}} \quad \Rightarrow \quad i_{MS} = 2\mu_{\text{B}} i_{Sp}.$$

Successes of the spintronics are based on the possibility of creating such structures which hot have the respective analogues and in which the interfaces play a decisive role. These magnetic systems are very different from the standard magnetic materials. The interlayer interfaces and the deformation energy can be used to control the magnetic anisotropy. It allows to obtain the magnetic ultrathin films, in which the magnetic moments can be formed either parallel or perpendicular to the film surface.

As already mentioned, the development of the technologies had allowed to synthesize entirely new multicomponent materials with controlled properties. In general, the nanostructures may consist of alternating quantum layers; this raises a set of unique physical phenomena, such as the spin-dependent dispersion of the conduction electrons, the indirect exchange coupling, the surface magnetic anisotropy.

The control of the exchange coupling can be achieved by varying material and the thickness of the streak between the magnetic layers, as well as by changing the crystalline structure.

Transformations of the magnetic and magnetoresistive properties in the layered structures in many respects are defined by the indirect exchange coupling that occurs between the thin ferromagnetic layers separated by the nonmagnetic layer. Under certain conditions, the usual ferromagnetic structure may be transformed into the antiferromagnetic with the antiparallel direction of the magnetic moments. For example, such magnetic phase transitions in the Co/Cu multilayers occur with a period of 1 nm, while the control by the structure of interfaces and streak allows to change the angle between the magnetic moments in the adjacent layers from 0 to 180°.

The best-known effect which appears in the metallic multilayer structures is a giant magnetoresistance effect due to the spin dependence of the dispersion of the conduction electrons on the type of the magnetic ordering of the adjacent layers in the film. The study of this phenomenon and its mechanisms has created a family of new materials with wide potential possibilities of the practical application: the structure with a magnetic tunnel junction, spin valves, transistors, and others.

Previously the magnetoresistance studied in the bulk materials, where the length of the magnetic inhomogeneities greatly exceeded the length of free path of electrons (the distance to the collision).

In the multilayers (for example such as Fe/Cr) ferromagnetic layers Fe of the thickness $\sim 30\overset{0}{A}$ ($1\overset{0}{A} = 10^{-10}\,\text{m} = 0.1\,\text{nm}$) alternated with layers of the non-ferromagnetic chromium Cr of the thickness $9-18\overset{0}{A}$ (Fig. A3.1) It was found that the magnetic moments of the Fe atoms within one layer are parallel and the magnetic moments of the adjacent layers of the Fe are oriented antiparallel (antiferromagnetically). The magnetic field which is greater than the saturation field H_s and applied in the plane of the layers destroys the antiferromagnetic exchange coupling and all the magnetic moments of the Fe atoms are parallel to each other (Fig. A3.1). As a result, the electrical resistance decreases sharply, that is, there is the colossal magnetoresistance.

Magnetic Transition Junction (MTJ) is composed of a very thin dielectric layer (about 1 nm) sandwiched between the two magnetic layers.

Each of the magnetic layers has own magnetic field vector.

The upper magnetic layer is called the free layer; it may change the vector of its field. The magnetic layer of the base is called the fixed layer; the vector of its magnetic field is blocked and does not change.

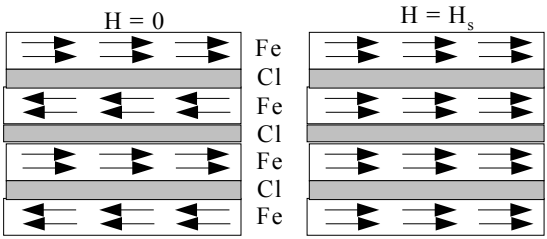

Fig. A3.1. Antiferromagnetic exchange coupling

The direction of the magnetic field vector of the free layer determines the state of the bit as a logical zero or one.

If the vectors of the free layer and fixed layer are oriented in one direction, then the resistance of the MTJ structure is low.

If the vectors are antiphase with respect to each other (are opposite), the structure of the MTJ has a high resistance.

This structure is used to create a magnetic random access memory.

The value of the transition resistance of the MTJ determines the following fact: the resistance of the cell with MTJ will be read as "0" or "1" under the passing of the read current through the cell.

To write the information in the cell the different ways may be used. In the simplest case each cell is located between two writing lines placed at right angle to each other, one line is above the cell and the other line is below the cell, Fig. A3.2.

When the current passes through them, the cross-induced magnetic field is induced in the writing lines intersection which changes the magnetic state of the respective layer.

High speed of the operation and low power consumption allow spintronic devices to form the basis for a new generation of the computers - quantum computers. To do this, it is necessary to create the basic elements – spin transistors capable to amplify the spin current. On the basis of these transistors will be necessary to create the new high-speed processors and nonvolatile memory of high density.

In the spin transistor the states "ON" and "OFF" depend on the direction of the spins of electrons taking part in the flow of the current. Any spintronic device, including the spin transistor must contain three essential elements [50]:

• mechanism of the electrical injection of the spin-polarized electrons in the semiconductor;

• means for the control by the spin current in the semiconductor (for example, the voltage);

• precise detection (measuring) of the resulting spin current.

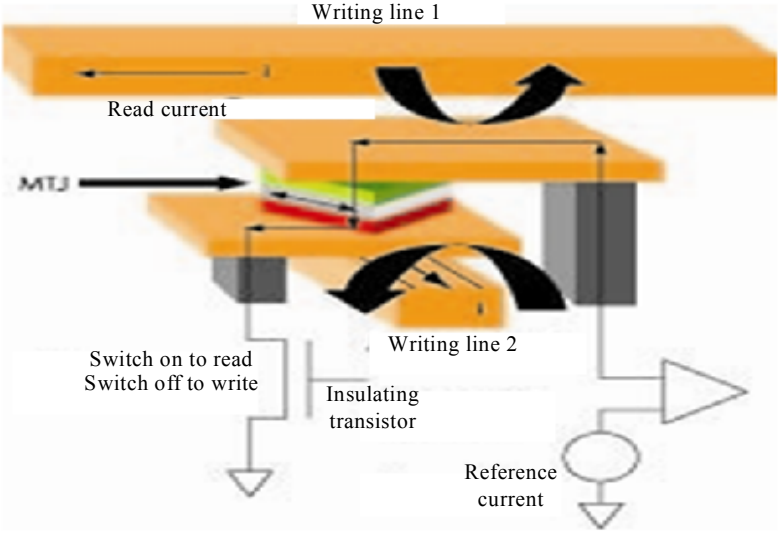

Fig. A3.2. Elementary cell of the MRAM-memory

In addition, it is necessary to achieve high efficiency of the electrical injection of the spin-polarized electrons in the semiconductor and enough spin diffusion length. This means that in order to estimate the effectiveness of the spin-polarized transport of the current carriers it is important to determine at what distances for a while moving the conduction electron "remembers" the spin (preserves the orientation of its spin). The characteristic length of this distance is proportional to the product of the average speed of the electron for a while the spin relaxation, during which the direction of the spin of the moving electron conductivity. In spite of the complexity of this question, recent studies have shown the possibility of transferring the spin current over a long distance (according to the standards of microelectronics) exceeding 300 μm through the unalloyed silicon substrate [100] – [102]. Using unalloyed substrate allows to achieve of the flow of "pure" spin current in the semiconductor, which is very important for precise detection of the resulting signal.

It was experimentally demonstrated that the spin current may be injected into the silicon substrate and controlled.

The degree of the spin polarization, which was reached by the researchers, was equaled to 37%. It means that 37% unidirectional spins of the total number of spins that have come to the injector, was delivered to the detector.

The experimental model of the chip with the spin transistors is shown in Fig. A3.3.

Fig. A3.3. The chip with the spin transistors

The spin transistor is a layered structure composed from the layer of the ferromagnetic, the pure silicon layer, the second ferromagnetic layer (of the different composition) and the silicon layer with the impurities.

The specially selected voltage controlling by the movement of the electrons is applied to the different layers of this structure. The electron flow at the input is not polarized, but after the passage of the ferromagnetic layer it becomes polarized. It means that it becomes by the spin current. These electrons fall into the layer from the pure silicon, pass enough great distance, and then fall into the second ferromagnetic layer, Fig. A3.4.

The experiments have shown that under the motion of the electrons through the silicon the polarization is partially retained. Due to this fact, changing the relative orientation of the magnetic fields in the two ferromagnetic layers allows to turn on or off the spin current on the output of the spin transistor. It allows to use two stable states of the transistor (in which the current is either there (logical "1") or not (logical "0")) to carry out ultra speed logic operations over data.

Under the applied voltage V_e the non-polarized electrons are injected from the aluminum emitter (the electron source) in the ferromagnetic

layer CoFe. Due to the spin-dependent dispersion of the electrons in the magnetic layer, the electrons with the selected spin direction (for example, "spin-down") are eliminated, since the direction of the magnetization of CoFe layer does not coincide with the direction of these spins.

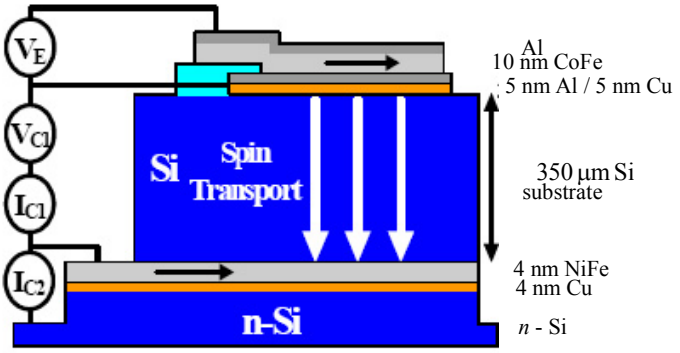

Fig. A3.4. The scheme of the spin transistor functioning

The selected electrons with the unidirectional spins tunnel through the thin layer of Al_2O_3. The electrons pass the barrier if they have a high enough energy to overcome energy barriers. These electrons create the emitter current. Further, the electrons passing through the potential Schottky barrier which arises at the boundary metal – semiconductor, enter in the pure monocrystalline silicon layer, where they occupy the free places in the conduction band of the semiconductor. Under the action of the applied voltage V_{c1} the electrons begin orderly movement, creating the collector current I_{c1} (the current through the detector). After passing through a 350 μm layer of the silicon the spin-polarized electrons are detected by the second spin transistor.

The ferromagnetic layer of NiFe registers the spins of the electrons that are injected into the *n*-type silicon, where the electrons are the basic carriers. It allows to increase the sensitivity of the detector (the excess electrons, which amplify the spin current are in the *n*-type silicon conduction band), creating the collector current I_{c2}.

When the constant voltage V_{c1} is on the emitter the "the first collector current" I_{c1} is measured on the NiFe-contact and "the second collector current" I_{c2} on the indium contact deposited on the *n*-type silicon substrate.

Obviously the spin current depends on the relative magnetization of the two ferromagnetic layers, Fig. A3.5.

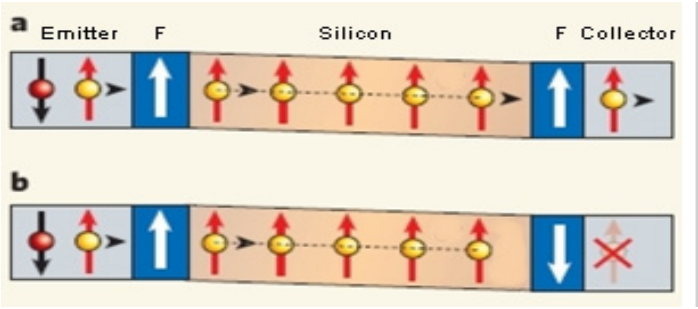

Fig. A3.5. The functioning of the injector and detector: (a) shows layers of CoFe and NiFe which are magnetized in parallel; (b) shows layers which are magnetized in antiparallel, *F* is the first and second ferromagnetic layers

Thus, the development, improvement and implementation of the spintronic devices allow to construct a new generation of ultra speed and economical electronics.

Educational edition

Sineglazov Viktor Mikhailovich,
Zelenkov Alexander Avramovich,
Askerov Shohraddin Isabali oglu

MEMRISTORS AND NONVOLATILE RANDOM ACCESS MEMORY (NVRAM) IN NANOELECTRONICS

Training book

Signed for printing 12.09.2017

Paper size 60×84/16. Offset paper.

Print run 300 copies.

Publishing house "Osvita Ukraini",
04136, Kyiv, Marshala Grechko, 13, of. 218

Certificate of entry in the State Registerpublishers DK N1957 of 27.09.2004
Tel./fax (044) 507-04-52, (097) 479-78-36, (050) 552-20-13
E-mail: osvita2005@gmail.com, www.rambook.ru